UNIVERSITY OF SOUTHAMPTON

Mixing in Anaerobic Digesters

by

Jacqueline S. Christodoulides

M. Eng (Hons), Mastère Spécialisé, CEng, MCIWEM

A Doctoral Thesis submitted in partial fulfilment of the requirements for the award of Doctor of Philosophy at the University of Southampton

Faculty of Engineering and Applied Science

Department of Civil and Environmental Engineering

February 2001

SUPERVISOR: Dr. C. J. Banks

This thesis is dedicated to:

My husband for his unconditional love and patience and my parents for giving me the insight to strive forwards in life.

UNIVERSITY OF SOUTHAMPTON

ABSTRACT

FACULTY OF ENGINEERING AND APPLIED SCIENCE
DEPARTMENT OF CIVIL AND ENVIRONMENTAL ENGINEERING

Doctor of Philosophy

MIXING IN ANAEROBIC DIGESTERS

by Jacqueline S. Christodoulides

Mixing in anaerobic sewage sludge digesters has been investigated using two scales of vessel with the overall aim of providing quantified design information in terms of the active volume expected with different gas sparger types and the blend times expected within this active volume.

Due to a greater sludge production and restrictions enforced on disposal routes, many sludge producers want to increase the available sludge digestion capacity using their existing digesters. This can be achieved both by reducing the size of any inactive volume and by digesting thicker sludges. In both cases, successful volume utilisation and digestion are dependent on the detailed design of the mixing systems involved, on which published information is sparse.

The United States Environmental Protection Agency (US EPA) and Degrèmont provide the only two quantified design guidelines in the literature. These design guidelines result in inconsistencies when changing scale, aspect ratio or mixer type.

An experimental programme was undertaken to study unconfined gas mixing using a sludge simulant. Measurements of blend time were made using an electrolyte tracer and conductivity probes positioned around the vessels. Video footage was taken to determine the size and location of any inactive volume within the vessel. Finally, the results were analysed and correlations produced to predict blend time and active volume.

It was found that a sequential gas sparger performed best overall, both in terms of active volume produced and also in terms of the active blend time. The choice of sparger layout had a considerable effect on mixer performance. The size and location of inactive volume depended on the mixer layout, the viscosity of the liquid and the power input. In general, an increase in viscosity resulted in a decrease in active volume and an increase in blend time. Conversely, an increase in power input resulted in an increase in active volume and a decrease in blend time.

Acknowledgements

I would like to express my thanks to Dr Nick Fawcett of Yorkshire Water Services and Mr Colin Brade of Monsal Ltd for their contributions to this work, both in terms of their sponsorship as well as their valuable experience and ideas.

I would like to thank my supervisor at Southampton, Dr Charles Banks for his continued support and enthusiasm for this work. I would also like to thank my supervisor at BHR Group Limited, Dr Mick Dawson for his encouragement and pearls of wisdom.

A special thankyou to my colleagues at BHR Group Limited for their support, friendship and welcome distractions.

The largest thankyou must go to Louis, without whom I would be losing my mind in Word instead of remaining calm with LaTeX, not to mention his constant love, encouragement, help and perseverance over the past three years and especially over the last few months. Thankyou.

Finally, I would like to thank my parents.

List of Publications

Due to the confidential nature of the work contained within this thesis, extensive publication of the results has not been possible. However, the following publications have been made as a result of this research:

J. Barker and M. Dawson "Digester Mixing: Theory and Practice", 3rd European Biosolids and Organic Residuals Conference, Aqua-Enviro, Wakefield, UK. 16-18 Nov. 1998

J. Christodoulides (née Barker), M. Dawson, N. Fawcett and C. Brade "A Comparison of Mixing Systems in Model Anaerobic Sewage Sludge Digesters", 5th European Biosolids and Organic Residuals Conference, Aqua-Enviro, Wakefield, UK. 19-22 Nov. 2000

Contents

List of Figures

List of Tables

Chapter 1

Introduction

Anaerobic digestion is a biological treatment process that has been used on wastewater treatment plants for almost a century. Figure 1.1 illustrates a typical wastewater treatment process flowchart. Anaerobic digestion is one of the final sludge treatment processes. Biological degradation of sewage sludge in the absence of oxygen produces a stable product with reduced Volatile Organic solids and pathogens, this can be disposed of to agricultural land, landfill or incinerators. In addition, the sludge gas produced (70% methane) during the digestion process can be used as fuel on the treatment plant itself and sometimes even to produce electricity for surrounding urban areas.

Legislation in the form of the Urban Wastewater Treatment Directive has led to the disposal of sewage sludge to sea being banned from December 1998 (EU, 1991). Pressure from food retailers has phased out spreading untreated sewage to land with untreated sludges banned after December 31st, 1999. As a result, investment is currently being directed towards upgrading existing digestion plants and towards the construction of new digesters.

As part of this investment, a project was undertaken at BHR Group Limited for Yorkshire Water Services, one of the largest water companies in the UK and Monsal Ltd, a smaller company that designs and manufactures digester equipment. One aspect of the BHR Group Limited project has been studied in detail

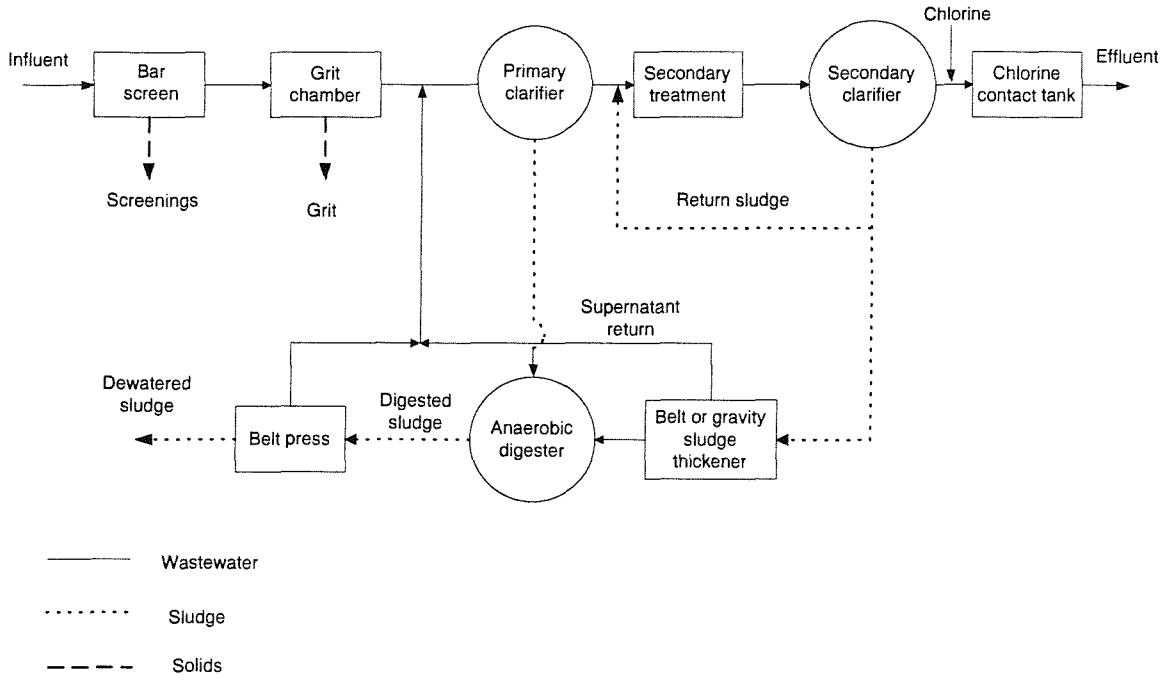

Figure 1.1: Flowchart showing a typical wastewater treatment process (Tchobanoglous and Burton, 1991)

in this thesis, namely digester mixing using unconfined gas mixing.

1.1 Digester mixing systems

The vast majority of digesters are fitted with mixing systems in order to (CIWEM, 1996; EPA, 1987):

1. Provide contact between the feed sludge and active biomass to maximise gas production

2. Provide physical, chemical and biological uniformity in order to maintain a satisfactory environment for both acid and methane forming bacteria

3. Dilute inhibitory substances

4. Prevent stratification and temperature gradients

5. Maintain the required biomass residence time by minimising short-circuiting and dead zones

6. Minimise the build-up of solids on the digester floor, which reduces the active volume

7. Minimise the formation of a scum layer on the sludge surface

Items 1 to 4 are functions of the rate of liquid blending. Item 5 is determined by the flowpattern and characterised by the residence time distribution (RTD). Item 6 is related to solid suspension and distribution, and item 7 to foam breaking and draw-down from the surface.

The rheology of a sewage sludge is non-Newtonian and usually shear-thinning (Frost, 1983; Ouziaux, 1997; Lotito et al., 1997; Slatter, 1997; Monteiro, 1997). As such, it does not behave like a Newtonian, water-like fluid, making items 1 to 7 more difficult to achieve.

Digesters are fed intermittently with incoming sludge. Usually, the feed sludge is heated as this provides a means of maintaining the digester contents at the required mesophilic temperature of 35°C. It is important to disperse the feed sludge throughout the digester quickly to avoid temperature gradients and also to prevent foaming on the sludge surface which can lead to blockages of the gas mixing and control devices and reduce the digestion efficiency and digester gas production (CIWEM, 1996).

A wide variety of different equipment types have been used for digester mixing. The commonest classes are confined and unconfined gas mixing systems, mechanical stirring and mechanical pumping systems. Large digesters commonly operate multiple mixing systems (CIWEM, 1996) .

Digester mixing systems are designed today on the basis of work expended in mixing. However, the design values used appear to be based on rules of thumb with current practice having evolved over many decades from observation and experimentation at the full scale on operational digesters (Brade, 1997; EPA,

1987) rather than a definitive mixing theory related to liquid blending, Residence Time Distribution (RTD) or solids suspension.

Highly evolved process mixing methods used in the Chemical, Food and Pharmaceutical industries have not yet been applied to digestion, perhaps due to insufficient research work on typical digester geometries and sludge rheologies. These areas were examined as part of this work to determine whether mixing technology from the process industries could be applied to anaerobic sewage sludge digesters.

The effect of poor flow characteristics and hence residence time distribution (RTD), can be linked to process performance by experimental results relating retention time (currently specified as 12 to 15 days (DoE, 1996)) to gas production and volatile solids reduction. If the available digester volume is being poorly used because sludge is short-circuiting, then gas production will be low and sludge treatment may not be optimal. Similarly, grit accumulation on the floor reduces the digester active volume, retention time, potential gas production and eventually leads to down-time of the digester for manual grit removal. Some studies have been carried out to measure digester RTDs and hence flowpattern using Lithium Chloride as a tracer (Smith, 1996; Williams, 1994). However, linking the process performance to the rate of liquid blending is difficult since no quantification of the optimum blending rates appears in the literature. Users are now typically specifying a blend time of 1 hour, although there does not appear to be any theoretical or empirical reason why this value has been chosen. The sizing of mixers, the primary function of which is blending, is being carried out with little knowledge of what the blending rates are or should be.

There are many designs for digester mixing systems, the details of which vary from one manufacturer to another. Three different parameters are described in the literature for digester mixing equipment sizing. These parameters are power input per unit volume of sludge (EPA, 1987), the gas flowrate per unit volume of sludge (EPA, 1987) and the gas flowrate per unit area of the digester (Degrémont, 1991). These three design parameters result in inconsistent mixer sizing when applied to

different scales of digester and aspect ratios (Barker and Dawson, 1998). There is, therefore, a clear need for mixing design criteria to be established for the design or retrofit of digesters. In addition, the effect of increasing the thickness of the feed sludges needs to be quantified in terms of mixer size requirements in order to allow a higher sludge volume through both new and existing digesters.

The mixer geometry and size affects both the blend time of the sludge and also the volume of the digester that is actively in motion (active volume). Problems have frequently been encountered with grit settling out into the base of digesters and accumulating on the digester walls. 'Scum' (a mixture of fats, grease, hair and sanitary items) is also reported to collect at the sludge surface. Many digester designs feature a sloping base with a sludge drain pipe located at the centre. This pipe was designed as a means of relieving the consolidation of grit and sludge that built up within the base of the digester. However, the pipe often became blocked and was not used, the digested sludge normally being drawn off by an overflow at the surface. This resulted in the digester contents becoming stratified and a reduction of the volume available to digest the sludge (reduced to approximately 60 to 80%) (CIWEM, 1996).

The periodic drain-down and de-silting of digesters has been an accepted aspect of digester maintenance. However, there is now more sludge to be digested and Water companies are constantly under pressure from the Office of Water Services (OFWAT) to improve their cost effectiveness. Therefore, this method of operating is no longer plausible and it has been recognised that digesting thicker sludges without uprating the mixing systems would increase the grit build-up and hence maintenance problem (Brade, 1997; Fawcett, 1997).

There is a wide variety of digester shapes, geometry and aspect ratios used worldwide and even within the UK. The traditional cylindrical digesters with shallow sloping or flat bases are found in most areas of the UK whilst the newer egg-shaped digesters, originating from Germany, feature at one site in the North West of England (Southport). The traditional cylindrical digesters have aspect

ratios that can vary from 0.5 to 1.5. In addition, there are many different types of digester mixing system, depending on the manufacturer and the Water Company involved. Southern Water is currently retrofitting and building new digesters using impellers for mixing whereas by far the most common mixing system found in Yorkshire Water (YWS) was unconfined gas mixing. Severn Trent Water have a large number of digesters, some of which contain no auxiliary mixing systems at all (however, a large retrofit programme is underway on their digesters).

1.2 Scope of Thesis

This thesis investigates the performance of gas-mixing systems employed within digesters. The thesis focuses on unconfined gas mixing with the aim of improving design by better understanding the effect of mixer size, type and sludge thickness on resultant blend time and active volume.

The mixer and digester test geometries were selected following an extensive survey of YWS digestion sites (Ouziaux, 1997).

Investigation was based on two different scales of vessel, a model (or laboratory) scale and a pilot (or prototype) scale vessel. The model digester was cylindrical in shape with a flat base and the aspect ratio was varied between 0.5 and 1 to represent the range found in practice. Unconfined gas mixing was chosen as Ouziaux (1997) found it to be the most common form of mixing installed in YWS digesters and other researchers have found this to be the case in other regions of the UK (Williams, 1994; Edgington, 2000; CIWEM, 1996; Truscott, 1980).

Six different sparger arrangements were selected, based on the survey by Ouziaux (1997) to investigate the effects of power input, viscosity, aspect ratio, sparger arrangement and scale on the blend time and active volume.

The aim of this work was to produce design guidelines for digesters mixed using unconfined gas injection, in terms of blend time and active volume. This

was achieved by:

- Identification of any literature data for blend time or active volume using non-Newtonian shear thinning liquids
- Designing a series of experiments to address the gaps in the knowledge highlighted in the literature
- Measuring the blend times and active volumes for six different sparger arrangements at different power inputs and in three different concentrations of sludge simulant (CMC), scaled down from the full-scale digester survey of Ouziaux (1997)
- Identification of the effect of power input, viscosity, aspect ratio, nozzle diameter, scale, sparger type and feed position on blend time and active volume
- Identification of an 'optimum' sparger arrangement from those tested
- Comparing the blending performance of the 'optimum' gas spargers with an impeller-mixed vessel

This thesis has looked at the mixing of digesters and does not attempt to address the area of biological breakdown of the sludge and there are many investigations reported in the literature (Gujer and Zehnder, 1983; Novaes, 1986; Elefsiniotis and Oldham, 1994).

Chapter 2

Background and literature

In this chapter, a history of anaerobic digestion is presented and the differences between water and sludge in terms of their rheological properties are highlighted. The evolution of mixing systems within anaerobic digesters is presented where particular attention is paid to the fundamentals of gas mixing. The current state of the art in digester mixing is discussed and comparisons drawn between the different systems that have been investigated in the literature. Finally, Chemical and Process industry mixing research has been reviewed for its applicability to mixing anaerobic digesters using unconfined gas mixing.

2.1 History of anaerobic digestion

The Chartered Institute of Water and Environmental Management, CIWEM (1996) reported that the first trials of digesting sludge anaerobically were recorded by W.J.Dibden more than a century ago in 1885. Originally, digesters were neither mixed nor heated with the turnover of the digester contents assumed to occur solely due to the evolution of biogas, a natural by-product of the anaerobic digestion process.

'Grit' has always been present in the digesting sludge despite screening of the sewage during earlier stages of the treatment process (Figure 1.1). It has been

common practice to provide digester capacity equivalent to 25 to 30 days retention to allow for grit accumulation, low dry-solids feed and variation in local operation. This has been reduced to 12 to 15 days retention in accordance with government guidelines (Department of the Environment, 1996).

During the 1920s and 30s, sludge digestion was becoming more widespread in the UK with several types of mixing and heating systems employed. Traditionally constructed from concrete, digesters were only found on large plants (population equivalent of approximately 25 000). They were typically cylindrical with a conical base, low aspect ratio and floor slope of less than 33°.

By comparison, Germany was using cylindrical digesters with a steeper conical base to enable grit to collect in the base of the digester which was removed periodically via a control valve. A steep conical rooftop reduced scum formation. This design became known as the 'conventional German digester'. Several years later in the early 1950s, the egg shaped digester was invented in Germany, as a result of improved concrete technology, to fulfill the need for large capacity, effectively mixed digesters. US research meanwhile was focused on improving anaerobic digestion by looking at the processes involved rather than the digester shape.

In the UK during the late 1960s and early 1970s, operating difficulties were being reported with digesters and the popularity of anaerobic digestion was suffering as a result. This prompted investigation by various researchers into the problems being encountered. The Water Pollution Research Laboratory (WPRL) survey of 1969 (Swanwick et al., 1969) was an important step towards correcting some of the most commonly reported problems as it led to a re-assessment of the design and operation of sludge digesters. A total of 142 sewage treatment works - thought to represent over 90% of digestion works - were forthcoming with information. Of this total, 56 reported problems due to inadequate design or operation. Nearly all of these problems were in some way, related to inadequate mixing.

During the early 1980s, the Severn Trent Water Authority published a series

of papers (Brade et al., 1982; Brade and Noone, 1981; Noone and Brade, 1982) describing their work into developing heating and mixing systems, the results of which were incorporated into current practice at that time. These developments allowed the retention time to be reduced to 15-18 days. This, together with the advent of pre-fabricated epoxy and glass-coated, flat-bottomed steel tanks, meant digestion became a viable option on smaller plants and its popularity increased (CIWEM, 1996).

During the same period, trials carried out by Rundle and Whyley (1981) at Stoke Bardolph wastewater treatment works (Nottingham) on several mixing devices showed unconfined gas mixing systems to be the most effective and CIWEM (1996) confirm that this method is now very popular. Research performed by Williams (1994), Ouziaux (1997) and Edgington (2000) confirmed that digesters within Wales, Yorkshire and Severn-Trent respectively, are mostly of the unconfined gas mixing type with an external sludge recirculation and heating loop. Williams (1994) even went as far as to suggest that there was something of a 'band-wagon' to use unconfined gas mixing at this time.

After the 1980s, published information concerning mixing quantification within anaerobic digesters is scarce. Design recommendations for digester mixing have been published by the United States Environmental Protection Agency (EPA) (EPA, 1987) and Degrémont (1991). EPA (1987) documented the benefits found from mixing and heating the digester contents, thickening the incoming raw sludge and providing a uniform sludge feed. The majority of the available literature relating to anaerobic digestion is limited to industrial wastewater practice, where Upflow Anaerobic Sludge Blanket (UASB) and filter or contact digester systems for example, are preferred. These systems are not comparable with sewage sludge digesters due to different operating conditions, solids loadings and rheologies. It is therefore, difficult to glean relevant information from them.

The EU Directive on the disposal of sewage sludge to sea (EU, 1991) came into force at the end of 1998 resulting in an increase in sludge requiring disposal

by alternative means. This requirement was a significant stimulus for the work described in this thesis, with the overall aim of increasing the throughput of existing digesters by improving the mixing within them, hence increasing their volume utilisation and ensuring efficient mixer design for new digesters. Other incentives were present in the form of requirements to minimise energy costs and new difficulties anticipated in handling the thicker sludges (sludges with a higher dry solids content) now increasingly available from the use of mechanical dewatering plant in the pre-thickening of municipal sludges (Brade, 1997; CIWEM, 1996).

Digester mixing research has been reported in the literature. The earliest of these studies failed to take the complex rheological properties of sludge into account, (Verhoff et al., 1974; Brade and Noone, 1981) despite Buzzell and Sawyer (1963) having reported that sludge exhibited shear-thinning properties many years previously. However, shear-thinning behaviour was not well understood in the industry at this time, and indeed, is only beginning to be understood thanks to the work of Lotito et al. (1997), Slatter (1997) and Monteiro (1997) among others. Therefore, prior to reviewing the research to date, an introduction to sludge rheology is given.

2.2 Sludge rheology

Rheology is the study of material flow behaviour. It is a complex subject and many books are available that cover this topic in detail (Skelland, 1967; Walters, 1975; Barnes et al., 1989). The material presented here is sufficient to allow the reader to understand the fundamental differences between a Newtonian and a non-Newtonian, shear-thinning (or pseudoplastic) fluid with and without a yield stress.

Water is a Newtonian liquid whereas Buzzell and Sawyer (1963), Frost (1983), Ouziaux (1997), Lotito et al. (1997), Slatter (1997) and Monteiro (1997) found that digested sludges behave as non-Newtonian liquids. The difference between

the two types is how they respond to shear, applied at a constant rate of strain (Jacobs, 1994). Newtonian fluids respond with a proportional increase in shear stress whereas non-Newtonian fluids deviate from this proportional shear stress response. In addition, some sludges may exhibit a yield stress. These fluids require a residual shear stress to be reached before flow can begin. This residual shear stress is defined as the yield stress. The flow curve for these fluids is similar to that for a shear-thinning fluid but it does not intercept the shear stress axis at the origin.

The flow curves for a Newtonian liquid and a shear-thinning non-Newtonian liquid with and without a yield stress are shown in Figure 2.1.

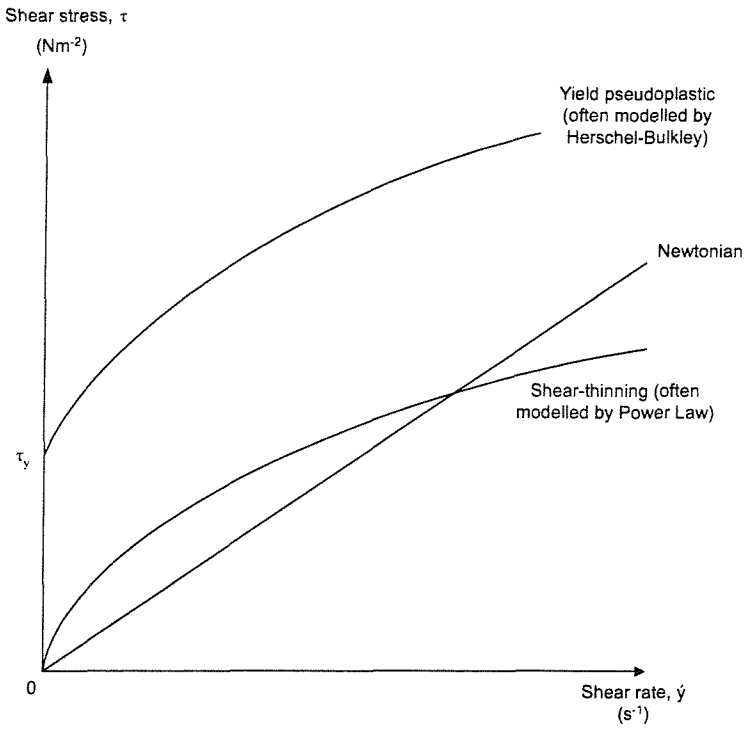

Figure 2.1: Examples of flow curves on linear axies

To determine the relationship between shear stress and shear-rate, a range of viscometers are available. The most common ones are the cone and plate, parallel plate, concentric cylinder and cylinder in 'inflnite' medium. These are illustrated in Figure 2.2.

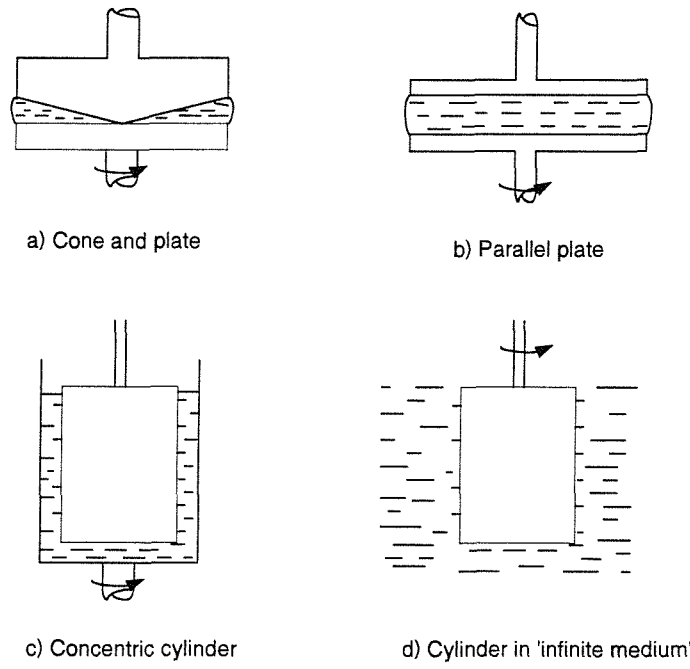

Figure 2.2: Examples of different rheometers (ESDU, 1982)

Anaerobically digested sludge is a slurry, dark brown to black in colour. When thoroughly digested, it is not offensive, its odour being relatively faint and like that of hot tar, or sealing wax according to Tchobanoglous and Burton (1993). Sludges contain solids in suspension. Typical values of dry solids in the digested sludges measured by Ouziaux (1997) ranged from 2% to 5% by weight. These solids are primarily inorganic mineral solids, often referred to as 'grit', as the majority of organic compounds decompose within the digester (Tchobanoglous and Burton, 1993; CIWEM, 1996).

The presence of solids can affect the rheological measurement when using the close-tolerance rheometers shown in Figures 2.2(a), (b) and (c). For sludge rheology determination, the cylinder in an 'infinite' medium is used, as shown in Figure 2.2(d). The bob is placed in a container whose diameter is much greater than that of the bob (Jacobs, 1994). This practice limits the range of shear rates available with the rheometer but avoids any relatively coarse particles from adversely affecting the results or jamming in the narrow annulus between the cup and bob

(in the case of a concentric cylinder arrangement).

2.3 The evolution of anaerobic digester mixing

Originally digesters were built with no auxiliary mixing systems. They operated at a low rate with long residence times. A digester with no auxiliary mixing system is referred to as a 'naturally mixed' digester in this thesis. The natural mixing input comes from a combination of three sources: isothermal expansion of naturally evolving gas, convection from the inflow and outflow of sludge and convection from the warmer feed or recirculated sludge within the bulk.

Casey (1984) suggested that the highest natural mixing energy input comes from the isothermal expansion of the rising gas bubbles but did not quantify this input. As a bubble rises through the sludge it expands due to a decrease in hydrostatic pressure. From thermodynamics:

$$\frac{p_1 V_1}{T_1} = \frac{p_2 V_2}{T_2} \tag{2.1}$$

where p = pressure, V = volume and T = temperature. The subscripts 1 and 2 refer to two different gases.

Eqn. 2.1 may be represented by the ideal gas equation, which can be written as:

$$P = \dot{n} R t \ln \left[\frac{p_1}{p_2} \right] \tag{2.2}$$

where P = Power input from isothermal gas expansion; $\dot{n}$ = molar gas flowrate; R = universal gas constant (8.314 $\mathrm{Jmol^{-1}K^{-1}}$); t = sludge temperature; p_1 = pressure at nozzle or bubble nucleation point; p_2 = pressure at sludge surface

The effectiveness of the natural gas evolution in terms of overall mixing efficiency of digester contents is however limited. For maximum mixing efficiency,

all of the gas needs to be produced at the base of the tank where the pressure differential between the surface and nozzles is highest (Eqn. 2.2). In practice, gas is produced at different heights in the digester, reducing the maximum mixing input available.

Rundle and Whyley (1981) showed that the volume of gas available for mixing in the lower parts of the tank was reduced because of the increased solubility of gases at greater pressures. Casey (1984) agreed, stating that the mixing input from isothermal expansion is not uniform, increasing from a zero value at floor level to a maximum value at the sludge surface.

Stafford (1982) stated that unless the digester aspect ratio (height to width: H/T) was small or the allowable blend time was long, natural mixing was insufficient to achieve adequate mixing, although this was not based on any experimental data.

Hertle and Lever (1987) found that the power inputs due to isothermal expansion of the evolved biogas ranged from 0.15 to 0.5 Wm^{-3}, which in terms of mixing energy, is very low (see Section 2.7). Zoltek and Gram (1975) measured the degree of mixing in a sludge-filled rectangular digester with no auxiliary mixing system using a radioactive tracer. They calculated the mixing input using Eqn. 2.2 as 1.21 Wm^{-3}, a much higher value than that found by Hertle and Lever (1987).

An explanation for this may be in how Zoltek and Gram (1975) determined a gas flowrate for Eqn. 2.2. Zoltek and Gram (1975) stated that the gas flowrate was observed as 0.085 m^3s^{-1}, but determination of the flowrate of the biogas produced could only have been made from measuring the gas flowrate as it left the digester rather than that produced at any point within the digester. Hence 0.085 m^3s^{-1} would have been an average gas flowrate. Taking this value as the gas flowrate and using the height of the digester in Eqn. 2.2, the power input would have been overestimated because in reality, only a fraction of the quoted gas flowrate would occur at the base of the digester and hence, rise through the full digester height. As further evidence, Zoltek and Gram (1975) measured no radioactivity at the

digester outlet 2 hours after injection and concluded that the intensity of natural mixing was small.

A second source of natural mixing energy is from the inflow and outflow of sludge to the digester. Sludge enters the digester through the inlet and is drawn off or overflows at the outlet. Casey (1984) showed that the convective mixing associated with feed and withdrawal was essentially localised and that the associated energy fluxes were less than 0.2% of the natural mixing energy input in a typical digester. Using the values from Hertle and Lever (1987), this would amount to $3x10^{-4}$ Wm^{-3}. Compared to that from isothermal gas expansion, this input can be considered as insignificant for typical digesters. In addition, Williams (1994), Edgington (2000) and Ouziaux (1997) found the location of the inlet and outlet to be within 90° of each other at the surface of the digesting sludge in some older digesters, promoting short-circuiting of the feed sludge thus reducing any mixing input further.

Verhoff et al. (1974) investigated the influence on the flowpattern of convection resulting from the warmer feed sludge entering the cooler digesting sludge. They derived from theory, using dimensionless numbers, that natural convection dominated the flow, contradicting the findings of Casey (1984). Verhoff et al. (1974) assumed that the sludge had the same properties as water, apart from viscosity, thereby considering the sludge as a viscous Newtonian liquid. However, Frost (1983), Ouziaux (1997), (Buzzell and Sawyer, 1963), Slatter (1997), Monteiro (1997) and Lotito et al. (1997) showed that digested sludges behave as non-Newtonian shear-thinning liquids (Section 2.2). By considering the digester inlet flow as a jet, Shekarriz et al. (1996) have shown that the decay rate of a jet is faster in a non-Newtonian shear-thinning liquid than in a Newtonian one, resulting in a smaller active volume. Therefore, the flowpattern derived by Verhoff et al. (1974) is likely to be an over-estimate.

Historically, 'natural' mixing was commonly relied upon. However, reduced retention times of 15 to 18 days meant that auxiliary mixing systems were required

to perform the following functions: quickly disperse the feed sludge within the digester; increase the solids loading by digesting thicker sludges; ensure increased volume utilisation by avoiding grit deposition and 'scum' formation due to the non-uniform distribution of the biogas produced. Scum consists of fats, oils, grease and soaps together with hair, plastics and sanitary items which rise to the surface of the sludge. If scum accumulates, it can reduce the effective volume of the digester, interfere with mixing and circulation and restrict the evolution of gas (CIWEM, 1996).

2.4 Anaerobic digester mixing systems

The main types of anaerobic digester mixing equipment can be classified as follows (CIWEM, 1996; EPA, 1987):

- Unconfined gas mixing
- Confined gas mixing
- Impeller mixing
- Mechanical pumping

Examples of these types of mixing systems have been taken from CIWEM (1996) and are shown in Figure 2.3 and discussed in the following sections. This is not an exhaustive list as different manufacturers have used variations of these types.

2.4.1 Unconfined gas mixing

This is the most common type of auxiliary mixing currently found in UK digesters (Ouziaux, 1997; CIWEM, 1996; Williams, 1994; Truscott, 1980; Edgington, 2000). In older designs fitted with a floating roof, the sludge gas was collected at the top of the digester. In newer designs, the gas is collected in a separate tank. In both

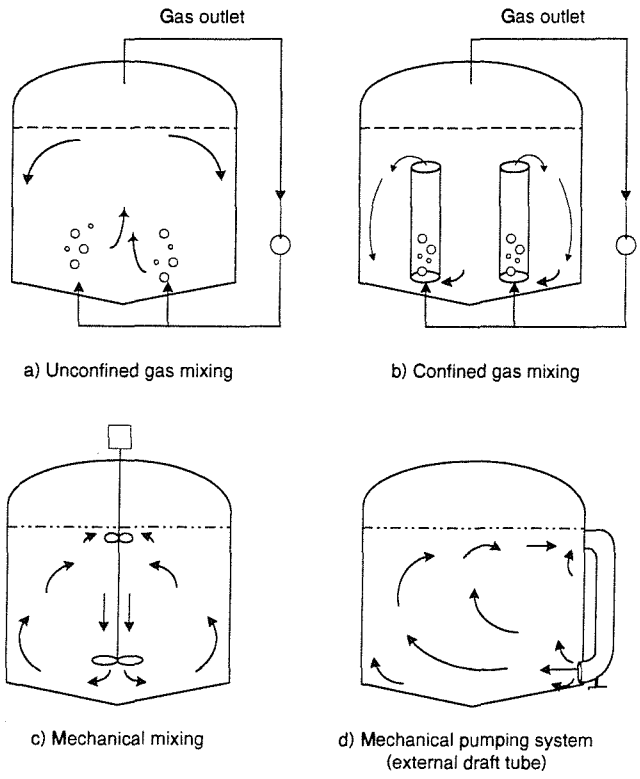

Figure 2.3: Main types of auxiliary mixing found in digesters (CIWEM, 1996)

cases, the gas is scrubbed, compressed and discharged into the digester. Figure 2.4(a) shows a bottom diffuser arrangement and Figure 2.4(b) shows a digester fitted with cover-mounted lances (EPA, 1987).

Diffusers are fixed to the base of the digester as a diffuser box or a simple nozzle or nozzles arranged across the digester base. Cover-mounted lances are suspended from the roof (base-mounted lances are also found). In cases where the cover-mounted lances were installed in a floating-roof digester, the lances would rise and fall with the production of gas allegedly aiding the suspension of grit in the base when they were lowered and the surface scum breakup when they were raised (EPA, 1987; CIWEM, 1996).

As a bubble of compressed sludge gas rises through the digester, it accelerates and the decrease in pressure produced behind it, the wake, is equalised by entrainment of the surrounding liquid into this space. As the bubble gets closer to the liquid surface, the hydrostatic head decreases and the bubble expands thus

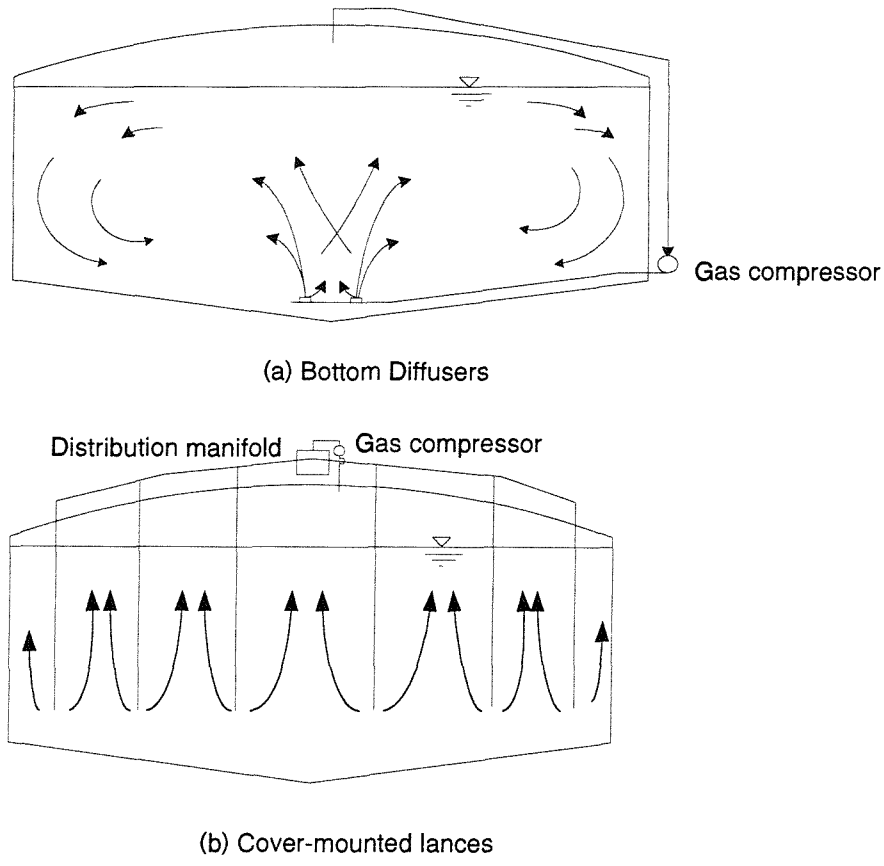

Figure 2.4: Unconfined gas mixing (EPA, 1987)

further increasing the eddies within the surrounding liquid. The overall effect of a single gas outlet is a vertical cone of rising liquid as shown in Figure 2.5 (Williams, 1994).

In the most simple arrangement, the diffusers are supplied simultaneously with sludge gas from the compressor, running intermittently or continually, to achieve the required intensity of mixing. In more complex systems, gas is supplied sequentially to selected diffusers either via a rotary valve, or by electric or pneumatic actuated valves opening and closing on signals from a programmable logic controller (CIWEM, 1996).

One argument given in favour of sequential gasing is that by diverting all the flow to a single nozzle, any blockages induced from sucking sludge into the gas lines after the gas is switched off, can be cleared due to the higher gas flowrate

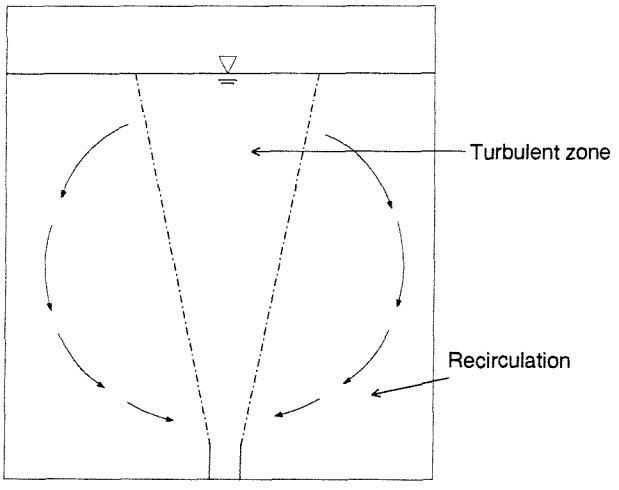

Figure 2.5: Zone of influence of rising gas bubble

through one nozzle compared to several (CIWEM, 1996). In addition, large quantities of gas passed through individual pipes results in vigorous local mixing. In electronically controlled plants, any blockage in the diffuser system would cause an over-pressure signal and indication of which pipe is blocked. Edgington (2000) recently investigated the performance of several Severn Trent Water digesters in terms of their active volumes. The sequentially mixed digester was reported to have a lower active volume than those mixed using several nozzles simultaneously.

The environment within an anaerobic digester is very corrosive. The main advantage of unconfined gas mixing over other types is the absence of internal moving parts which are prone to corrosion, thus reducing the down-time of the digester for maintenance. However, mixing of the vessel contents below the injection nozzles is relatively ineffective which can result in solids build up on the base of the digester and foaming problems at the sludge surface (EPA, 1987; CIWEM, 1996; Williams, 1994). A separate secondary mixing system is often required (although seldom employed) for scum control and for shifting grit deposits.

2.4.2 Confined gas mixing

These systems are less common nowadays but some of the older digesters are fitted with them and will generally continue to be used until the plants are refurbished. Compressed gas is fed into the base of a draft tube in which it rises as a stream of small bubbles (or as a slug, depending on the tube diameter and gas flowrate) causing the sludge to rise up the tube in the bubble wakes and be distributed over the surface of the sludge (CIWEM, 1996).

The claimed advantages of confined gas mixing over unconfined gas mixing are that it is more energy efficient and provides better movement of bottom deposits as the draft tubes are located close to the base of the digester (EPA, 1987). However, as much of the equipment is within the digester, corrosion can be a problem and the draft-tubes can become plugged with rags as the sludge moves within them.

2.4.3 Impeller mixing

Examples of impeller systems are illustrated in Figures 2.4(c), 2.6 and 2.7. Their use appears to be more common in Scandinavian countries than in the UK.

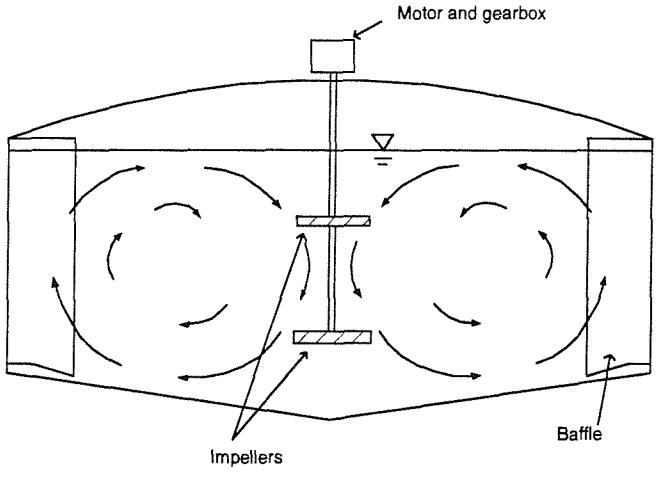

Figure 2.6: Mechanical stirring system

In impeller systems, one or more shaft mounted rotating impellers are installed in the centre of the digester, suspended from the roof. If an upper impeller is used,

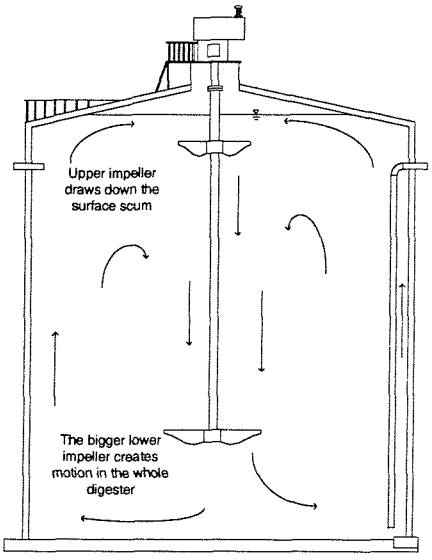

Figure 2.7: The Vaahto impeller system

it is usually smaller than the lower one and is used to draw-down scum into the rest of the digester whilst the lower impeller provides bulk fluid motion and prevents grit settlement. The vessels may be baffled to avoid a central vortex formation which is reported to hinder the mixing process (EPA, 1987), however the Vaahto digesters are unbaffled (Vaahto, 1996).

The widespread use of impellers in the UK has been limited although plants in the USA and Sweden are reported to have used impellers successfully (Rundle and Whyley, 1981; Balmer, 1999). This aversion to impellers is partly due to the problems reported in the 1980s (EPA, 1987) with the corrosion of internal equipment and partly due to concern about 'rags' accumulating on the impeller and shaft, making the shaft imbalanced. Rag accumulation will increase the load on the impeller and shaft requiring a reinforced tank roof and an oversized motor and gear box. This is an important consideration for package plant designs (EPA, 1987). Internal equipment can be replaced but the digester must be drained, put out of service and any grit accumulation manually dug out.

Rag accumulation can be alleviated by installing a reversible motor causing the rags to unappend themselves from the impeller although the rags would soon accumulate in the reverse direction. Alternatively, improved screening upstream

would reduce the rag volume reaching the digester, but increase the headloss over the screens and the risk of blockage.

2.4.4 Jet mixing

A mechanical pumping system was shown in Figure 2.3(d). An axial-flow pump circulates digesting sludge from a high level to return it into the lower part of a digester (CIWEM, 1996).

Digesters that operate using an external heat exchanger withdraw sludge periodically from the digester and pass it through the heat exchanger. It is then pumped back into the digester, either with a batch of fresh feed, or on its own (CIWEM, 1996) and can therefore be considered as a jet. Casey (1984) found that the power input from the sludge recirculation loop was small at approximately 0.2% of the mixing input from gas evolution within his model digester.

2.5 Gas mixing fundamentals

This section aims to introduce the reader to the fundamentals of gas mixing, firstly for Newtonian fluids and then for non-Newtonian fluids. Liquid motion in gas mixed systems is caused by the movement of the rising gas bubbles within the liquid. Such a system is a two-phase system, the gas being the dispersed phase and the liquid being the continuous phase.

Much work has been performed on bubbles in Newtonian fluids and the state of the art is given by Clift et al. (1978). Much less work has been performed in non-Newtonian fluids, although an extensive review of the available literature has been performed by Chhabra (1993).

The simplest form of gas-liquid movement is that produced by a single bubble. Two models exist to determine bubble formation and these are discussed in detail later in this section. The bubble is formed at an orifice by injecting gas. As the bubble forms, it gradually moves upward with a velocity determined by the

buoyancy and inertia forces.

Schmidt et al. (1992) described the local mixing in the liquid phase of two-phase gas-liquid flows agitated by rising gas bubbles. The authors assumed that the transport of liquid in the bubble wakes was the dominant mixing mechanism and used experimental results on single bubbles to describe this mechanism. They concluded that as a bubble rises through a liquid, the liquid in front of the bubble is continuously replaced by the bubble gas causing the liquid to flow downwards along the interfacial area between the bubble and liquid. During this process, the liquid carries dissolved gas from the bubble with it which is preferentially transferred into the bubble wake, leading to local liquid flow around the bubble. As the bubble continues to rise, the vortices which follow in the bubble's path can be regarded as liquid volume trapped in the wake and carried along with the rising bubble through the liquid bulk phase. There is continuous leakage of the wake liquid into the bulk fluid allowing transportation of liquid within the vessel.

2.5.1 Bubble formation and coalescence

The size of a bubble is influenced to varying degrees by both the system and physical parameters, such as the physical properties of the two phases, gas flowrate, pressure above the orifice, height of the liquid, etc. Consequently, a general model encompassing bubble formation under all conditions would be desirable although such a model is yet to emerge, even for Newtonian liquids (Chhabra, 1993).

Newtonian fluids

There are essentially two models to determine bubble volume (or diameter) at the point of formation that have been used in the literature (Chhabra, 1993). These models have also been extended to describe bubble formation in non-Newtonian media.

These are the Davidson-Schuler model (Davidson and Schuler, 1960a; Davidson and Schuler, 1960b) and the Kumar-Kuloor model (Kumar and Kuloor, 1970). In

the Davidson-Schuler model the bubble is assumed to form at a point source where the gas is introduced. As the bubble forms, it gradually moves upwards with a velocity determined by the net resultant of the forces applied, i.e. the bubble buoyancy, the inertia of the liquid moving with the bubble and the viscous drag force. The combination of forces depends upon the liquid phase physical properties (surface tension, density and viscosity) and the gas flowrate (Chhabra, 1993). The bubble detachment from the source orifice is assumed to occur when the centre of the bubble has moved a distance equal to the sum of the radius of the orifice and of the bubble.

In low-viscosity Newtonian fluids and at relatively large gas flowrates (no definition in terms of Reynolds number was given to determine the size of these gas flowrates), the liquid flow can be assumed to be inviscid (Davidson and Schuler, 1960b) and the surface tension effects are negligible. The resultant forces acting on the bubble therefore are buoyancy and inertia of the liquid moving with the bubble, ie.:

$$V_b(\rho_L - \rho_g) = \frac{d}{dt}\left[\left(\frac{11}{16}\rho_L + \rho_g\right)V_b\frac{dx}{dt}\right] \tag{2.3}$$

where V_b =bubble volume; ρ_L = liquid density; ρ_g = gas density and x = distance

In highly viscous Newtonian systems and at low gas flowrates (again, no guidance was provided as to these values), the inertial force of the liquid being carried by the bubble would be negligibly small and instead the buoyancy force would be balanced by the viscous drag force, ie.:

$$V_{bf} = \frac{4\pi}{3}\left(\frac{15\mu Q}{2\rho_L g}\right) \tag{2.4}$$

where V_{bf} = final bubble volume; μ = liquid viscosity; Q = gas flowrate and g = acceleration due to gravity

In the Kumar-Kuloor model the bubble is assumed to form in two stages, namely the growth (or expansion) stage followed by the detachment stage. This

model differs from that of Davidson-Schuler in that the bubble stays at the orifice during the growth stage whereas in the second stage, it moves away from (but remains in contact with) the orifice tip, via a neck, until detachment.

The volume of the bubble at the end of the first stage can be expressed as:

$$V_{bl} = 0.0474\frac{Q^2 V_{bl}^{-2/3}}{g} + 2.42\left(\frac{\mu}{\rho_L}\right)V_{bl}^{-1/3}\left(\frac{Q}{g}\right) \tag{2.5}$$

where V_{bl} = volume of bubble at the end of the first stage

Despite their widely different physical background, under inviscid liquid flow conditions and without any surface tension effects, the two models for final bubble volume at detachment can be reduced to:

$$V_{bf} = C\left(\frac{Q^2}{g}\right)^{3/5} \tag{2.6}$$

where C is a constant, dependent on the liquid viscosity, gas and liquid densities. Davidson and Schuler (1960a) found the value of C to be 1.387 which was subsequently modified to 1.138 and Kumar and Kuloor (1970) found C to equal 0.976.

The use of these two models in non-Newtonian media is discussed in the following section.

The recent work of Colella et al. (1999) has investigated the coalescence and breakage mechanisms of air bubbles in water. The researchers found a distinct lack of bubble size distribution measurements reported in the literature. According to Colella et al. (1999), this is because of an unsatisfactory understanding of the physical mechanisms that lead to breakage and coalescence and the enormous difficulty in obtaining reliable data. The bubble size distribution in a vessel is not constant, but can change due to bubble-bubble interactions than can lead to breakage or coalescence. Almost all of the published data refer to the evaluation of a mean bubble diameter usually estimated from a single height measurement.

Figure 2.8 illustrates the phenomenon of a wake behind a rising bubble. A smaller bubble rises upwards, accelerating towards the larger bubble due to a reduction in the drag experienced by the smaller bubble, where it collides with the large bubble and coalesces.

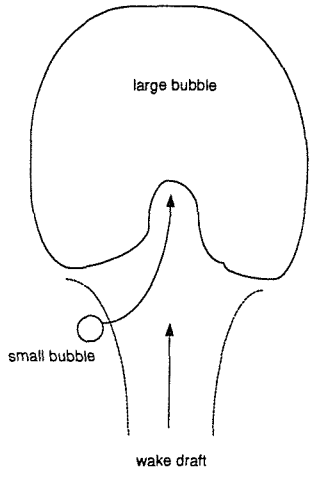

Figure 2.8: Illustration of the existence of a wake behind a rising bubble

Figure 2.9 is a simplified illustration of coalescence. Dekée et al. (1986) defined three distinct stages of coalescence and these are illustrated in Figure 2.9. Initially, two spherical bubbles rise with their own bubble rise velocities (Figure 2.9(a)). In Dekée's stage one definition, the trailing bubble enters the wake left behind by the leading bubble (Figure 2.9(b)). In stage two, the trailing bubble experiencing less drag in the wake, accelerates towards the leading bubble until collision occurs (Figure 2.9(c)). In stage three, a process of film thinning takes place until coalescence occurs, when the resulting bubble continues to rise upwards, with a larger volume (Figure 2.9(d)). However, as Shiloh et al. (1973) point out, coalescence times should be distinguished from collision times as two bubbles may collide but not coalesce.

Therefore, a bubble volume at detachment from the nozzle can be determined using either Eqns 2.4 or 2.5. The volume of a bubble at a higher point in the vessel can reasonably be expected to be larger, assuming coalescence occurs (coalescence is influenced by the liquid physical properties). Following the laws of

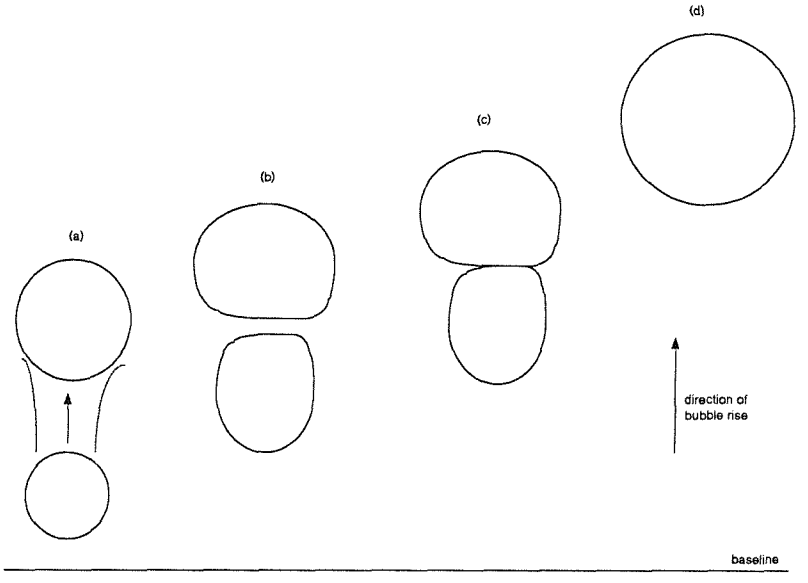

Figure 2.9: Illustration of liquid thinning leading to bubble coalescence

thermodynamics, at a constant temperature, as a bubble rises through a liquid, the static head is reduced and the bubble expands due to isothermal gas expansion (Eqn. 2.2). However, the size of this bubble cannot currently be determined for all systems and all liquids.

The effect of orifice diameter on bubble volume appears to be negligible. According to the models of Davidson-Shuler and Kumar-Kuloor (Eqns 2.4 and 2.5), bubble volume at detachment is only a function of liquid viscosity, gas flowrate and liquid density. If two nozzles of different diameter were used in the same liquid with constant physical properties and at a constant gas flowrate therefore, it would appear that the bubble volume would be the same.

Non-Newtonian fluids

Chhabra (1993) has reviewed the area of bubble formation in non-Newtonian systems and found that in contrast to Newtonian fluids, few studies have been performed in well-characterised non-Newtonian systems. Chhabra (1993) suggested that inviscid flow models are likely to only be applicable at extremely high gas flowrates and therefore, in view of the current work, not to a gas-mixed anaerobic

digester.

Researchers (Bhavaraju et al., 1978; Hirose and Moo-Young, 1969; Hirose and Moo-Young, 1972) have obtained approximate solutions for single bubble motion in non-Newtonian fluids, although due to the complex rheology and presence of inertia terms in the equations of motion, exact solutions are difficult to obtain and hence, the techniques applied have led to approximate models (Dekée et al., 1986).

The applicability of the Davidson-Schuler and Kumar-Kuloor models presented previously was studied by Costes and Alran (1978). Their paper discussed the formation of bubbles in one CMC solution ($k = 3.04$ Pas^n and $n = 0.68$) under constant pressure and constant flowrate conditions. The bubble volumes determined experimentally were compared with those calculated from the Davidson-Shuler and Kumar-Kuloor methods. The measured values of bubble volumes showed slightly better agreement with the model of Davidson and Schuler (1960a) than that of Kumar and Kuloor (1970).

Recently Li (1999) has studied in-line interactions between bubbles for two viscoelastic liquids. Li (1999) simulated the passage of bubbles by imposing consecutive shear rates (pulses) to a fluid sample using a rheometer that measured the response in terms of shear stress. Li (1999) proposed that the dynamical competition between the creation of stresses after the passage of a bubble and the relaxation of these stresses, temporarily formed a corridor of reduced viscosity. If a trailing bubble enters this region before the viscosity returns to that of the bulk liquid, then the trailing bubble accelerates towards the leading bubble, as defined by Dekée et al. (1986) in stage two of bubble coalescence.

Bhaga and Weber (1980) studied the interaction of bubbles in a viscous aqueous sugar solution. They determined that the shape and rise velocity of the leading bubble was essentially unaffected until coalescence, confirming the findings of Crabtree and Bridgwater (1971). The trailing bubble was deformed under the influence of the leading bubble's wake.

As for Newtonian fluids, isothermal gas expansion and coalescence may occur, depending on the liquid properties and gas flowrates used. However, theoretical determination of the bubble diameter at different liquid heights is not yet possible, although growth rates of bubbles in power-law fluids have been studied (Chhabra, 1993). The number of studies performed are limited with many more studies having been performed on viscoelastic fluids.

2.5.2 Bubble shapes

Extensive reports on bubble shape in Newtonian and non-Newtonian fluids have been presented in the literature (Acharya et al., 1977; Clift et al., 1978; Calderbank et al., 1970; Barnett et al., 1966). Bubble shape has been reported by these researchers as being a function of bubble volume and the physical properties of the surrounding liquid. According to Eqns 2.4 and 2.5, the bubble volume at the time of detachment from the nozzle is a function of the liquid viscosity, gas flowrate and liquid density.

Different bubble shapes are formed as the bubble rises through the height of the liquid and in different liquid viscosity systems. Bubble shapes in Newtonian liquids are presented first, followed by those in non-Newtonian liquids.

Newtonian fluids

Chhabra (1993) has reviewed the literature available on bubble shapes in Newtonian fluids. Bubbles will deform when subjected to external flow fields until the shear stresses reach an equilibrium at the bubble-liquid interface because of a bubble's mobile interface. In Newtonian media, ignoring wall effects, there are three main categories. These are illustrated in Figure 2.10 and can be described as:

- Spherical - occurs at low bubble Reynolds number. Interfacial tension and viscous forces essentially govern the bubble shape

- Ellipsoidal - bubbles are oblate with a convex interface around the entire surface (when viewed from inside). These bubbles generally undergo periodic dilation or wobbling motion thus further complicating their characterisation.
- Spherical-cap or ellipsoidal-cap - the bubbles are large and usually have flat or indented bases, resembling segments cut from spheres

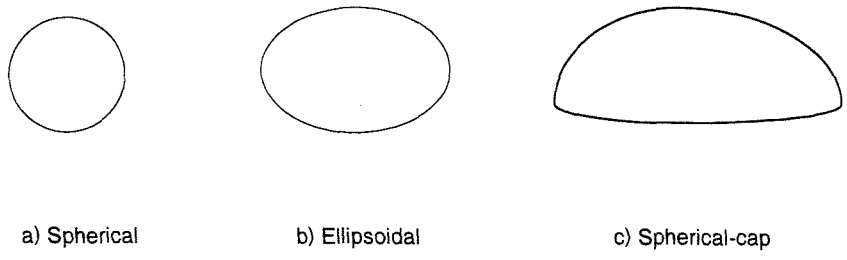

Figure 2.10: Bubble shapes in water and viscous Newtonian fluids

Astarita and Apuzzo (1965) reviewed existing knowledge in Newtonian liquids and expanded these concepts to non-Newtonian and viscoelastic fluids. They identified four flow regimes in Newtonian fluids where different bubble properties were defined. Increasing the bubble Reynolds number changed the regime the bubbles were in.

In the Stokes regime, small diameter spherical bubbles of low Reynolds number follow the same fundamental rules as spherical particles and are considered to have a rigid interface between their surface and the surrounding liquid. At higher Reynolds number, bubbles enter the Hadamard regime. The bubbles are still spherical but now move in the creeping flow regime and have a free interface. At high Reynolds number, the bubbles continue to have a free interface and are still spherical but have a larger volume than the two preceding regimes. Finally, in the Taylor regime, the bubbles take on a spherical-cap shape, retaining their free interface. However, no Reynolds number values were provided to define the transition between these regimes.

The bubble rise velocities for the Stokes and Hadamard regimes are defined as (Astarita and Apuzzo, 1965):

$$\text{Stokes:} \qquad U_{br} = \frac{84}{\nu} V^{\frac{2}{3}} \tag{2.7}$$

where U_{br} = bubble rise velocity; ν = kinematic viscosity $(=\frac{\mu}{\rho})$ and V = bubble volume. The value of the constant requires the units of U_{br} to be cms^{-1}; ν to be cm^2s^{-1} and V to be cm^3.

$$\text{Hadamard:} \qquad U_{br} = \frac{126}{\nu} V^{\frac{2}{3}} \tag{2.8}$$

Only these two regimes are defined here because in non-Newtonian, shear-thinning fluids, the governing equations are extremely complex, therefore, only the creeping flow is considered, that is, the flow regime defined by Eqns 2.7 and 2.8 (Chhabra, 1993).

Non-Newtonian fluids

The same forces of buoyancy and inertia that act on a bubble in Newtonian liquids, act on a bubble in non-Newtonian liquids (Chhabra, 1993). However the size of these forces are different, resulting in different bubble shapes from those in Newtonian fluids.

Bubble shapes in 1% CMC solution are illustrated in Figure 2.11, taken from Chhabra (1993).

Dekée et al. (1986) observed similar bubble shapes in 1% CMC solution. The bubble shapes changed as bubble Reynolds number increased, beginning with small inverted tear drop shaped bubbles at low Reynolds number increasing in volume to the oblate shape as Reynolds number increased, until finally, the spherical cap shape was observed at the highest bubble Reynolds number. Values for the bubble Reynolds numbers were not given but later work by Dekée and Chhabra

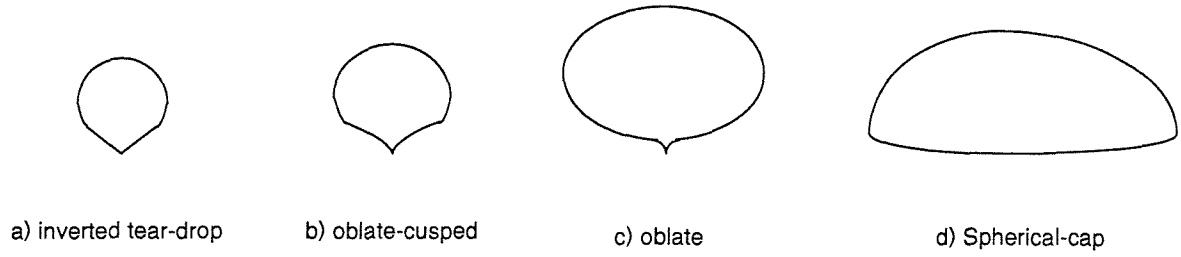

Figure 2.11: Illustration of bubble shapes in 1% CMC solution

(1988) varied bubble Reynolds from 0.087 to 6 and found the same bubble shape range as shown in Figure 2.11.

Chhabra (1993) has summarised the findings regarding bubble shapes in free rise in non-Newtonian media as follows: at very low Reynolds numbers (no exact definition was given for the Reynolds number referred to by Chhabra (1993) but it is likely to be the bubble Reynolds number), the surface tension forces tend to maintain the spherical shape. The bubble shape changes through the range shown in Figure 2.11 as a function of the physical properties and its volume. An oscillating negative wake is often reported behind a bubble in non-Newtonian viscoelastic media, although no physical explanation for this phenomenon is yet available (Chhabra, 1993).

Barnett et al. (1966) examined experimentally bubble motion in non-Newtonian fluids. Their paper outlined transitional bubble shapes in aqueous solutions of carboxymethylcellulose (CMC) and highlighted the observed relationship existing between tailing at the rear of the bubble and an increase in the drag coefficient. Hassager, Bisgaard, and Ostergaard (1980) claimed that the phenomenon of bubble tailing was related to a negative wake forming directly behind the rising bubbles due to the liquid velocity being in the downward direction, away from the rising bubble. This liquid movement is in agreement with that found by Schmidt et al. (1992) who concluded that the liquid surrounding a rising bubble was continuously replaced by the bubble gas as it rose.

Dekée et al. (1986) and Dewsbury et al. (1999) observed the same bubble

shapes in non-Newtonian solutions of CMC (as well as the viscoelastic polyacrylamide, PAA) as have been presented, and concluded that this reflected the increased friction in these solutions of CMC and the bubbles therefore travelled slower with less liquid entrainment.

Information on determining the bubble rise velocity in non-Newtonian fluids is scarce. Chhabra (1993) concludes that an exact solution that can rival the work in Newtonian fluids is not possible due to the shear-rate dependent viscosity of non-Newtonian shear-thinning liquids. Therefore, only solutions for the creeping flow regime are considered, these are the Stokes and Hadamard equations (Eqns 2.7 and 2.8). These equations require measurement or calculation of the bubble volume using the Davidson-Shuler model or Kumar-Kuloor model, as discussed in Section 2.5.1.

2.5.3 Bubble plumes

When bubbles are continuously released from a single localised source at the bottom of a liquid layer, a plume of bubbles is produced. Chen and Cardoso (2000) investigated the motion of a plume of low Reynolds number bubbles in a stratified liquid consisting of two liquids of different density. Mixing between the two liquid layers occurred when the bubbles broke through the liquid-liquid interface. They carried in their wake, a certain volume of the higher density liquid, the volume of which depended on the bubble sizes.

If a single orifice is used, this plume may be a single column of rising bubbles as observed by Crabtree and Bridgwater (1969) or using multiple orifices, several columns of rising bubbles as observed by Rietema and Ottengraph (1970). Ulbrecht et al. (1985) studied the form of this plume at different gas flowrates in three solutions: Corn syrup (Newtonian), polyvinyl pyrrolidon - PVP (non-Newtonian, shear-thinning, inelastic) and polyacryl amide - PAA (non-Newtonian, shear-thinning, elastic). They found the existence of three modes, depending on the gas flowrate, the column diameter and liquid viscosity. These were the viscous

mode; the helical flow mode and the vortex mode.

In the viscous mode, the bubbles had almost uniform sizes (0.005 to 0.006m in diameter) and rose slowly with very little interaction with each other. Immediately above the sparger, the motion of the bubbles was more erratic. Slightly higher up, the bubbles arranged themselves into a relatively narrow plume which rose upwards with a slight rocking motion (although this was only observed for narrow bubble columns). In this mode, they observed that most of the liquid moves upwards in a straight line, following the plume before flowing downwards in the annulus. This results in high axial mixing but very little radial mixing.

Increasing the gas flowrate increased the rocking motion of the plume, aiding the radial mixing. Simultaneously, the plume rotated so that the resulting motion was helical. They found frequent bubble coalescence and a widening of the plume with liquid height.

Finally, increasing the gas flowrate further intensified the bubble coalescence forming large bubbles which absorbed smaller bubbles. The regular structure of the plume broke down and vortices formed in the wakes behind the large bubbles, trapping portions of liquid, carrying it from the bottom to the top of the column, essentially unmixed.

In terms of blend time, they found that it was highest in the viscous mode, decreasing with increased gas flowrate until reaching a minimum in the vortex mode.

Although it was not studied in the work of Ulbrecht et al. (1985), they concluded that a ring sparger would produce a different plume than that from a single nozzle. They identified a 'cooling tower' plume shape in viscous liquids where the gas bubbles released from a ring sparger would first move towards the centre of the column before forming the continuously widening plume.

2.5.4 Power input

Power input due to the isothermal expansion of rising gas bubbles has been presented earlier as Eqn. 2.2. A second form of power input can also arise from the jetting action of the gas as it passes through the nozzles or orifices. This form of power input has been used by Sridhar and Potter (1980) and is mentioned in Tatterson (1991) and can be calculated using:

$$P_j = 0.5 Q_g \rho_g u_{nozzle}^2 \tag{2.9}$$

where P_j = power input from jetting action of gas; Q_g = gas flowrate; ρ_g = gas density and u_{nozzle} = velocity of gas through the nozzle

This kinetic energy input has received little attention in the literature. Much of the literature that discusses power input is for gas-liquid stirred vessels where the power input from the gas sparging is insignificant compared to that of impeller mixed systems. However, at high gas flowrates and small nozzle diameters, the contribution from the kinetic energy should not be ignored.

It is not at all clear however, how much of this nozzle kinetic energy is transferred to the surrounding liquid. Sridhar and Potter (1980) studied a gas-liquid impeller stirred vessel and did consider the kinetic energy input from the gas. The inlet gas was assumed to dissipate its entire kinetic energy near the sparger exit.

At high enough gas flowrates, the gas jet issuing from the nozzle will be in the form of a jet, but this will shortly dissipate into smaller bubbles which will then rise to the liquid surface.

To determine the magnitude of the kinetic energy input from the gas for a full-scale digester, Ouziaux (1997) supplied information on digester volume, nozzle diameter, gas flowrate and the number of nozzles in use. This information was available for 8 of the 14 unconfined gas mixed digesters surveyed. Using Eqn. 2.9, the kinetic energy contribution was calculated as 3.75 to 4.56 W. The sludge volumes of these digesters ranged from 450 to 1076 m^3, therefore the power in-

put per unit volume range was negligible, being 4.24 x 10^{-3} 8.33 x 10^{-3} Wm^{-3}. The following discussions concerning power input for full-scale digesters are therefore considered only in terms of the power input from isothermal gas expansion. However, both of these energy inputs are considered for the experimental work performed in this thesis.

2.6 State of the art in digester mixing

In reviewing the available literature on mixing within anaerobic digesters, the most prominent finding is that there is very little published information on digester mixer sizing. Only the EPA (1987) and Degrémont (1991) have published any target values for power input or gas flowrate. These values are presented in Table 2.1. Actual power inputs used in practice may differ depending on the type of mixing system used and the manufacturer.

Converting the EPA (1987) and Degrémont (1991) flowrates to the same units and assuming an aspect ratio of one, the ratio of the flowrates is:

$$\frac{Q_{EPA}}{Q_{Deg}} = \frac{0.27}{0.8} \times \left(\frac{4V}{\pi}\right)^{1/3} = 0.366V^{1/3} \tag{2.10}$$

where V is the digester volume

Table 2.6 illustrates the ratio between the EPA (1987) and Degrémont (1991) flowrates for increasing vessel volume, assuming a digester aspect ratio of one. For vessels of a realistic size, the EPA (1987) flowrate is between 1.7 and 6.3 times larger than that recommended by Degrémont (1991).

There is conflict in the published design literature therefore regarding firstly, which design parameter to use: P/V, Q_g/V or Q_g/A and secondly, which value to use. The following section discusses the comparisons made in the literature between different mixing systems and where available, comments on the values of power input quoted.

Table 2.1: Common design parameters for mixing systems

Parameter	Definition	Unit	Typical Value	Applies to:
Unit power	Power input by mixing equipment divided by digester volume (EPA, 1987)	Wm^{-3}	5-8 2-4	US/UK Egg shapes
Unit gas flow EPA : Degrémont:	 Quantity of gas delivered divided by digester volume Quantity of gas delivered divided by digester area	 $m^3/h/m^3$ $m^3/h/m^2$	 0.27-0.3 0.3-0.42 0.8	 Unconfined Confined -
Velocity gradient	Square root of power used per unit volume divided by sludge viscosity * (EPA, 1987)	s^{-1}	50-80	-
Turnover time	Volumetric flowrate divided by sludge volume (Stukenberg et al., 1992)	day^{-1}	0.3-18	-
Draft-tube velocity	Volumetric flowrate divided by cross sectional area (Stukenberg et al., 1992))	ms^{-1}	0.75-1.8	Jet pump or impeller pump

*The viscosity used appears to be that of water $\mu = 0.001$ Pa.s. If the viscosity of the sludge is taken as this value then:

$$\text{Velocity gradient, } G = 50 = (P/(\mu\ V))^{0.5}$$
$$P/V = (0.001)(2500) = 2.5\ \text{Wm}^{-3}$$

This is comparable with the P/V values given by EPA (1987). If a typical sludge viscosity was used, say 0.1 Pas, then P/V becomes 250 Wm^{-3}.

Table 2.2: EPA and Degrémont flowrates when H/T=1

V (m^3)	Q_{EPA}/Q_{Deg}(-)
100	1.7
500	2.9
1000	3.7
5000	6.3

2.6.1 Determination of the power input

Williams (1994) surveyed six Welsh Water sites. The gas flowrates ranged from 0.031 to 1.34 $m^3/m^3/hr$ which compare with those recommended by Degrémont (1991) in Table 2.1. Williams (1994) recorded the corresponding power inputs as

1.93 to 12.3 Wm^{-3}, the higher values of which compare with the range of power inputs recommended by EPA (1987).

Brade (1997) suggested that a typical gas compressor used for the unconfined gas mixing of digesters has an efficiency of 30% due to small leaks at glands, seals, joints and drains, reported by CIWEM (1996). Therefore, if the power rating of a compressor was 5kW and the digester volume was $1000m^3$, for example, then the gross power input per unit volume would be 5 Wm^{-3} but the net power input would be 30% of this value, 1.5 Wm^{-3}. To clarify this further, a power input of 5 Wm^{-3} to the compressor would result in a power input of only 1.5 Wm^{-3} to the digester itself.

The work reported by Williams (1994) does not mention the gas compressor efficiency and in the cases where the compressor power ratings were supplied, it is clear that the power inputs per unit volume quoted were those from the compressor, i.e. gross power input. If an efficiency of 30% is assumed then the power inputs reduce to 0.58 to 3.69 Wm^{-3} (the net power inputs).

As a comparison, the power inputs from isothermal expansion using the gas flowrates supplied by Williams (1994) and Eqn. 2.2 have been calculated. The resulting power inputs range from 0.79 to 2.50 Wm^{-3}, very similar to the net compressor values, obtained assuming 30% efficiency.

Ouziaux (1997) recorded the compressor power ratings and digester volumes for a selection of YWS sites and calculated the gross power input. The isothermal expansion of gas was also calculated using the recorded gas flowrates through the compressor and Eqn. 2.2 and compared with the net compressor power inputs, assuming an efficiency of 30%. Good agreement was found between the net and isothermal power inputs, both being lower than the gross power input based on the compressor power ratings.

Table 2.6.1 lists the gross, net (assuming an efficiency of 30%) and isothermal power inputs for the Welsh sites (Williams, 1994) and the Yorkshire sites (Ouziaux, 1997). Only those sites with sufficient data have been included.

Table 2.3: Comparison between power inputs

Site	**Digester Volume (m^3)**	**Gross P/V (Wm^{-3})**	**Net P/V (Wm^{-3})**	**Iso. expansion P/V (Wm^{-3})**
Llanfoist	1500	12.3	3.69	2.50
Monmouth	245	4.60	1.38	1.44
Penybont	1000	5.00	1.50	0.91
Gresford	777	1.93	0.58	0.81
Queensferry	1590	9.43	2.83	0.79
Caldervale	1755	10.5	3.15	3.50
Harrogate North	978	3.1	0.93	0.93
Harrogate South	450	6.7	2.01	2.18
Malton	715	4.2	1.26	1.43
Marley	700	7.8	2.34	2.11
Rawcliffe	530	5.7	1.71	1.84
Sutton	715	4.2	1.26	1.65
Walbutts	537	5.6	1.68	1.54
Wombwell	1076	2.8	0.84	0.94

In all cases apart from Queensferry, the net power input is in close agreement with that calculated from isothermal gas expansion. This indicates that a compressor efficiency in the order of 30% should be accounted for when stating power inputs. As will be shown in the following sections, this is not often the case in the literature.

2.7 Comparison of mixing system performance

2.7.1 Confined and unconfined gas mixing

In addition to the naturally mixed rectangular digester introduced in Section 2.3, Zoltek and Gram (1975) also investigated one confined and one unconfined gas mixer, both in sludge filled digesters using a radioactive tracer. The digesters used were all rectangular (5.2m high, 29.9m x 16.8m) and of similar volume, with the inlet and outlet at opposite ends of the tank. The diffusers were located in the bottom of the tank in a circle 2 m in diameter. They were positioned towards the inlet of the digester. The confined gas system consisted of one draft tube located along the same axis as the diffusers, but towards the outlet end of the digester.

Two methods of measurement were made: one using a scintillation detector in the middle of the digester and the second method used a portable scintillation detector that could be positioned at different locations in the digester due to sampling ports located across the digester roof. Using the first method, Zoltek and Gram (1975) reported tracer detected within 10 minutes from injection and the count rate levelled off after 40 minutes. Using the second method however, large differences in tracer concentration were detected in different parts of the tank even after 100 minutes.

The injected tracer in the confined gas case took longer to reach the probe in method one, some 30 minutes, the concentration rose relatively slowly and erratically, levelling off at about 100 minutes. Method two was not used for this digester.

The authors were unable to determine whether the differences in blend time were due to the confined or unconfined nature of the mixing systems or whether they were due to the different layouts of the systems within the tank, which would produce different flowpatterns. The power inputs to the digesters were reported as 10.1 Wm^{-3} for the unconfined gas and 6.05 Wm^{-3} for the confined gas mixers, which would suggest that the observed differences may have been due to different

power inputs.

Rundle and Whyley (1981) compared confined and unconfined gas mixing systems at Severn Trent's Stoke Bardolph wastewater treatment plant. All eight of the digesters were originally mixed by the intermittent operation of a screw-pump mixer in a central uptake draft-tube. Rags and other debris collected around the impeller and at the bottom of the uptake tube, which was unsatisfactory and replacements were sought.

The choice was between confined gas mixing using draft-tubes, unconfined gas mixing using diffuser boxes and unconfined mixing using leaf-spring diffusers.

Rundle and Whyley (1981) used an existing open-topped digester at the plant to measure the blend times of the different systems using real sludge. Three methods were used to evaluate mixing: radioactive tracer, Lithium Chloride tracer, and solids distribution. The power input used was not specified, but the total airflow rate was given as 0.085 m^3s^{-1}. The liquid volume was recorded as 5300 m^3. With this information, assuming as aspect ratio of one, this author calculated the height as 19m and using Eqn. 2.2, calculated a power input of 1.95 Wm^{-3}.

The leaf-spring diffusers blended in the shortest time and were used to optimise the gas flowrate required. Decreasing the gas flowrate increased the dispersion time. Even at a power input of 0.49 Wm^{-3}, the tracer concentration at the probes was reported to lie within $\pm 10\%$ of the theoretical completely mixed value within 40 minutes.

The exact locations of the probes used in the work of Rundle and Whyley (1981) are given only as a 2-dimensional side-elevation of the digester. It would appear that the number of readings by the digester wall and near the base (typically less actively mixed regions) were limited with the majority of readings taken in well-mixed regions. This would result in a faster blend time because the probes were in an active volume, as suggested by the two methods of detection used by Zoltek and Gram (1975).

Baumann and Huibregste (1982) compared simultaneous and sequential gas

mixing processes for the following systems: a draft tube mixer (confined gas mixing), multiple sequential discharge lances (unconfined gas mixing) and floor-mounted diffuser boxes consisting of 8 diffusers located around a small diameter central ring (also unconfined gas mixing). The draft tube mixer and multiple sequential discharge lances were studied using water in a laboratory scale rectangular tank 24.4 x 24.4 x 6.1 m in dimension. All three mixer types were also studied at the full-scale at different sites using real sludge.

The power input to the confined gas mixed systems were higher than those supplied to either of the unconfined gas mixed systems and yet the authors were unable to specify whether one system was better than another in terms of mixing efficiency, providing each system was designed 'properly' although what exactly this means was not defined.

A review of digestion plant in the United States was performed by EPA (1987) collating together a review of the literature and discussions with design engineers and operators of existing plant. Both confined and unconfined gas mixed systems reported high maintenance of the compressor and potential gas seal problems. The confined gas system also reported problems with corrosion of the gas lifter, scum buildup, poor mixing in the top region of the digester and plugging of the draft tubes, but did provide better movement of bottom deposits than cover-mounted lances (unconfined gas) and lower power requirements.

The bottom-mounted diffusers fared worse than cover-mounted lances for the unconfined systems with problems reported of scum formation, plugging of diffusers, breakage of bottom-mounted gas piping but reported better movement of bottom deposits than cover-mounted lances. The cover-mounted lances were effective against scum buildup and required less maintenance than the bottom-mounted diffusers although suffered from plugging of the lances.

From this comparison between confined and unconfined gas mixing systems, there is no clear conclusion as to whether one system is better than another, either in terms of required power input, measured blend time (Zoltek and Gram,

1975; Rundle and Whyley, 1981), mixing efficiency (Baumann and Huibregste, 1982) or operational use (EPA, 1987). The comparisons made in the literature have often used different power inputs, different digester geometries and mixer layouts making direct comparison difficult. To determine whether one system is better than another, equal digester geometries, sludge rheology, power inputs and measurement systems should be used so that clear conclusions can be drawn.

2.7.2 Impellers and unconfined gas mixing

Brade and Noone (1981) performed blend time measurement tests using a water-filled digester fitted with an impeller and unconfined gas diffusers. They found that the impeller was up to four times more efficient than the gas injection system in terms of energy utilisation. However, this may have been due to a poor diffuser layout compared to the impeller or due to the tests having been performed in water, which would produce different flowpatterns to sludge.

In a later paper, Brade et al. (1982) carried out mixing tests using an open-topped digester filled with digesting sludge and a four-bladed turbine of diameter equal to one quarter of the digester diameter. The power input was varied from 0.52 to 5.74 Wm^{-3} and recorded blend times were from 12 to 40 minutes. No mention of how the blend times were recorded or the location of any probes used was made, only that these blend times were subsequently confirmed using radio-tracing when the tank was an active digester.

Balmer (1999) quoted a value of 1 Wm^{-3} for Rya treatment works in Sweden, stating that propeller mixers are used in all modern flat-bottomed tanks. This power input is low compared to that quoted by Brade et al. (1982) but the tanks at Rya are also supplemented with an unconfined gas mixing system, which would suggest that the impeller requires less power input. There were eight gas injection ports, equally spaced around the periphery of the tank where gas was supplied to each nozzle sequentially. Unfortunately, there is not enough information supplied to calculate the power input from the gas so the total power input is unknown.

During commissioning of the plant at Rya, LiCl was injected as a tracer to determine the blend time. After injection, the tracer concentration increased rapidly, achieving 89% of the theoretical concentration for complete mixing within 20 minutes, 93% after 30 minutes and 99% within 60 minutes. After two and a half years of operation, the bolts on the axle of one of the mixers worked loose and the propeller and half the axle dropped to the bottom of the tank. The tank was emptied to repair the damage, allowing a visual inspection of the conditions within the tank.

The inspection revealed that the centre of the tank bottom was free from deposits. However, along the periphery there were deposits with a triangular cross-section of about 3m by 3m, with a conical hole at each diffuser location. Balmer (1999) interpreted this as meaning that the gas injection did not contribute much to the tank mixing, but this author would argue that the grit buildup around the periphery would also indicate that the impeller mixing was not reaching the periphery due to the flowpattern and low power input. Without knowing the gas power input, it is not possible to compare Balmer's (1999) conclusions about the gas performance as the gas power input may have been too low.

Casey (1984) discussed the results found by other authors (Imhoff, 1983; Carrol and Ross, 1983; Wiedemann, 1977) when comparing impeller and gas mixing systems. Imhoff (1983) reviewed impeller mixing systems in Germany and Wiedemann (1977) reviewed gas mixing systems. Casey (1984) concluded that impeller systems provided reliable performance over extended service periods and consumed less energy than gas mixing systems. In contrast, Carrol and Ross (1983) reviewed operating experience in Canada that showed impeller mixing to be costly and difficult to maintain. These apparently conflicting experiences should be considered with caution since detailed information on the systems involved is lacking.

The review from the EPA (1987) listed problems of wear for impellers and shafts, bearing failures, accumulation of rags on the impellers and requirements for oversized gear boxes and gas leaks at the shaft seals. However, they were listed

as having good mixing efficiency.

As an interesting comparison, Lin and Pearce (1991) recommended a power input of 1.5 kWm^{-3} for the impeller system used in the anaerobic digestion of potato processing wastewater, a figure almost 1000 times higher than quoted by Balmer (1999).

No firm conclusion has been drawn as to whether the power input required for an impeller is higher or lower than that required for equivalent mixing using unconfined gas. As for the confined and unconfined gas mixing comparisons, it is very difficult to compare the work of different researchers because different systems have been used and insufficient detail supplied about the different systems, such as sludge rheology, percentage dry solids content, mixer configuration and gas power inputs. This illustrates the futility of quoting power inputs without further details of the system used and similarly, quoting system information with insufficient data to calculate the power input.

2.7.3 Unconfined gas mixing and other systems

The EPA (1987) produced a comprehensive list of the advantages and disadvantages of the main types of digester mixers. The list was based on a review of technical literature and numerous discussions with American wastewater treatment plant operatives.

Every mixer had a longer list of disadvantages than advantages with corrosion cited as a disadvantage in almost every case. In terms of mixing efficiency, impeller mixed systems and confined gas mixing systems were listed by EPA (1987) as being better than other types of mixer and yet the majority of UK digesters are unconfined gas mixing systems with base mounted diffusers (Williams, 1994; Ouziaux, 1997; Truscott, 1980; CIWEM, 1996).

Stukenberg et al. (1992) carried out a survey of several digestion plants in the USA and their results are shown in Table 2.4.

The primary mixing system is either the system that provided the greatest

Table 2.4: Values for mixing energy found in several American and German digesters (Stukenberg et al., 1992)

Shape	Volume (m^3)	Primary P_{in} (Wm^{-3})	Secondary P_{in} (Wm^{-3})	Recirculation P_{in} (Wm^{-3})	Primary Turnover (d^{-1})
Egg	6000	2.5	6.1	2.5	3.3
Sphere/cone	3200	0.3	3.6	0.3	0.3
Egg	8000	2.3	-	2.0	11
German conventional	7500	2.0	1.8	2.9	8
Egg	7500	2.3	1.8	2.9	8
Sphere/cone	2700	0.8	-	0.8	1.3
Egg	4700	3.2	5.0	3.0	18
Egg	11400	3.5	5.5	4.7	10
Egg	11400	3.0	-	2.0	7.6
German conventional	9500	3.8	-	2.4	9

amount of energy or that which had the greatest influence on digester mixing as it was the only system operated continuously. The majority of the primary systems were a form of impeller mixing consisting of an internal draft tube with an impeller at the top. The secondary mixing systems were usually gas injection systems.

The overall power input per unit volume range was 0.3 to 6.1 Wm^{-3}. Unfortunately, no information is given concerning their actively mixed volumes or the extent of any solids build up and therefore, any comparison with other digesters is limited to the power input. The highest primary power input was for the German conventional digester shape, closely followed by the egg-shaped digesters, but the sphere/cone shape (UK digesters) had the lowest power input, four to ten times lower than that for the egg-shaped digesters.

Bode and Klauwer (1999) claimed an energy demand of 3 to 5 Wm^{-3} is required for unconfined gas mixing systems in digesters of a reasonable size referring to Figure 2.12. Once again though, it was not stated whether this was the power

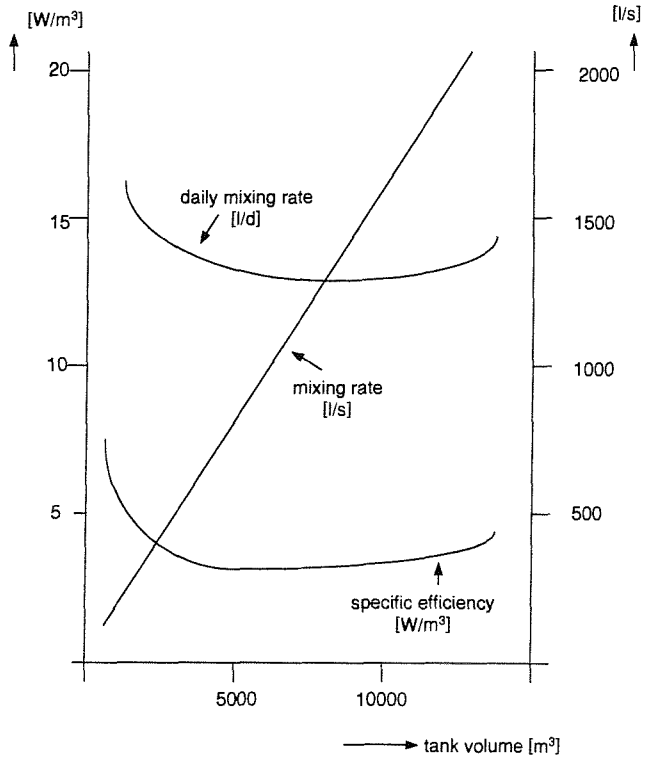

Figure 2.12: Characteristic values of digester mixing quoted in Bode and Klauwer (1999)

input to the compressor or that to the digesting sludge. If the specific efficiency is actually the power input (the units are Wm^{-3}), then the figure suggests that the required power input decreases from 7 Wm^{-3} to 2.5 Wm^{-3} when the tank volume is increased from 500 to 7000 m^3. Beyond this volume, the power input increases again up to 4.5 Wm^{-3} when the volume is 14000 m^3. How these figures have been obtained is not provided by Bode and Klauwer (1999) and the reason for the decrease and subsequent increase in required power input is not at all clear.

The purpose of the other two lines in Figure 2.12 is not clear either. The units of 'daily mixing rate' and 'mixing rate' are those of flowrate but whether these refer to feed flowrate, circulation flowrate, pumping rate or even gas flowrate is not specified. However, this is one of the few investigations in the literature where an attempt at suggesting power input values to use has been made.

2.7.4 Effect of power input on active volume

The extent of the grit build-up that can occur was graphically described by Baumann and Huibregste (1982). Table 2.5 shows the sites studied and their respective power inputs, calculated from the information supplied in the paper. An extensive accumulation of solids at the bottom of the S.E.Wisconsin digester was recorded during their studies on solids profiling. A 'Pango' sampler was used, a spring loaded device that collected samples within the digester which were then analysed for solids content and used to build up a solids profile of the digester. The digester was fitted with a central diffuser box. The sampler was unable to penetrate the lower 3m of the digester and the digester was taken out of service for cleaning.

The solids build-up consisted primarily of grit and inorganic solids and formed a steep pile which sloped downward from the digester wall to the diffuser box. The draining down of the digester caused these grit slopes to slide, tearing out sludge piping supports and the diffusers along with the gas supply piping.

The power inputs to the digesters studied by Baumann and Huibregste (1982) are shown in Table 2.5. The overall range of power inputs was 0.7 to 11 Wm^{-3}

Table 2.5: Theoretical power inputs and mixing effectiveness for different confined and unconfined gas mixing systems

Site	D (m)	H (m)	V (m^3)	Theo.P_{in} (kW)	P/V (Wm^{-3})	Mixer	Grit deposition
Texas 1	19.8	7.5	2460	27.5	11.0	Draft	Slight
Texas 2	19.8	7.5	2460	15.7	6.4	Draft	Slight
N. Illinois	18.3	6.1	1600	3.0	1.9	Draft	Significant
C.Virginia	12.2	-	1426	2.5	1.75	Lances	Insignificant
C. Wisconsin 1	18.3	-	4813	3.3	0.7	Lances	Slight *
C. Wisconsin 2	18.3	-	4813	4.8	1.0	Lances	Slight *
S.E. Wisconsin	18.3	-	4813	3.6	0.75	Diffusers	Significant

* Grit build-up was evident below the lances, although lengthening the lances to extend further into the digester reduced the height of this build-up. Above this layer of grit, there was evidence that solids were moving around and therefore, not accumulating.

and if the compressor is assumed to be 30% efficient (see Section 2.6.1), these reduce to 0.21 to 3.3 Wm^{-3}.

The power input per unit volume for the digester at S.E.Wisconsin was given as 0.75 Wm^{-3}. This is a very low power input as it is and by assuming 30% efficiency of the compressor, this value drops further to 0.225 Wm^{-3}. Baumann and Huibregste (1982) concluded that the mixing arrangement was not maintaining a completely mixed condition within the digester and anticipated that increasing the gas flowrate (and hence power input) would improve the solids suspension.

These tests revealed an apparent, albeit loose, correlation between floor deposits and power supplied between the different mixers.

Each of the draft-tube systems recorded slight or significant grit depositions compared to slight or insignificant depositions for the lances which used a much lower theoretical power input range (0.7 to 1.75 Wm^{-3}) compared to 1.9 to 11.0 Wm^{-3} for the draft-tube systems.

The diffuser box and confined systems produced similar flowpatterns since the mixing energy was concentrated at the centre of the digester. Both systems experienced problems with accumulated solids on the bottom of the digester and floating solids at the surface. Increasing the power inputs to those closer to the confined gas mixing values would increase the active volume by entraining the base deposits and surface solids into the bulk.

The lances suffered less from grit deposition as they were positioned more evenly throughout the tank however, grit was reported on the digester base up to approximately 1m below the lances.

The power inputs to the Welsh digesters studied by Williams (1994) were given as 1.93 to 12.3 Wm^{-3}, which become 0.58 to 3.69 Wm^{-3} assuming an efficiency of 30% (These values have been discussed previously in Section 2.6.1). Williams (1994) performed Lithium Chloride tracer studies and reported that the majority of the digesters tested were performing 'satisfactorily' with the minimum volume utilisation determined as 78% for Queensferry and Gresford. Queensferry had

been in service for 10 years whereas Gresford had been in service for only 2 years. Gresford had the lowest power input in the survey - a quoted value of 1.93 Wm^{-3} (0.58 Wm^{-3} if 30% efficiency assumed) compared to 9.43 Wm^{-3} for Queensferry (2.83 Wm^{-3}) suggesting that a higher power input reduced the grit deposition, in accordance with the conclusions of Baumann and Huibregste (1982).

The active volume of a digester can be reduced when solids are able to accumulate around the periphery of the digester base. This is the case for confined gas mixers (draft tubes) and unconfined gas mixers (diffusers and lances). The work of Baumann and Huibregste (1982) and Williams (1994) suggest that the active volume can be increased by increasing the power input to the digester.

2.8 Relating Chemical Industry research to anaerobic digestion

Mixing has been studied for Chemical Process Industry applications for many years. Good mixing ensures high product yields by providing sufficient contact between the different chemicals present to allow the necessary chemical reactions or heat transfer to be optimised.

Bubble columns used in chemical and pharmaceutical production, are similar to anaerobic digesters in that it is the rising gas bubbles that induce mixing within the reactor. For this reason, bubble column mixing has been reviewed in this thesis, paying particular attention to non-Newtonian systems.

2.8.1 Bubble columns

Bubble columns are inexpensive gas-liquid contactors which have found a wide application in all branches of the chemical and processing industries. Mixing is supplied entirely by forcing compressed gas into the reactor, which then rises through the liquid height. This gas-liquid mixture has been termed the 'plume'

by Ulbrecht and Baykara (1981) and Ulbrecht et al. (1985).

Although bubble columns are of simple construction, they are difficult to design due to the complexity of the flowpatterns, especially when they contain viscous and non-Newtonian liquids (Ulbrecht et al., 1985). Much research has been carried out into these systems to investigate mass transfer and gas holdup with less work to investigate the blending processes involved.

There has been very little research on bubble columns of low aspect ratio and large diameter employing non-Newtonian shear-thinning liquids, as in a digester. Only the work of Haque et al. (1987) has studied such a geometry using a shear-thinning fluid, but the gas flowrates were much higher than those found for digesters.

Work has been performed using shear-thinning fluids to simulate fermentation processes. However, much of this work has concentrated on mass transfer, solids suspension and heat transfer. In addition, fermenters are often mixed with an impeller and gas rather than gas alone, which is not applicable to this work.

2.8.2 Flow regimes

There are three main flow regimes within which bubble columns operate:

- Chain bubbling (single orifice) or Bubbly homogeneous flow (multiple orifices)
- Churn-turbulent/heterogeneous flow
- Slug flow

The regime encountered depends on the superficial gas velocity within the column, that is the gas flowrate divided by the bubble column cross-sectional area. The exact values at which the regime changes depends on the liquid type and column diameter. The values in the following descriptions have been taken from Ulbrecht and Baykara (1981), Wadley (1994) and Shah et al. (1982) and

apply to air-water systems. Figure 2.13 is taken from Shah et al. (1982) and illustrates the effect of column diameter and superficial gas velocity on the flow regime encountered.

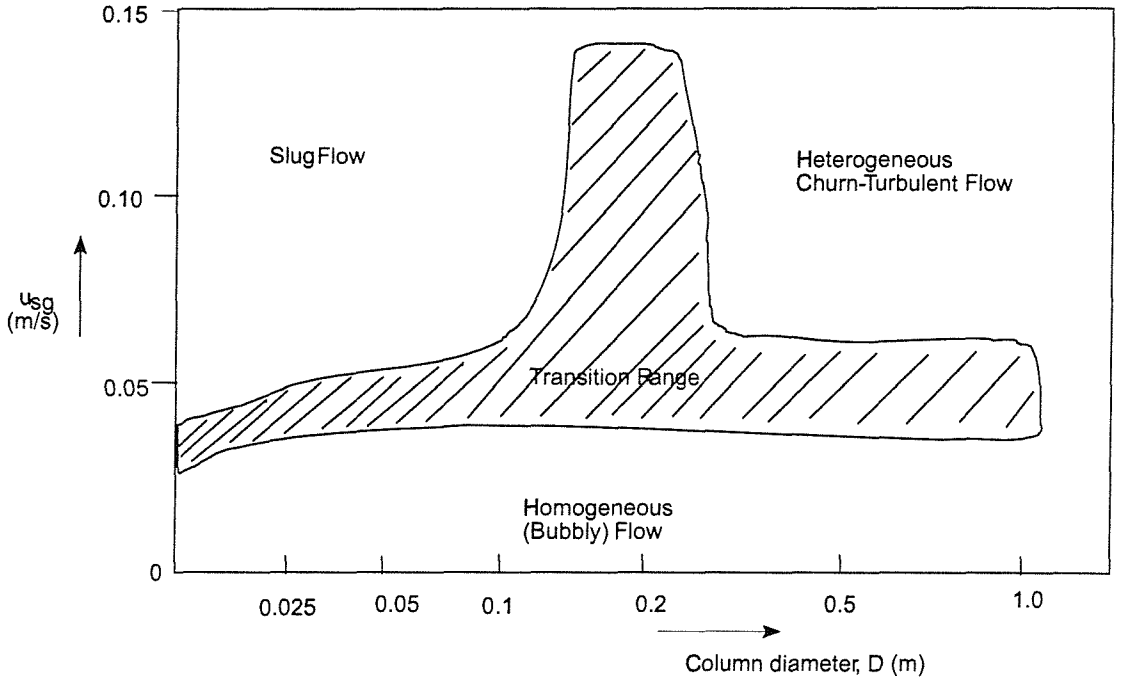

Figure 2.13: Transition between flow regimes as defined by Shah et al. (1982)

Bubbly homogeneous flow occurs at very low gas flowrates, where the superficial gas velocity is less than approximately 0.1 ms^{-1}. The gas enters via a single or multiple orifice sparger. The bubbles are small, typically less than 5mm in diameter. For a single nozzle, the bubbles tend to form a chain along the central axis of the column and rise with uniform velocities and no coalescence, as shown in Figure 2.14(a). This is termed 'chain bubbling'. For a multiple orifice sparger, columns of bubbles rise with uniform velocities and no coalescence as shown in Figure 2.14(b).

Churn-turbulent or heterogeneous flow occurs at high gas flowrates, typically with superficial gas velocities greater than 0.1 ms^{-1} and is much more disorderly than bubbly homogeneous flow. Small spherical bubbles are present together with larger, irregular slugs of gas.

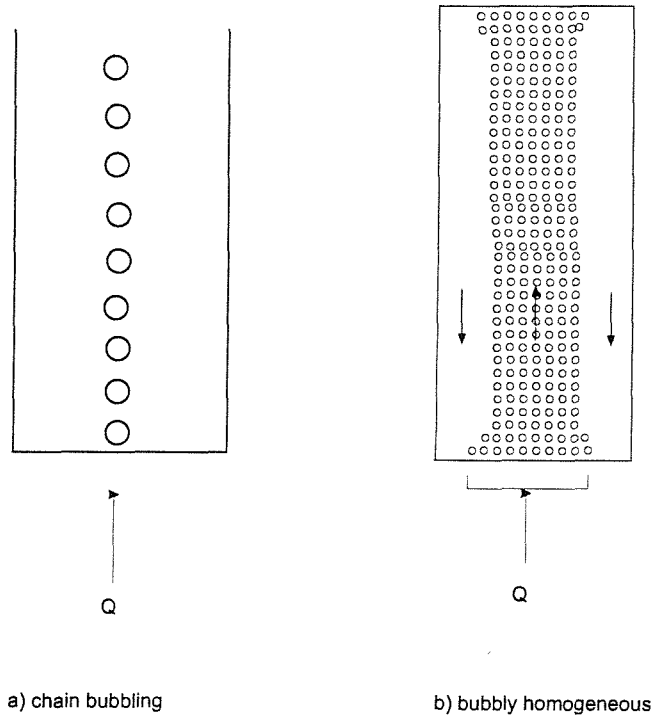

Figure 2.14: Bubble column flow regimes

Finally, slug flow can only occur in narrow columns where the large diameter bubbles are stabilised by the column walls. Superficial gas velocities of 0.5 ms^{-1} and above are required.

Increasing the viscosity of the liquid phase, reduces the terminal rise velocity of the bubbles, as discussed previously in Section 2.5 (Clift et al., 1978). Pandit and Joshi (1983) investigated the effect of liquid viscosity using aqueous solutions of glycerine of various concentrations and found that in viscous systems, the bubbly homogeneous flow regime may extend to higher values of superficial gas velocity in the order of 0.028 - 0.03 ms^{-1}.

The superficial gas velocities for the Welsh digesters investigated by Williams (1994) and the Yorkshire digesters, (Ouziaux, 1997) have been calculated. In the absence of detailed information for the Welsh digesters, an aspect ratio of one has been assumed and the cross-sectional area calculated. The superficial gas velocities for the Welsh digesters ranged from 0.0001 to 0.0003 ms^{-1} and

the Yorkshire digesters ranged from 0.0001 to 0.0005 ms^{-1}, putting the digesters within the bubbly homogeneous regime.

The definition of the different regimes may be misleading when applied to digesters because the ratio of the cross-sectional area of the mixing equipment to that of the digester is often much smaller than that of a bubble column. Calculating the superficial gas velocity does not account for the number of nozzles in use. If a multiple orifice sparger is used in a digester, where gas is supplied simultaneously, then each nozzle receives a smaller amount of gas than if a single nozzle was in use at the same gas flowrate. As discussed in Section 2.5, the size and shape of a bubble in a non-Newtonian shear-thinning liquid changes with increasing flowrate. Therefore, for the same gas flowrate, the region immediately surrounding a single nozzle may in fact be churn-turbulent in terms of bubble diameter variation and shape, even though the superficial gas velocity lies within the bubbly-homogeneous regime.

Slug flow will not occur in an unconfined gas mixed digester because the digester diameter is much larger than the bubble diameters. However, it may occur in confined gas mixing systems employing draft tubes.

2.8.3 Blend time

Blend times in digesters have been measured by many researchers, (Zoltek and Gram, 1975; Rundle and Whyley, 1981; Brade et al., 1982). It is a measure of the distribution of concentration within a vessel, thereby influencing the rate of transfer of fluid between poorly and well-mixed regions of the vessel (Ruszkowski, 1994; Grenville and Tilton, 1997).

Ulbrecht and Baykara (1981) measured blend time in bubble columns using a decolourisation technique. Sodium starch glycollate was added to the solution in the bubble column to form a dark blue complex. Thiosulphate was injected onto the surface of the bubble column and the decolourisation of the solution was monitored with a photocolorimeter. Solutions of water and three shear-thinning

liquids: carboxymethylcellulose (CMC), polyethyleneoxide (PEO) and polyacrylamide (PAA) were used. The latter two were also viscoelastic and therefore, unrepresentative of a digesting sludge. The rheological properties of the CMC were only slightly shear-thinning with a flow behaviour index of 0.95 and 1.0.

In addition to blend time, Ulbrecht and Baykara (1981) measured the liquid velocity in the plume. The authors were able to show that the liquid phase mixing rate was influenced by the liquid rheological properties, namely the viscosity and the viscoelasticity of the continuous phase. At low gas superficial velocities they were able to correlate the blend time with the velocity of the liquid in the central plume.

Using the same technique and equipment, Ulbrecht et al. (1985) increased the gas flowrate further and were able to extend their previous correlation to higher superficial gas velocities.

This model requires measurement of the liquid velocity in the rising plume. The column diameters used in the work of Ulbrecht et al. (1985) were 0.102, 0.127 and 0.152m over a range of aspect ratios from 6 to 10. The gas was injected using a multi-hole sparger with the result that a plume of bubbles filled the column. The velocity profile of the column was determined and a definite central riser and annular downcomer were found as shown in Figure 2.15.

In an anaerobic digester however, gas is usually injected via a single orifice Ouziaux (1997) resulting in regions of differing shear rates within the digester cross-section. The velocity profile shown in Figure 2.15 would differ for a digester with one nozzle in operation in that the regions defined as 's' and 't' would be narrower relative to the vessel radius, 'R'. The blend time correlation produced by Ulbrecht and Baykara (1981) and adapted by Ulbrecht et al. (1985) applies to a small diameter bubble column. To extrapolate it to wider columns relies on the measurement of the liquid velocities across the diameter of a model-scale digester, which is difficult, as admitted by the authors themselves.

Pandit and Joshi (1983) built on an earlier model by Joshi and Sharma (1976)

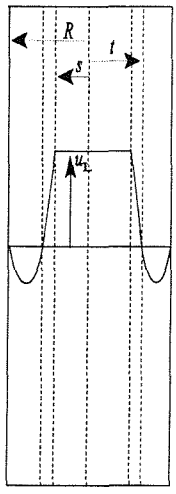

where R = radius of the column; t = locus of the liquid flow reversal; s = radius of the central plume and u_L = liquid phase velocity in the central plume

Figure 2.15: Velocity profile assumed by Ulbrecht and Baykara (1981)

who showed that an air/water bubble column was made up of a series of circulation cells in the axial direction. Blending occurred initially within each cell and extended to adjacent cells.

Pandit and Joshi (1983) measured blend times in bubble columns filled with water, CMC and Guar gum, sparged with air. They measured changes in pH and conductivity to determine the blend time. A pulse of acid or alkali of known volume was added via a hypodermic syringe near the bottom of the column. One pH electrode was located at the other extreme of the dispersion and their responses recorded. Similarly, a known concentration and volume of salt solution (NaCl) was added as for the acid or alkali and one conductivity probe recorded the response at the other end of the column. The location of these probes was varied in a transverse direction and found to have practically no effect on the blend time. This implies that the column was fully-mixed with no active or inactive volume present.

The gas flowrate range that Pandit and Joshi (1983) were operating in resulted in a high range of superficial gas velocity: 0.010 - 0.25 ms^{-1} in a column diameter of

0.15m with the result that the column was fully active. They found that increasing the superficial gas velocity (by increasing the gas flowrate) initially caused the blend time to decrease until reaching a minimum. Increasing the superficial gas velocity further caused the blend time to increase. The authors explained that blend time decreased with an increase in intercell velocity, whereas it decreased with an increase in gas dispersion height. The combined effect of these two factors resulted in a minimum value of blend time at a certain value of superficial gas velocity. Ulbrecht et al. (1985) also observed a minimum value of blend time at a certain value of superficial gas velocity. However, this was attributed to a change in flow regime between a viscous mode when most of the liquid moves upwards in the plume and down in the annulus with very little back mixing and a 'helical mode', where radial mixing developed.

Pandit and Joshi (1983) reported that increasing the aspect ratio from 2 to 8 under otherwise identical conditions caused the blend time to increase. They also found that blend time increased with an increase in column diameter (0.15 to 0.20m).

Pandit and Joshi (1983) proposed the following model for blend time:

$$\theta = \theta_{cell}\left[1 - 0.174\left(\frac{H}{T} - 1\right) + 0.179\left(\frac{H}{T} - 1\right)^2\right] \tag{2.11}$$

where θ = total blend time; H = liquid height; T = column diameter; θ_{cell} = blend time in an individual cell:

$$\theta_{cell} = \frac{5(1.5T)}{V_{cS}} \tag{2.12}$$

where V_{cS} is the average liquid circulation velocity due to gas sparging.

Eqn. 2.11 reduces to Eqn. 2.12 when the aspect ratio of the column is 1, as in the case of a typical digester, and θ_{cell} then becomes the total blend time. The average liquid circulation velocity due to gas sparging can be determined using:

$$V_{cS} = 2\left(\frac{u_{sg}}{\epsilon_g}\right)\left(\frac{T}{1.0}\right)^{1/3} \tag{2.13}$$

where u_{sg} = superficial gas velocity (gas flowrate divided by column cross-sectional area); ϵ_g = fractional gas holdup in the column

The effect of viscosity has been accounted for in the fractional gas holdup. Pandit and Joshi (1983) reported that the overall effect of increased viscosity and surface tension led to an increase in fractional gas holdup. Using Eqns 2.12 and 2.13, Pandit and Joshi (1983) plotted predicted against measured blend times for a range of Newtonian and non-Newtonian liquids with good agreement.

The use of this blend time equation depends on there being sufficient gas retained within the column to have some gas holdup. If the gas holdup is zero, then Eqn. 2.13 reduces to zero. Shah et al. (1982) reported that gas holdup is proportional to superficial gas velocity such that:

$$\epsilon_g \propto u_{sg}^n \tag{2.14}$$

where n is a positive value between 0.7 and 1.2 for the bubbly homogeneous regime (Shah et al., 1982).

Typically, at digester superficial gas velocities of 0.0001 to 0.0005 ms^{-1} quoted earlier, Eqn. 2.14 suggests that the gas holdup in a digester would be minimal. To support this, Pandit and Joshi (1983) reported that Eqn. 2.13 was invalid for low superficial gas velocities and hence, data on blend time could not be correlated (the minimum superficial gas velocity used by Pandit and Joshi (1983) was 0.028 ms^{-1}).

Haque et al. (1987) measured blend time using non-Newtonian shear-thinning carboxymethylcellulose (CMC) solution in a bubble column 1.0m in diameter. The aspect ratio was held at either 1 or 2. The flow behaviour indices and consistency coefficient values for the concentrations of CMC used are shown in Table 2.6. The

relative geometry and solutions used are comparable with those found by Ouziaux (1997) for anaerobic digesters.

Table 2.6: Rheological properties of the aqueous CMC solutions used by Haque et al. (1987)

CMC concentration (% wt)	**Flow behaviour index** n	**Consistency coefficient** k
0.1	0.80	0.012
0.5	0.70	0.061
1.0	0.67	0.102

The range of superficial gas velocities used was 0.008 to 0.057 ms^{-1}, which are much higher than those calculated for a digester (0.0001 to 0.0005 ms^{-1}).

Haque et al. (1987) measured the blend time using a single pH cell and a single conductivity probe, located in the base of the column. Acid or alkali were injected at the liquid surface when using the pH method. A solution of Sodium Chloride in water was injected at the liquid surface when using the conductivity technique. The location of the pH cell and conductivity probe was varied transversely and found to have no effect on the blend time. The use of a single probe is not advocated by other blend time researchers when larger vessels are used: (Ruszkowski, 1994) recommended 3 probes in different regions of the vessel to measure probe responses in well-mixed and less well-mixed regions of the vessel.

Haque et al. (1987) found an exponential decrease in blend time with increasing superficial gas velocity which is shown in Figure 2.16. Pandit and Joshi (1983) found the same result, with almost identical blend times as shown in Figure 2.17. Both researchers also found an effect of viscosity on blend time where an increase in viscosity resulted in an increase in blend time, as shown in Figures 2.16 and 2.17.

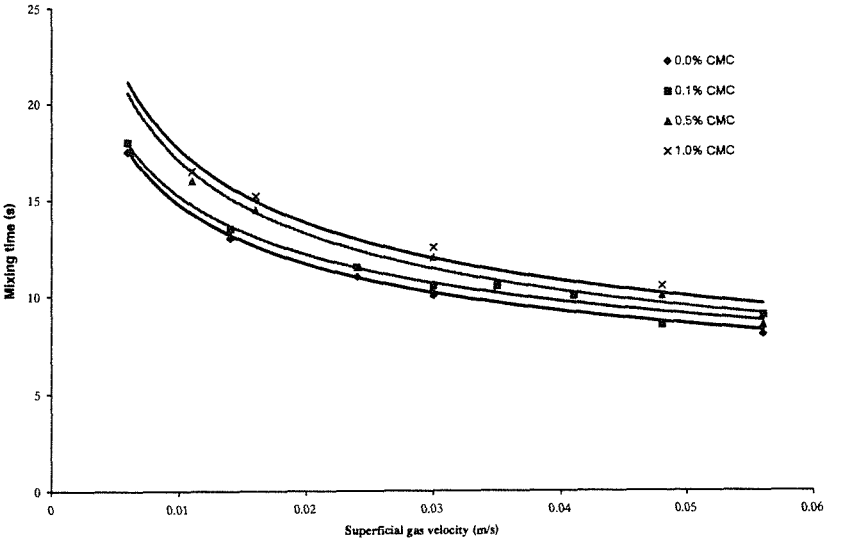

Figure 2.16: Blend time against u_{sg} for $H/T = 1$. (Haque et al., 1987)

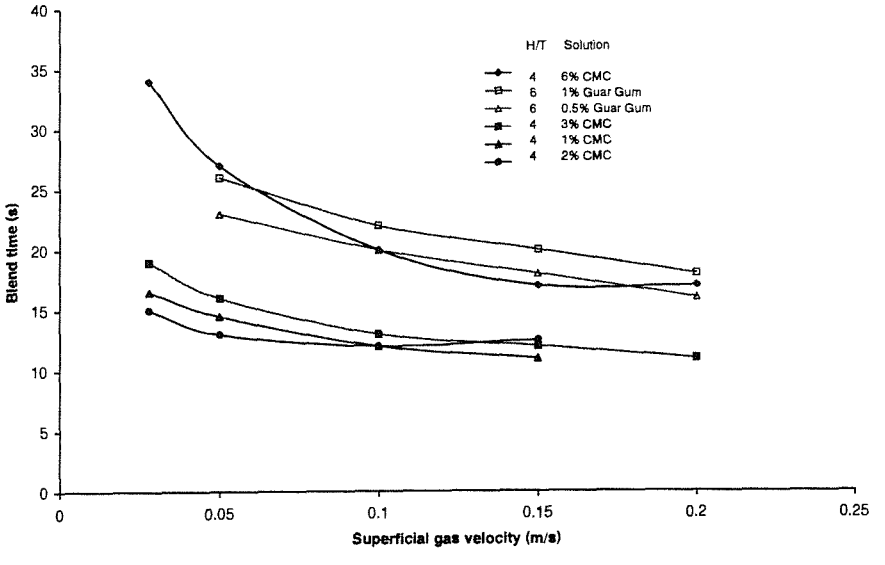

Figure 2.17: Blend time against u_{sg} for $H/T = 1$. (Pandit and Joshi, 1983)

2.8.4 Reynolds number determination

The determination of the Reynolds number within a digester is important for scaling between different sizes of vessel. Various Reynolds numbers can be determined based on different geometries:

- Based on the vessel
- Based on the rising liquid and gas plume
- Based on a single bubble

The vessel Reynolds number for a Newtonian fluid is calculated using:

$$Re = \frac{\rho u_L T}{\mu} \tag{2.15}$$

For a non-Newtonian fluid, the viscosity varies with shear-rate:

$$Re_{n-N} = \frac{\rho u_L^{2-n} T^n}{k} \tag{2.16}$$

where Re_{n-N} = non-Newtonian Reynolds number; n = Power Law fluid consistency index and k = Power Law consistency coefficient

Two equations for Reynolds number based on the rising liquid plume in non-Newtonian fluids have been put forward in the literature, one an empirical one (Ulbrecht et al., 1985) and the other a theoretical one (Kawase and Moo-Young, 1986b).

Ulbrecht et al. (1985) measured the velocity within the rising bubble plume. Freely suspended polystyrene tracer particles were used. Up to fifty passages of the tracer particle between two marks (one close to the bottom and one close to the top of the column) were visually observed and the time of passage calculated. They used a viscous Newtonian fluid (corn-syrup in water), a non-Newtonian

shear-thinning fluid (Polyvinyl pyrrolidon - PVP) and a non-Newtonian shear-thinning and elastic fluid (polyacryl amide - PAA). They correlated their data and the data of others for air/water and air/viscous fluid systems as:

$$Re_L^* = 3.34(Re_{sg}^* Fr_{sg}^{-0.25})^{0.92} \tag{2.17}$$

where Re^*_L = modified Reynolds number for the liquid phase using the velocity of the liquid in the central plume ($= \frac{\rho u_L^{2-n} T^n}{k}$); Re^*_{sg} = modified Reynolds number using the superficial gas velocity ($= \frac{\rho u_{sg}^{2-n} T^n}{k}$); Fr_{sg} = Froude number ($= \frac{u_{sg}^2}{gT}$)

This method of determining the Reynolds number does take into account non-Newtonian behaviour although its applicability to vessels of a larger diameter than most bubble columns (such as in a lab-scale digester) is unknown. Eqn. 2.17 was produced in the bubbly homogeneous flow regime where the whole cross-sectional area was filled with bubbles. This may not be the case in an anaerobic digester where Ouziaux (1997) found that the gas typically enters via a single nozzle, agitating one area of the digester at a time, leaving other areas undisturbed. However, there is no reason why it should not apply within the rising plume.

Kawase and Moo-Young (1986b) theoretically derived a similar expression to Ulbrecht et al. (1985) based on an energy balance between the energy input, energy dissipation rate in the liquid motion and that at the gas-liquid interface:

$$Re_L^* = (0.787 n^{-2/3})^{2-n} Re_{sg}^* Fr_{sg}^{-\left(\frac{(2-n)}{3}\right)} \tag{2.18}$$

where the liquid velocity at the column axis used in the calculation of Re^*_L was defined as:

$$u_L = 0.787 n^{-2/3} g^{1/3} T^{1/3} u_{sg}^{1/3} \tag{2.19}$$

where n = flow index in a Power Law model and g = acceleration due to gravity. Fr^*_{sg} and Re^*_{sg} were calculated as for Eqn. 2.17.

Kawase and Moo-Young (1986b) compared the non-Newtonian data produced by Ulbrecht et al. (1985) with Eqn. 2.19 and found good agreement. Kawase and Moo-Young (1986b) explained the difference between the two equations for Re^*_L by suggesting that the non-Newtonian flow behaviour has been inaccurately taken into account by the empirical equation, Eqn. 2.17.

Both of these forms of Reynolds number use the Power Law rheological parameters k and n thus avoiding the determination of an average shear-rate (see Section 3.2.2). However, equations to determine the average shear-rate within a bubble column have been proposed which could be used to determine a value of apparent viscosity within a digester and hence Reynolds number, using Eqn. 2.15.

Nishikawa et al. (1977) proposed the following empirical relation for average shear-rate:

$$\dot{\gamma} = 5000 u_{sg} \tag{2.20}$$

This relation was obtained from heat transfer data and is applicable to a relatively narrow gas flowrate range corresponding to a superficial gas velocity range of 0.04 to 0.1 ms^{-1}. These values are much greater than those of a digester (0.0001 - 0.0005 ms^{-1}). Kawase and Moo-Young (1986a) questioned the general applicability of this relation, acknowledging that despite its limitations, is widely used. Kawase and Moo-Young (1986a) proposed a further relation stating that the average shear-rate in a bubble column should be proportional to the ratio of the characteristic velocity to characteristic length:

$$\dot{\gamma}_{av} = \frac{u_{sg}}{R} \tag{2.21}$$

where R = radius of the column

They acknowledged that a constant of proportionality would be required depending on the hydrodynamics of the system but for convenience, assumed this value to be 1.

Haque et al. (1988) proposed a similar relationship for average shear-rate, approximating it to:

$$\dot{\gamma} = \frac{u_{br}}{d_B} \tag{2.22}$$

where u_{br} = bubble terminal rise velocity and d_B = diameter of a single bubble

This equation relates to the shear-rate around the bubble whereas Eqn. 2.21 refers to the average shear-rate across the column radius. The literature does not state which is the better equation to use. Neither Eqns 2.20 nor 2.21 take the liquid viscosity into account, whereas Eqn. 2.22 does in that the bubble rise velocity and bubble diameter will change with viscosity. However, Eqn. 2.22 requires an accurate determination of the bubble rise velocity and bubble diameter. In the creeping flow regime, the equations of Stokes (Eqn. 2.7) or Hadamard (Eqn. 2.8) have been proposed in Section 2.5.2. However, the values obtained using these equations are much higher than those observed experimentally with flow followers. In addition, these equations were developed for Newtonian liquids.

The work of Deckwer and Schumpe (1993) and Haque et al. (1988) on the relationship between bubble rise velocity and gas holdup can provide estimations for the bubble rise velocity that more closely match those measured. There is no single equation that has been produced for non-Newtonian liquids to determine the bubble rise velocity due to the complexities of the rheological characteristics (Chhabra, 1993). By relating the theoretical equations of Deckwer and Schumpe (1993) and Haque et al. (1988), the following equation has been derived:

$$u_{br} = [101.15(u_{sg})^{0.13}(gT)^{0.5}]^{-1} \tag{2.23}$$

where u_{br} = bubble terminal rise velocity

The shear rate using Eqn. 2.22 can then be calculated. The form of Eqns 2.21 and 2.20 are similar but the shear rates calculated with Eqns 2.21 and 2.22

are five orders of magnitude less than those calculated using Eqn. 2.20 for the Yorkshire digesters surveyed by Ouziaux (1997) and the Welsh digesters surveyed by Williams (1994) as shown in Table 2.7.

Table 2.7: Comparison of shear-rate values for the digesters surveyed by Ouziaux (1997) and Williams (1994)

Equation 2.21 (s^{-1})	**Equation 2.20** (s^{-1})	**Equation 2.22** (s^{-1})
1.7 x 10^{-5} - 4.7 x 10^{-4}	0.5 - 10	5 - 13

The shear-rate has been estimated using Eqn. 2.22 in this work as it takes the liquid viscosity into account and produces more believable results than those calculated using Eqns 2.21 or 2.20.

There is one further Reynolds number to consider and that is the bubble Reynolds number.

$$Re_{bubble} = \frac{\rho u_{br} d_B}{k\dot{\gamma}^{n-1}} \tag{2.24}$$

where $\dot{\gamma}$ = average shear-rate around the bubble, calculated using Eqn. 2.22.

The bubble Reynolds number can be determined using the bubble diameter calculated from Eqn. 2.4 (Davidson and Schuler, 1960a; Davidson and Schuler, 1960b) and the bubble rise velocity calculated using Eqn. 2.23. The bubble Reynolds number calculated in this way uses the bubble diameter calculated as it detaches from the orifice. As the bubble rises through the height of the liquid, it expands, therefore, the bubble diameter will increase. Interpreting Eqn. 2.24 with this in mind, implies that the bubble Reynolds number calculated will be an underestimate as a larger bubble diameter will result in a larger Reynolds number. In addition, the rise velocity of a bubble increases with height and will reach its terminal rise velocity at some point, although when is not defined in the literature. However, providing the Reynolds numbers between different scales remain within the same regime, it is not critical that the values remain equal.

Ideally, the bubble rise velocity should be measured in the absence of a definitive calculation method, although this is not always possible.

2.9 Conclusions

The literature relating directly to mixing in anaerobic digesters lacks any fundamental understanding of the liquid properties or the mixing mechanisms involved. Unconfined gas mixing has been stated previously as the most common form of mixing found in UK anaerobic digesters and yet a definitive mixing theory for these systems has not been found in the literature.

Impellers have been used in some digesters but there is no definitive mixing design theory for them in this application. It is not clear whether baffles are consistently employed or not and what this decision may be based on. The power inputs to the different digesters vary from site to site and appear to be derived from 'rules of thumb' and experience.

Direct comparison of the power inputs to digesters between the work of different researchers is difficult because of a lack of system definition and a consistent method of qualifying the mixing results reported. The power inputs currently used in unconfined gas mixed digesters appear to be too low to avoid grit buildup in the digester base.

Comparisons have been made in the literature between different mixing types, sometimes in lab-scale models and sometimes at the full-scale. For the majority of cases, the difference between water and sludge rheology has not been understood and water has been used to simulate the sludge.

The mixing objectives have not been understood either with the emphasis of these comparisons being on the efficiency of the different systems and therefore, their running costs, believing the digesters to be 'properly' mixed.

The published work on bubble columns cannot be directly translated to anaerobic digesters as bubble column diameters are much smaller than those required

in a lab-scale digester with the exception of Haque et al. (1987). The aspect ratio of most UK anaerobic digesters is approximately 1 whereas bubble columns are typically 4 or greater. Work has been performed using non-Newtonian sludge-like fluid although the superficial gas velocities used are high compared to those known to occur in a digester. No mention is made of an inactive volume in these bubble columns compared to digesters where there are many examples of volume reductions due to grit accumulation and scum formation.

In this thesis, investigations on unconfined gas mixing at the laboratory scale using different sparger arrangements, gas flowrates and liquid viscosities have simulated digesters found in practice to provide mixer design guidelines. To the author's knowledge, no other physical study to investigate the blend times and flowpatterns within a laboratory scale digester has been performed under conditions representative of full-scale digesters.

Chapter 3

Materials and Methods

A survey of a selection of digesters within Yorkshire Water's catchment area was undertaken by Ouziaux (1997) to provide information on digester shapes, geometries, mixing systems and sludge rheology. Once collected, these data were used to design two scales of digester in the laboratory.

This chapter will discuss and present the survey results, including the sludge rheology data that was collected. The collected geometric and mixer geometries and operational conditions had to first be scaled-down from the full-scale to a laboratory-scale and then scaled-up to a pilot-scale vessel. The considerations given to this scaling are presented. The procedure used to select a simulant fluid to model the digester sludge is also presented. There follows a description of the experimental techniques used in this work, detailing the gas blending experiments, blend time measurement, active volume measurement and the experimental programme for both gas and impeller mixing.

3.1 Survey results

Seventeen digestion sites were surveyed within the Yorkshire region with a total of 24 digesters. The volumes of the selected digesters varied between 530 m^3 and 5140 m^3. There were 39 years between the commissioning dates of the most recent

digester in 1996 and the oldest in 1957.

3.1.1 Digester geometry

All of the digesters were vertical cylinders in shape apart from that at Bedale, which was a horizontal cylinder shaped digester. The aspect ratios (digester height to diameter) ranged from 0.36 (for Bedale) to 1.2. The digesters built before 1980 all had a low aspect ratio (less than 0.6) compared to those built after 1980 which had an aspect ratio of between 0.8 and 1.2 (65% of those surveyed).

The base shapes varied. Six digesters had a shallow base at an angle of inclination of approximately 7°, two were steep with an angle of 20° and nine did not have this information.

The inlet positions also varied. Nine feed locations were into the top of the digester by the wall and two were into the base of the digester, by the wall. One was into the digester at mid-depth and in the centre. All of the digester outlets were overflow weirs positioned at the top of the digester. This system keeps the digester full, however in some cases, the inlet and outlet were positioned very close to each other, which could suggest short circuiting of the feed sludge.

The digesters were usually fed for a period of several minutes in a 20 to 30 minute cycle. Most digesters used an external heat exchanger to heat and maintain the sludge at the required mesophilic digestion temperature of 35°C. A volume of sludge was removed from the digester and passed through the heat exchanger before re-entering. To avoid any temperature gradient between the colder feed sludge and the warmer digesting sludge, the feed sludge was sometimes fed into the recirculation loop.

3.1.2 Mixing systems

Unconfined gas mixing was by far the most common form of digester mixing system employed in the Yorkshire digesters. A total of 82% of those surveyed used

this system, typically designed by Farmgas but not exclusively so. Half of these digesters employed sludge recirculation through an external heat exchanger and the remaining half did not. Two digesters employed confined gas and one digester employed impellers although these were located within the sludge recirculation loop rather than in the digester bulk.

The method of gas addition for the unconfined gas cases varied. Eleven were fitted with nozzles in the base. A common design was two concentric rings with 8 nozzles in the outer ring and 4 in the inner ring. Usually, (Farmgas designs) the gas was supplied in a sequence around the nozzles by means of a rotary valve, beginning with one nozzle and working around the sequence until it was complete. However, no indication of the actual sequence used was found. In this arrangement, gas was usually supplied to each nozzle for a period of 60 seconds. Alternatively, gas was supplied to all or a group of nozzles simultaneously. The gas was rarely supplied on a continuous basis and the usual procedure was to supply the gas intermittently for set periods throughout the day, for example, Farmgas designs supplied gas for a 12 minute period every 30 minutes.

3.1.3 Power inputs

The power input for the unconfined gas mixing mixing systems was recorded in two ways. Firstly the power supplied by the compressor was recorded directly and secondly, the power input was calculated in terms of the isothermal expansion of the rising gas bubbles (Eqn. 2.2) based on gas flowrates from the compressor.

The compressor power inputs ranged from 2.5 to 12.9 Wm^{-3} and yet the power input due to isothermal expansion ranged from 1.52 to 3.5 Wm^{-3}, much lower than the compressor values. Compressors are very inefficient devices with a typical quoted efficiency of 30% (Brade, 1997). Using this value, the power inputs on the outlet side of the compressor would be 0.75 to 3.87 Wm^{-3} which are in closer agreement with the power inputs from isothermal expansion.

The individual site values are given in Table 3.1 together with information on

Table 3.1: Survey information collected for each digestion site (sludge data were not collected for all of the sites in the survey)

Site name	Mixing system	Compressor P/V (Wm^{-3})	Isothermal P/V (Wm^{-3})	Average % Dry solids	Sludge Volume (m^3)
Calder Vale	Unconfined gas	10.5	3.5	3.7	4900
Harrogate South	Unconfined gas	6.7	2.18	3.4	530
Malton	Unconfined gas	4.2	1.43	-	728
Old Whittington	Unconfined gas	-	-	-	4586
Rawcliffe	Unconfined gas	5.7	1.84	-	1130
Sandall	Unconfined gas	12.9	-	2.5	3500
Sutton	Unconfined gas	4.2	1.65	-	1540
Walbutts	Unconfined gas	5.6	1.54	-	565
Wombwell	Unconfined gas	2.8	0.92	3.1	2276
Aldwarke	Unconfined gas	-	-	3.3	5670
Bedale	Unconfined gas	-	-	4.9	105
Harrogate North	Unconfined gas	3.1	0.93	2.4	1005
Marley	Unconfined gas	7.8	2.11	4.6	2920
Northallerton	Unconfined gas	8	-	3.3	500
Mitchell Laithes	Confined gas	2.5	0.52	4.0	10280
Naburn	Confined gas	8.8	1.03	-	3400
Lundwood	Impellers	-	-	2.4	4038

the digester volume and mixing systems installed at each of the sites surveyed. In some cases, more than one digester was located at each site, and in those cases, the information in Table 3.1 refers to individual digesters. The sludge dry solids content was not always the same for these digesters and the average dry solids content has been taken.

3.2 Sludge rheology

Digested sludge samples were removed from eleven of the sites surveyed (Ouziaux, 1997) to measure the sludge rheology. The percentage dry solids (%DS) is a standard measurement taken daily at most digestion sites. The %DS range found was from 2.4 to 4.9% DS with most digesters operating at between 2 and 3.5% DS.

The sludge rheologies were measured using a concentric cylinder rheometer in the infinite sea condition as shown in Figure 2.2(d).

It is important to match the shear-rate range for the rheology test to the range found in the full-scale system to ensure that meaningful rheological data are obtained (ESDU, 1982; Nienow, 1997).

The shear-rate range for the surveyed digesters was calculated using Eqn. 2.22. The shear-rates calculated for the full-scale digesters ranged from 5 to 13 s^{-1}. The values used for the rheology tests was extended to as high as possible with the equipment used, covering the range 0.066 to 22 s^{-1}.

Two viscometers were used, both made by Brookfield. YWS used a Brookfield LVDV-II+ viscometer with spindles LV1 and LV4 and this author used a Brookfield DVIII viscometer using spindles LV1, LV2, LV3 and LV4. The data was collected and stored using Brookfield's 'Rheocalc for Windows' software. The spindle used was chosen to cover the widest possible torque range (between 10 and 90% of the maximum) and hence shear-rate to obtain the most accurate results. A low-form Griffin 600 ml beaker with the LV guard leg in place was used for all tests, as specified by Brookfield (Brookfield, 1996).

3.2.1 Thickened sludges

Sludge thickening is sometimes carried out before digestion to increase the dry solids content (%DS) of the feed sludge to 8%, or to as high a figure as possible (CIWEM, 1996). This is not normally achievable by gravity settlement alone

and often thickening agents are employed. The reduction in water content by thickening allows a reduction in size and heat requirement of the digester. It also allows a higher throughput of sludge solids, which is desirable in the absence of sludge disposal to sea to treat the increased volume of sludge that is now produced. The highest feed sludge found by Ouziaux (1997) was at Bedale and contained approximately 6 to 7%DS resulting in a digested sludge of 4.9%DS.

The effect of digesting 'thicker' sludges with dry solids contents of 8% upwards on the mixing systems has not been quantified in the literature and was to be investigated in this work. However, no digested sludges were found with these %DS contents. To provide rheological data for these sludges, samples of digested sludges were taken from a selection of the Yorkshire sites and thickened by slow evaporation in an oven at 35°C, the same temperature as found inside a mesophilic anaerobic digester. This process was chosen rather than filtration as it would not change the structural properties of the sludges (although the biological activity may have changed due to oxidation).

Before the collected site samples were thickened, it was necessary to ensure that their rheological properties had not changed during transit. This was done by repeating the site measurements in the laboratory using samples collected from the sites and kept in a refrigerator at 4°C. The sludge samples were brought up to the temperatures measured on site using a hot water bath and thermometer prior to measuring their rheological properties. Figure 3.1 shows that only a very slight change in apparent viscosity occurred for the two sites concerned and so the thickening tests were performed.

To perform the thickening process, aluminium foil trays were used. The samples taken from Marley digester 3 and Bedale were thickened in an oven at 35°C. These sludges were chosen because of the quality of the results taken on site. The sludges were regularly checked to ensure that no crust formed on the surface which may have affected the rheological properties.

The un-thickened digested sludges ranged from 2.5% to 4.9% DS and were

thickened up to 10% DS (by weight). Figure 3.2 illustrates the increase in apparent viscosity caused by increasing the dry solids content of the Bedale sludge. Lines of best fit have been drawn through the individual data sets to illustrate the trends more clearly.

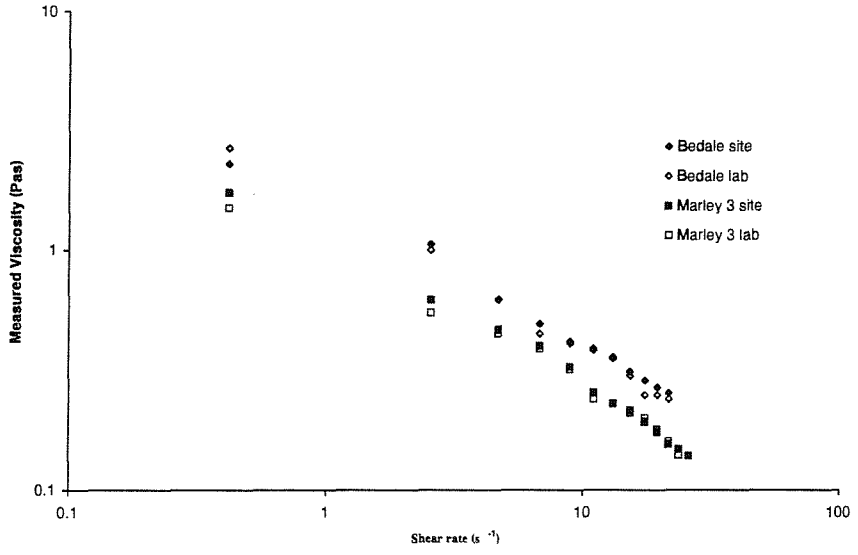

Figure 3.1: Viscosity values between site and lab samples

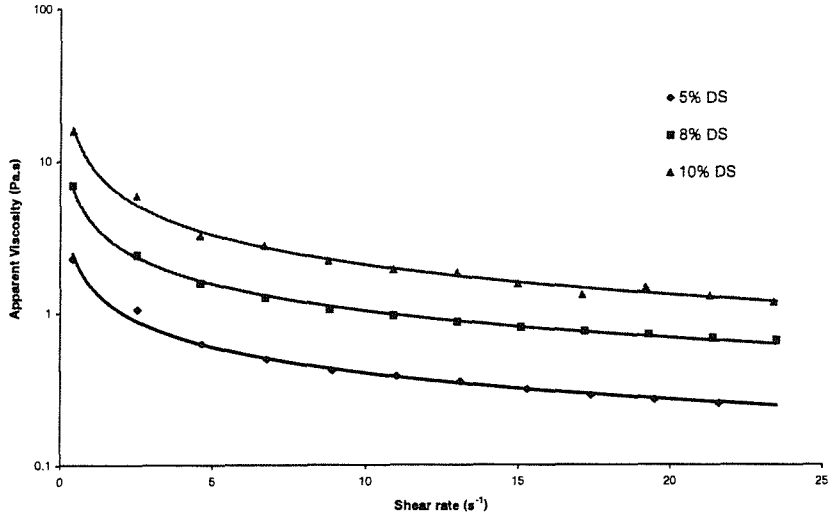

Figure 3.2: Effect of increasing %DS content on apparent viscosity

3.2.2 Sludge simulant selection

A sludge simulant solution was required to perform the mixing experiments as using real sludge would pose several problems. The biogas production and potential microbiological hazard had implications for health and safety. The nature of the sludge would lead to experimental difficulties in performing tracer studies to measure blend times and to determine the location of any inactive volume as sludge is not transparent. Further difficulties would be encountered in trying to maintain a uniform solids concentration between different batches of sludge. Therefore, the rheological properties of the simulant solutions chosen had to match those found for the digested sludges.

Figure 1.1 showed that sludge is produced at different stages in the wastewater treatment process. Some of these sludge types exhibit a yield stress whereas others do not (Frost, 1983). To determine whether the digested sludges exhibited a yield stress, plots of shear stress verses shear-rate were produced for each sludge tested and are shown in Appendix A. Extrapolating these curves back to intersect the y-axis gave a value of shear stress when the shear-rate was zero, which was the yield stress (Chhabra, 1993; Walters, 1975; Barnes et al., 1989). The values of yield stress so obtained are extremely sensitive to the range of data being extrapolated, particularly the lowest value of shear-rate (Chhabra, 1993). For example, if the lowest shear-rate used was $2s^{-1}$, then extrapolating the data back to intersect the shear stress axis, would give a higher yield stress than if the lowest shear-rate of $0.066s^{-1}$ was used. The values of yield stress determined in this way for the digested sludges are shown in Table 3.2.

The shear stress/shear-rate relationship for shear-thinning fluids can often be described by the Power Law model:

$$\tau = k\dot{\gamma}^n \tag{3.1}$$

where τ = shear stress; $\dot{\gamma}$ = shear-rate; k = consistency coefficient; n = flow

Table 3.2: Yorkshire Water sludge rheological data

Site	**Yield stress** (Nm^{-2})	**%DS**	**Power Law *k*** (-)	**Power Law *n*** (Pa.s ^{n})	**Herschel-Bulkley *k*** (-)	**Herschel-Bulkley *n*** (Pa.s ^{n})
Mitchell Laithes 1	0.3	4	0.569	0.229	0.260	0.390
Mitchell Laithes 2	0.2	4	0.451	0.263	0.166	0.647
Wombwell	0.10	3.1	0.250	0.275	0.105	0.609
Lundwood 1	0.48	2.4	0.872	0.180	0.187	0.967
Lundwood 2	0.42	2.4	0.762	0.164	0.180	0.770
Harrogate South	0.29	3.4	0.507	0.213	0.204	0.413
Calder Vale 1	0.12	3.7	0.374	0.493	0.143	0.930
Calder Vale 2	0.15	3.8	0.408	0.473	0.192	0.830
Sandall 1	0.37	2.5	0.639	0.194	0.444	1.290
Sandall 2	0.17	2.5	0.715	0.586	0.450	1.220
Marley 2	0.5	4.5	1.036	0.503	1.290	0.360
Marley 3	0.5	4.7	1.123	0.384	0.658	0.477
Marley 4	0.3	3.7	0.612	0.388	0.085	0.98
Harrogate North	0.3	2.4	0.420	0.329	0.0927	0.710
Bedale	0.6	5.5	1.511	0.406	0.797	0.620
Bedale (thickened)	5	10	9.413	0.347	3.72	0.610

behaviour index

Yield pseudoplastic fluids require a finite stress to be reached before flow can occur (yield stress) and the shear stress/shear-rate relationship for these fluids can be described by the Herschel-Bulkley model:

$$\tau = \tau_y + k_{hb}\dot{\gamma}^{n_{hb}} \tag{3.2}$$

where τ_y = yield stress; k_{hb} = Herschel-Bulkley k value; n_{hb} = Herschel-Bulkley n value

Values of k and n were determined for both models using linear regression. For the Power Law, linear regressions were performed on $ln(\tau)$ and $ln(\dot{\gamma})$. For the

Herschel-Bulkley model, $ln(\tau_y - \tau)$ and $ln(\dot{\gamma})$ were used. The values for k and n are given in Table 3.2.

The apparent viscosity of a non-Newtonian fluid can be determined experimentally or calculated knowing the k and n values.

Experimentally, the apparent viscosity can be calculated for a given shear-rate using (Walters, 1975; Barnes et al., 1989):

$$\mu_a = \frac{\tau}{\dot{\gamma}} \tag{3.3}$$

μ_a = apparent viscosity

For Power Law fluids, the shear stress component of Eqn. 3.3 is rewritten as:

$$\mu_a = k\dot{\gamma}^{n-1} \tag{3.4}$$

For Herschel-Bulkley fluids:

$$\mu_a = \frac{\tau_y + k_{(hb)}\dot{\gamma}^{n_{(hb)}}}{\dot{\gamma}} \tag{3.5}$$

To determine the model that was most applicable to the sludges tested, these three apparent viscosities were calculated and plotted as shown in Appendix B.

The measured data for 12 out of the 14 sites were visually closer to the Power Law model than the Herschel-Bulkley model. Only the experimental data points for Marley 2 and 3 were in closer agreement to the Herschel-Bulkley model than the Power Law model. In addition, comparing the correlation coefficients for all of the sites showed a better fit of the experimental data to the Power Law compared to Herschel-Bulkley as shown in Table 3.3. The two thickest sludges (ie. highest %DS contents) had correlation coefficients slightly closer to the Power Law model than the Herschel-Bulkley model despite suggesting higher yield stress values from their rheograms. Lotito et al. (1997) also measured the rheological properties of

Table 3.3: Goodness of fit values for the Yorkshire digested sludges

Site	Power Law r^2	Herschel-Bulkley r^2
Mitchell Laithes 1	0.999	0.993
Mitchell Laithes 2	0.999	0.992
Wombwell	0.997	0.986
Lundwood 1	0.998	0.989
Lundwood 2	0.999	0.993
Harrogate South	0.999	0.997
Calder Vale 1	0.934	0.889
Calder Vale 2	0.893	0.847
Harrogate North	0.998	0.991
Marley 2	0.852	0.852
Marley 3	0.995	0.986
Marley 4	0.993	0.983
Bedale 4.9%DS	0.997	0.976
Bedale 5.5%DS	0.987	0.973
Bedale 10%DS	0.995	0.987

8 digested sludges and found correlation coefficients of 0.996 and upwards using the Power Law (only one had a lower value of 0.975).

Based on these results, a Power Law fluid was chosen as the simulant.

It is important to realise that a sewage sludge will vary from one site to another depending on the effluents that enter the sewage works (i.e. industrial and/or domestic) and even on the time of day. So as to not be site specific, the simulant(s) had to cover the range of sludge rheological properties found at the full-scale.

Figure 3.3 is a plot of the experimentally determined apparent viscosity against shear-rate for all of the sludges tested. The three lines mark the three sludges chosen for simulation in the laboratory experiments. This would allow a low %DS sludge, commonly found in the survey (Ouziaux, 1997), a higher %DS sludge that was in use at Bedale and possibly at other sites around the country (Brade, 1997) and finally, a very high %DS sludge to be used in the future.

The following section discusses the selection procedure for three simulants for

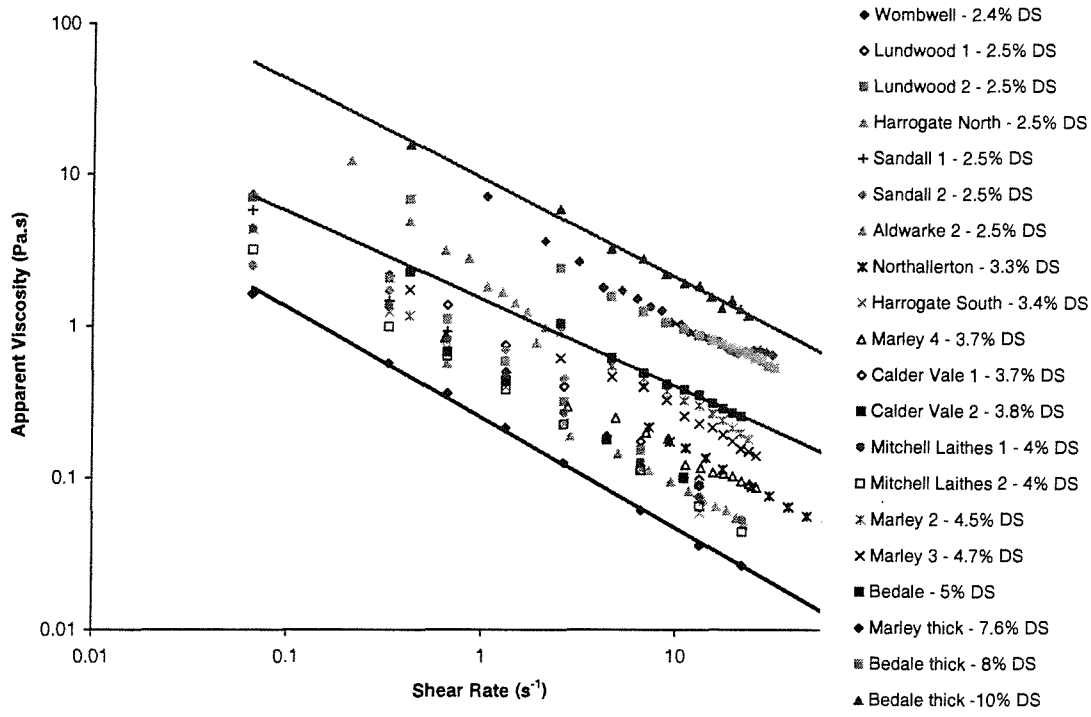

Figure 3.3: Apparent viscosity vs. shear-rate for site sludge and thickened samples

these three %DS sludges.

3.2.3 Selection procedure

The flowpatterns set up within the laboratory digesters were to be observed, hence the simulant needed to be transparent once made-up. The simulant rheology had to withstand the addition of salt as this was to be the tracer for the blend time measurements. As the experimental work was to be conducted over a period of several months, the simulant needed to be durable so as to avoid the high costs of purchase and disposal. It also needed to be easy to handle, store and make-up with no health and safety implications.

A short-list of suitable solutions was drawn up and samples of these polymers obtained from the manufacturers. Initial test solutions were made-up in a one litre impeller mixed container to produce samples of different concentrations. Samples

of 600ml were taken and measured using the Brookfield DVIII rheometer in the laboratory. The results were recorded in terms of shear stress and shear-rate. The viscosity range for each sample was calculated using Eqn. 3.3 and values for k and n were calculated using the Power Law (Eqn. 3.1). These values were then compared between the selected sludges and simulant concentrations.

The shear-rate range over which the rheometer operated was the same as for the sludge samples.

Power Law polymer fluids were tried initially. Natrasol (hydroxymethylcellulose), Carbopol and different grades of Sodium hydroxymethylcellulose (CMC) were tried. Both Natrasol and Carbopol were difficult to make up. Natrasol was opaque once made-up and Carbopol was white. The k and n values did not match well with the sludges either. Xanthan and Guar gum are yield pseudoplatic fluids and were also tried to compare between the Power Law fluids but did not match the range of sludges well. In addition, their rheologies were very sensitive to salt addition, becoming less viscous as salt was added.

Sodium carboxymethylcellulose (CMC) is a granular powder in its packaged form and is made up by adding the required quantity (by weight) to a stirred vessel of water (tap water in this work). Once the particles had dissolved, the solution needed time to fully hydrolyse (approximately 12 hours) before its final rheology was attained.

The highest grade of CMC, grade 7H4C, was the most shear thinning polymer solution available in the CMC range (available from Crestchem Ltd in Amersham, Buckinghamshire) and produced a good match for the k and n values for the selected sludges. In addition, it was easy to make-up and transparent. Its rheology was slightly affected by the addition of salt and this is detailed in the next section.

Figure 3.4 shows rheograms of the three selected sludge concentrations together with rheograms of their corresponding CMC concentrations. Solutions of 0.3%, 0.6% and 1% CMC were found to have similar apparent viscosity values to 2.4% DS, 5% DS and 10% DS digested sludge respectively.

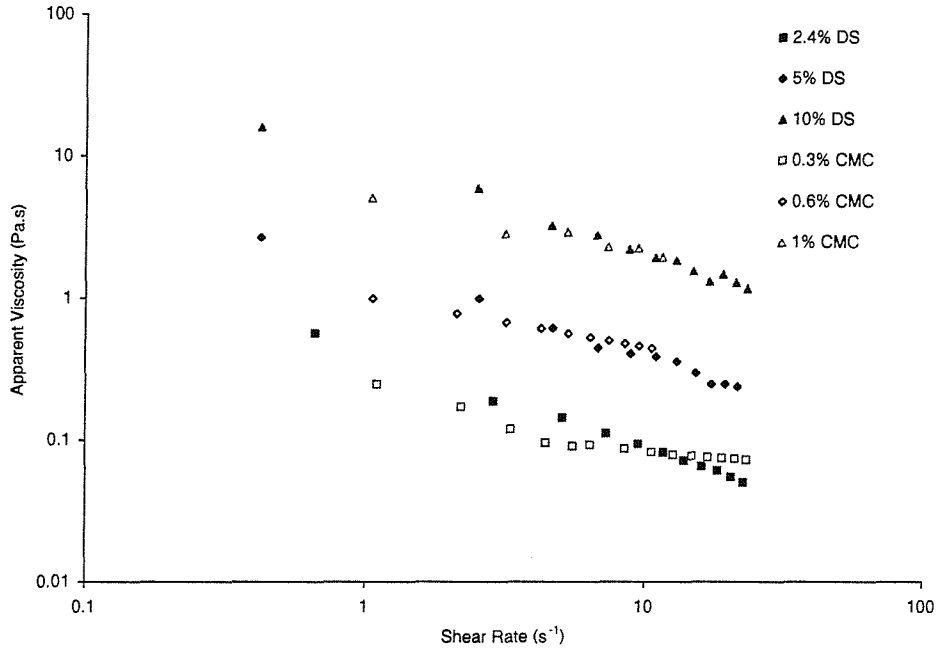

Figure 3.4: Comparison of apparent viscosities and shear-rates of three digested sludges with 0.3%, 0.6% and 1.0% CMC

3.2.4 Effect of salt tracer addition on simulant

Researchers (Haque et al., 1986; Haque et al., 1987; Pandit and Joshi, 1983; Ulbrecht and Baykara, 1981) have reported changes in CMC rheology when an electrolyte was added. It was therefore important to quantify this change before testing began. In addition, the tracer dosing technique used for the experimental work was intended to reflect the addition of feed sludge at the full scale. The ratio of the volume of feed added to the digesting sludge volume recorded at the full scale varied from one site to another and so the most common volume ratios were averaged and used in the laboratory scale tests.

Initially, salt was added to 500 ml of CMC taken from the bulk CMC in the mixing vessel. A small amount of food dye was added to the tracer and poured through a funnel at a fixed inlet position, into the bulk. The tracer sank to the bottom of the vessel where it was quickly entrained into the rising column of gas bubbles which gave a short blend time. The blend times recorded in this way

could not be reproduced and after investigation, this was found to be due to the tracer addition technique. This was changed so that the tracer was added via a pump with a fixed outlet pipe. The pipe internal diameter was 13.5mm and the tracer was added at a constant rate of 5 x 10^{-6} m^3s^{-1}. This meant that the tracer was always added at the same rate and at the same location for all tests. This improved the reproducibility, however, the tracer was still sinking.

To overcome the density effect, the tracer needed to have the same density as the bulk CMC so that it was neutrally buoyant. Samples of 0.3%, 0.6% and 1% CMC were made up and their density measured at ambient temperature. Adding salt to these concentrations would increase their densities, therefore salt water was used as the tracer instead of salt and CMC. The concentration of salt was added to match the densities of the three CMC solutions. Heating the tracer to 2°C higher than the bulk CMC temperature, removed any remaining density effect.

Table 3.4 shows the densities measured for the different CMC concentrations and the corresponding salt concentrations used in water.

Table 3.4: Salt concentrations used to obtain a neutrally buoyant tracer

CMC concentration (%)	**Density of CMC (kgm^{-3})**	**Salt concentration in water (gl^{-1})**
0.3	1000.92	1.5
0.6	1001.43	2.5
1.0	1003.37	4.0

This resulted in the extension of this phase of work to include the effect on rheology of diluting the CMC with water as well as the effect of the salt itself.

Three batches of CMC were made up in the three concentrations (0.3%, 0.6% and 1%) in the lab-scale vessel to an aspect ratio of 1. Samples were taken from each batch before adding a dose of salt and again afterwards.

The addition of the salt solution had a detrimental effect on the viscosity of the simulant, decreasing its viscosity. The sludge rheologies measured from full-scale sites varied over a wide range and the simulant concentrations were chosen to

reflect this range. Therefore the fact that the viscosity decreased with the addition of salt solution was acceptable, provided that the rheological data was known for each test performed. A threshold percentage decrease in apparent viscosity was required in order to determine at what point a particular concentration of CMC was no longer representative. A fresh batch of CMC was prepared prior to any alterations in sparger geometry, thus providing a standard starting rheology for the different sparger types.

After analysing the results for all of the tests and comparing them with the viscosity ranges of the site sludges, a threshold decrease in apparent viscosity was determined as 30%. Once the measured viscosity had decreased by 30% from its original value (i.e. the value after being made up) for any shear rate, the batch was deemed to have degraded and was disposed of.

3.3 Scaling considerations

The majority of tests were to be performed in the lab-scale vessel (0.61m internal diameter). These results would provide insight into the flowpatterns, blend times and active volumes produced under different conditions. However, the effect of scale was also to be investigated and therefore, a pilot-scale vessel, (2.67m internal diameter) was also used.

It is well documented in the literature that scaling between different sizes of vessel is fraught with difficulties and perfect scaling is generally not possible because some phenomena scale in different ways that are incompatible (Zlokarnik, 1998; McDonough, 1992; Tatterson, 1994; Harnby et al., 1997). Even so, the results obtained from tests that are not exactly scaled can be interpreted using appropriate scaling relationships. The processes of mixing are controlled by the geometric, kinematic, and dynamic factors. Hence, tests were conducted in geometrically similar vessels in a manner that was as kinematically and dynamically similar as practical.

Table 3.5: Comparison of geometric data for lab-, pilot- and full-scales

Parameter	**Lab-scale (m)**	**Pilot-scale (m)**	**Full-scale (m)**
Liquid height, H Vessel diameter, T Aspect ratio, H/T	0.61 0.61 1, 0.5	2.67 2.67 1	6.5 - 14.0 8.4 - 23.0 0.36 - 1.2
Nozzle arrangement	2 rings: 4 nozzles at $0.2T$, 8 nozzles at $0.72T$	1 ring: 4 nozzles at $0.2T$	2 rings: 4 nozzles at $\approx 0.2T$, 8 nozzles at $\approx 0.72T$ *
Nozzle diameter	0.002	0.010	0.032
Inlet location	$T/10$ below surface and $T/10$ from wall	$T/10$ below surface and $T/10$ from wall	$\approx T/10$ below surface and $T/10$ from wall *
Outlet location	At surface, opposite inlet	At surface, opposite inlet	At surface, opposite inlet *

* indicates that not all digesters had this information due to loss of records and turnover of staff

This discussion on scaling will initially consider the scale-down of an unconfined gas mixed digester to the lab-scale followed by scale-up from the lab- to pilot-scale.

3.3.1 Geometric similarity

Geometric similarity means that all pertinent dimensions have constant ratios for scaling (McDonough, 1992; Tatterson, 1994).

The collected full-scale data was scaled down to be used at the lab-scale and subsequently, scaled up for the pilot-scale. Only one vessel shape could be tested and therefore, the most common aspects of all the different designs were considered. The geometric parameters for each scale are listed in Table 3.5.

3.3.2 Kinematic similarity

Kinematic similarity requires the same velocity ratios between the different scales. Reynolds number contains a velocity term and is used to define the flow regime that exists around a bubble, impeller or in a flow field, for example. If the full-scale digesters were found to operate in the laminar flow regime for example, then it is essential that the lab- and pilot-scale vessels also operate within the laminar flow regime. If a flow regime change does occur and is ignored, then there is a serious question as to whether the information gained in the pilot studies is useful (Tatterson, 1994).

In the process industries, scaling of power per unit volume and power dissipation are important and are often used as scaling terms. The power inputs for an anaerobic digester come from the isothermal expansion of the gas and a smaller portion may come from the kinetic energy of the gas injection. Isothermal gas expansion is a function of gas flowrate and static pressure whereas kinetic energy is a function of the velocity of gas as it passes through the nozzles.

In a gas mixed digester, there is more than one possible velocity ratio to consider and there are implications on the Reynolds numbers and power inputs for those chosen. Possible velocity terms are the superficial gas velocity (the ratio of the gas flowrate to the vessel cross-sectional area); the nozzle velocity from gas injection; terminal bubble rise velocity and the velocity of the feed as it is added through the inlet. In addition, the superficial gas velocity is an average velocity for the vessel cross-section, but the wall velocity or the plume velocity could also be considered. It is necessary therefore, to prioritise these velocities in terms of their impact on the mixing process and the ease with which they can be determined.

According to Tatterson (1994) and McDonough (1992), scaling of a mixing process requires the identification of the dominant mixing mechanism. In a gas mixed vessel, the mixing is caused by the rising gas bubbles and can take the form

of isothermal gas expansion and/or kinetic energy.

The terminal bubble rise velocity is determined by the liquid properties and the geometry of the system (Eqn. 2.23). It can be used to determine the bubble Reynolds number (Eqn. 2.24). The velocity of the feed as it is added through the inlet jet results in an inlet Reynolds number, which should be in the same regime between the scales. The wall velocity is not very useful for this work because of the existence of active and inactive zones. Consequently, the wall velocity may be zero for several gas flowrates and liquid viscosities. In this instance, the superficial gas velocity is an easier parameter to determine. The plume velocity has been measured by Ulbrecht et al. (1985) and Kawase and Moo-Young (1986a) in non-Newtonian systems and both researchers produced Reynolds number equations for this velocity term, as given in Section 2.8.4.

Table 3.6 lists the relevant velocity terms and Reynolds numbers for the three scales, in order of their importance to blend time and active volume.

Table 3.6: Comparison of kinematic data for lab-, pilot- and full-scales

Parameter	Lab-scale	Pilot-scale	Full-scale
Re_L^* U	3.97 - 587	24 - 1412	-[†]
Re_L^* K-M	15 - 1116	186 - 5638	1078 - 4078[††]
Re_{bubble}	0.16 - 1.70	0.27 - 2.00	0.32 - 0.41
u_{sg} [ms^{-1}]	$6.84x10^{-5}$ - $6.84x10^{-4}$	$7.11x10^{-5}$ - $7.11x10^{-4}$	$0.123x10^{-3}$ - $0.551x10^{-3}$
u_{nozzle} [ms^{-1}]	1.59 - 15.9	1.27 - 12.68	17.42 - 21.10[‡]
Re_{inlet}	5.4	6	5 - 20

U refers to Ulbrecht et al. (1985)
K-M refers to Kawase and Moo-Young (1986b)
[†] = unable to determine because requires measurement of liquid circulation velocity.
[††] = Re_L^* K-M takes account of the liquid rheological values. The full-scale sites used here had low %DS sludges corresponding to 0.3% CMC. Up to 1% CMC was used at the lab-scale and up to 0.6% was used at the pilot-scale, thus reducing the minimum Reynolds numbers compared with the full-scale.
[‡] = sufficient data was only available for sequential gas addition through a single orifice. No flowrates were supplied by Ouziaux (1997) for multiple orifice injection, therefore, these values are likely to be maximum values.

Re^*_L U and Re^*_L K-M were calculated using Eqn. 2.17 and Eqn. 2.18 respectively. The resulting values of Re^*_L are quite different between the two methods, but individually, cover similar ranges at lab- and pilot-scales.

In terms of the liquid circulation, the plume Reynolds numbers of Ulbrecht et al. (1985) and Kawase and Moo-Young (1986b) are important parameters. These together with the bubble Reynolds number strongly influence the liquid circulation in terms of the blend time and active volume. The exact numbers of these three Reynolds numbers are not constant between the scales due to differences in their calculation methods, but individually, they remained within the same orders of magnitude for each scale, indicating the same flow regimes on scaling.

The superficial gas velocity and nozzle velocity covered the same ranges at each scale, although their direct influences on the liquid circulation are less than the Reynolds numbers already discussed.

The inlet Reynolds number refers to the Reynolds number of the feed. Maintaining the same range between the scales ensured no extra mixing energy was added to the system from the feed jet.

3.3.3 Dynamic similarity

Dynamic similarity occurs when all forces are constant. According to McDonough (1992), there are four forces that are readily used for the analysis and evaluation of scale-up criteria: the input force from the mixer and three opposing forces - viscosity, gravity and surface tension. Dynamic similarity is predicted on the ratios between full-scale and lab-scale, lab-scale and pilot-scale of all four of these forces being constant on scale-up:

$$\frac{(F_p)_m}{(F_p)_p} = \frac{(F_v)_m}{(F_v)_p} = \frac{(F_g)_m}{(F_g)_p} = \frac{(F_s)_m}{(F_s)_p} \tag{3.6}$$

where the subscripts m and p refer to model and pilot scales respectively; F_p

= power input; F_v = viscous forces; F_g = gravitational forces and F_s = surface tension forces.

The aim was to determine the flowpatterns and blend times in a shear-thinning fluid that exhibited the same properties as digested sewage sludge. Therefore, the shear-rate distribution and flowpatterns within the vessels should be similar, precluding the use of a different liquid between the lab- and pilot-scales. Hence, the liquid rheological properties were a constraint that could not be changed. Thus the dynamic forces involved were the input from the mixer and gravity (which can be assumed as constant for the full-, lab- and pilot-scales).

The ratios of the viscosity, gravitational and tension forces were the same between the different scales. The input force from the mixer was determined by the power input to the surrounding liquid. The actual power input values were different between the scales, but the values of power input per unit volume were constant between the scales. Therefore, all four force ratios were constant between the different scales used and dynamic similarity was maintained.

3.3.4 Scaling ratios employed

The vessel shapes at the full-, lab- and pilot- scales were cylindrical. The sites at the full-scale ranged in aspect ratio from 0.36 to 1.2. The power inputs supplied to these different aspect ratios varied with some low aspect ratio sites receiving more power than some of the higher aspect ratio sites. Part of this work was to investigate how the flowpatterns, blend times and active volumes changed with aspect ratio, keeping the vessel diameter constant. Geometric similarity was maintained between the lab- and full-scale vessels for the respective aspect ratios.

The feed position, feed addition rate and feed volume to vessel volume ratio were held constant between the different scales. The feed entered at $T/10$ from the wall (where T is the vessel diameter) and $T/10$ below the surface at a rate of 0.012 x 10^{-3} m^3s^{-1} with a total volume of 0.3% of the vessel volume added. The nozzles in the base were arranged in two concentric rings with diameters

representative of those found at the full scale.

The dynamic scaling ratio employed was power input per unit volume since the power input from the mixer will be proportional on scaling if it is considered as the power input per unit volume (Tatterson, 1994; McDonough, 1992).

The power input per unit volume at the full-scale was calculated using isothermal expansion. The values ranged from 0.5 to 5.0 Wm^{-3}. It was clear from the literature that these values were producing problems with grit deposition and reduced active volume, therefore the range (calculated using isothermal gas expansion) was extended for the lab-scale from 0.7 to 7 Wm^{-3} and maintained at the pilot-scale.

Kinematic similarity was maintained in terms of the plume Reynolds numbers of Ulbrecht et al. (1985) and Kawase and Moo-Young (1986b), bubble Reynolds number, superficial gas velocity and nozzle velocity.

The nozzle velocities were determined from the gas flowrates through the systems, which in turn, were determined from the power inputs. The nozzle diameters varied between the three scales was shown in Table 3.5 in order to maintain constant nozzle velocities.

3.4 Gas mixing experiments

The lab-scale gas-mixing vessel is shown in Figure 3.5. Air was supplied to the vessel from a compressor. The flow was regulated by up to three rotameters. Two manifolds were used, one with thirteen 1.0mm internal diameter branches and one with eight 0.5mm internal diameter branches. The spacing between branches was the same for both manifolds as was the manifold diameter. Uniform gas flow distribution at the lowest gas flowrates was only achievable with the 8-branch manifold.

A total of 13 nozzles were positioned in the vessel base in two concentric rings as shown in Figure 3.6 and one central nozzle. The internal diameters of the

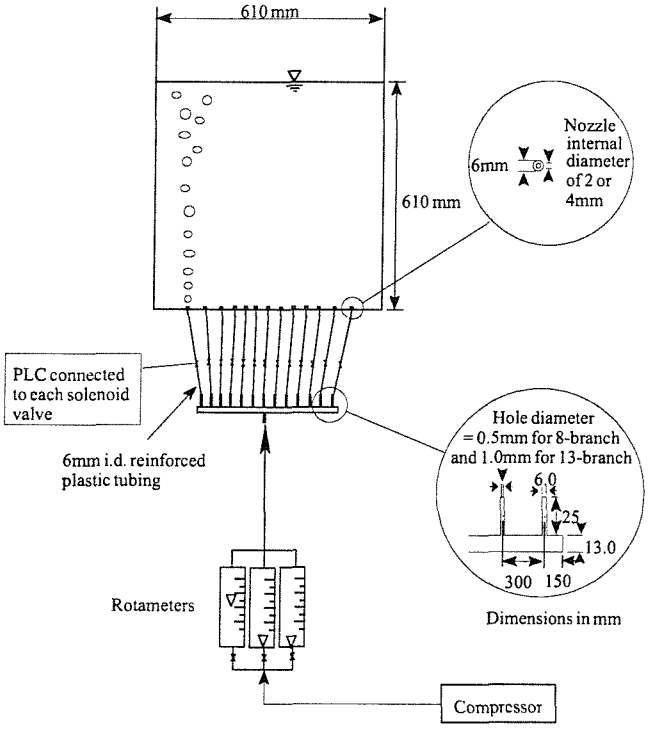

Figure 3.5: Air supply to gas mixing vessel

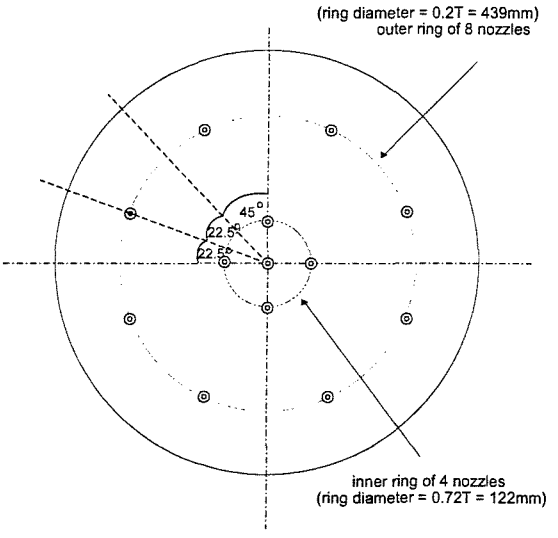

Figure 3.6: Nozzle arrangement in vessel base for unconfined gas mixing

nozzles were 2mm and they were interchangeable with nozzles of 4mm internal diameter.

The gas flowrate was the parameter that was physically changed and this resulted in a change in power input per unit volume. The gas flowrates used were

0.02, 0.04, 0.1 and 0.2 x 10^{-3} m^3s^{-1} corresponding to a power input per unit volume range of 0.7 to 7.0 Wm^{-3}.

Six different sparger arrangements were tested and are shown in Figure 3.7. The sparger arrangements are defined in Table 3.7.

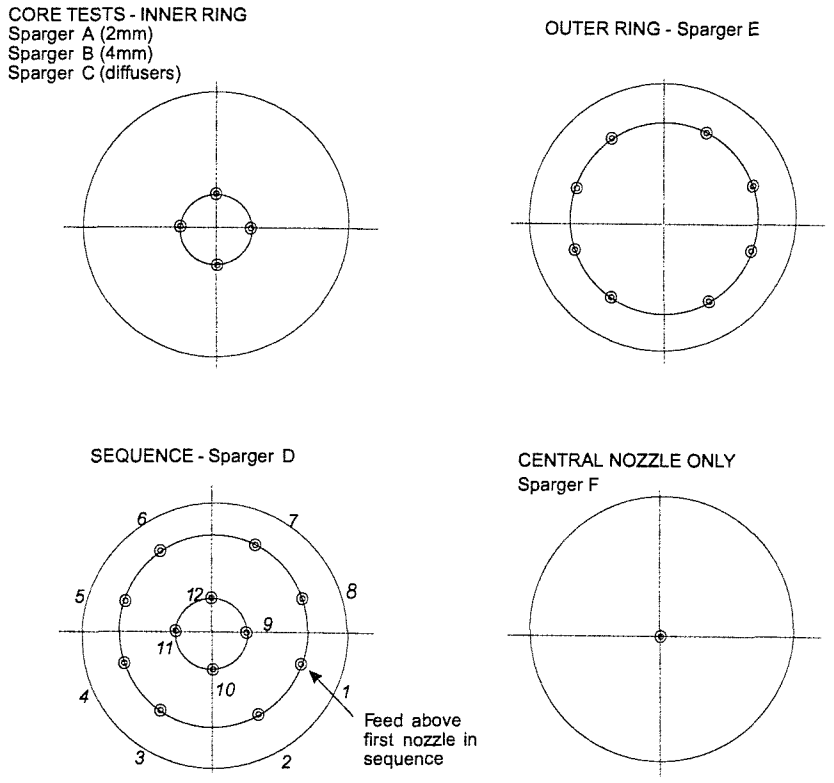

Figure 3.7: Sparger arrangements tested (not drawn to scale)

Table 3.7: Sparger arrangements tested

Sparger	Description	No. of nozzles	Gas supply
A	Inner ring	4 of 2mm diameter	simultaneous
B	Inner ring	4 of 4mm diameter	simultaneous
C	Inner ring	4 diffusers	simultaneous
D	Sequence	12 of 2mm diameter	sequential
E	Outer ring	8 of 2mm diameter	simultaneous
F	Central nozzle	1 of 2mm diameter	simultaneous

Figure 3.8 illustrates one of the four fine bubble diffusers used in Sparger C. These diffusers were fitted to the inner ring of Sparger A to investigate the effect of many small bubbles compared to larger, single bubbles on active volume and blend time.

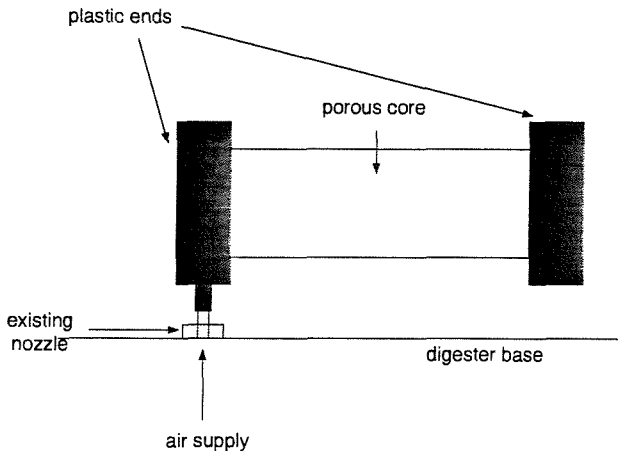

Figure 3.8: Illustration of fine bubble diffuser for Sparger C (lab-scale)

A programmable logic controller (PLC) controlled which nozzle or nozzles were in use by opening and closing the solenoid valves attached to each nozzle. The gas was supplied simultaneously to all nozzles apart from Sparger D where gas was supplied to the first nozzle in the sequence, located below the feed position on the outer ring as shown in Figure 3.7. After 60 seconds, the programmable logic controller (PLC) closed the solenoid valve feeding this nozzle, and opened the next one in the sequence allowing gas through. A value of 60 seconds per nozzle was widely quoted at the full-scale (Ouziaux, 1997). The same addition period was directly transferred to the lab-scale work. No attempt was made to scale this down. The location and extent of inactive volume was determined visually and it was thought that this period would allow time to observe the flowpatterns set up for each nozzle in the sequence. The effect of reducing this period is something that would be interesting to study in further work.

After 60 seconds, the gas then moved to the next nozzle and so on until each nozzle in the outer ring had been used. The sequence then moved to the inner

ring and continued supplying gas for 60 seconds to each nozzle until the 4 nozzles had been used. This constituted 1 sequence and took 12 minutes. The PLC would then continue with the first nozzle in the sequence as before.

3.5 Blend time measurement

The degree of mixing within a vessel is reflected by the distribution of concentration within the vessel thereby influencing the rate of transfer of fluid between poorly and well-mixed regions of the vessel.

The rate of blending can be followed using a tracer. The existence of well-mixed and less well-mixed zones within a digester precludes the use of the decolourisation technique of Ulbrecht and Baykara (1981) and Ulbrecht et al. (1985) as in the extreme cases, there would be regions where decolourisation was complete within a short time and regions where no decolourisation had occurred. Visual determination of the end point of the reaction is open to inaccuracies as the sparger geometry and liquid viscosity changed.

A conductivity technique has been used in the literature for bubble columns employing non-Newtonian liquids by Pandit and Joshi (1983) and Haque et al. (1987). It is also widely used in Chemical Industry research (Ruszkowski, 1994; Edwards, 1997; Grenville, 1992; Revill, 1997). As mixing was thought to occur at different rates within the vessel (Zoltek and Gram, 1975), multiple probes were positioned in the vessel in both regions (Ruszkowski, 1994; Grenville, 1992; Edwards, 1997).

Grenville (1992) has produced correlations to predict the blend time using non-Newtonian shear-thinning fluids blended with an impeller. In order to validate the blend time approach taken in the current work and in the absence of relevant literature data for blend times in gas-mixed vessels using non-Newtonian liquids in geometries similar to digesters, a series of tests were performed using an impeller mixed vessel to measure blend time. The experimental blend times were compared

with those predicted using Grenville's (1992) correlations.

Two empirical correlations were produced, one for the transitional and turbulent regimes, defined by the impeller Reynolds number:

$$Re_{impeller} = \frac{\rho N D^2}{\mu} \tag{3.7}$$

where N = impeller speed; D = impeller diameter and μ = liquid dynamic viscosity calculated using the average shear-rate determination of Metzner and Otto (1957) who found that the average shear-rate was directly proportional to impeller speed:

$$\dot{\gamma}_A = k_s N \tag{3.8}$$

where $\dot{\gamma}_A$ = average shear-rate and k_s is the mixer shear-rate constant (values for k_s are given in Metzner et al. (1961) for different impellers).

Experiments were performed in a vessel 0.61m in diameter at an aspect ratio of one. The turbulent regime was defined as $Re > 10^4$ and the transitional regime as $10 < Re < 10^4$ according to the ranges used by Grenville (1992).

The correlations are given by equations 3.9 and 3.11 respectively.

$$\theta_{95\%} = \frac{4.10^4 T^2 \mu_w}{P_o^{2/3} N^2 D^4 \rho} \pm (38.4\%) \tag{3.9}$$

where $\theta_{95\%}$ = time taken from tracer addition for fluctuations to remain within $\pm$ 5% of the final value; T = vessel diameter; $P_o = \frac{P}{\rho N^3 D^5}$ (P = power input from impeller) and μ_w = apparent viscosity of liquid at the vessel wall, calculated using a torque balance:

$$\tau_w = \frac{1}{1.622}\left(\frac{\Lambda}{T^3} - 0.00638\rho(\Delta v)^2\right) \tag{3.10}$$

where τ_w = the shear stress at the wall; Λ = the shaft torque; Δv = change in velocity of the fluid as it impinges on the baffles.

The turbulent correlation is given by:

$$\theta_{95\%} = \frac{5.47T^2}{P_o^{1/3}ND^2} \pm 13.6\% \tag{3.11}$$

N = impeller speed and D = impeller diameter

There is no viscosity term in this correlation since Grenville (1992) found that blend time was independent of viscosity in the turbulent regime.

Both Eqns 3.9 and 3.11 have upper and lower bounds defined as being 2 relative standard deviations either side of the blend time prediction.

In this thesis, a tracer of salt (NaCl) dissolved in tap water was used. The tracer was added to the vessel and its dispersion recorded using conductivity probes located within the vessel volume. A rise in conductivity would indicate a pulse of high tracer concentration passing the probe and similarly, a drop in conductivity would indicate the passing of lower conductivity fluid at the probe. Once the readings for all of the probes within the mixing vessel were constant for a given length of time, the vessel contents were assumed to be fully blended. It was therefore important that the probes were positioned in both active and less active volumes so that a complete picture of the vessel mixing pattern could be built.

The conductivity probes used were made according to the design originally described by Khang and Fitzgerald (1975) and shown in Figure 3.9.

Five conductivity probes were used for the lab-scale tests. Once the pilot-scale vessel was filled with liquid, the probes were inaccessible from the surface and so as a precaution, ten probes were used, positioned within the same five regions of the vessel as at the smaller scale in anticipation of any problems during testing. If one probe malfunctioned for example, there would be a second probe there to record the tracer's movements within that region.

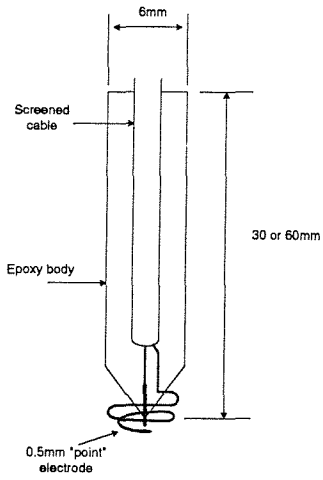

Figure 3.9: Conductivity Probe

To ensure the probes were positioned in both active and less active volume, an initial dye test was performed at the lab-scale to locate these zones. The probes were then distributed within these parts of the vessel.

Figure 3.10 illustrates the probe positions for the gas mixing experiments. The positions were held constant for all of the gas mixing tests. Probe 1 was located below the tracer inlet pipe and as the tests were run as batch tests, a probe (probe 2) was positioned so as to represent the outlet. Probe 3 was fixed against the vessel wall, approximately one third of the liquid depth. This region was active at high flowrates but less active at lower flowrates, depending on the sparger arrangement in question. Probe 4 was positioned in the base against the vessel wall. This was usually an inactive volume but again, depended on the sparger arrangement and gas flowrate supplied. Probe 5 was positioned within the vessel bulk in a zone that was usually active.

The probes were connected to a 6-channel conductivity box which amplified the difference in resistance recorded by the probes as the tracer passed them, converting this reading into 'bits' which was then displayed on a computer. The data were collected using Labview, version 4.0, a Windows compatible graphical based programming language that uses 'G', marketed by National Instruments.

Figure 3.11 illustrates a typical conductivity probe response. The tracer con-

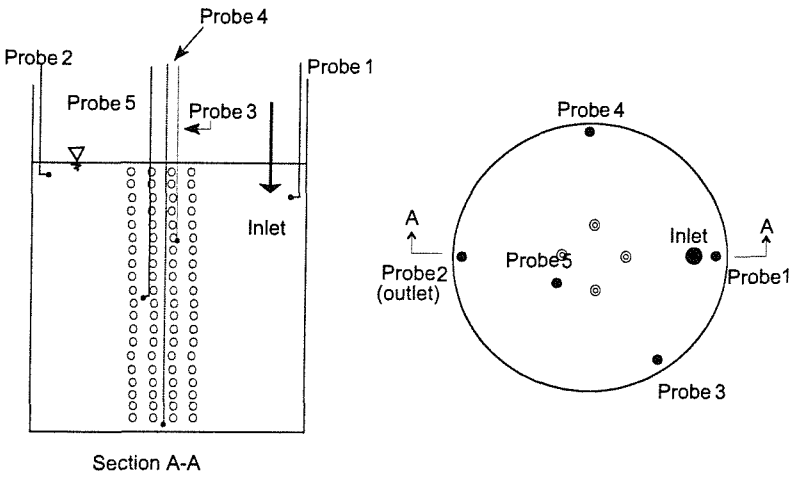

Figure 3.10: Location of probes for all gas mixing experiments

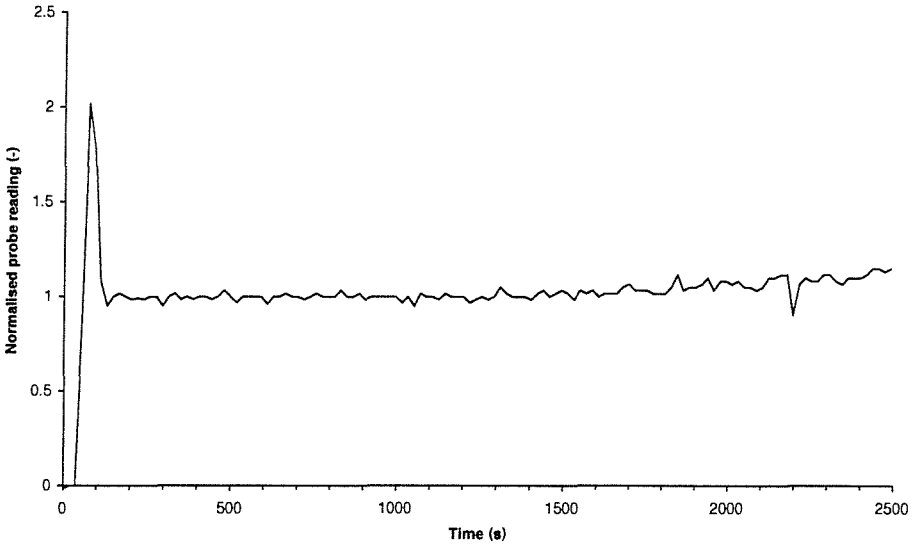

Figure 3.11: Typical conductivity probe response for blend time measurement

centration at this probe location has increased, peaked and fallen until finally reaching an equilibrium concentration. The blend time can then be defined as the time required from the addition of tracer to the time when this equilibrium value is reached (Ruszkowski, 1994; Grenville, 1992; Edwards, 1997). However, the concentration approaches this equilibrium value in an asymptotic manner and the end point of the experiment is difficult to detect with precision.

The analysis method used in this work is described in detail by Ruszkowski (1994) and Grenville (1992) and is briefly described here. The blend time is determined as the time taken for the tracer concentration fluctuations to fall within a pre-determined percentage about the mean. If the volume of tracer is known, the equilibrium concentration can be calculated using:

$$\bar{C} = C_i' - C_i \tag{3.12}$$

where $\bar{C}$ = the mean concentration; C_i = local concentration at time t; C_i' = local fluctuating component of concentration at time t

At any time the concentration variance about the equilibrium value can be calculated as:

$$\sigma^2 = \frac{1}{N-1}\sum_{i=1}^{n}(C_i - \bar{C})^2 \tag{3.13}$$

where σ^2 = concentration variance; N = the number of probes; i = probe number

The change of this variance with time for the data shown in Figure 3.11 would take the form shown in Figure 3.12.

The blend time is taken as the time at which the tracer concentration at the measurement location has reached the expected final mean concentration to within the required variance (Ruszkowski, 1994; Grenville, 1992; Revill, 1997).

If there is no tracer initially present in the tank, then a blend time can be defined as:

$$m = \frac{C_i - \bar{C}}{\bar{C}} \tag{3.14}$$

where m is the maximum acceptable absolute value of the variance. At the start of the mixing process, $m = 1.0$ and when complete homogeneity has been achieved, $m = 0$.

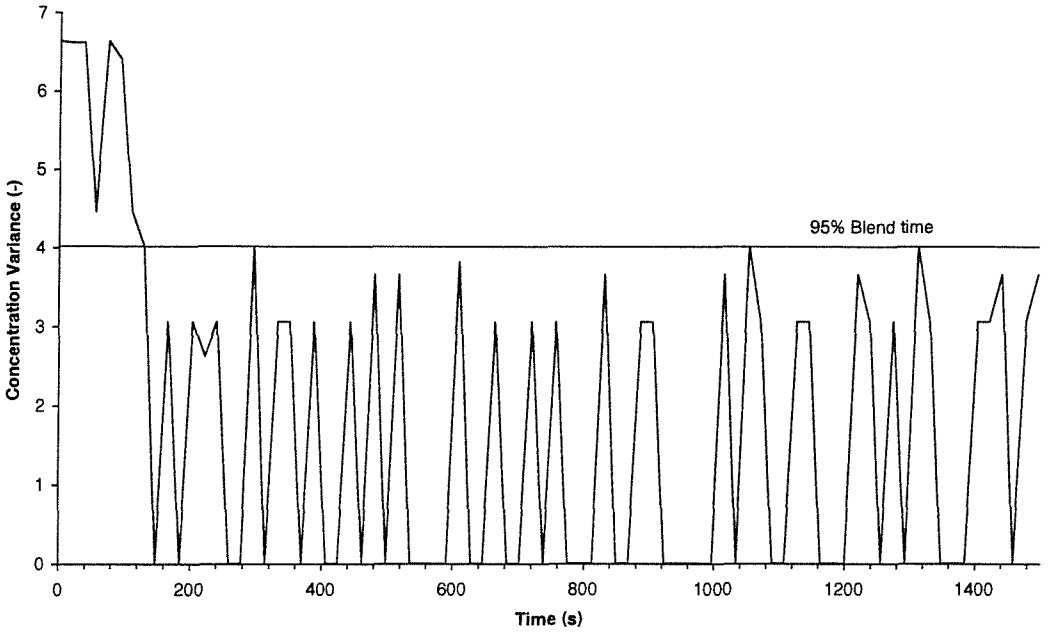

Figure 3.12: Reduction in variance with time

However, as the equilibrium value is approached asymptotically, a 95% blend time is often measured. This is the time from tracer addition to the time when $m = 0.05$ (Revill, 1997). For this example, rather than collecting changes in electrical conductivity (concentration) as Volts, the data logging card (A/D card) used collected integers in the form of bits as these were easier to store. The card range was $\pm$ 2048 bits. Figure 3.12 shows a line corresponding to the 95% blend time with a value of 4.02 on the log variance scale. This value comes from the log of $(0.05 \times 2048)^2$, where 0.05 is the concentration variation of $\pm 5\%$ about the mean. The blend time from Figure 3.12 is taken as approximately 130 seconds. The final (active) blend time results for the current work, were based on $m = 0.05$.

The variance for each probe was calculated. Probes in the active regions of the vessel reached equilibrium faster than those in less active regions of the vessel with the result that the probes in the active regions often exhibited probe drift. This can be caused by slight increases in temperature and are noticeable on a probe response plot by an increase in gradient as shown in Figure 3.13. This drift was

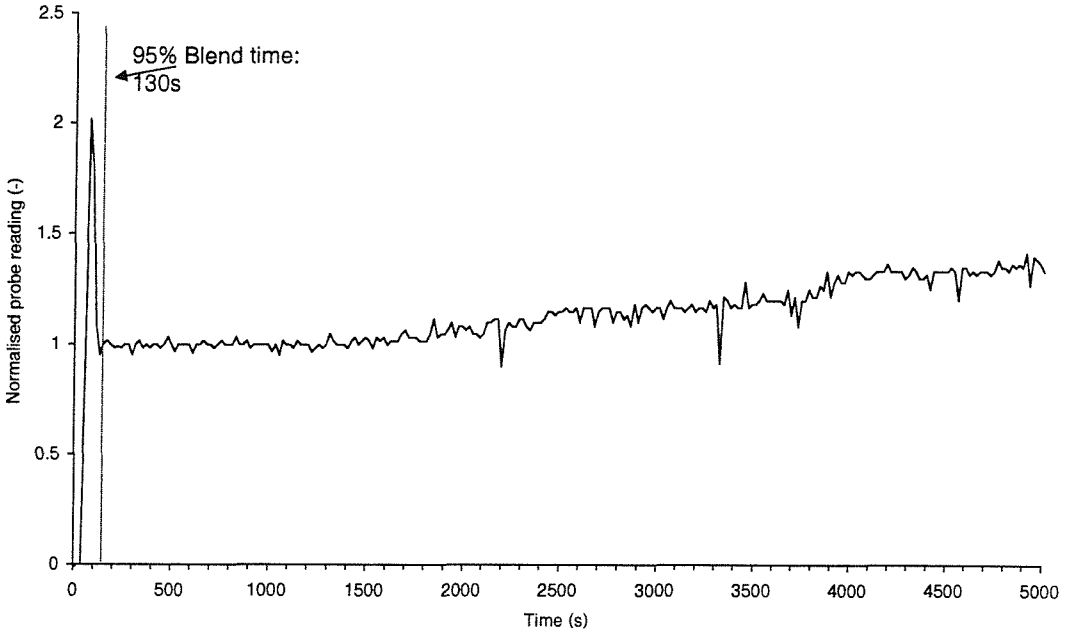

Figure 3.13: Example of probe response and drift

removed before the variance was calculated. If this was not done, then the end concentration would be that at the end of the test and would therefore include the drift.

Dye was added to the salt tracer initially and its progress followed throughout the test length. This provided confirmation of the order of magnitude for the active blend time measurements.

Grenville (1992) produced empirical correlations in the literature to predict the blend time using non-Newtonian shear-thinning fluids blended with an impeller. In order to validate the blend time approach taken, a series of tests were performed using an impeller mixed vessel to measure blend time. Details of these experiments are given shortly and the results can be found in Appendix C. Good agreement was found between the measured blend times and those predicted using Grenville's correlations (1992), providing confidence in the experimental method used.

3.6 Active and inactive volume measurement

It is important to identify the location of any poorly-mixed zones within the digester. To maximise the throughput of sludge through a digester, there should be no reduction in volume due to stagnant zones or grit deposition. Grit will deposit when the settling velocity of the particles is greater than the local velocity, i.e. in regions of low shear-rate. The bubble column literature does not contain any work on determining the location or extent of these zones as the gas flowrates used have been high so as to ensure good mixing and mass transfer. The diameter of a bubble column is small so as to maximise the contacting from the gas and therefore, inactive volume are not encountered. A visual technique can be used to determine the location of any inactive volume and whether these change for different sparger arrangements.

Flow patterns were recorded on video using a combination of flow followers and dye. At the lab-scale, the dye in the vessel enabled visual identification of the location of the last regions to mix in the vessel. Further visual aid was supplied by flow followers (neutrally buoyant coloured particles) to identify velocities and flowpatterns.

Video footage was taken throughout the duration of each test condition and studied to determine the size and locations of both active and inactive volumes within the vessel. By studying the video and superimposing the positions of the probes, the location of the probes could be determined in terms of active and inactive volumes.

The video also enabled bubble rise velocities to be estimated and a quantitative visual comparison of the bubble sizes produced by the different sparger arrangements. At the pilot-scale, flow observation was not possible because the vessel was buried in the floor. Only surface visualisation was possible. The location of any inactive volume was determined by looking at the probe responses but the size of these zones was difficult to determine accurately.

3.7 Experimental Programme

One configuration of sparger, Sparger A, was chosen to investigate the full range of variables, based on the findings at the full-scale (Ouziaux, 1997). These were the effects of viscosity, power input, aspect ratio, nozzle diameter and scale. Tests were performed using the remaining sparger geometries over a narrower range of conditions to compare the effect of sparger arrangement on blend time and active volume.

3.7.1 Gas mixing

The range of parameters investigated was based on the findings of Ouziaux (1997) and scaled down to the laboratory scale. These parameters were:

- Sparger arrangement
- Nozzle diameter - either 2 or 4mm
- Simulant rheology - 0.3%, 0.6% or 1.0% CMC
- Aspect ratio (H/T) - 0.5 and 1
- Gas flowrate (Q) - 0.02, 0.04, 0.1 and 0.2 x 10^{-3} m^3s^{-1} which resulted in power inputs of 0.7, 1.4, 3.6 and 7.0 Wm^{-3} based on isothermal gas expansion ($H/T = 1$)
- Inlet position - Two inlet positions were tested using Sparger A as shown in Figure 3.14(a) and two were tested for Sparger D, shown in Figure 3.14(b). This was only investigated for 0.6% CMC as this would show any effects more markedly than 0.3% CMC.
- Scale - 0.61m and 2.67m diameter vessels

Table 3.8 shows the power inputs, viscosities, aspect ratios and scales studied in this phase of work.

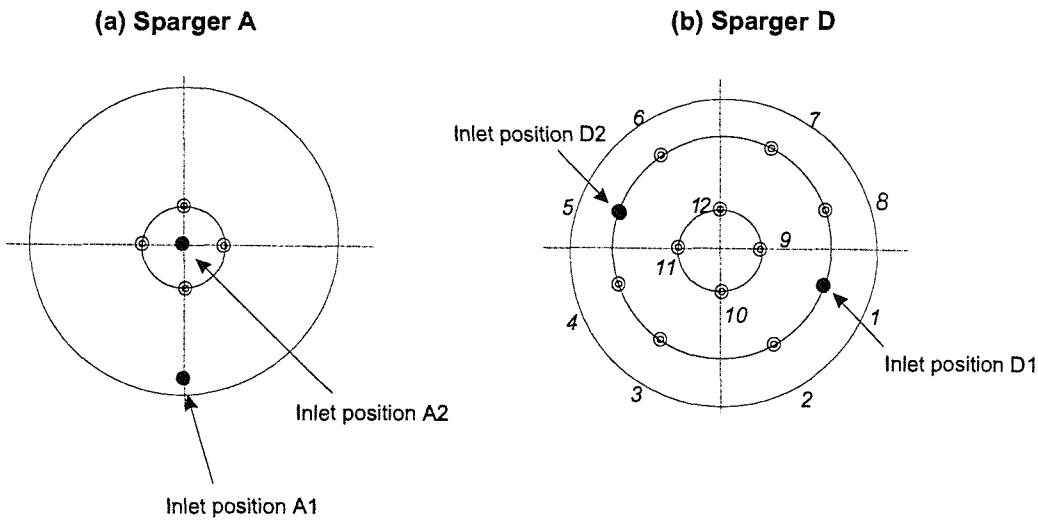

Figure 3.14: Location of inlet positions tested with Spargers A and D

Table 3.8: Test matrix for unconfined gas mixing experiments

Type	Sparger details	Aspect ratio (H/T)	% CMC wt/wt	Scale (m)	Inlet	Q_g x10^{-3} (m^3s^{-1})	P/V (Wm^{-3})
A	Inner ring (2mm nozzles)	1	0.3, 0.6, 1	0.61, 2.67	A1 A2	0.02, 0.04 0.1, 0.2	0.7, 1.4, 3.6, 7.0
A	Inner ring (2mm nozzles)	0.5	0.3, 0.6, 1	0.61	A1	0.02, 0.1	0.7, 3.6
B	Inner ring (4mm nozzles)	1	0.3	0.61	A1	0.02, 0.1	0.7, 3.6
C	Inner ring (diffusers)	1	0.3, 0.6	0.61	A1	0.02, 0.1	3.6, 7.0
D	Inner and outer ring in a sequence (2mm nozzles)	1	0.3, 0.6	0.61	D1 D2	0.02, 0.1	3.6, 7.0
E	Outer ring (2mm nozzles)	1	0.3, 0.6	0.61	A1	0.02, 0.1	3.6, 7.0
F	Central nozzle (2mm nozzle)	1	0.3, 0.6	0.61	A1	0.02, 0.1	3.6, 7.0

Sparger D was the only sparger where gas was supplied sequentially to each nozzle.

3.7.2 Impeller mixing

A 45° downward pumping pitch blade turbine (PBT) was used for the experimental phase of work, details of which are given in Table 3.9. The probes were positioned in the locations shown in Figure 3.15.

Table 3.9: Table of impeller dimensions

Parameter	Value
Number of blades	4
Blade angle to horizontal	45°
Impeller diameter (mm)	203
Blade length (mm)	73
Blade thickness (mm)	3
Blade width (mm)	57
Hub diameter (mm)	57
Hub height (mm)	56
Shaft diameter (mm)	34

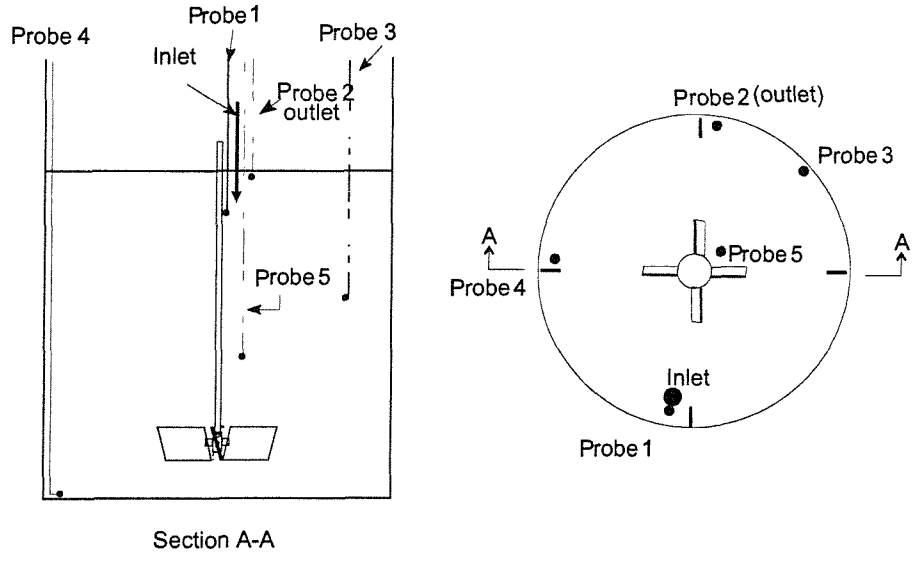

Figure 3.15: Probe positions for all impeller experiments

Experiments were performed using 2 concentrations of CMC: 0.3% and 0.6% CMC. The power inputs selected were representative of those used for gas mixing in 0.3% CMC to serve as a comparison of the two mixer types. These concentrations and power inputs resulted in operation in the transitional regime based on the impeller Reynolds number, calculated using Eqn. 3.7. The test matrix is shown in Table 3.10.

Table 3.10: Test matrix for impeller blending

Conditions	%CMC	Re	P/V (Wm^{-3})
Baffled, unbaffled	0.3	416, 544, 710, 773	3.6, 7.2, 14.4, 18
Baffled, unbaffled	0.6	228, 304, 374	150, 300, 500

3.8 Summary

Two scales of vessel were selected to investigate the effect of different parameters on blend time and active volume. A laboratory-scale 0.61m internal diameter vessel and a pilot-scale 2.67m internal diameter vessel were used for this work. Their geometries and aspect ratios were geometrically scaled down from the full-scale findings of Ouziaux (1997). Three concentrations of Grade 7H4C CMC, 0.3%, 0.6% and 1% by weight, were selected to model three digested sludges of 2.4%, 5% and 10%DS respectively.

Four gas flowrates were chosen to represent the range of power input per unit volume values found at the full-scale (Ouziaux, 1997). These were 0.02, 0.04, 0.1 and 0.2 x 10^{-3} m^3s^{-1} corresponding to power inputs of 0.7, 1.4, 3.6 and 7.0 Wm^{-3}. Sparger A was selected to investigate the effects of viscosity, power input, aspect ratio, nozzle diameter and scale on blend time and active volume, using this full range of power inputs. Tests were performed using the remaining sparger geometries over a narrower range of conditions to compare the effect of sparger arrangement on blend time and active volume.

A conductivity blend time measurement technique was selected from the literature. As no literature was found that measured blend time in a vessel similar to the digesters being modelled, validation was performed by measuring the blend time in an impeller-mixed vessel using the method of Grenville (1992). The blend time results agreed well with the literature correlations proposed by Grenville (1992).

Active volume was studied at the lab-scale and estimated using visual observation. Dye was added with the tracer and neutrally buoyant flow followers were present in the vessel bulk. Video footage was taken throughout the duration of each test condition and studied to determine the size and locations of both active and inactive volumes within the vessel.

The following chapter presents the results of the experimental work.

Chapter 4

Unconfined Gas Mixing

The experimental matrix performed using unconfined gas mixing was presented in Section 3.4. This chapter will present the results from the experimental work performed using unconfined gas mixing at both vessel scales.

4.1 Reproducibility of blend time results

A number of repeat tests were performed both during commissioning and during the experimental work programme to ensure that the results obtained were repeatable and therefore, reliable.

The graphs that are introduced later in the report do not show these repeats. Instead, the graphs show the mean of these repeat tests in order to make the graphical interpretation of the results easier (however, all data was used in the production of the blend time and active volume correlations presented in Sections 4.8.2 and 4.8.3 respectively). An example of this averaging is shown in Figure 4.1.

The reproducibility of the blend time results has been expressed as a percentage difference about the mean as the sample sizes were too small to perform a statistical analysis such as an f-test or a t-test, such as would be performed to assess differences in data sets, eg. Sparger A vs. Sparger B at 95% confidence.

The maximum variation about the mean for the active blend time was $\pm 28\%$

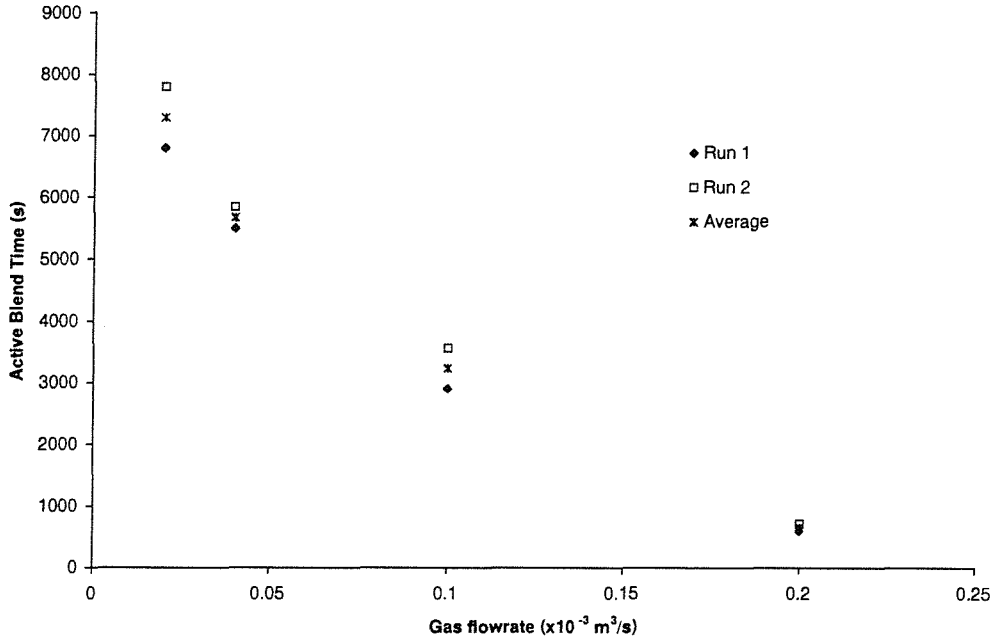

Figure 4.1: Averaging of two sets of active blend time data for Sparger A in 0.6% CMC

with most being less than ±10%. Besides experimental error, these differences may have arisen due to changes in the CMC rheology between tests. As discussed in Section 3.2.4, adding salt to the CMC reduced its viscosity. As more than one test was performed per batch of CMC, this reduction was unavoidable and may have influenced comparisons of the different spargers, although this influence was kept to a minimum by making up a fresh batch of CMC prior to any alterations in sparger geometry, thus providing a standard starting rheology for the different sparger types. In addition, as presented in Section 3.2.4, a fresh batch of CMC was made up once the viscosity at different shear rates had decreased by 30%.

The accuracy of the final correlations was unaffected by any change in rheology because the rheology was measured before and after every test and these measured values were used in the correlation production.

When mixed, the flowpattern in the vessel exhibited an active volume which was the volume of vessel in motion and an inactive volume where no motion occurred. The region in and around the rising bubble plumes moved faster than

those regions further away making the choice between labelling a slow moving region active or inactive somewhat subjective. However, if there was movement, these regions were included in the active volume.

4.2 Interpretation of blend time results

The conductivity probes were positioned within the vessel bulk volume as described in Section 3.4. The blend time recorded for each probe varied due to the movement of tracer throughout the vessel. During the analysis phase, it became apparent that some probes responded very quickly to the tracer addition whilst others took considerably longer. After performing dye tests, the slow responding probes were found to lie in the inactive volume.

The literature was consulted for ways in which to interpret the blend time data. However, there was a distinct lack of references where researchers had encountered significant active and inactive volumes. In all cases in the literature, turbulent blending has been investigated where the power inputs to gas mixed systems were sufficiently large and the diameters of vessels used sufficiently small so as to avoid inactive zones forming.

Overall, the blend time results in this thesis could have been determined by averaging the readings from the five probes in the vessel. However, this carried the risk that the results may be skewed as the average would include the probes within the inactive volume, the extent of which varied with power input and sparger arrangement. For example Figure 4.2 shows the blend times for two tests using the average of all 5 probes ('Total') and using only those probes located in the active volume ('Active'). Considering the active blend time, Sparger B mixed faster than A at the higher power input but considering the total blend time, Sparger A mixed faster than B, despite the higher power input for B.

Alternatively, the vessel bulk could be divided into active and inactive volumes (based on observed flowpatterns) where the blend time in the active volume would

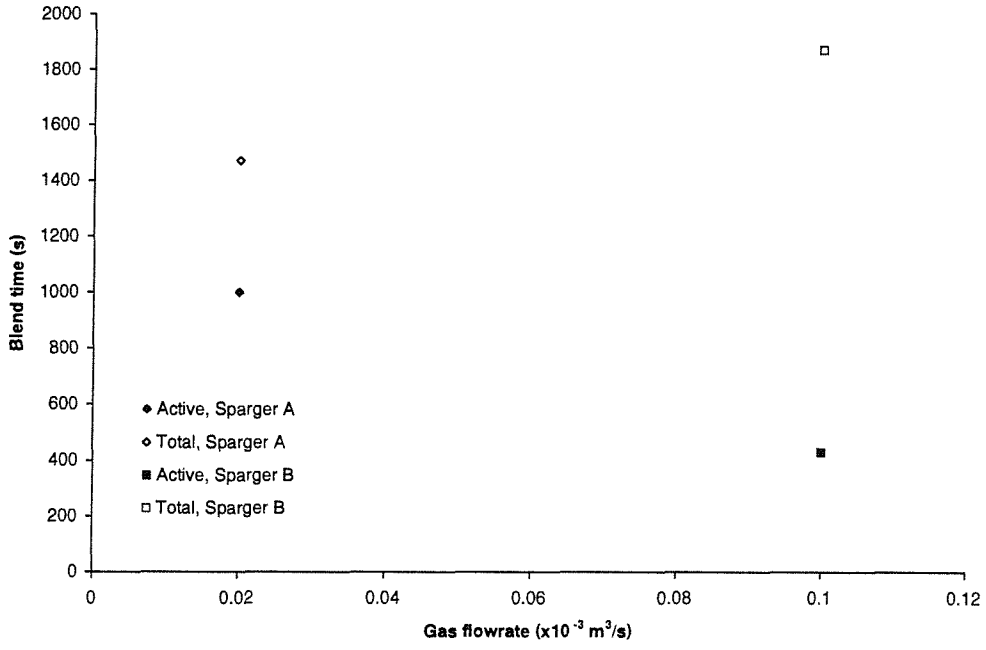

Figure 4.2: Comparison of 'total' and 'active' blend times for Spargers A and B in 0.3% CMC

be an average of those probes within that zone. This would result in an average 'active' blend time from the probes in the active volume and an average 'inactive' blend time from the probes present in any inactive volume.

Water Companies are only now just beginning to specify a blend time for new digesters (previously, no such requirement was made) and in their view, new digesters should have an active volume of at least 90% and therefore, the blend time within the active volume was of more use to them than a blend time for the whole vessel (Fawcett, 1997; Brade, 1997).

Therefore, it is this second method that has been employed and the graphs that follow show active and total blend times.

As expected, the longest blend times were recorded by probes located in the inactive volume and the shortest blend times recorded by probes in the active volumes. The results for 0.6% CMC showed some anomalies however. There were cases where it would appear that shorter blend times were recorded in the inactive volume than in the active volumes. An example of this is shown in Figure 4.3

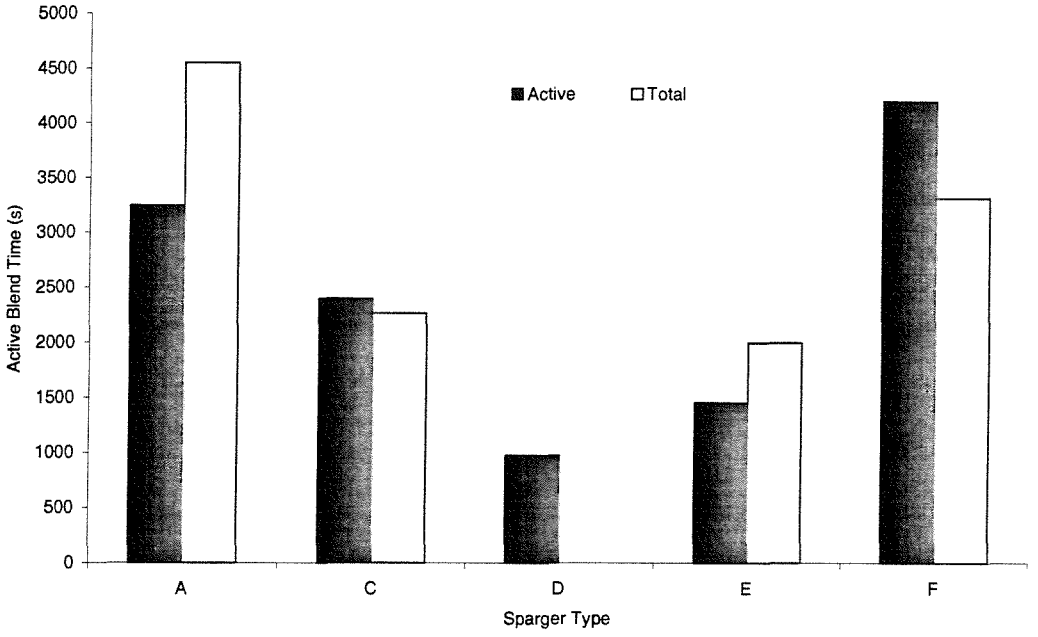

Figure 4.3: Effect of sparger type on blend time in 0.6% CMC at 3.6 Wm^{-3} (Q_g = 0.1 ls $^{-1}$)

for the central nozzle (Sparger F). In this instance, the tracer was added into an inactive volume at the surface. It was slowly entrained into the active region but the time taken to do this was greater than the blend time of the tracer within the inactive volume, highlighting that at full-scale conditions, the feed sludge should always be added into an active volume. Knowledge of the inactive volume locations will allow this.

4.3 Bubble shapes and plumes using Sparger A

The results are firstly presented for Sparger A as this sparger was used to determine the effects of gas flowrate, viscosity, aspect ratio, nozzle diameter and scale. A comparison between different sparger types will then be made to determine their performance.

Overall, Sparger A produced a central plume of bubbles that rose upwards, with an annular downcomer section as observed by other researchers in bubble

columns (Ulbrecht and Baykara, 1981; Crabtree and Bridgwater, 1969; Rietema and Ottengraph, 1970).

The observed bubble shapes are illustrated in Figure 4.4 for the different CMC solutions used. The bubble diameter increased with increasing viscosity at a given gas flowrate, in accordance with both the Davidson-Schuler and Kumar-Kuloor models (Eqns 2.4 and 2.5). The bubble formed at the nozzle had a larger volume with increasing liquid viscosity and as bubble detachment only occurs when the buoyancy force of the bubble can overcome the inertia force of the liquid, an increase in viscosity must result in an increase in inertia, requiring a greater bubble buoyancy before detachment can occur, hence, a larger bubble volume.

The bubble shape changed with increasing flowrate and increasing viscosity, as was noted in the literature (Section 2.5). In addition, bubble shape also changed as the bubbles rose through the height of the liquid. Bubble shape is a function of bubble volume and the liquid properties. As the larger bubbles rose through the liquid, their diameter increased due to expansion, resulting in higher bubble Reynolds numbers with height. According to Dekée et al. (1986), the bubble

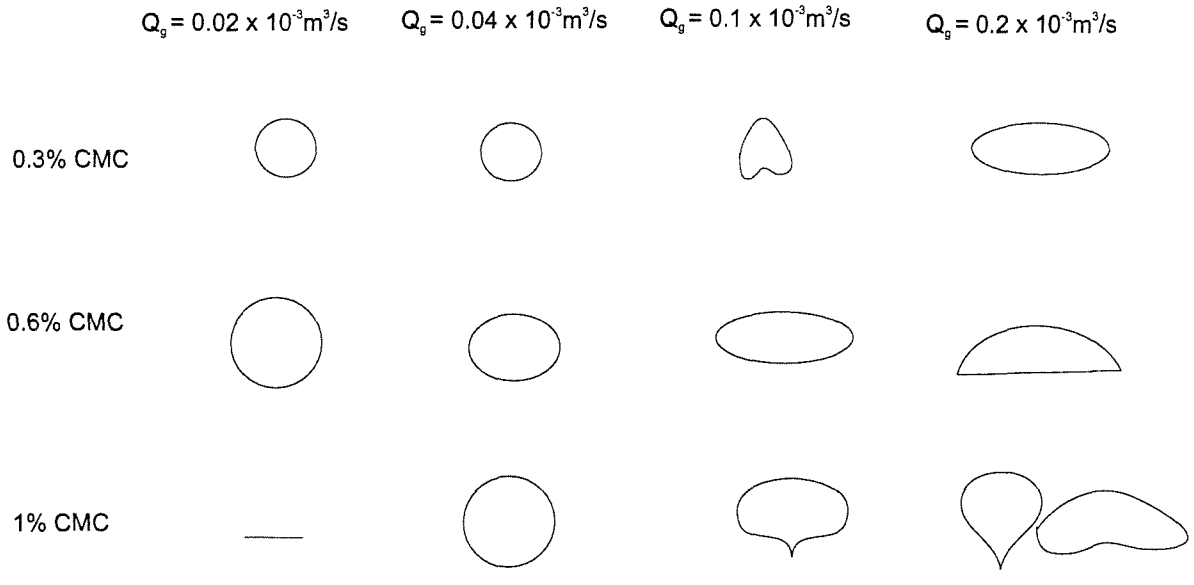

Figure 4.4: Bubble shapes observed for Sparger A at the lab-scale in each CMC solution

shape is dictated by the bubble Reynolds number. In the current work, the bubble shape was observed to change with liquid height. This was more marked in the 1% CMC and 0.6% CMC than the 03% CMC solution.

The bubbles tended to be spherical at the two lowest gas flowrates, for each CMC solution. As the flowrate increased, the bubble volumes increased. At 0.1 x $10^{-3}m^3s^{-1}$, the bubbles increased in volume and changed in shape due to coalescence as they rose through the height of the liquid.

At this flowrate, in 0.3% CMC, the bubble was no longer spherical but at an intermediate stage between spherical and ellipsoidal, being convex at the top and concave at the bottom. As the bubbles rose through the height of the liquid, coalescence occurred in the top half of the vessel, changing the bubble shapes to ellipsoidal in the top one third of the vessel.

In 0.6% CMC, the bubbles were similar in shape to those in the lower half of the 0.3% CMC filled vessel, although the base of these bubbles was flat rather than concave. Due to coalescence in the top half of the vessel, the bubble shape became ellipsoidal.

In 1% CMC, the bubble shape changed from spherical to ellipsoidal and finally, spherical capped due to coalescence as the bubbles rose through the liquid height.

At the highest gas flowrate, the bubbles increased in volume once more and again, changed shape as they rose through the height of the liquid. The bubble shapes in the lower half of the vessel were similar to those described above in 0.3% CMC and 0.6% CMC, although in 1% CMC the bubble shape began as the inverted teardrop shape, becoming oblate-cusped and finally, spherical capped with increasing height. Such bubble shapes were observed in the literature for viscoelastic fluids.

Figure 4.5 illustrates the rising bubble plumes for each gas flowrate and each CMC concentration for Sparger A.

Ulbrecht et al. (1985) noted that the bubble plume wavered with increasing vessel height. This was observed in the current work but only at the highest

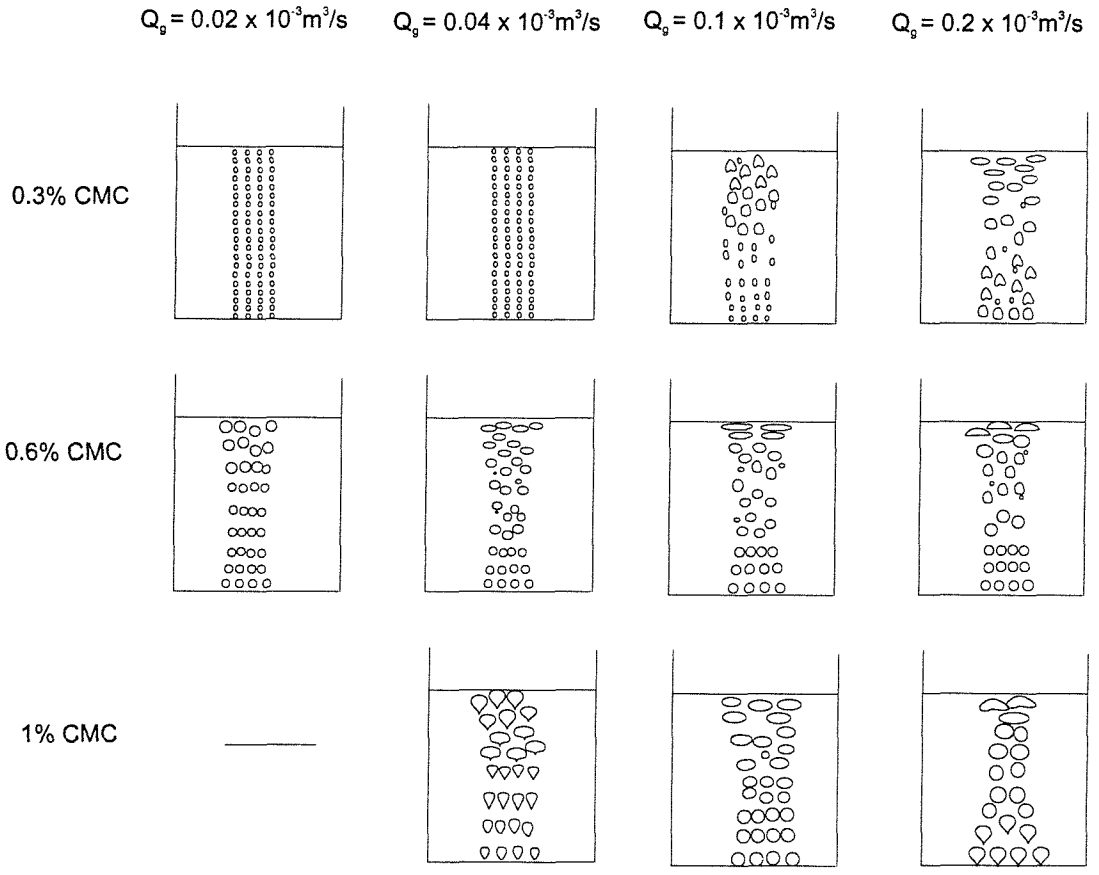

Figure 4.5: Bubble plumes observed for Sparger A in each CMC solution (lab-scale)

gas flowrate and within the top one third of the liquid height in 0.3% CMC. This phenomenon was caused by the thimble shaped bubbles coalescing, at which point, ellipsoidal bubbles were formed that rose upwards in a zigzag form until reaching the liquid surface. This effect may have been more prominent in the work of Ulbrecht et al. (1985) as although they used a slightly shear-thinning inelastic solution of polyvinylchloride (n = 0.93 and 0.92, similar to those values for the 0.3% CMC, n_{avg} = 0.82), they used higher gas flowrates than were used in the current work.

4.4 Active volume results using Sparger, A

4.4.1 Effect of power input

At the lab-scale, four gas flowrates were used ranging from 0.02 x 10^{-3} m^3s^{-1} to 0.20 x 10^{-3} m^3s^{-1} which correspond to power inputs per unit volume of 0.7, 1.4, 3.6 and 7.0 Wm^{-3}, based on isothermal expansion (Eqn. 2.2).

The highest contribution from kinetic energy would arise at the highest gas flowrate. Table 4.1 lists the power inputs to the digester both in terms of kinetic energy for a single nozzle (KE_{nozzle}), all nozzles used (KE_{tot}) and isothermal gas expansion using Eqns 2.2 and 2.9. The kinetic energy input is only important for Spargers D and F at the highest gas flowrate, assuming that all of the kinetic energy is dissipated into the surrounding liquid. In all other cases, the kinetic energy contribution is negligible compared to that of isothermal gas expansion.

Figure 4.6 shows that increasing the power input per unit volume increased the active volume. The gradient of the line of best fit for the 0.3% CMC was the steepest. The gradient of these lines for the 0.6% and 1% CMC were similar to each other, but less steep than that for the 0.3% CMC. This suggests that increasing the viscosity reduced the effect of power input on active volume.

Table 4.1: Table of power inputs per unit volume from kinetic energy and isothermal expansion

Sparger	$(P/V)_{iso}$	$(P/V)_{KE_{nozzle}}$	$(P/V)_{KE_{tot}}$	$(P/V)_{total}$
A_{lab}	0.7 - 7.0	0.0002 - 0.17	0.0055 - 0.68	0.7 - 7.68
A_{pilot}	0.7 - 7.0	0 - 0.0406	0 - 0.163	0.7 - 7.16
B	0.7 - 3.6	0 - 0.0013	0 - 0.0053	0.7 - 3.6
D	3.6 - 7.0	0.34 - 2.86	0.34 - 2.86	3.94 - 9.86
E	1.7 - 7.0	0.0003 - 0.043	0.0027 - 0.342	1.4 - 7.35
F	3.6 - 7.0	0.34 - 2.86	0.34 - 2.86	3.94 - 9.86

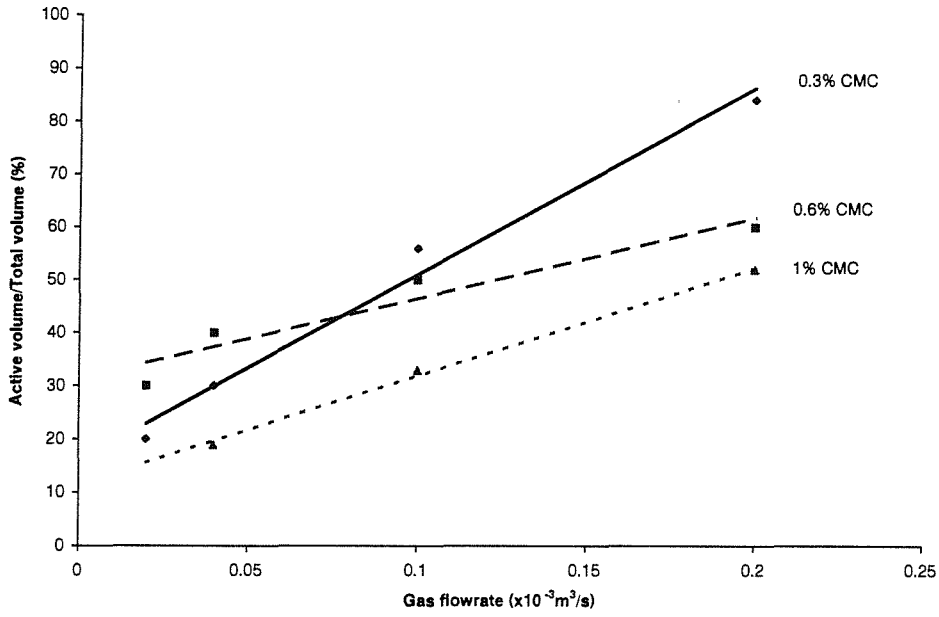

Figure 4.6: Effect of gas flowrate and viscosity on active volume (Sparger A, lab-scale)

Figure 4.7 illustrates the flowpatterns set up at each of the power inputs. In a shear-thinning non-Newtonian fluid, the flowpatterns produced by the different gas spargers were different and are useful in understanding the results obtained. For Sparger A, at the lowest power input only the central core of the vessel was active. As for bubble columns in Section 2.8.1, increasing the gas flowrate increased both the velocity of the rising bubbles and coalescence causing the bubble volumes to increase. Hence, the volume of liquid entrained increased with increasing gas flowrate extending the active volume to encompass the walls and finally at the highest gas flowrate, the surface.

The entrainment of surrounding liquid into the rising columns of gas bubbles was small at the lowest gas flowate and resulted in an active volume of 20% in 0.3% CMC. Increasing the gas flowrate increased the frequency with which the bubbles were produced at the nozzle, which in turn, increased the entrainment of the surrounding bulk liquid thereby increasing the circulation within the vessel. At the highest gas flowrate, the active volume increased to 85% in 0.3% CMC and

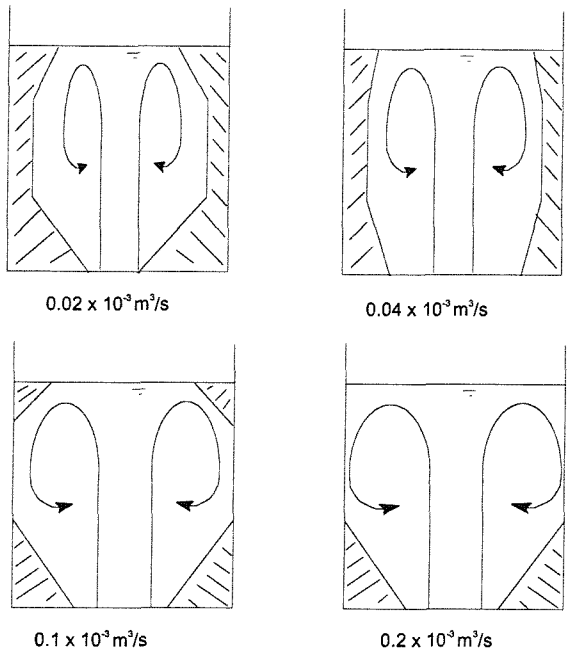

Figure 4.7: Flowpatterns and active volumes for Sparger A at 0.02, 0.04, 0.1 and 0.2 x 10^{-3} $m^{-3}s^{-1}$ in 0.3% CMC

also increased for both 0.6% and 1% CMC as shown in Figure 4.6.

The range of superficial gas velocities was calculated as 6.84 x 10^{-5} to 6.84 x 10^{-4} ms^{-1}, which suggest that the two-phase flow regime was bubbly homogeneous according to Figure 2.13 and the definitions given by Ulbrecht and Baykara (1981, Wadley (1994) and Shah et al. (1982) in Section 2.8.1.

Observation confirmed this flow regime for the two lowest gas flowrates, as shown in Figure 4.5. In each CMC concentration at these flowrates, the bubbles formed were individual bubbles rising with uniform velocity and with limited coalescence and therefore, fell into the bubbly-homogeneous regime according to the descriptions of Ulbrecht and Baykara (1981) and Shah et al. (1982). At the two highest flowrates, the two-phase flow regime changed with an increase in viscosity. The definitions of Ulbrecht and Baykara (1981, Wadley (1994) and Shah et al. (1982) imply that the flow regime remained bubbly homogeneous at these higher flowrates as the superficial gas velocity was still low, however, the pictorial representations of the different flow regimes given in Shah et al.

(1982) show a uniform distribution of single bubbles of similar volume (Figure 2.14). This does not fit with the observations made in the current work, where coalescence occurred in the top half of the vessel for each CMC concentration at the two highest gas flowrates. The definition of churn-turbulent flow did not fit these images either, and therefore, a transition region was perhaps encountered, although the superficial gas velocity for this to occur was shown (Shah et al., 1982) as a minimum of 0.04 ms^{-1} at a column diameter of 0.6m, compared with a maximum of 6.84 x 10^{-4} ms^{-1} in the current work. Therefore, it would appear that for solutions with viscosity higher than water and in large diameter vessels, the flow regime transitions occur at lower superficial gas velocities than defined in the literature for air-water systems, in narrow columns.

4.4.2 Effect of viscosity

Changing the rheologies by using different concentrations of CMC had a dramatic effect on the active volume. Figure 4.6 illustrated that increasing the CMC concentration reduced the active volume over the gas flowrate range used in this work despite an increase in bubble diameter (see Figure 4.4). However, an increase in viscosity results in an increase in bubble volume as a greater bubble buoyancy force is required to overcome the liquid inertia force, therefore, the bubble remains at the nozzle for longer before detachment. Hence, the bubble release frequency is reduced, resulting in fewer bubbles and subsequently, fewer wakes and a reduced liquid entrainment.

At all flowrates and in 0.3% and 0.6% CMC, four columns of bubbles were observed (see Figure 4.5). This was also the case for 1% CMC apart from the highest gas flowrate, where four columns were only observed in the lower half of the liquid height. The rising bubble columns in the 0.3% CMC remained very straight at each flowrate. In 0.6% CMC, the diameter of the circle outlined by the rising bubble plumes was similar at the surface to that in the vessel base, but the diameter at mid-depth was smaller, the plumes exhibiting a true cooling tower

shape, as observed in the literature by Ulbrecht et al. (1985). In 1% CMC, the diameter of the rising plumes was narrower at the liquid surface than elsewhere in the liquid height. Towards the liquid surface, rather than coalescence occurring solely within each bubble plume, coalescence occurred between neighbouring plumes reducing the number of rising bubble columns. This effect was visible at the lowest gas flowrate and became more marked as the flowrate increased until at the highest gas flowrate, only one effective plume of large spherical cap bubbles was observed at the liquid surface.

Chhabra (1993) noted an increase in interfacial tension in non-Newtonian shear-thinning liquids as viscosity increased. The bubble volume models of Davidson and Schuler (1960a) and Kumar and Kuloor (1970) show that the bubble volume formed at the orifice is proportional to the viscosity of the liquid (Eqns 2.4 and 2.5). This supports the findings of larger bubble volumes in 1% CMC compared to 0.6% and 0.3% CMC. However, the rise velocity of the bubbles decreased with an increase in volume. The rise velocities for the Stokes regime and Hadamard regime for creeping flow were defined in Eqns 2.7 and 2.8 in Section 2.5.2 where the rise velocity was inversely proportional to the dynamic viscosity (and kinematic viscosity) although it was proportional to the bubble volume. That is to say, that an increase in bubble volume would increase the bubble rise velocity in the same fluid. An increase in liquid viscosity would result in a decrease in bubble rise velocity. From the current work, it would appear that for the gas flowrate range and the solutions tested, the effect of the liquid viscosity was greater than the increased volume on bubble rise velocity.

Figure 4.8 illustrates the flowpatterns setup in the three CMC concentrations for the highest and lowest gas flowrates.

Increasing the viscosity increased the drag on the bubbles. The rise velocity of the bubbles was reduced in the thicker CMC solutions. This resulted in reduced circulation velocities and lower active volumes than in the thinner CMC solutions.

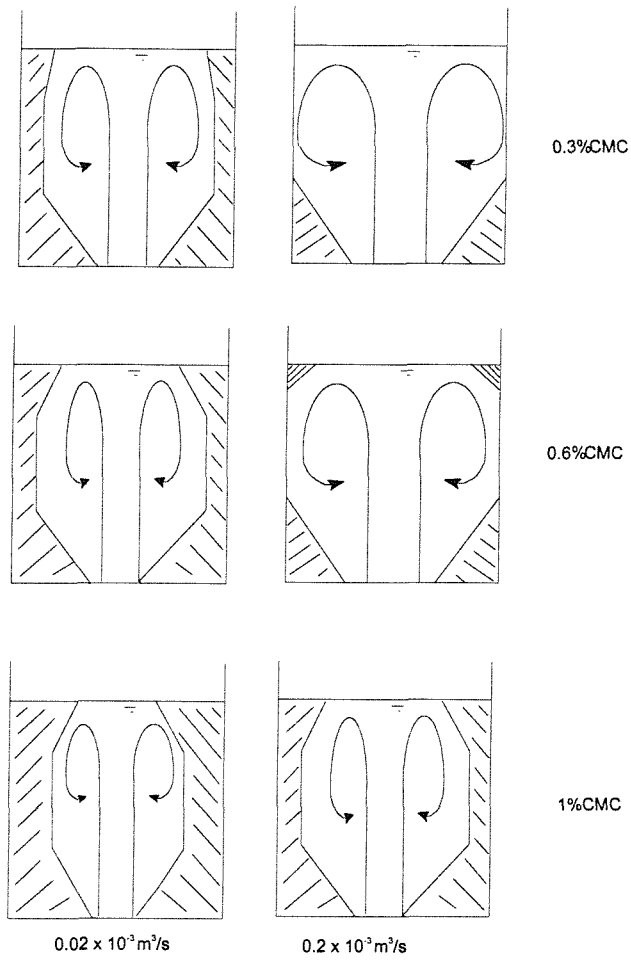

Figure 4.8: Flowpatterns and active volumes for Sparger A at 0.02 and 0.2 x 10^{-3} $m^{-3}s^{-1}$ in 0.3%, 0.6% and 1% CMC (lab-scale)

4.4.3 Effect of aspect ratio

To investigate active volumes and blend times of digester geometries found at the full-scale, the aspect ratio was reduced from 1 to 0.5 to cover the range found by Ouziaux (1997). The liquid height was reduced to 0.305m whilst maintaining the diameter as 0.61m and using Sparger A. Three gas flowrates of 0.02, 0.1 and 0.2 x 10^{-3} m^3s^{-1} were used in the three CMC concentrations.

Figure 4.9 shows the difference in active volumes recorded at different gas flowrates in each CMC concentration at the two aspect ratios. Although data were not recorded in all cases, at each gas flowrate and in the same CMC concentration,

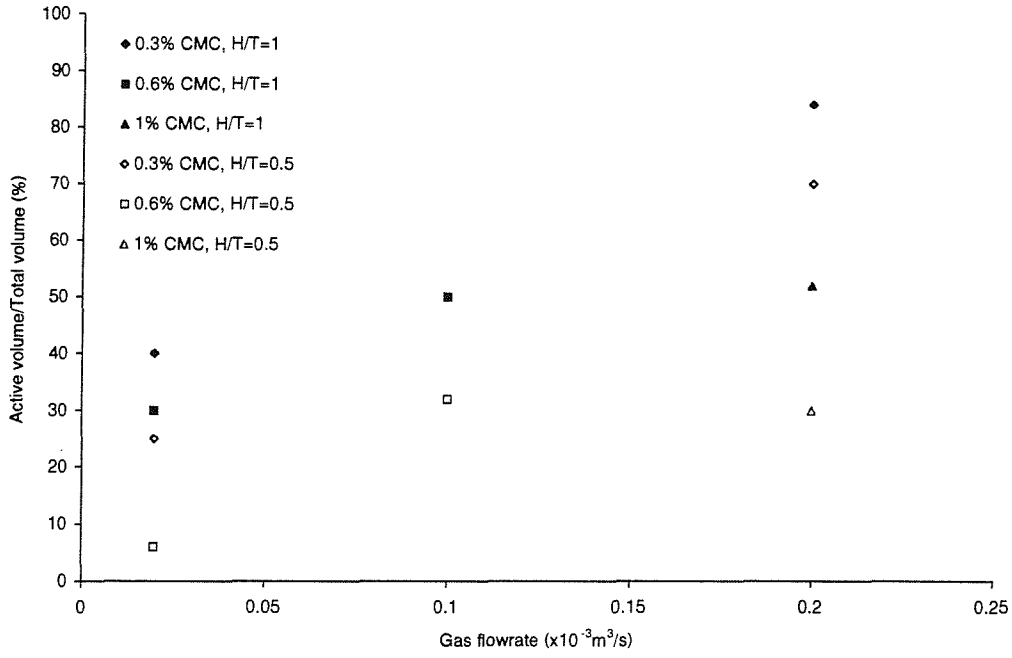

Figure 4.9: Effect of aspect ratio on active volume for Sparger A (lab-scale)

the percentage active volume was lower at the aspect ratio of 0.5 than at the aspect ratio of 1.

The gas flowrate to the two aspect ratios was held constant and the only difference between the two vessels was the height of liquid.

By considering the power input due to isothermal gas expansion, keeping all parameters constant apart from the liquid height, the power input becomes:

$$P \propto \ln\left[\frac{p_n}{p_a}\right] \tag{4.1}$$

where P = power input; p_n = pressure at nozzle and p_a = pressure at liquid surface

The power inputs at the two aspect ratios can be compared as:

$$\frac{P_1}{P_{0.5}} = \frac{\ln\left(\frac{p_n}{p_a}\right)_1}{\ln\left(\frac{p_n}{p_a}\right)_{0.5}} \tag{4.2}$$

where P_1 = power input for digester with aspect ratio 1; $P_{0.5}$ = power input for digester with aspect ratio 0.5

In Eqn. 4.2, the pressure at the surface is the same (taken as 10.33m head of water in this case), but the pressure at the nozzles is different due to the difference in static head, ie:

$$\frac{(p_n)_1}{(p_n)_{0.5}} = \frac{10.33 + H}{10.33 + \frac{H}{2}} \tag{4.3}$$

where H = liquid height = 0.61m

and Eqn. 4.2 becomes:

$$\frac{P_1}{P_{0.5}} = \frac{\ln\left(\frac{10.33+0.61}{10.33}\right)}{\ln\left(\frac{10.33+0.305}{10.33}\right)} = \frac{0.0574}{0.0291} = 1.972 \tag{4.4}$$

Hence:

$$P_{0.5} = 0.507P_1 \tag{4.5}$$

The total power input almost halved by halving the aspect ratio and the volume of liquid has been halved by halving the aspect ratio. Therefore:

$$\left(\frac{P}{V}\right)_{0.5} = \frac{0.507P_1}{0.5V_1} = 1.041\left(\frac{P}{V}\right)_1 \tag{4.6}$$

where V = volume

Therefore, the power input per unit volume is almost the same when halving the aspect ratio at constant gas flowrate, yet the percentage active volume has decreased.

The reduced liquid height has a second impact on the active volume. The greater the liquid height, the more the bubbles will coalesce and expand, resulting in greater liquid entrainment. Reducing the liquid height reduced the chances of coalescence, thus reducing the bubble expansion and liquid entrainment. For the cases where coalescence occurred, Figure 4.5 showed that coalescence only occurred in the top half of the vessel. By reducing the liquid height, coalescence was reduced, which resulted in a reduced active volume due to reduced entrainment.

This would suggest that digesters with a high aspect ratio would induce more liquid circulation than those of lower aspect ratios because of increased coalescence and therefore, have a higher percentage active volume than a low aspect ratio digester. Therefore, aspect ratio is an important consideration in design.

4.4.4 Effect of nozzle diameter

The nozzle diameter for Sparger A was 2mm, this was increased to 4mm for Sparger B. Measurements were taken at two gas flowrates (0.2 and 0.1 x 10^{-3} $m^{-3}s^{-1}$) in 0.3% CMC only. Sparger C consisted of fine bubble diffusers fitted to the Sparger A layout. This sparger was tested at 0.1 and 0.2 x 10^{-3} $m^{-3}s^{-1}$. Spargers A, B and C are compared in this section although only 1 gas flowrate can be compared directly (0.1 x 10^{-3} $m^{-3}s^{-1}$).

Figure 4.10 shows the active volumes recorded for Spargers A, B and C. The active volumes for each sparger were very similar to each other suggesting that the nozzle sizes used for this sparger had little effect on active volume at a given power input.

It was noted in the literature review (Section 2.5.1) that the effect of orifice diameter on bubble volume appeared to be negligible. According to the models of Davidson-Shuler and Kumar-Kuloor (Eqns 2.4 and 2.5), bubble volume at de-

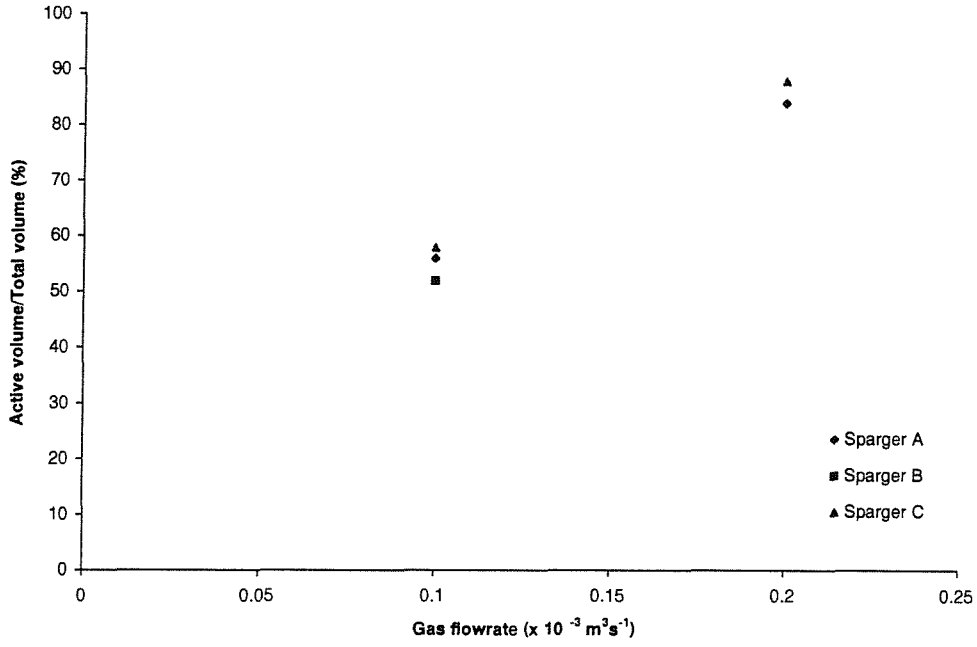

Figure 4.10: Active volumes for Spargers A, B and C (lab-scale)

tachment was only a function of liquid viscosity, gas flowrate and liquid density. If two nozzles of different diameter were used in the same liquid with constant physical properties and at a constant gas flowrate therefore, it would appear that the bubble volume would be the same.

Figures 4.11(a), (b) and (c) illustrate the observed bubble diameters for Spargers A, B and C respectively.

The diffusers produced many tiny bubbles which coalesced as they rose through the liquid height. The bubble volumes towards the liquid surface were spherical and much larger than those produced at the diffuser itself. These larger bubbles were mixed with smaller bubbles, as shown in Figure 4.11(a). The 2mm nozzles produced fewer bubbles with larger diameters than those produced by the sparger and they rose with a lower velocity than those from the diffuser. The 4mm nozzles produced fewer bubbles with larger diameters that rose with a lower velocity than either the 2mm nozzles or diffusers. Therefore, observation showed that increasing nozzle diameter increased the bubble volume, but reduced the formation frequency

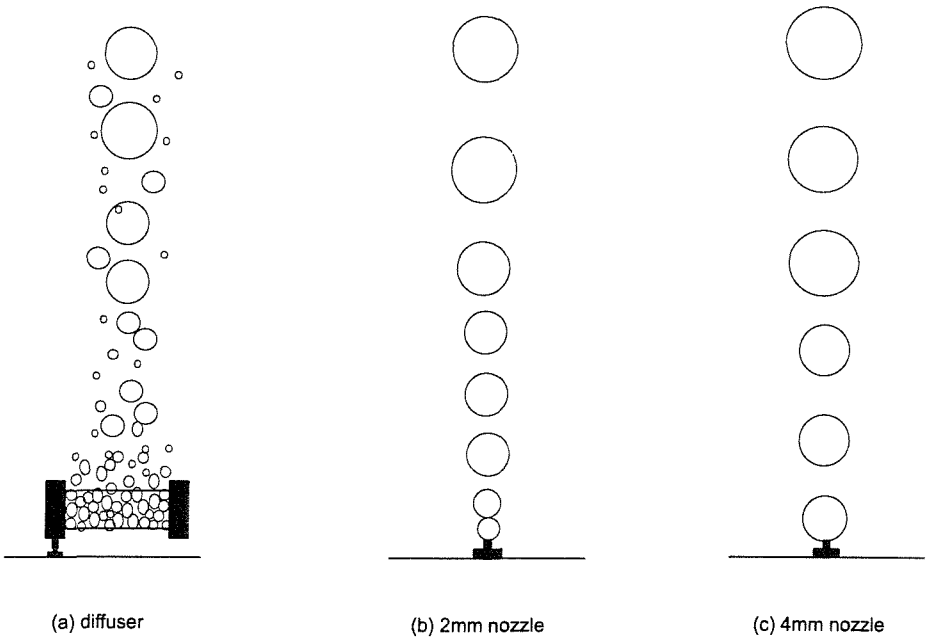

Figure 4.11: Bubble plumes produced by Spargers A, B and C (lab-scale)

and the rise velocity. However, these effects have had little effect on the active volume, suggesting that the overall liquid entrainment for each sparger type was similar.

4.5 Blend time results using Sparger A

4.5.1 Effect of power input

As expected, increasing the gas flowrate decreased the active blend time at a constant CMC concentration. This was true for each of the CMC concentrations used. Figure 4.12 illustrates the effect of gas flowrate on blend time in the active volume.

Increasing the gas flowrate increased the volume and velocity of the rising gas bubbles thus increasing the rate at which the surrounding liquid was entrained into the bubble wakes. This results in increased bulk flow and reduced blend times.

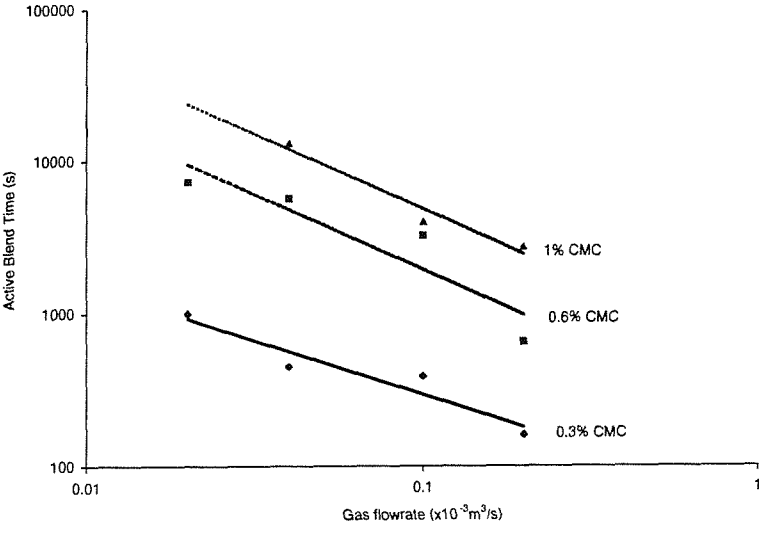

Figure 4.12: Effect of gas flowrate and viscosity on blend time for Sparger A (lab-scale)

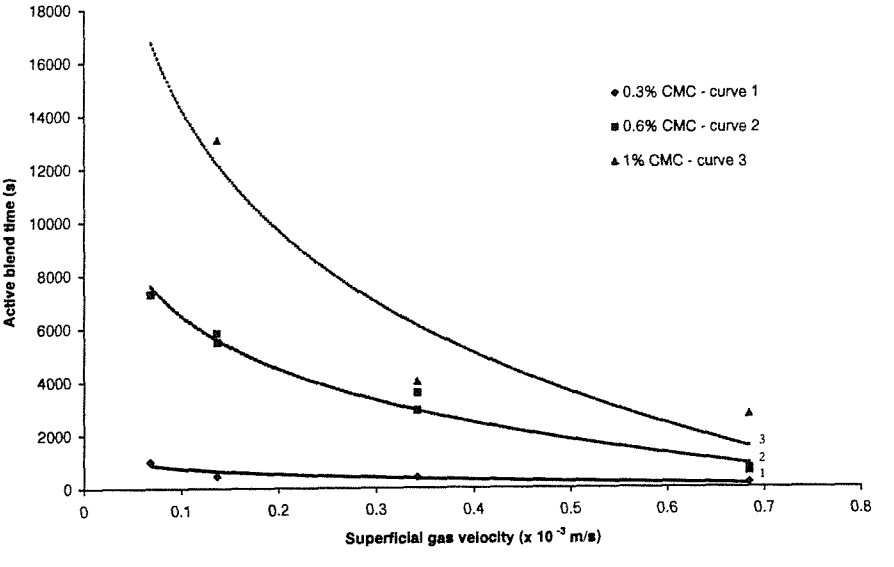

Figure 4.13: Effect of superficial gas velocity for Sparger A on blend time (lab-scale)

The gradient of the three lines shown in Figure 4.12 are very similar, suggesting that the degree of the blend time reduction was strongly proportional to gas flowrate for the three liquid viscosities tested.

Pandit and Joshi (1983) and Haque et al. (1987) both observed a decrease in blend time with an increase in superficial gas velocity (gas flowrate). Figure 4.13 shows active blend time against superficial velocity for the current work and shows similar trends to Figures 2.16 and 2.17. Despite a lower range of superficial gas velocity compared to the literature, the blend time decreased exponentially as superficial gas velocity increased. However, no minimum value was observed as reported by Pandit and Joshi (1983) and Ulbrecht et al. (1985). Ulbrecht et al. (1985) attributed this minimum value to a change in plume flow regime, such as viscous to helical. No such change was observed during the current work, perhaps because the superficial gas velocity range used was much lower than the value at which Ulbrecht et al. (1985) observed this minimum.

4.5.2 Effect of viscosity

Figure 4.12 showed that increasing the viscosity increased the active blend time. The increase in active blend time with concentration for a given power input was a direct result of the increased drag and reduced wake entrainment for a given power input.

Pandit and Joshi (1983) and Haque et al. (1987) also observed an increase in blend time with increased viscosity. The differences in blend times becoming less marked with increasing gas flowrate (superficial gas velocity) as shown previously in Figures 2.16 and 2.17.

4.5.3 Effect of aspect ratio

Figure 4.14 shows the effect of aspect ratio on blend time. In 0.3% CMC, the active blend times recorded were similar for both aspect ratios, decreasing with

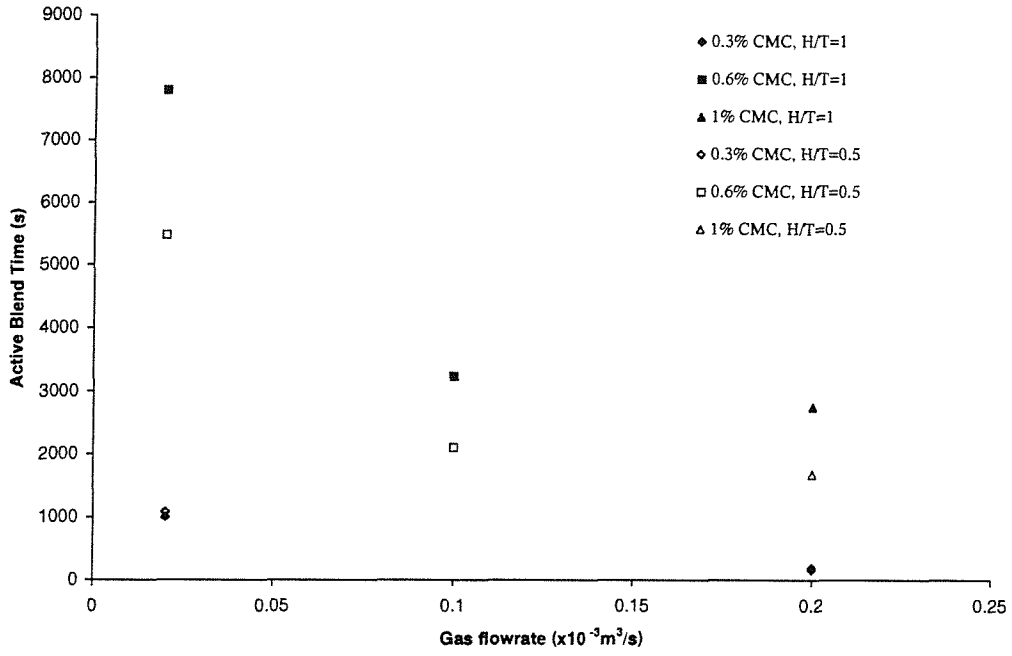

Figure 4.14: Effect of aspect ratio on blend time for Sparger A (lab-scale)

an increase in gas flowrate. In 0.6% and 1% CMC, the active blend times at the lower aspect ratio were shorter than those at an aspect ratio of one, for all gas flowrates. As the active volume was smaller at $H/T = 0.5$, there was a smaller volume to mix, resulting in a shorter active blend time.

Pandit and Joshi (1983) and Haque et al. (1987) both studied the effect of aspect ratio on blend time, over a total range of aspect ratios from 1 to 8. Both research groups observed a shorter blend time at constant gas flowrate as the aspect ratio was reduced.

4.5.4 Effect of nozzle diameter

Figure 4.15 shows the active blend times recorded in 0.3% CMC for Spargers A, B and C. Sparger C recorded the shortest blend time followed by Sparger B and finally, Sparger A.

Section 4.4.4 presented the observed bubble plumes from the individual spargers and concluded that an increase in nozzle diameter resulted in fewer, slightly

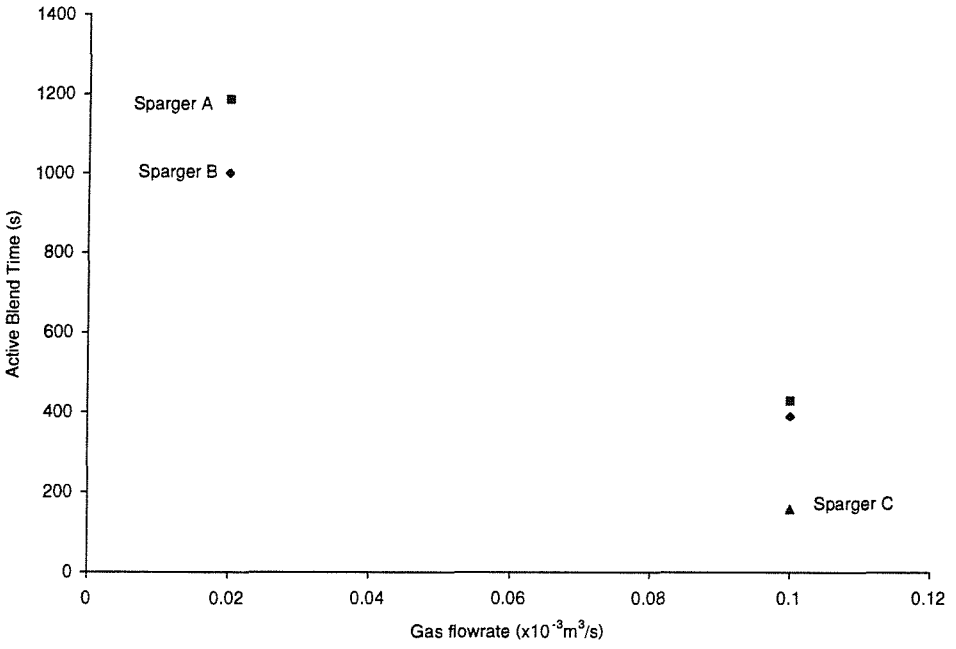

Figure 4.15: Effect of nozzle diameter on active blend time in 0.3% CMC (lab-scale)

larger bubbles, spaced further apart but rising slightly faster than those produced by smaller diameter nozzles, at equal gas flowrate. The kinetic energy based on gas flow through the nozzles would have been slightly less for the 4mm nozzles than the 2mm nozzles (a maximum of 0.011 Wm^{-3} with 4mm nozzles and 0.17 Wm^{-3} with 2mm nozzles at the highest gas flowrate). However, in both cases, the kinetic energy contribution was negligible compared to that from isothermal gas expansion.

Fewer bubbles would result in fewer wakes in the vessel with Sparger B. However the bubbles produced with Sparger B entrained more liquid into each wake because of their increased velocity and larger diameter. It would appear that the overall entrainment was similar since the active blend times and active volumes were similar at both nozzle sizes. Therefore, the overall effect of increasing the nozzle diameter from 2mm to 4mm had little influence on active blend time.

4.5.5 Effect of scale

Figure 4.16 illustrates the effect of power input and viscosity for both scales of vessel. The trends at the two scales are identical. For constant power input per unit volume, the active blend times at the pilot-scale were very similar to those recorded at the lab-scale.

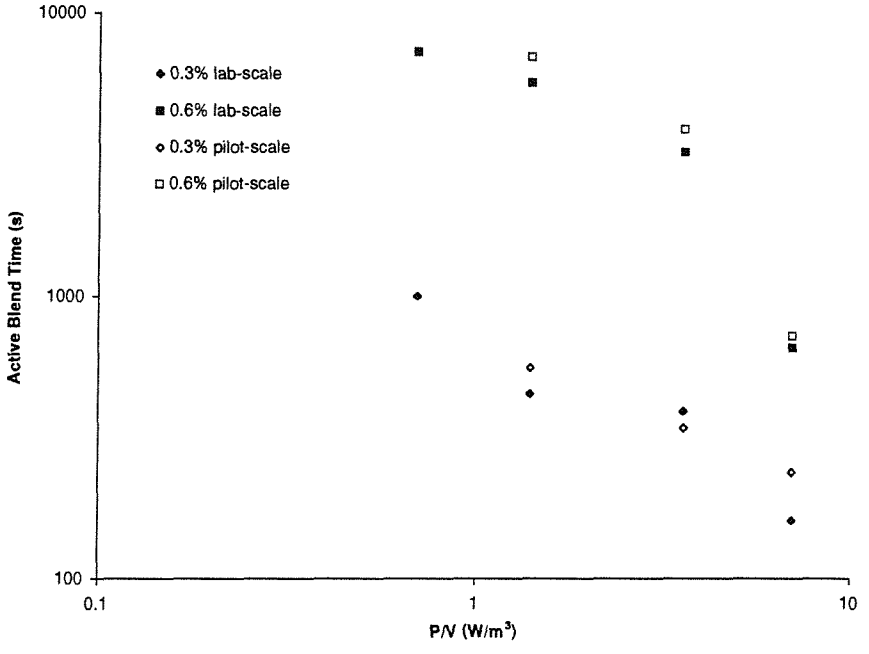

Figure 4.16: Effect of scale on active blend time

The work performed at the pilot-scale has suggested that scaling active blend time based on equal P/V is a valid method.

4.6 Comparison of sparger types

The six spargers listed in Section 3.4 and illustrated in Figure 3.7 were compared at the lab-scale over two gas flowrates, 0.1 and 0.2 x 10^{-3} m^3s^{-1} in both 0.3% and 0.6% CMC. Sparger B was compared at 0.02 and 0.1 x 10^{-3} m^3s^{-1} and therefore, does not appear at 0.2 x 10^{-3} m^3s^{-1} on all of the figures that follow.

4.6.1 Comparison of active volumes

Figures 4.17 and 4.18 illustrate the active volumes achieved by each of the spargers in 0.3% and 0.6% CMC respectively.

The order of performance was the same in both CMC concentrations for the 3 spargers recording the shortest blend times. In all cases, the sequence sparger (D) performed best with an active volume of 100%. Spargers A, B and C all had similar active volumes although C recorded the lowest at $Q_g = 0.1$ x 10^{-3} m^3s^{-1}, in 0.6% CMC.

At any one time during the sequencing of Sparger D, an inactive volume was observed at the base of the vessel opposite the nozzle in use. As this nozzle changed every 60 seconds, the inactive volume became active as the gas supply moved to the next nozzle in the sequence. In so doing, the inactive volume moved to the next nozzle, causing the base of the vessel opposite the active nozzle to become inactive. For the majority of the time therefore, the probes were located in an active volume, the inactive volume moving around the vessel base.

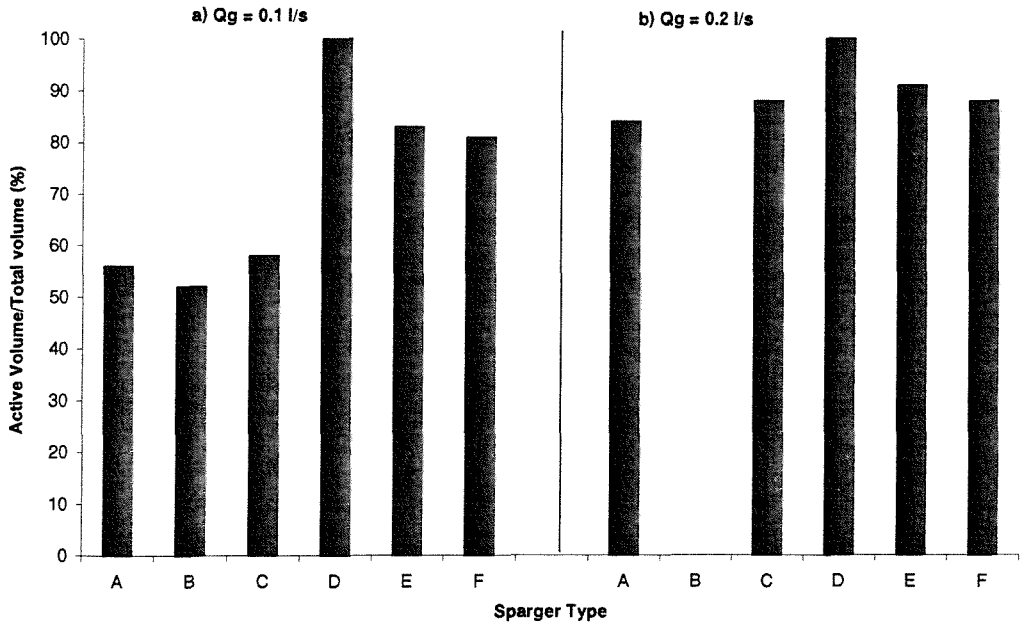

Figure 4.17: Effect of sparger type on active volume (in 0.3% CMC)

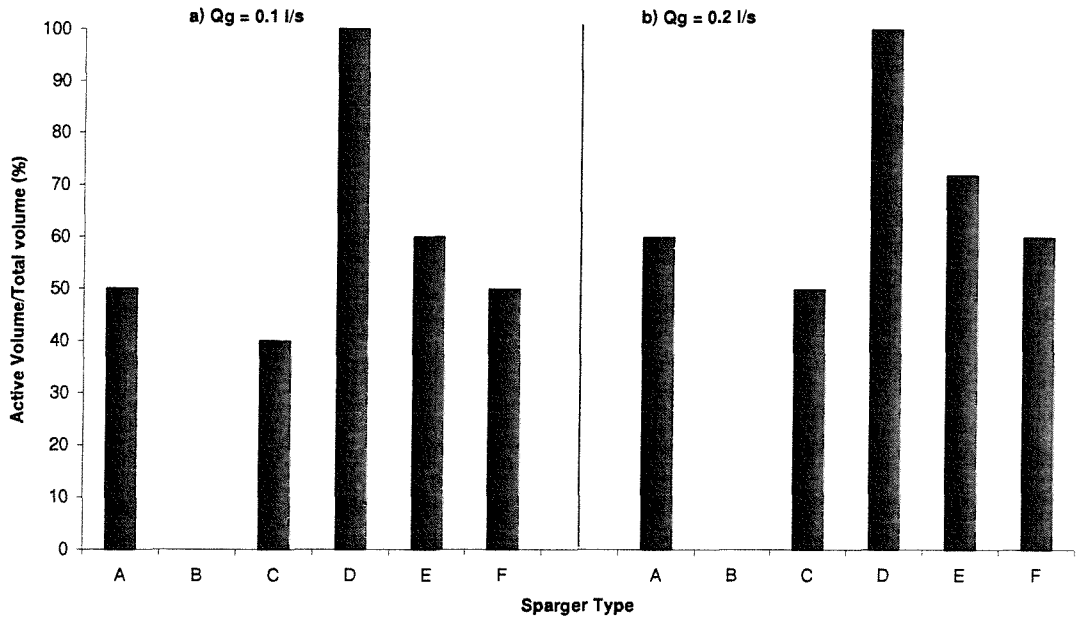

Figure 4.18: Effect of sparger type on active volume (in 0.6% CMC)

Sparger E consisted of 8 nozzles in the outer ring. The entire vessel was active apart from the central cylinder and the flowpattern was reversed compared to Spargers A, B, C and F. An annular upward flow region formed by the walls, and the central cylinder was downward flowing. This cylinder decreased to a central cone in 0.3% CMC at a gas flowrate of 0.2 x 10^{-3} m^3s^{-1} as shown in Figure 4.19.

Spargers A, B, C and F all had similar flowpatterns consisting of a central rising plume of liquid and gas and an annular downcomer.

In each case tested, Sparger F had an equal or higher active volume than Spargers A, B and C, despite having a smaller initial sparger area (1 nozzle opposed to 4 nozzles of diameter $0.2T$).

However, the kinetic energy contribution from Sparger F was greater than for the other spargers. From Table 4.4, at 0.2 x 10^{-3} m^3s^{-1}, the total power input from Sparger A was 7.68 Wm^{-3}, compared to 7 Wm^{-3} for isothermal expansion alone. At the same flowrate, the total power input from Sparger F was 9.86 Wm^{-3}. As discussed in Section 2.5.4, it is not clear whether all of this kinetic

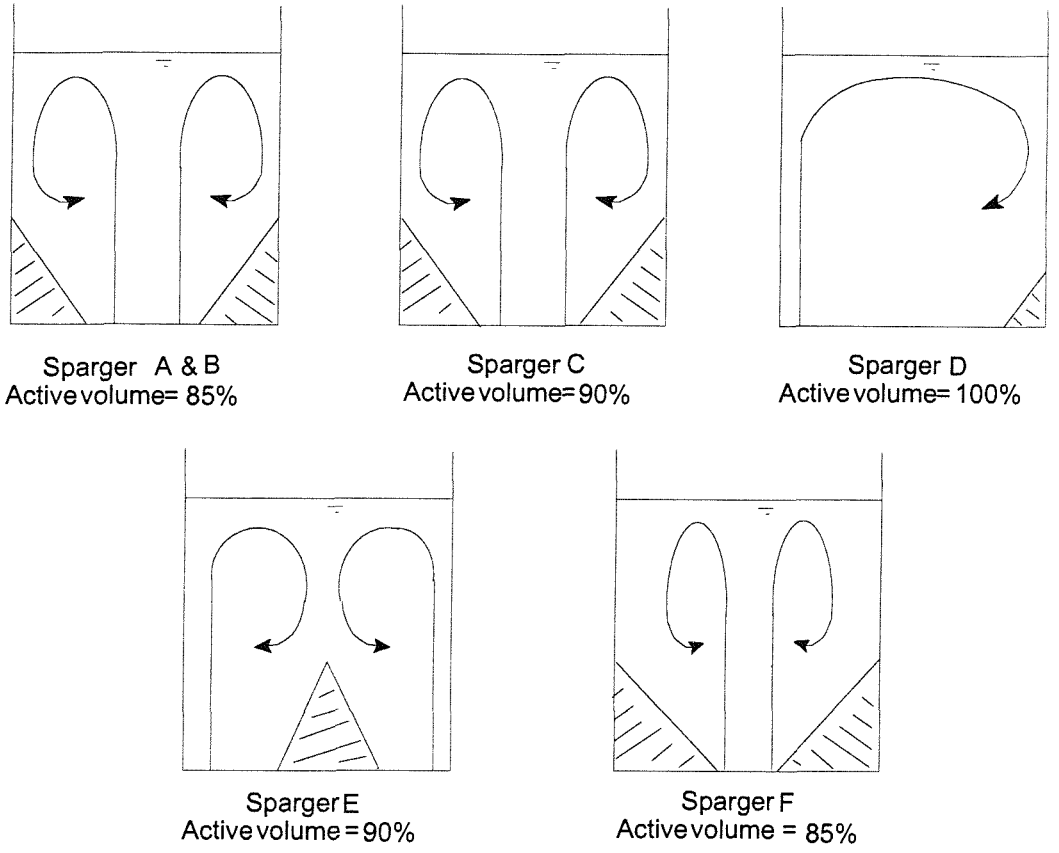

Figure 4.19: Flowpatterns and active volumes for Spargers A, C, D, E and F at Q_g = 0.2 x 10^{-3} m^3s^{-1} in 0.3% CMC

energy would be transferred to the surrounding liquid, as some may remain within the bubbles, leaving the vessel at the liquid surface Chhabra (1993). At 0.1 x 10^{-3} m^3s^{-1}, the power input was reduced to 3.69 Wm^{-3} for Sparger A and 3.95 Wm^{-3} for Sparger F. The kinetic energy from Sparger F was always sixteen times that from Sparger A at all gas flowrates because Sparger A contained 4 nozzles. The bubble diameters were also larger with Sparger F than Sparger A. In addition, the frequency of bubble production at the orifice of Sparger F was greater than Sparger A, therefore, the rate of coalescence was greater for Sparger F, hence, larger bubbles.

Spargers F and D both used single nozzles, therefore comparison can be made on equal power inputs, considering both isothermal gas expansion and kinetic

energy. The active volume of Sparger F was less than that achieved by Sparger D for each flowrate and in each CMC solution. The movement of the inactive volume around the vessel as the sequence moved around the digester has resulted in a high active volume.

The active volumes obtained in 0.6% CMC were lower for each sparger than in 0.3% CMC due to the increased drag on the bubbles. In the higher viscosity, Sparger D consistently produced the highest active volume.

The size of the active volume was dependent on the sparger arrangement, liquid viscosity and gas flowrate. In addition, the power input due to the kinetic energy of the gas through the nozzles may be significant, depending on the sparger type, nozzle diameter and gas flowrate. It should initially be calculated before deciding whether it can be neglected or not.

4.6.2 Comparison of blend times

Figure 4.20 shows the results for gas flowrates of 0.1 and 0.2 x 10^{-3} m^3s^{-1} in 0.3% CMC. At the lower gas flowrate, Sparger C produced the shortest active blend time, closely followed by Spargers F and D. A slightly higher active blend time was recorded for Sparger A which was similar to Sparger B and finally, Sparger E.

Increasing the gas flowrate to 0.2 x 10^{-3} m^3s^{-1} changed the order slightly, but the differences between the active blend times were very small and could be considered as equal, at least between Spargers A, C and D.

Figure 4.21 presents the effect of increasing viscosity. Sparger D performed well with increased viscosity.

Previously, in the discussion of the effect of sparger type on the active volume, Sparger F was shown to have up to an extra 2.86 Wm^{-3} (assuming all of the kinetic energy was transferred to the liquid) at the highest gas flowrate of 0.2 x 10^{-3} m^3s^{-1}. This potential extra power input did not noticeably improve the active blend time results in either CMC concentration in relation to other spargers.

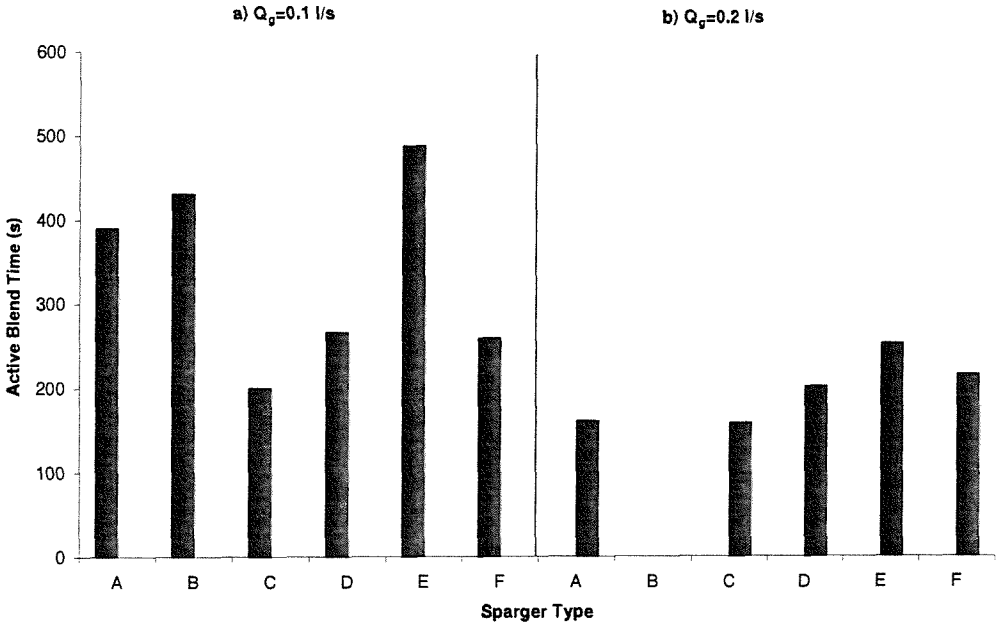

Figure 4.20: Effect of sparger type and gas flowrate on blend time (in 0.3% CMC)

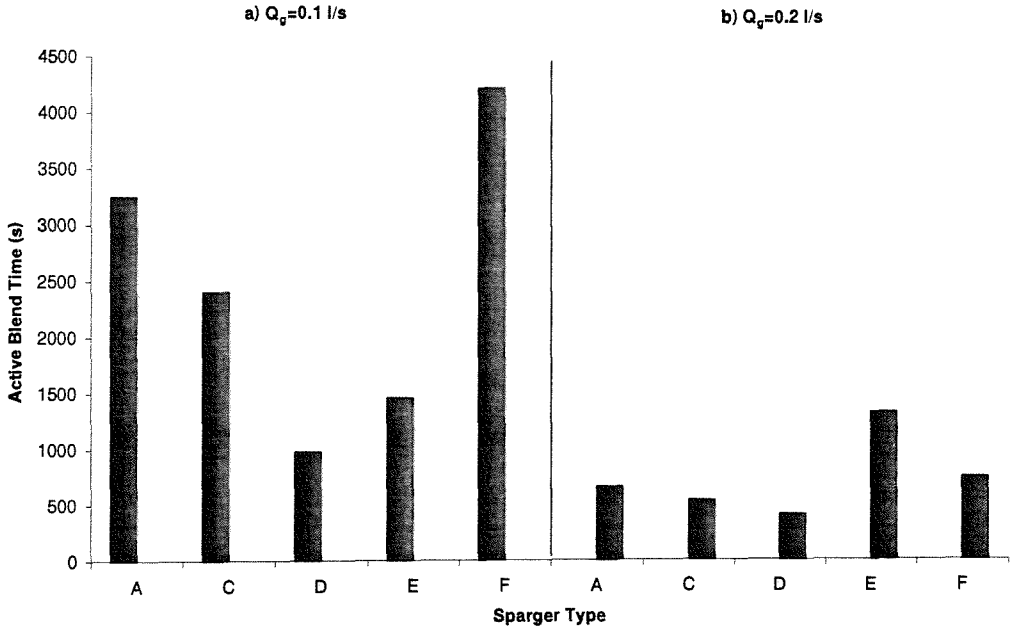

Figure 4.21: Effect of sparger type and gas flowrate on blend time (in 0.6% CMC)

Thus, it may be assumed that not all of the kinetic energy is transferred to the surrounding liquid.

The difference between the active and total blend times was not as great in 0.6% CMC as for 0.3% CMC. The active and total blend times for each sparger were shorter in 0.3% CMC than 0.6% CMC due to reduced viscosity, increased rise velocity, increased liquid entrainment and increased liquid circulation velocity.

Overall, Sparger D produced the shortest active blend times in both CMC solutions.

4.7 Effect of inlet position

The inlet position was selected based on the full-scale findings of Ouziaux (1997) and was at a fixed distance from the wall and below the surface. To investigate the effect of inlet position, a second location was used. Figures 3.14(a) and (b) illustrated the different inlet positions that were studied in this work for Spargers A and D respectively.

4.7.1 Sparger A

Figure 4.22 shows the results for the different feed position for Sparger A. The active blend times recorded were almost identical at each gas flowrate and for each feed position. Therefore, there was no effect of feed position on active blend time.

4.7.2 Sparger D

Figure 4.23 shows the results for the different feed position for Sparger D, although only in terms of active blend time as there were no inactive zones for this sparger over the conditions tested.

The original inlet position for Sparger D was against the wall, as for A1, but above the first nozzle in the sequence. To determine whether inlet location had

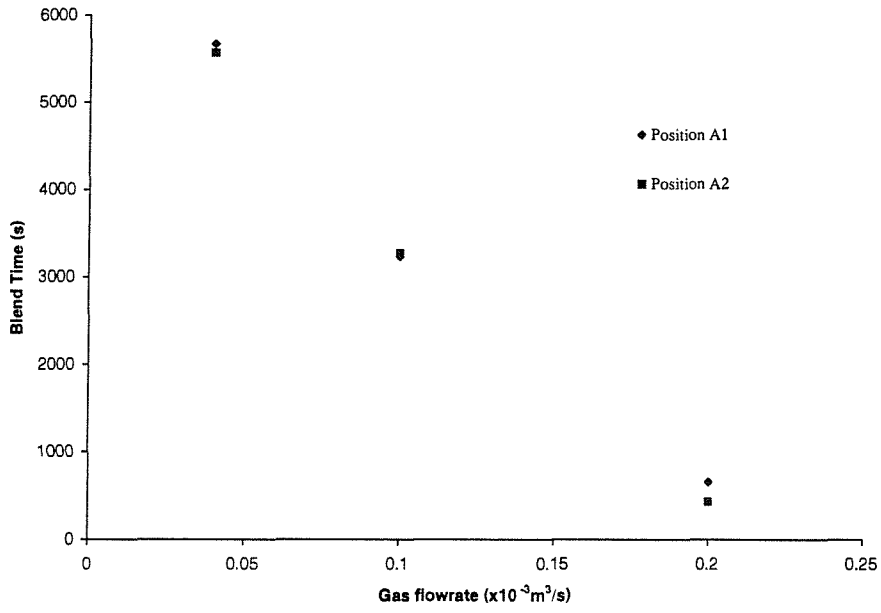

Figure 4.22: Effect of feed position on Sparger A's blend times in 0.6% CMC

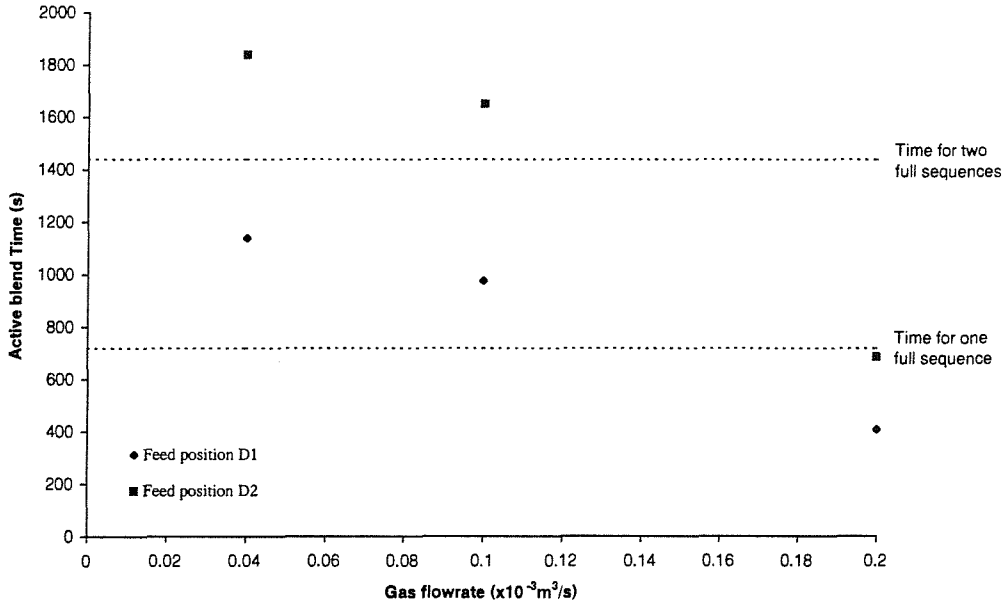

Figure 4.23: Effect of feed position on Sparger D's blend times in 0.6% CMC

an effect on blend time, the inlet was moved to the opposite side of the vessel so that it was as far away as possible from the influence of the first nozzle in the sequence. This was position D2.

Adding the feed at position D2 increased the blend time compared to D1. However, the vessel surface was fully active at each of the gas flowrates used and the tracer was not added into an inactive volume. The measured increase in blend time was least at the highest power input and greatest at the lowest power input. In all cases though, the blend time increased by the time taken for one full sequence to take place, or less (Section 3.4).

4.8 Correlating Blend Time and Active Volume Data

4.8.1 Literature correlations

The Literature review performed within this thesis (Chapter 2) focused both on anaerobic digestion work and bubble column work. No correlations were found for either blend time or active volume prediction in the area of anaerobic digestion of sewage sludge.

Circulation time approach

Ulbrecht et al. (1985) developed their work from Ulbrecht and Baykara (1981) coming up with a circulation time approach using Equation 2.17 which expands to:

$$Re_L^* = \frac{\rho_L u_L^{2-n} T^n}{k} = 3.34 \left[\frac{\rho_L u_{sg}^{2-n} T^n}{k} \left(\frac{u_{sg}^2}{gT} \right)^{-0.25} \right]^{0.92} \tag{4.7}$$

This model was used in the current work to predict the liquid plume velocity in the laboratory model digester which was then used to determine a circulation

time. In the current work, liquid plume velocity proved very difficult to measure because of the extent of liquid between the rising plume and the vessel wall. The velocities in this region were observed by means of neutrally buoyant flow followers and were shown to vary extensively with radial distance as a result of the decrease in shear-rate from the plume to the wall. The predicted liquid plume velocities from Eqn. 4.7 were much lower than those measured due to the difficulty experienced by the flow followers in entering the bubble plume itself. The flow followers were usually entrained into the liquid rising next to the plume as a result of the rising bubble wakes.

Ulbrecht et al. (1985) found a relationship between the number of circulations required to blend the vessel and the liquid velocity, however in the lab-scale digester used in the current work, it was impossible to allocate a fixed number of circulations to the blend time because of the variation in shear-rate between the rising plume and the wall. Although the model of Ulbrecht et al. (1985) does take the non-Newtonian rheological behaviour into account, their column did not exhibit this shear-rate variation because of higher flowrates and a smaller column diameter. For these reasons, their model could not be used to correlate the blend time data.

Kawase and Moo-Young (1986b) produced a similar correlation to Ulbrecht et al. (1985), shown in Eqn. 2.18, which could not be applied for the same reasons given above.

Inter-cell blend time

Pandit and Joshi (1983) produced a blend time model that considered a bubble column to consist of a series of 'cells' of equal height and diameter, given in Eqn. 2.11. If the column aspect ratio was 1, this equation reduced to Eqn. 2.12. However, this also required a circulation velocity, which was not measured during this work for the reasons specified in Section 2.8.1.

Active volume

No model was found to predict the active volume proportion of a vessel.

New correlations

New correlations have been produced using the experimental data from the current work. In the absence of other workers' data to compare these results with, their applicability is currently limited to this work. However, these are the only equations to the author's knowledge that predict blend time and active volume for an anaerobic digester.

4.8.2 Production of active volume correlations

Due to the lack of adequate literature correlations for active volume, new correlations were developed. The operating variables that influenced the active volume were:

$$\text{Active volume} = f\ \{Q_g,\ (H/T),\ T,\ \mu_a,\ \rho,\ g\ \}$$

where P/V = power input per unit volume from isothermal gas expansion (Eqn. 2.2); μ_a = apparent viscosity of liquid; H/T = liquid height/vessel diameter; T = vessel diameter; ρ = liquid density and g = acceleration due to gravity

The size of the active volumes within the pilot-scale vessel could not be determined accurately as the vessel could not be viewed from the side. Only the locations of the active and inactive volumes could be determined using the probe responses. Therefore, the vessel diameter term was removed from the list of operating variables.

The apparent viscosity term in the above list requires knowledge of the shear-rates in the vessel. According to Haque et al. (1988), in a gas-mixed non-Newtonian system at low vessel Reynolds number, viscous stresses in the neighbourhood of the bubble dominate over the inertial forces and the shear-rate between the bubble and liquid film can be approximated by Eqn. 2.22.

The viscosity was calculated by inserting this calculated value of shear-rate into the Power Law equation, Eqn. 3.4. A more accurate method however, would be to measure the sludge rheology directly. The apparent viscosity at a given shear-rate can then be calculated using Eqn. 3.3.

Least squares regression was used on the natural logs of each of the operating parameters that were found to influence active volume, to produce best linear fits. Although the gas flowrate was the parameter varied during the experiments, it is related to the superficial gas velocity and to the power input due to isothermal expansion. The effect of including each of these parameters separately into the combination of regression parameters was investigated.

The flowpatterns for the different spargers could be grouped into three categories:

- Centrally rising plume with an annular downcomer (Spargers A, B, C and F)
- Sequence (Sparger D)
- Outer ring (Sparger E)

The majority of data were collected for the centrally rising plume with annular downcomer flowpattern, the sequence and outer ring types providing data for comparison between the different flowpatterns, albeit with a smaller number of data points. A correlation has been produced for the centrally rising plume type to predict the percentage active volume:

$$\frac{V_A}{V} = 37.4\mu^{-0.15}\left(\frac{P}{V}\right)^{0.17}\left(\frac{H}{T}\right)^{0.70} \qquad r^2 = 0.81 \tag{4.8}$$

where $\frac{V_A}{V}$ = percentage active volume of the vessel

Figure 4.24 demonstrates the measured and predicted active volumes.

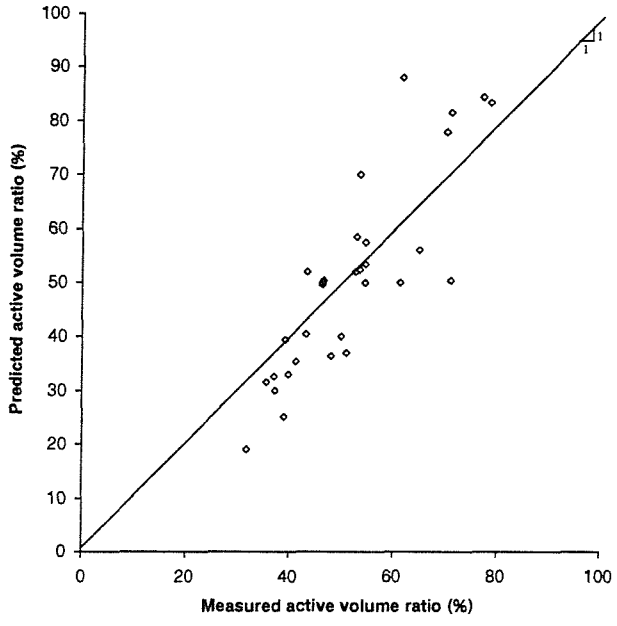

Figure 4.24: Central riser active volume correlation

4.8.3 Production of active volume blend time correlations

The literature correlations presented in Section 2.8.1 and summarised in Section 4.8.1 require knowledge of the liquid circulation velocity (Eqns 2.11; 2.12; 2.17 and 2.18). For the same reasons given in Section 4.8.1, this is not an easy measurement to make for a digester because of the range of shear-rates and therefore, liquid circulation velocities between the central rising plume and the vessel wall.

With this lack of liquid circulation information, these literature correlations have not been successfully applied to predict the blend time within the experimental digesters and therefore, new correlations have been produced from the experimental data.

The blend times that are predicted from these correlations are the blend times within the actively mixed zone of the vessel.

The same procedure as active volume prediction was followed to produce a blend time correlation for the centrally rising plume with an annular downcomer.

The operational parameters found to influence the blend time were:

$$\text{Active blend time} = f\ \{Q_g,\ (H/T),\ T,\ \mu,\ \rho,\ \text{g}\ \}$$

where Q_g = gas flowrate; μ_a = apparent viscosity of liquid; H/T = liquid height/vessel diameter; T = vessel diameter; ρ = liquid density and g = acceleration due to gravity

$$\theta = 5.14 \times 10^3 \mu^{0.84} T^{-0.20} \left(\frac{P}{V}\right)^{-0.63} \left(\frac{H}{T}\right)^{-1.23} \qquad r^2 = 0.84 \qquad (4.9)$$

Figure 4.25 shows the predicted active blend times compared to those measured.

The active volumes calculated using Eqn. 4.8 assume that the power input is continuous. On full-scale sites, gas supply can either be continuous or intermittent.

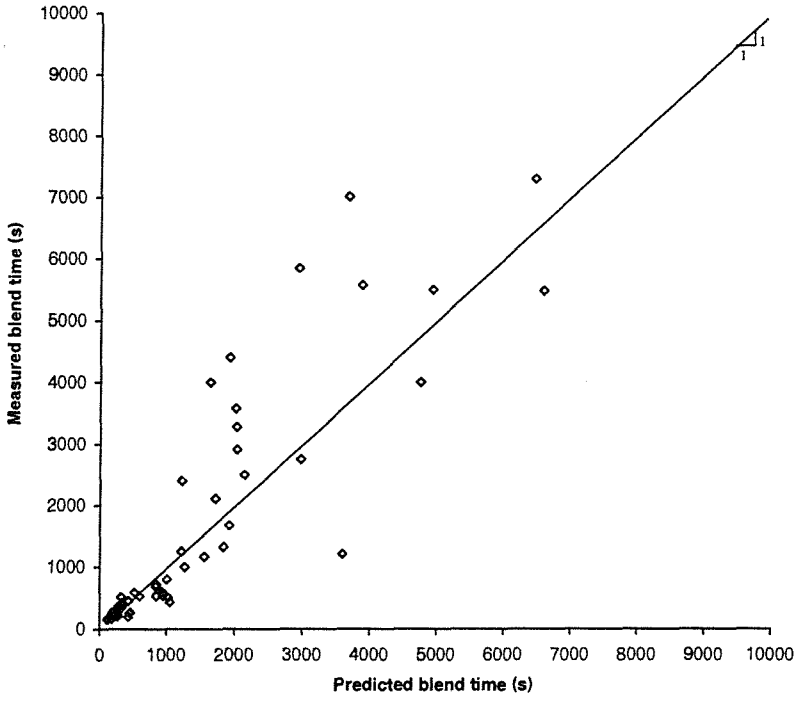

Figure 4.25: Central riser active blend time correlation

The usual practice is to supply gas to the digester intermittently as this is often more economic than continuous addition. The most common supply rate from the site survey of Ouziaux (1997) was 12 minutes of gas supplied every half an hour, although one site was only supplied gas for 10 minutes every 4 hours. In these cases, to ensure thorough mixing, the feed sludge should be completely mixed with the digesting sludge within the time that the gas is supplied. It follows therefore, that the gas should be supplied for a minimum of the digester blend time.

In addition to an intermittent gas supply, digesters are often fed intermittently too. The frequency with which the digester is fed will depend on the feed volume to be added to the digester per day. On large scale works, the digester will be fed several times a day whereas on a small scale works, this may only be once a day.

To ensure good mixing, the feed sludge should only be added when the gas is switched on, preferably at the start of the mixing cycle. At the end of the feed addition, the blend time period must be allowed for before any further feed is added.

Once the blend time and feed times have been determined, assuming the feed and mixing times start together, the required duration of gas addition can be determined since:

$$t_{on} = t_{feed} + t_{mix}$$

where t_{on} = the duration of gas addition, t_{feed} = duration of feed addition and t_{mix} = digester blend time

For example, if the blend time for a digester is 30 minutes and sludge is added to the digester for 12 minutes every hour, the required gas supply duration would be:

$$t_{on} = 12 + 30 = 42 \text{ minutes}$$

Therefore, the gas should be supplied for a minimum of 42 minutes every time feed is added.

If the blend time was longer, say 48 minutes with the same feed frequency and duration, the gas supply would be required for a full hour, every hour, i.e., contin-

uously. In this instance, increasing the feed volume would allow the feed frequency to be reduced or adding it at a higher flowrate would allow an intermittent gas addition if required.

4.9 Summary

The effects of power input, viscosity, nozzle diameter, scale, feed position and aspect ratio were investigated using Sparger A. Increasing the gas flowrate increased the active volume and decreased the active blend time. Increasing the viscosity reduced the active volume at equal power inputs.

There appeared to be little or no effect of nozzle diameter on active blend time or active volume. Increasing the nozzle diameter reduced the number of bubbles slightly but slightly increased their diameters and rise velocities due to a longer formation time, hence a reduced production rate.

In the case of the diffusers, the bubbles rose as a swarm. As they rose, they began to coalesce until at the liquid surface, their diameters were almost equal to the bubbles rising from the 4mm nozzles.

In terms of aspect ratio, the results suggest that if two digesters of equal diameter but one is half the height of the other are compared at equal gas flowrate, sparger arrangement and liquid viscosity, then the lower aspect ratio will have a smaller active volume and as a result, the active blend time will be shorter.

Increasing the vessel scale using the same sparger (Sparger A) and scaling on equal power input per unit volume resulted in similar blend times for both vessels under equal flow regimes. This suggested that equal power input per unit volume was the correct scale factor to use. The values of Q_g/V and Q_g/A were not constant between the two scales which would suggest that these scale up parameters, which are recommended in the literature are not the correct scale up parameters to use.

It has been found at constant gas flowrate and CMC concentration that the

sparger type can have a significant effect both on active and total blend time and the vessel's active volume. In the lowest viscosity CMC solution (equivalent to a digester sludge of 2.4% DS), the effect of sparger type was less marked. Differentiation between sparger performance was more apparent when the total blend times were considered due to the location and size of the inactive volumes set up by the different spargers.

Increasing the viscosity to 0.6% CMC (5.5% DS equivalent) clearly showed an effect of sparger type, as a result of the size and location of the inactive volume produced.

Sparger D (sequence sparger) performed consistently well in all cases and under all conditions. Although an inactive volume was formed in the base of the vessel opposite the active nozzle, as the sequence moved around the base, the flow-patterns moved around the vessel, thus avoiding any one area becoming stagnant.

Correlations have been produced to predict the active and the blend time within that active volume. Currently, the active volume correlation only applies to lab-scale digesters as it has not been tested at a larger scale. Both correlations only apply to spargers consisting of an inner ring of four nozzles with a diameter equal to one fifth of the vessel diameter. However, these are the only correlations, to the author's knowledge, that exist in the literature to quantify the effects of power input, viscosity and aspect ratio on active volume and active blend time in digesters.

Chapter 5

Comparison of Mixer Types

The focus of this work has been on unconfined gas mixing, although some experiments have been performed using an impeller in 0.3% and 0.6% CMC and these results are shown in Appendix C.

The performance of the different sparger configurations has been investigated and compared. This chapter will compare the active volumes and active blend times achieved with the two sparger types - Sparger D, the sequence sparger, which performed best overall and Sparger A, the sparger used to investigate the effects of aspect ratio, viscosity, power input, etc. In addition, the results from the impeller work will be compared.

5.1 Active volumes

Figure 5.1 shows the active volumes measured for the different spargers and impeller in 0.3% and 0.6% CMC respectively. The different mixers overlap over the power input range of 3 to 9 Wm^{-3}. Sparger A performed poorly with low active volumes compared to the other mixers at each power input.

Sparger D had an active volume of 100% at each power input used in 0.3% CMC. The impeller also had an active volume of 100%. However, Sparger A did not quite reach this value, even at 7 Wm^{-3}.

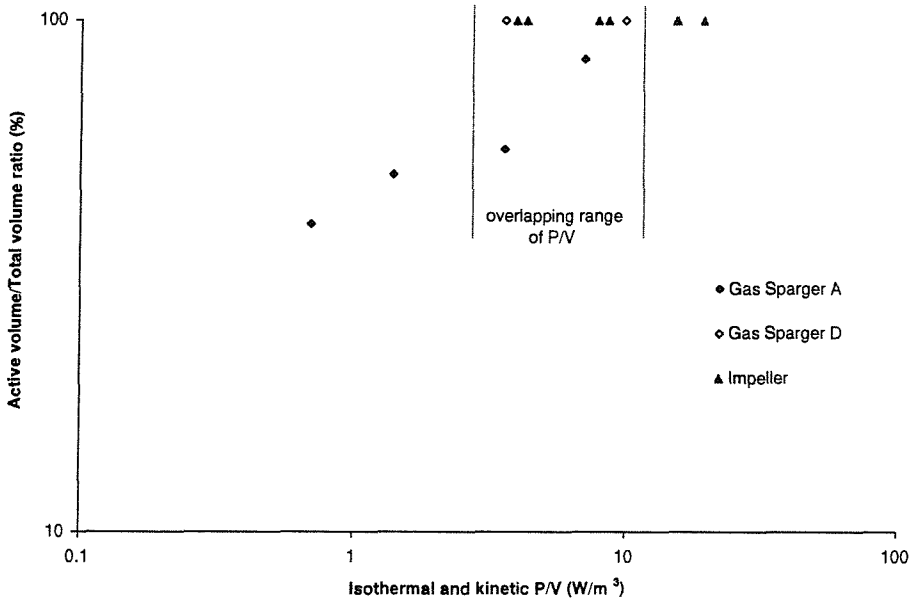

Figure 5.1: Comparison of active volumes from different mixers in 0.3% CMC

Tests were performed with the impeller in 0.6% CMC. However, to keep the vessel in the transitional/turbulent flow regime, it was necessary to increase the power input to such an extent that it fell far beyond the power input range used for the two gas spargers, although the impeller vessel volume was fully active.

Figures 4.17 and 4.18 in Section 4.6.1 showed that Sparger D consistently produced a higher active volume than Sparger A in 0.3% and 0.6% CMC. In both solutions, the active volume of Sparger D was consistently 100% hence, for the gas flowrates used, the sequence sparger was less affected by increasing viscosity than the other mixer types studied.

5.2 Blend times

The active blend times achieved for the power input range tested have been compared for Sparger A, Sparger D and the impeller, both with and without baffles. It is important to note that these are the active blend times and not the total blend times. Therefore, for each mixer type the active volume produced should

also be considered if a full comparison between mixer types is to be made. Further, the power inputs used are the net power inputs ie. actual power delivered to the liquid, rather than the gross power inputs. The power input values therefore do not account for inefficiencies in gas compressors for example or friction losses in the impeller motor and gearbox.

Figures 5.2 and 5.3 show the active blend times achieved for the range of power inputs used in 0.3% and 0.6% CMC respectively. The removal of the baffles during the impeller blending work resulted in a reduction in blend time for all conditions tested.

In 0.3% CMC, the overall trend of reducing blend time with increasing power input is the same for all mixers. There is approximately, a two fold variation in blend time at any given power input between mixers. Impeller mixing with baffles performed poorly compared to no baffles present and also compared to both sparger types.

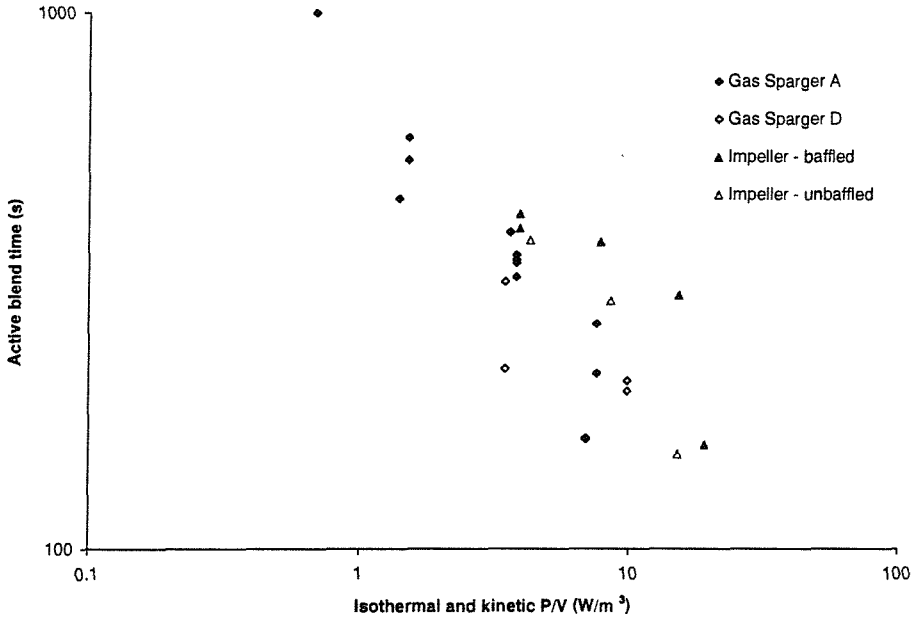

Figure 5.2: Comparison of active blend times achieved with different mixer types in 0.3% CMC

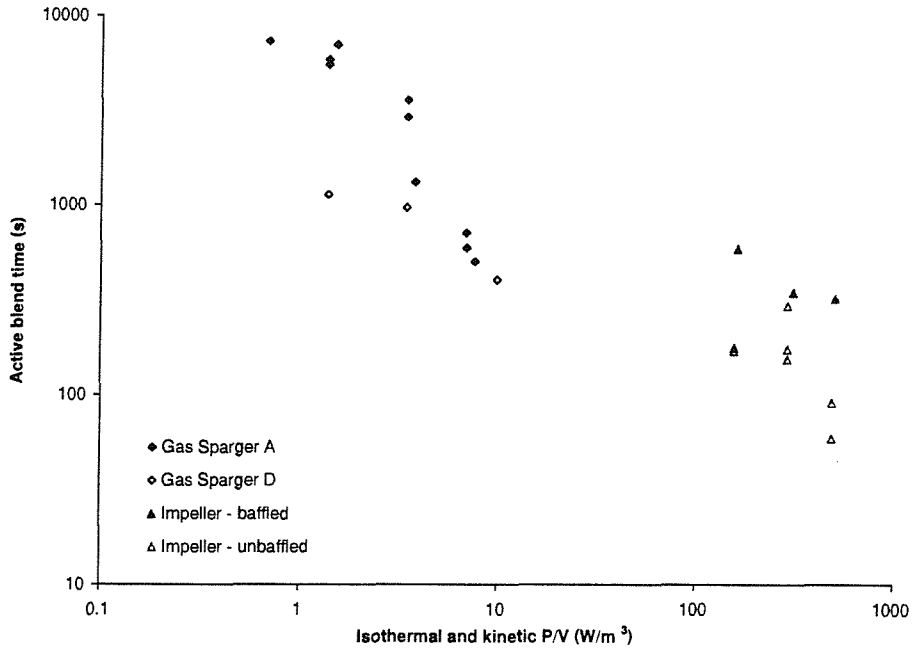

Figure 5.3: Comparison of active blend times achieved with different mixer types in 0.6% CMC

In 0.6% CMC, Sparger D performed best followed by Sparger A, the difference being greater than in 0.3% CMC. The impeller tests were not performed over a comparable power input range (in order to ensure Reynolds number remained in the transitional regime) and therefore, the active volumes achieved were not known. In 0.6% CMC, the gas sequential sparger (D) produced the highest active volume and would therefore, produce the shortest total blend time.

Figure 5.3 shows the active blend times achieved in 0.6% CMC over the full range of power inputs. Although the power inputs do not overlap, the data do appear to lie along the same line and increasing the net power input to the digester decreased the active blend time. However, a shorter blend time may not necessarily mean a high active volume as this is also a function of the mixer type and arrangement.

5.3 Discussion

In evaluating the performance of a mixer, there are three things to consider:

- the power input needed to achieve the required active volume
- the blend time produced in this active volume at that power input
- the viscosity of sludge used

It has been shown that in terms of active blend time, there is no one mixer that clearly performs significantly better than the rest under all conditions However, Sparger D (sequence gas) is good overall. The active volumes produced by the different mixers varied. In 0.3% CMC, Sparger D and the impeller both produced the highest active volumes compared to the other mixers for the same power input. In 0.6% CMC, Sparger D gave the highest active volume at a given power input (the impeller was not used over the same power input range).

Therefore, the mixer type chosen will depend on the mixing requirements for a given duty. If a large active volume is required for a low power input, then either Sparger D or the impeller should be used. If active volume is not important but blend time is, then any of the mixers could be used at the required power input. However, there is usually an economic constraint affecting the choice made in that the mixer needs to be efficient. The power inputs shown in Figures 5.1 to 5.3 inclusive are in terms of the net energy, that is the energy transferred directly to the sludge or CMC and not the power entering the gas compressor or impeller motor. The economics involved in the choice of mixer type has not been addressed in this thesis but is something that should be taken into account before choosing a mixer type.

Chapter 6

Conclusions

This thesis investigated the performance of gas-mixing systems employed within anaerobic sewage sludge digesters. The focus has been on unconfined gas mixing with the aim of improving digester mixing design by better understanding the effect of mixer size, type and sludge thickness on resultant blend time and active volume.

The literature review has highlighted gaps in the current state of the art regarding anaerobic digester mixer design. In terms of mixer design information, only two sources were found. These were EPA (1987) and Degrémont (1991). The values used in practice tend to lie closer to those recommended by Degrémont (1991) than the EPA (1987), although the exact values used vary from one manufacturer to another.

These two references quoted three design values:

- Power input per unit volume (Wm^{-3})
- Gas flowrate per unit volume of sludge ($m^3/h/m^3$)
- Gas flowrate per unit area of digester ($m^3/h/m^2$)

The different approaches result in inconsistencies with a change in scale, aspect ratio or mixer type. When the published power and gas flowrate design values are

compared at equal volumes and aspect ratios, these values vary over one order of magnitude. In addition, there is no provision for different types of sludge or their composition.

There were many references concerning the reduction in digester active volume over time due to grit accumulation in the base and scum formation at the surface, yet there has been no work performed to relate this reduction to the flowpatterns within a digester, the power input or the sludge properties. Similarly, blend time within a digester has not been addressed, although in the past two years or so, some new designs have specified a blend time requirement of one hour, although this value seems to be an arbitrary one as there is no record of its background.

A wide range of mixer types have been applied to digesters suggesting that market availability rather than applicability has dictated the selection of mixing equipment. Comparisons have been made in the literature between different digestion sites in terms of their mixing performance. Tests to compare different mixing systems have been limited in their scope due to their high cost, as the majority of them have been performed in full-scale digesters. Different methods have been used to assess the mixing performance and it has been widely accepted that grit deposition, active volume reduction and downtime for cleaning is par for the course for digesters.

The power input values for gas mixing systems quoted by researchers appear to be calculated from the power rating of the compressor and divided by the vessel volume. It has been quoted by Brade (1997) that compressors can have an efficiency as low as 30% and therefore, the power inputs quoted are often much higher than the actual power inputs. This has been confirmed by calculating the power input due to isothermal gas expansion (Eqn. 2.2) whose values are similar to the compressor inputs, assuming 30% efficiency. The power input from the kinetic energy of the gas as it is injected through the nozzles was found to be negligible at the full-scale.

Unconfined gas mixing was found to be the most common form of mixing in

anaerobic digesters within the UK and therefore, this type of digester has been studied in this thesis. Six different sparger arrangements and four different power inputs have been investigated under laboratory conditions to compare the active volumes and active blend times for these different sparger arrangements in three solutions of aqueous carboxymethylcellulose (CMC) at 0.3%, 0.6% and 1% by weight.

The effects of power input, viscosity, aspect ratio, nozzle diameter, scale, sparger type and inlet position on active volume and active blend time have been investigated. The optimum sparger arrangement from those tested was found to be a sequential gas addition where the nozzles were located in two concentric rings, 8 in the outer ring and 4 in the inner ring. Under the conditions tested, this sparger produced an active volume of 100% and lower active blend times than other sparger types.

To date, a definitive mixing theory has not been developed largely due to a lack of understanding of the processes, but also due to:

- variable sludge composition
- limited information on sludge rheology effects
- lack of data linking process performance to mixing parameters

Process mixing theory for blend time, using bubble columns has been reviewed within this thesis. Relating Chemical industry research to anaerobic digesters has not been done previously, perhaps due to insufficient published research work on typical digester geometries and sludge rheologies.

6.1 Data collection and sludge rheology

A survey was performed on 17 digestion sites within the Yorkshire Water catchment area to determine a 'common' digester geometry and a range of sludge

thicknesses encountered both currently and potentially in the future. The majority of digesters surveyed employed unconfined gas mixing. The compressor power input values ranged from 2.5 to 12.9 Wm^{-3} whereas the values calculated from isothermal gas expansion ranged from 1.52 to 3.5 Wm^{-3}. It is often the case, that the power input to the digesting sludge is based on the power input to the compressor which has been found to have efficiencies as low as 30%.

A sludge simulant was required to perform the experiments in the laboratory. This would allow visual observations of flowpatterns which would not be possible with real sludge because it is not transparent. Therefore, the rheological properties of a selection of digested sludges were measured from a total of eleven sites. The Power Law model was found to match the experimental apparent viscosities better than the Herschel-Bulkley model. A Power-Law polymer solution, Grade 7H4C sodium carboxymethylcellulose (CMC), was used as the simulant. Three concentrations, 0.3%, 0.6% and 1% (by weight) of CMC were found to simulate sludges of approximately 2-3% dry solids content, 5% DS and 10% DS respectively, in terms of their rheological behaviour.

6.2 Experimental results using gas mixing

The sparger type employed can have a significant influence on both the active and total blend times under all conditions tested. The sequence (Sparger D) arrangement gave the shortest blend times overall and the highest active volumes. The diffuser (Sparger C) arrangement was the better arrangement from the central riser continuous types, giving short active volume blend times but much longer total blend times.

By scaling up at constant P/V, (taking both isothermal and kinetic energies into account where applicable) and maintaining geometric, kinematic (in terms of bubble Reynolds number, superficial gas velocity, nozzle velocity and inlet Reynolds number) and dynamic similarity similar active blend times were

achieved at the lab-scale and pilot-scale suggesting that this is the correct scale-up parameter to use.

Decreasing aspect ratio at constant diameter and gas flowrate resulted did not alter the power input per unit volume for the same gas flowrate, yet a smaller active volume was achieved and a shorter active blend time. Increasing the gas flowrate increased the active volume and decreased the active blend time. Conversely, increasing the liquid viscosity reduced the active volume and increased the active blend times. Nozzle diameter had little effect on active volume and active blend time.

Correlations have been produced to predict the active volume and active blend time using one sparger arrangement, Sparger A.

6.3 Comparing the different mixers tested

The gas sparger, D and the impeller produced the largest active volumes for a given power input when used in 0.3% CMC. Sparger A produced the lowest active volumes in both 0.3% CMC and 0.6% CMC for all power inputs used.

Sparger D appeared to be the most efficient mixer type overall in terms of blend time and active volume when comparing all of the sparger configurations at equal P/V.

These results have implications on the retro-fitting of mixing equipment within digesters. If an active volume of 90% or more can be maintained, then there is a reduced requirement to periodically drain-down the digester and manually remove the grit build-up by hand. This would save money in terms of the operational costs at a digestion site. In addition, with a sequential sparger, there are no internals, as there are for an impeller mixed system, to corrode and therefore, there is a potential saving in terms of capital expenditure.

6.4 Future Work

In this thesis, the author has presented results for six different gas sparger arrangements at a 0.61m diameter laboratory scale and one of these spargers was also tested at a larger 2.67m diameter pilot scale. The sequence sparger (D) was found to perform much better overall than the other sparger types. Further work should investigate this sparger to determine the scale parameter for the active volume and blend time correlations to provide confidence when scaling up these results to the full-scale.

Active volume measurement and assessment at the full-scale is performed by evaluating residence time distribution (RTD) data, obtained with a tracer of Lithium Chloride (LiCl) (Williams, 1994; Edgington, 2000). Future work could use this technique at the laboratory scale to compare the inactive volume found visually with that found using RTDs. If the two techniques can be shown to agree, then the active volumes at the pilot scale can be determined. In addition, full-scale LiCl RTD data would provide active volume data for the full scale and therefore, scale-up information.

Impellers have been shown to be very effective as mixing devices and require similar net mixing power inputs to unconfined gas. Solids suspension has not been considered in the current work and is the area of research that would naturally follow. The spargers studied within this thesis should now be studied for their effectiveness at maintaining solids in suspension to determine their overall effectiveness.

Further adaptations of the gas spargers used should also be studied to determine alternative arrangements. A different sequence arrangement could be studied together with the effect of employing two or more nozzles simultaneously. For example, maintaining the nozzle under the feed location during the entire feed time whilst the other nozzles perform the sequence. There is likely to be an optimum nozzle spacing to allow the maximum mixing effect of each nozzle to be

attained. The effect of reducing the period that gas is supplied to the nozzles in the sequence sparger (D) should be investigated to identify whether 60 seconds is the optimum timescale.

Appendix A

Shear stress - shear-rate curves

The following series of graphs represent the raw rheological data for the sample of sludges taken from Yorkshire Water's catchment. Lines of best fit have been drawn through the points, the equations of which and correlation coefficients are shown on the graphs.

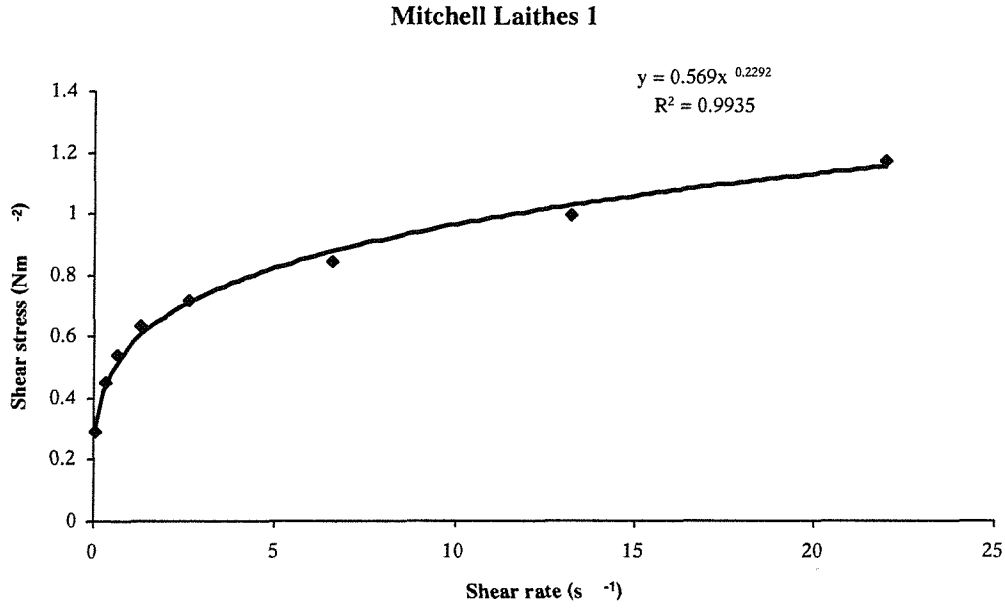

Figure A.1: Shear stress - shear-rate curves for Mitchell Laithes 1

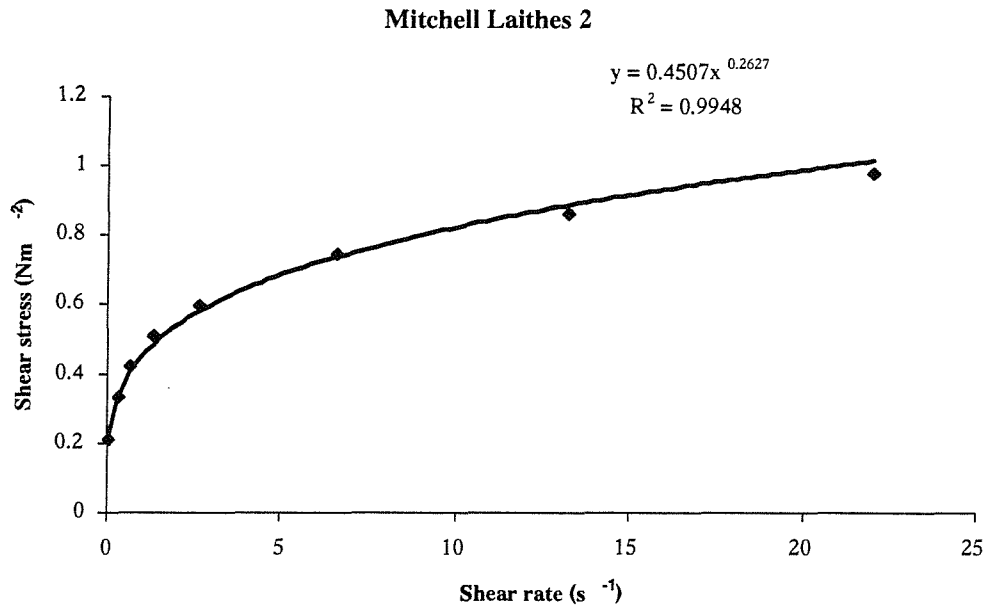

Figure A.2: Shear stress - shear-rate curves for Mitchell Laithes 2

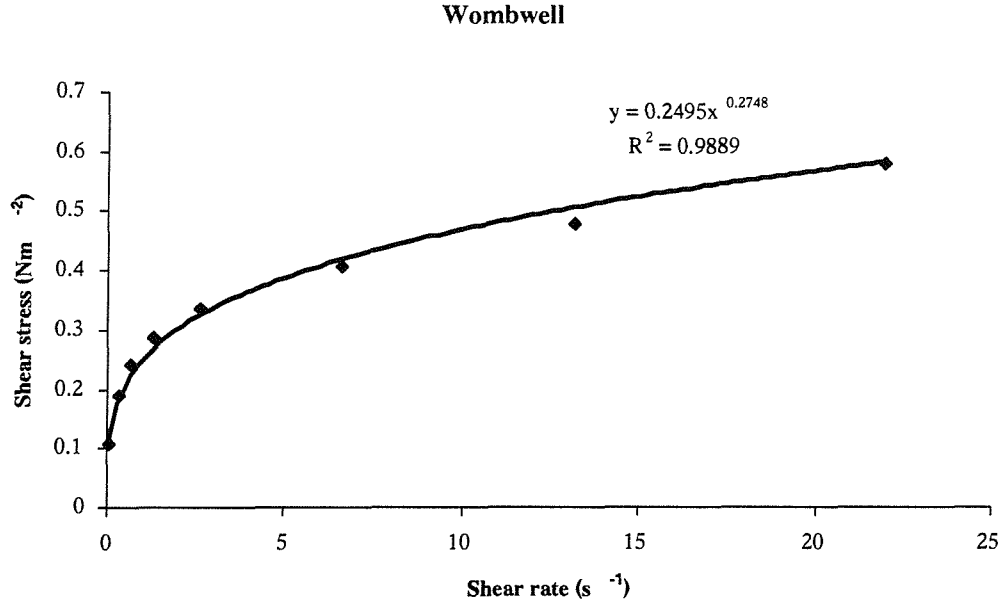

Figure A.3: Shear stress - shear-rate curves for Wombwell

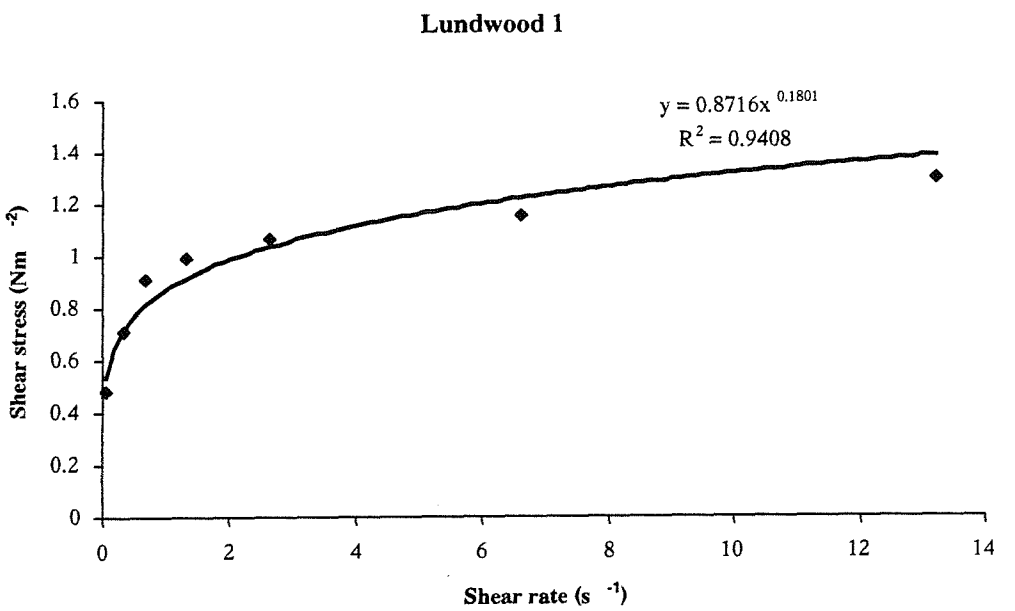

Figure A.4: Shear stress - shear-rate curves for Lundwood 1

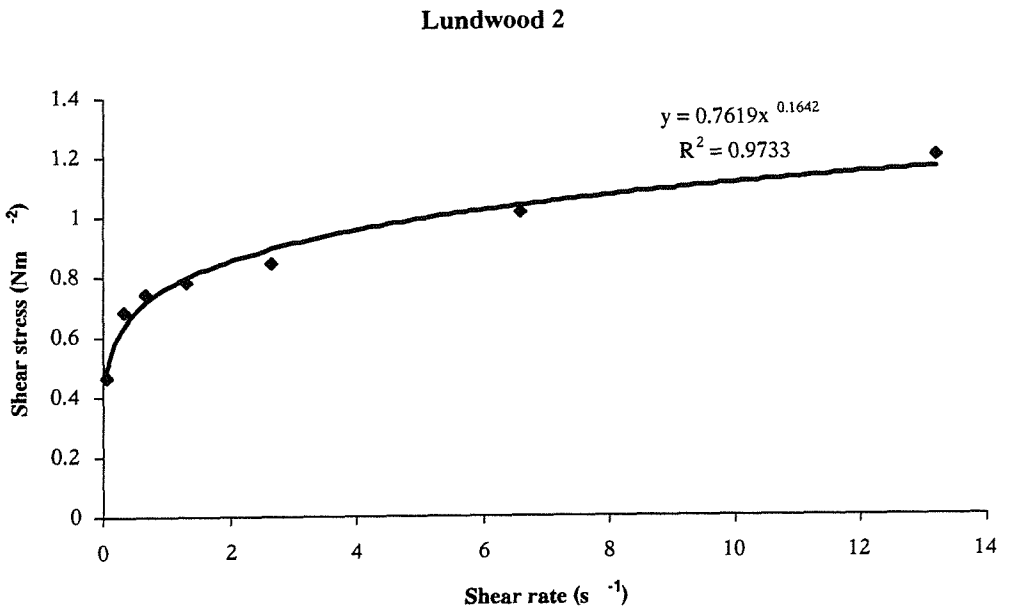

Figure A.5: Shear stress - shear-rate curves for Lundwood 2

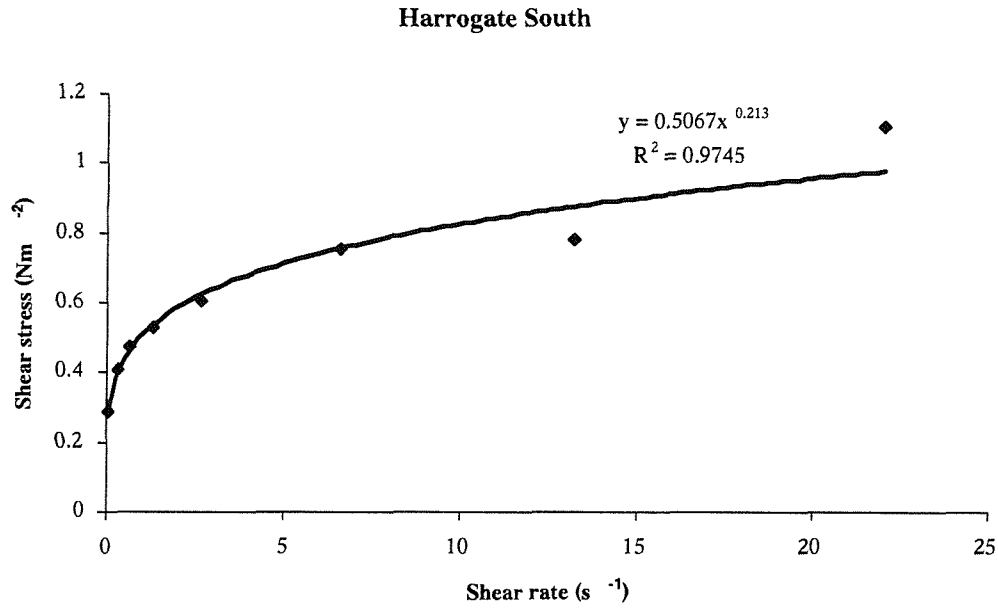

Figure A.6: Shear stress - shear-rate curves for Harrogate South

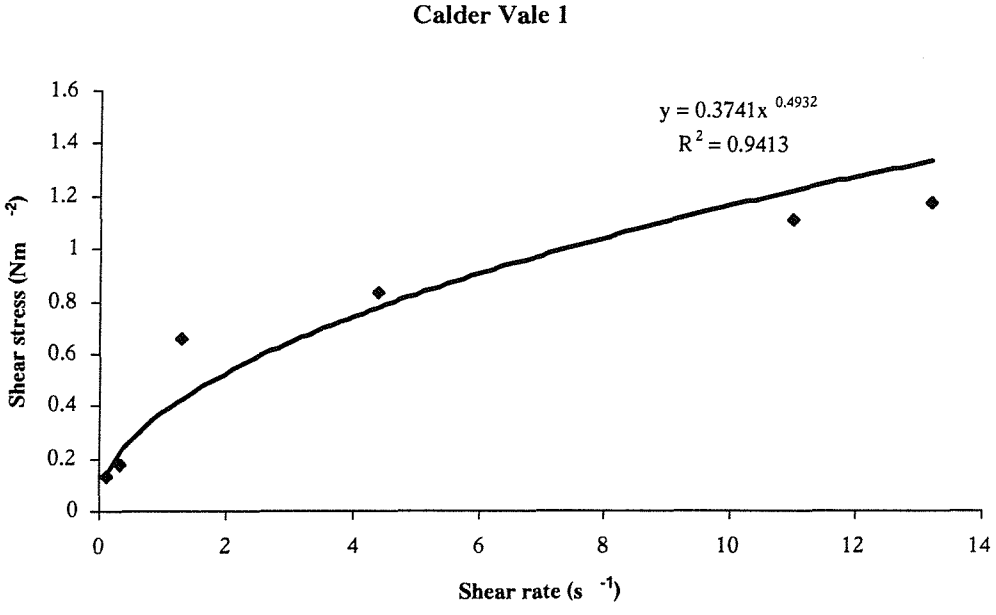

Figure A.7: Shear stress - shear-rate curves for Calder Vale 1

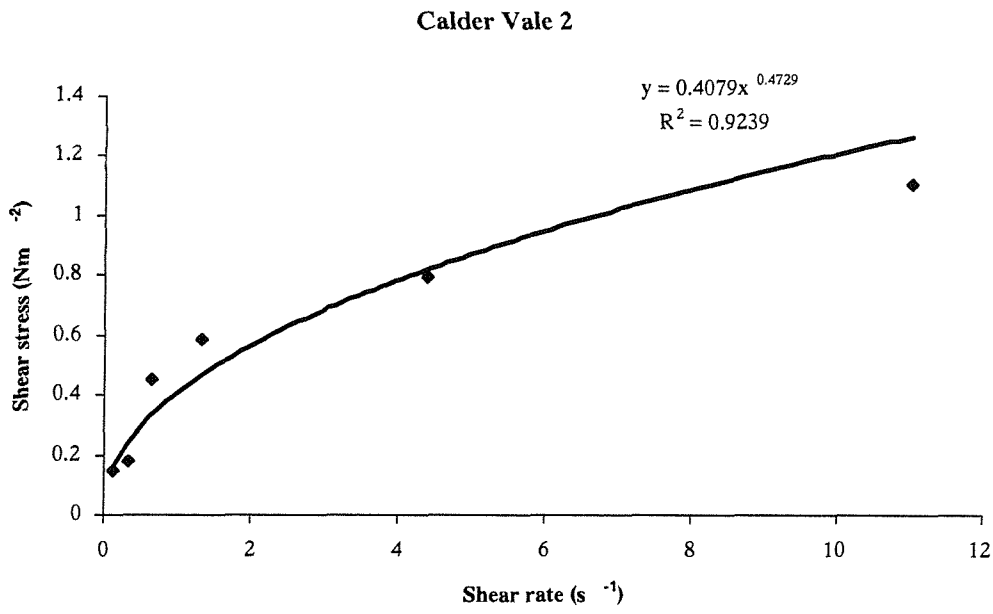

Figure A.8: Shear stress - shear-rate curves for Calder Vale 2

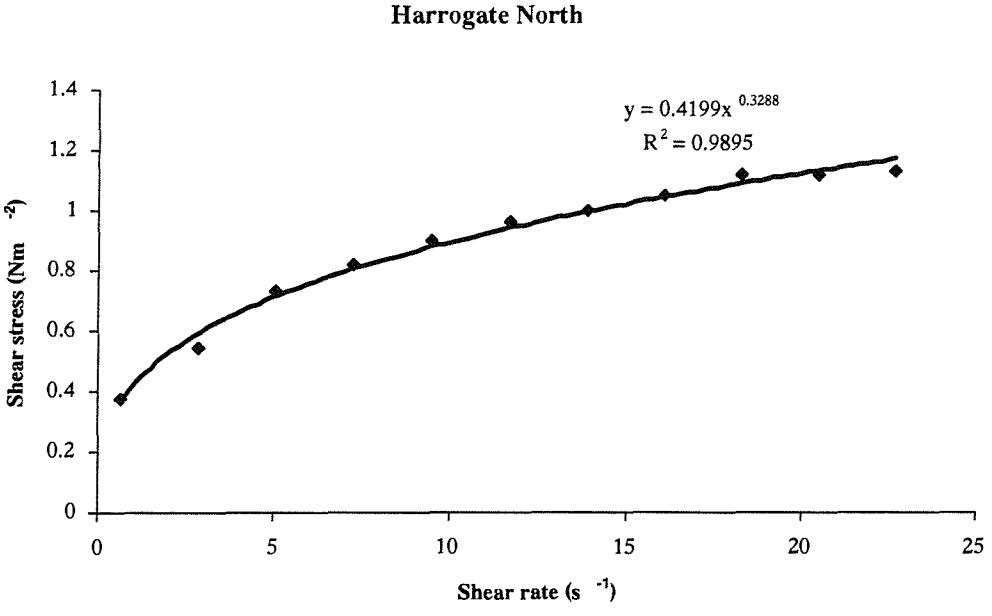

Figure A.9: Shear stress - shear-rate curves for Harrogate North

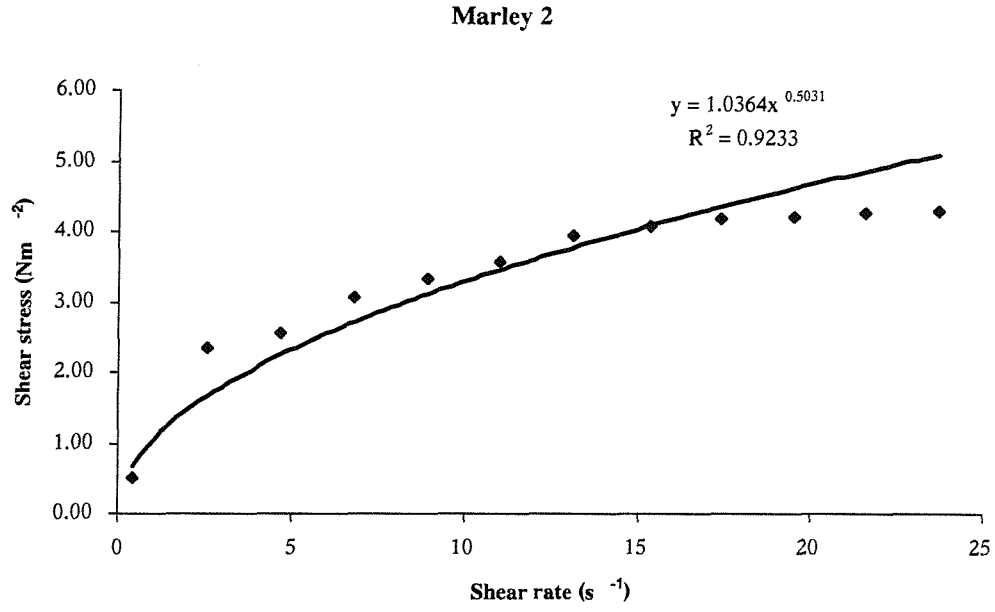

Figure A.10: Shear stress - shear-rate curves for Marley 2

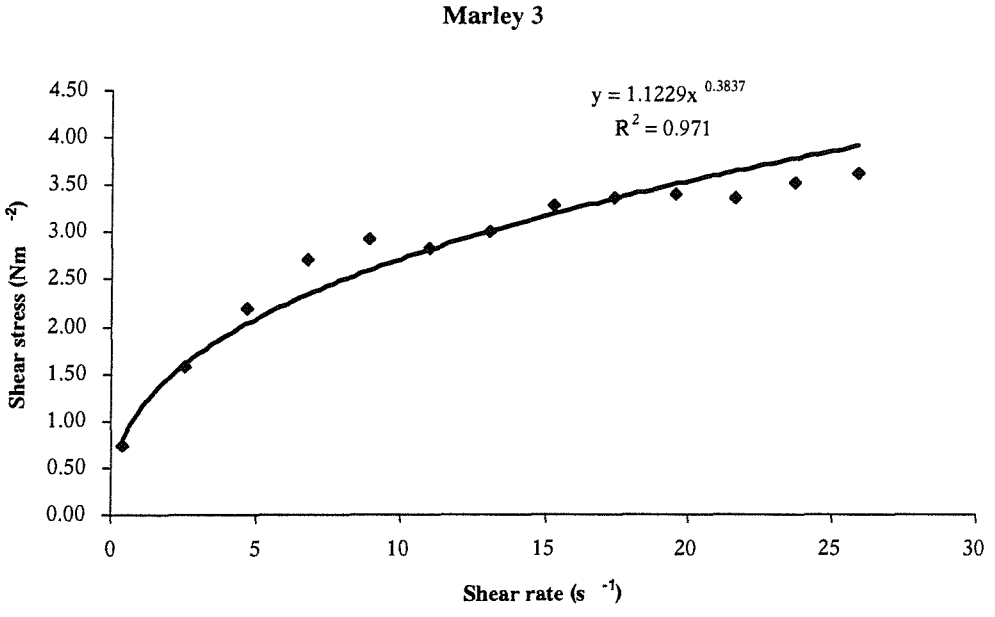

Figure A.11: Shear stress - shear-rate curves for Marley 3

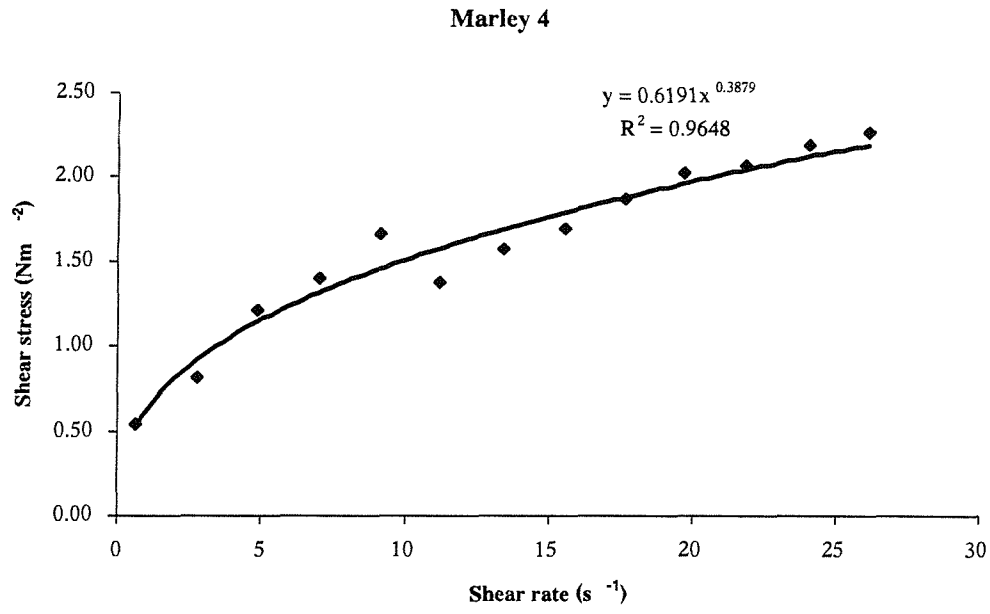

Figure A.12: Shear stress - shear-rate curves for Marley 4

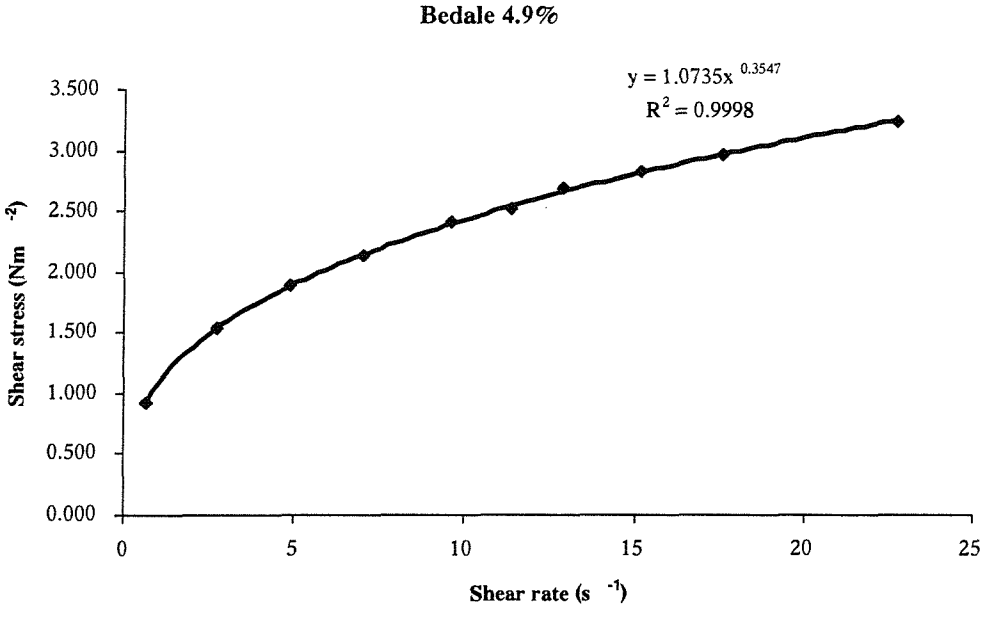

Figure A.13: Shear stress - shear-rate curves for Bedale

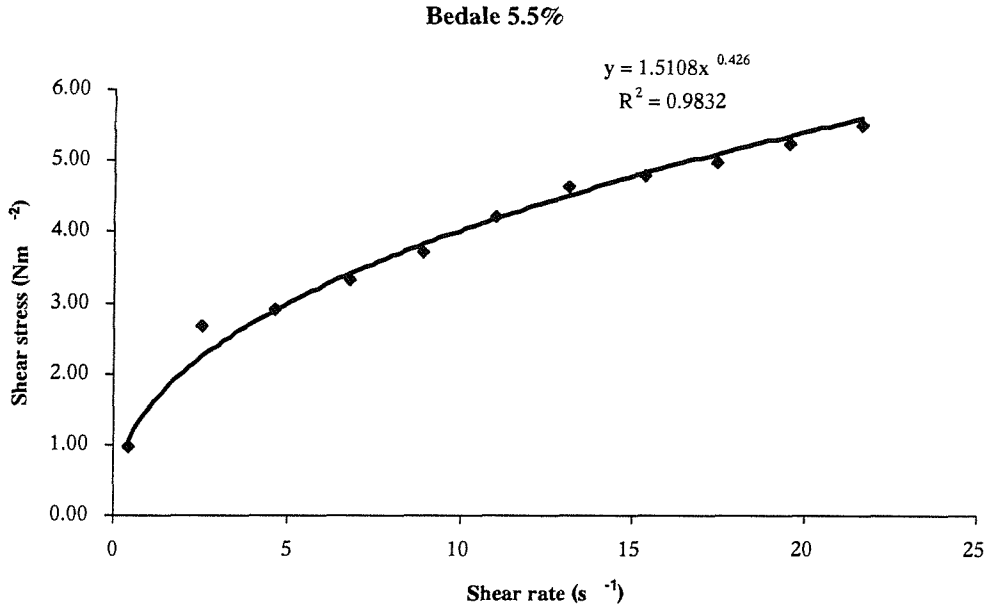

Figure A.14: Shear stress - shear-rate curves for Bedale (thickened to 5.5% DS)

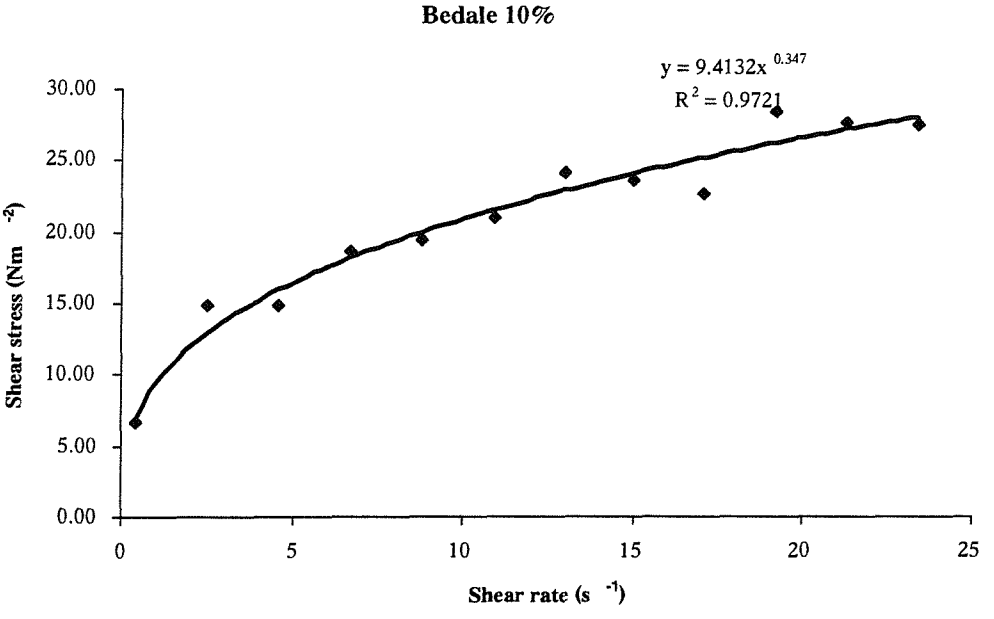

Figure A.15: Shear stress - shear-rate curves for Bedale (thickened to 10% DS)

Appendix B

Rheological models

This Appendix presents graphs of apparent viscosity against shear-rate for the sampled sludges using the Power Law model (Eqn. 3.1), Herschel-Bulkley model (Eqn. 3.2) and those obtained experimentally. Lines of best fit have been drawn through the points, the equations of which and correlation coefficients are shown on the graphs.

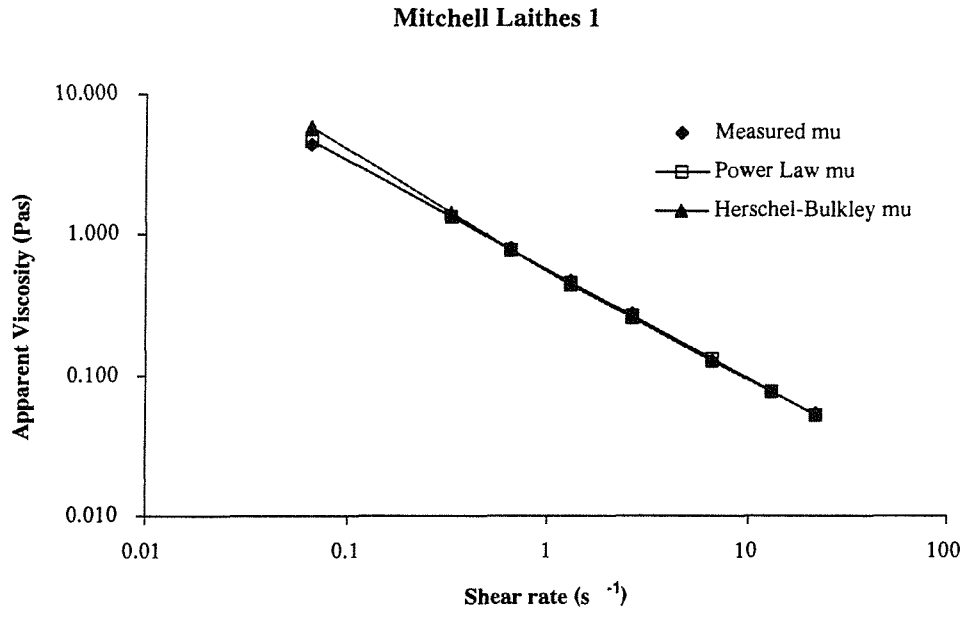

Figure B.1: Apparent viscosity - shear-rate curves for Mitchell Laithes 1

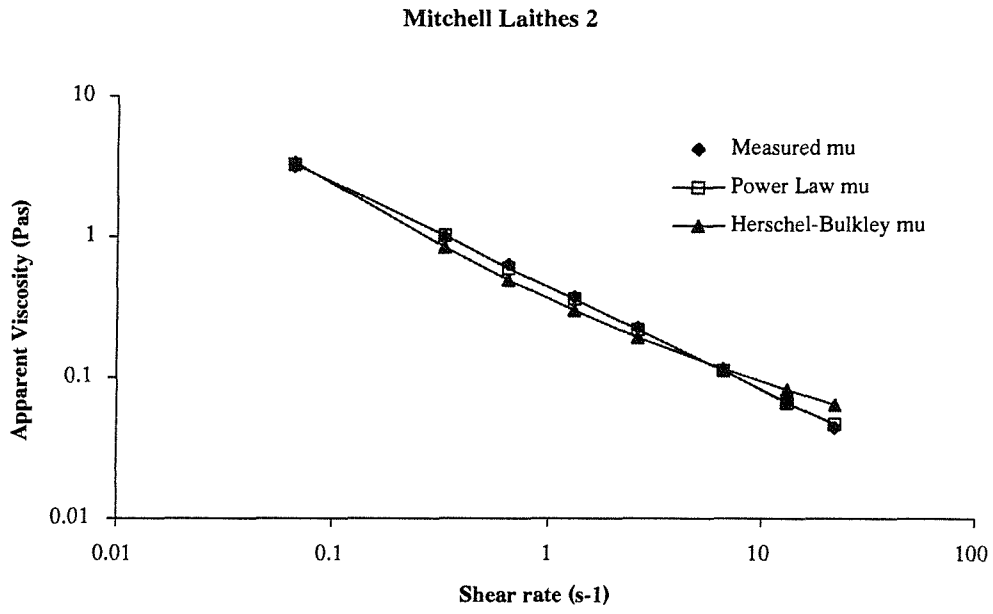

Figure B.2: Apparent viscosity - shear-rate curves for Mitchell Laithes 2

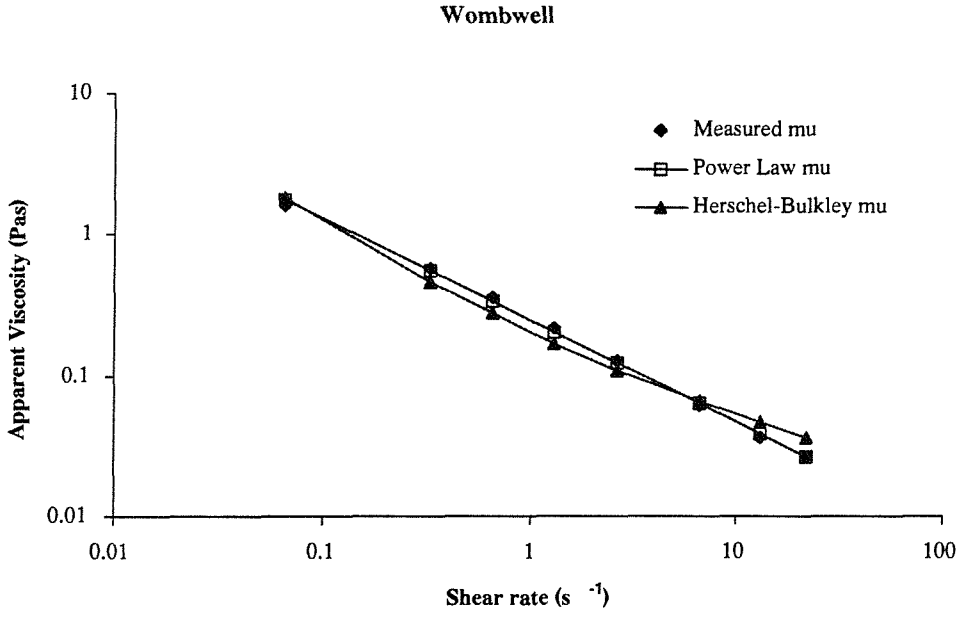

Figure B.3: Apparent viscosity - shear-rate curves for Wombwell

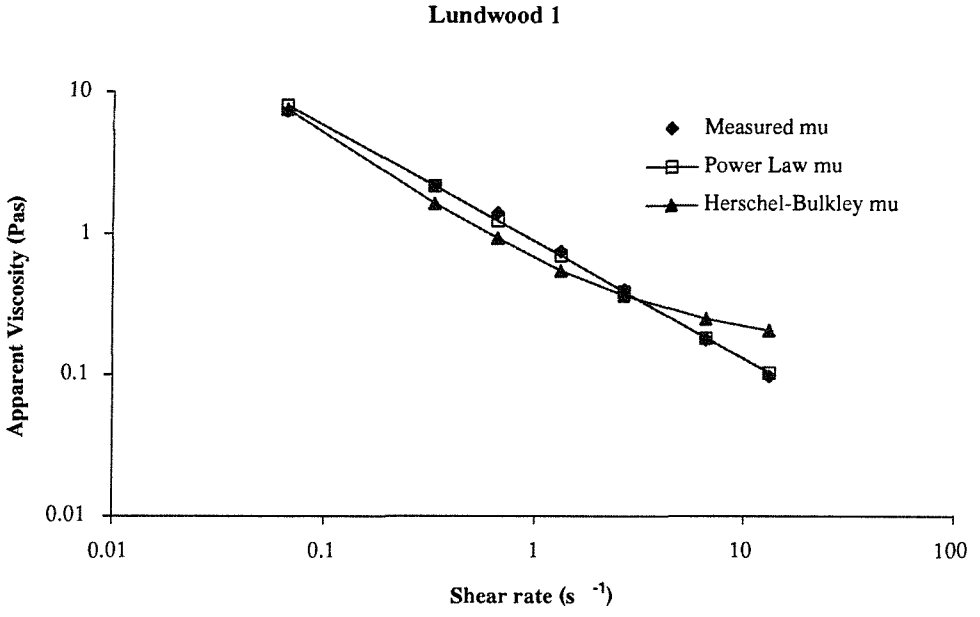

Figure B.4: Apparent viscosity - shear-rate curves for Lundwood 1

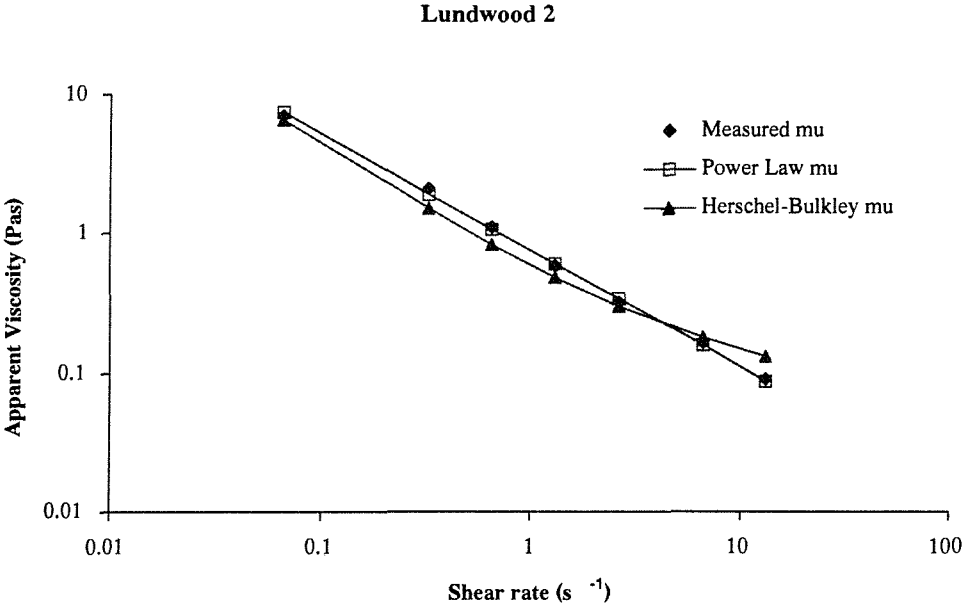

Figure B.5: Apparent viscosity - shear-rate curves for Lundwood 2

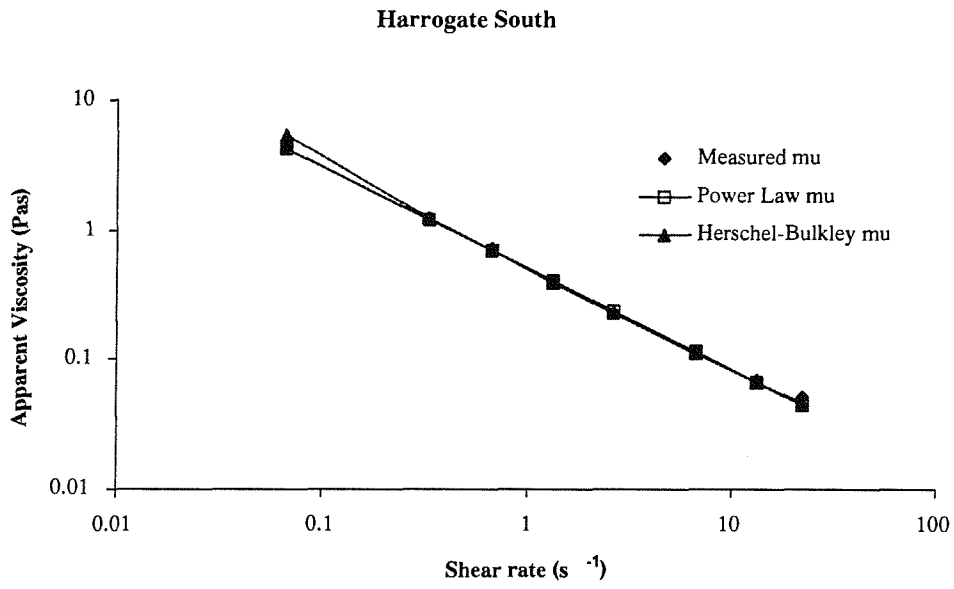

Figure B.6: Apparent viscosity - shear-rate curves for Harrogate South

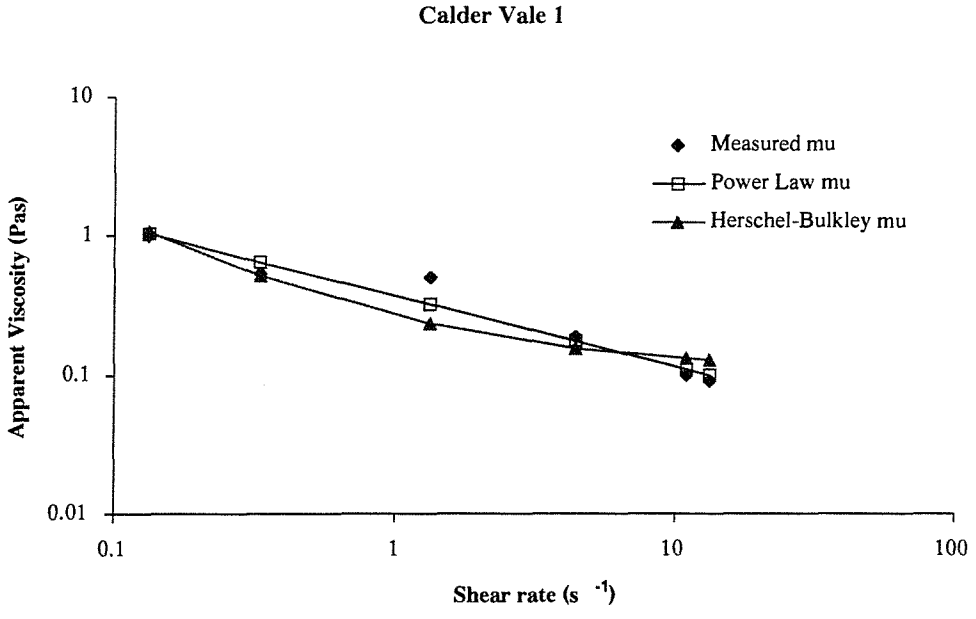

Figure B.7: Apparent viscosity - shear-rate curves for Calder Vale 1

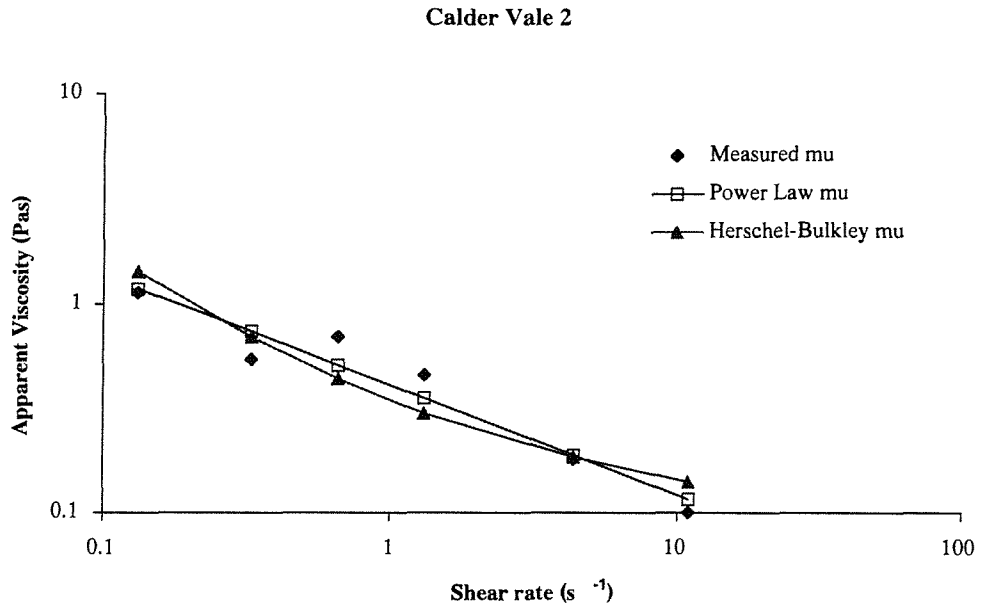

Figure B.8: Apparent viscosity - shear-rate curves for Calder Vale 2

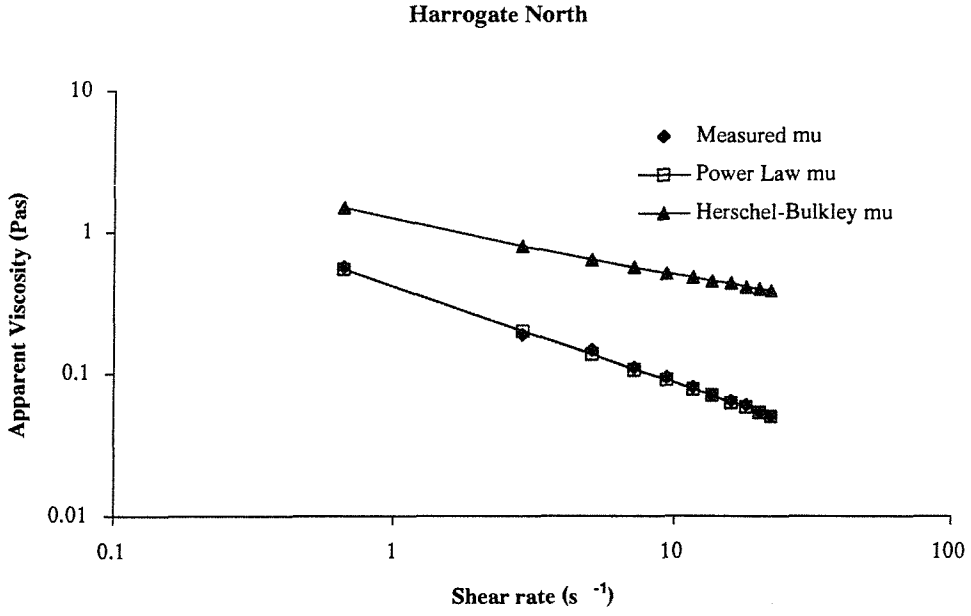

Figure B.9: Apparent viscosity - shear-rate curves for Harrogate North

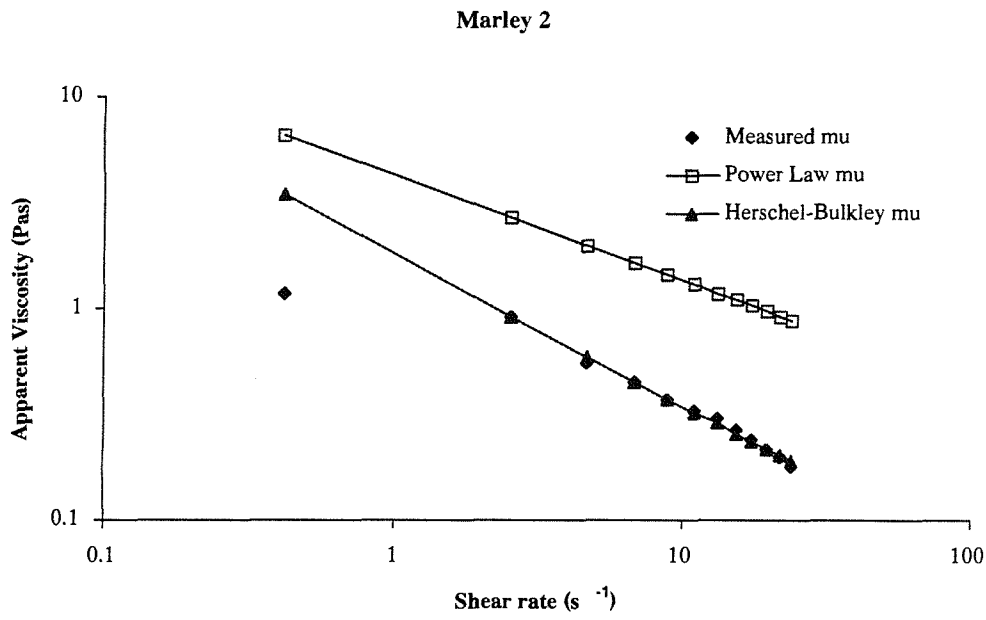

Figure B.10: Apparent viscosity - shear-rate curves for Marley 2

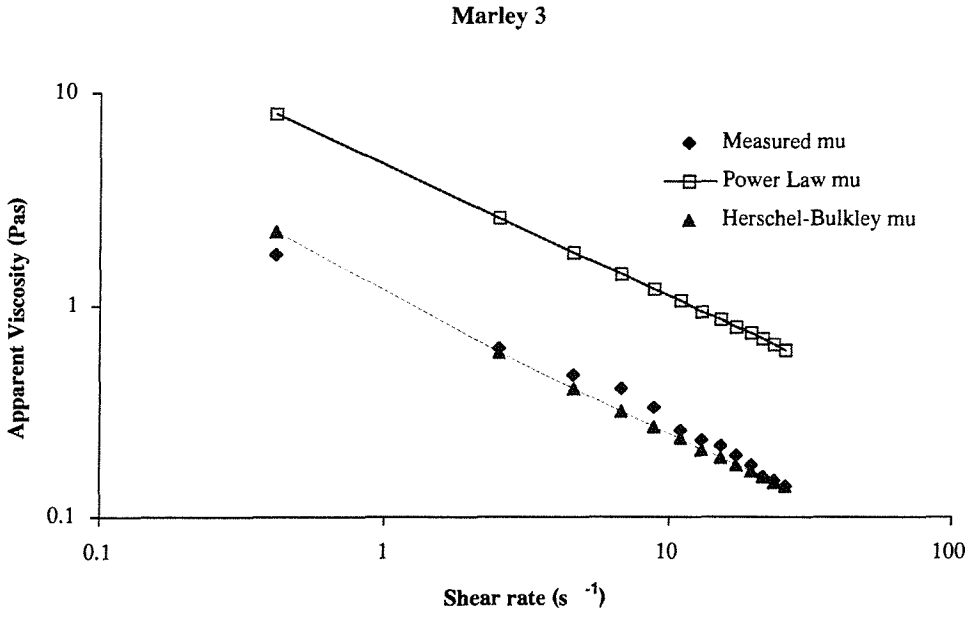

Figure B.11: Apparent viscosity - shear-rate curves for Marley 3

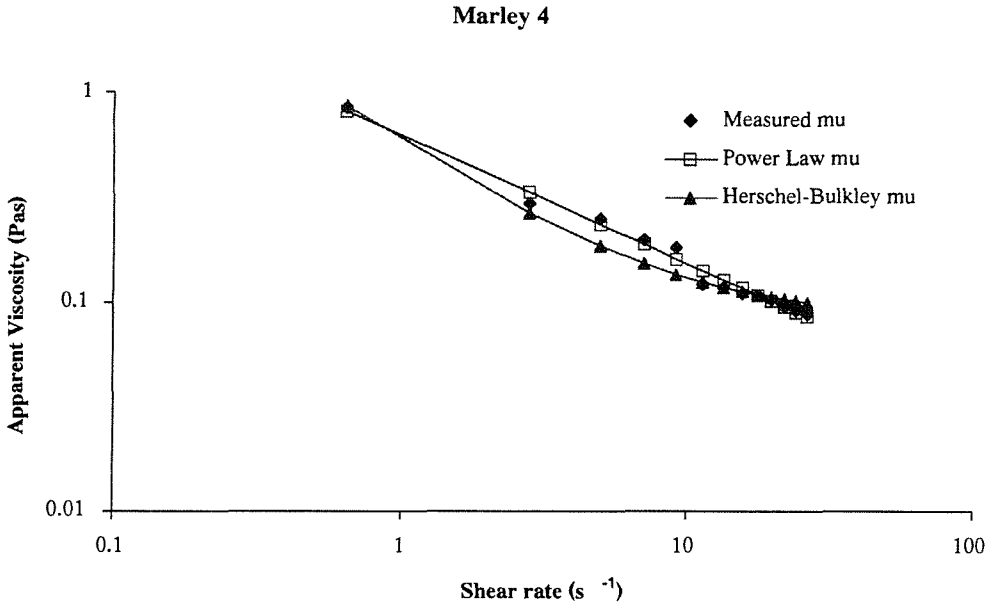

Figure B.12: Apparent viscosity - shear-rate curves for Marley 4

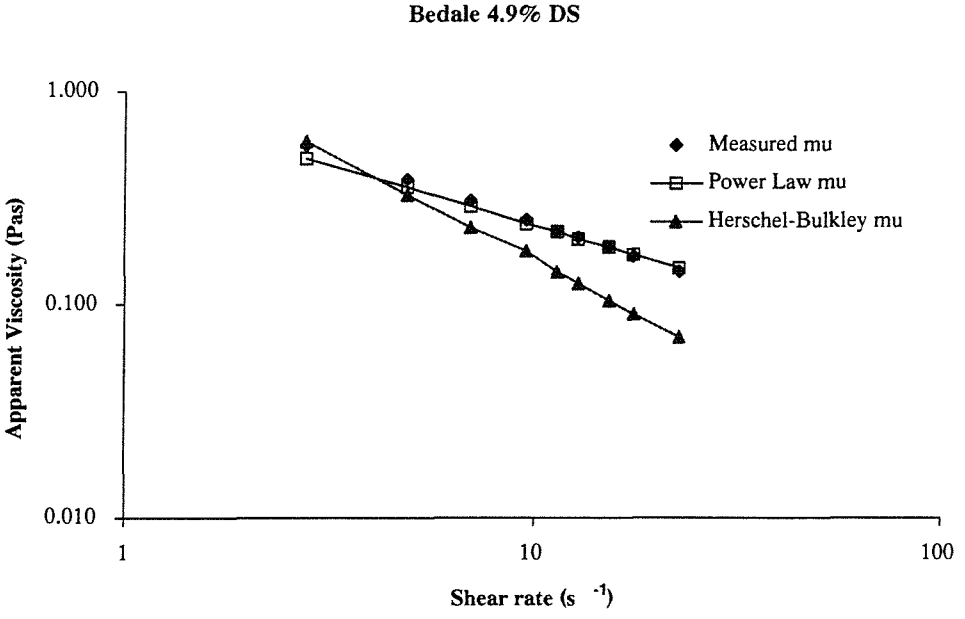

Figure B.13: Apparent viscosity - shear-rate curves for Bedale

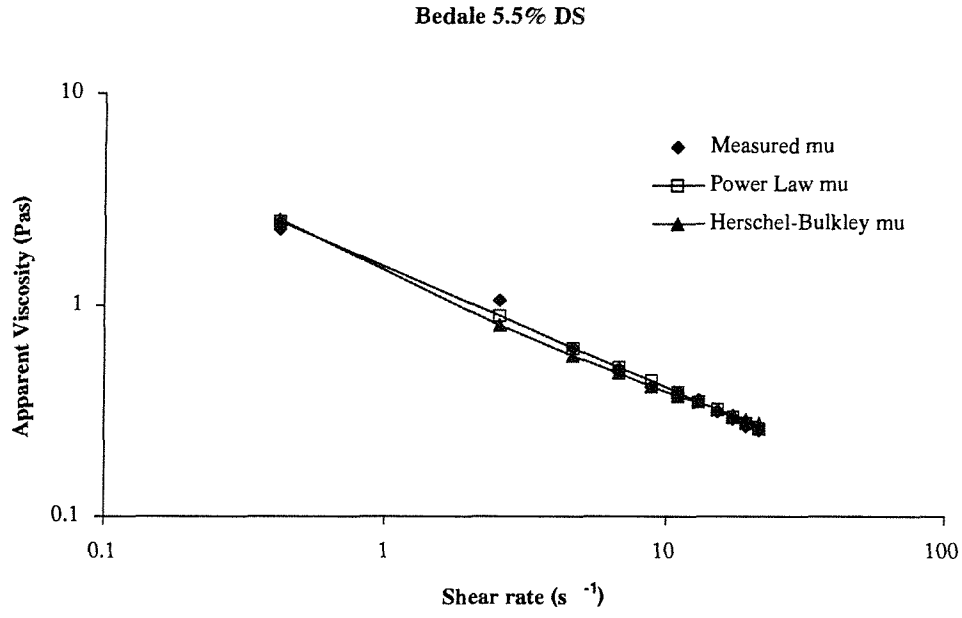

Figure B.14: Apparent viscosity - shear-rate curves for Bedale (thickened to 5.5% DS)

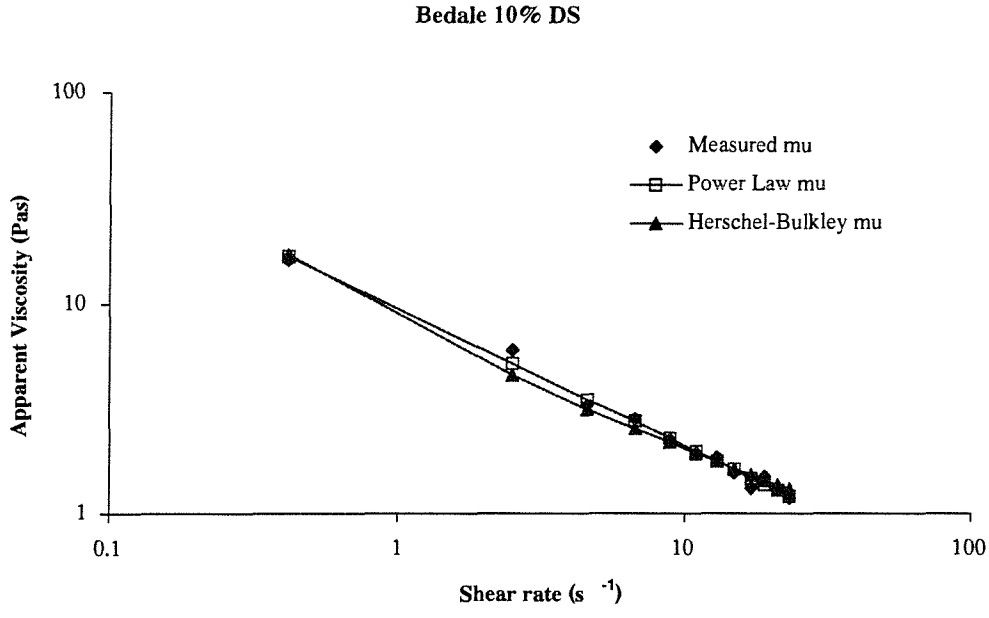

Figure B.15: Apparent viscosity - shear-rate curves for Bedale (thickened to 10% DS)

Appendix C

Impeller blending results

The correlation for blend time in the transitional regime (Eqn. 3.9) compared well with the measured values, both for baffled and unbaffled conditions. This was true for both the 0.3% and 0.6% CMC solutions.

Figures C.1 and C.2 illustrate the experimental results compared to those predicted for solutions of 0.3% and 0.6% CMC respectively.

All bar 2 of the data points lie within ± 2 standard deviations about the mean as defined in Eqn. 3.9. These 2 points were from unbaffled conditions and are only just outside the upper limit.

In addition, Grenville (1992) used 3 conductivity probes for his work rather than 5. These 3 probes were positioned in the impeller region, behind a baffle and in the vessel bulk. The last place to mix was behind a baffle and the first was in the impeller region. As Grenville (1992) produced this correlation in a vessel 0.61m in diameter at an aspect ratio of one, there does not appear to be an adverse effect on blend time of introducing 2 more probes into the same vessel geometry.

All bar 2 of the data points lie within ± 2 standard deviations about the mean as defined in Eqn. 3.9. These 2 points were from unbaffled conditions and are only just outside the upper limit.

The slight differences between the measured and predicted values may be ex-

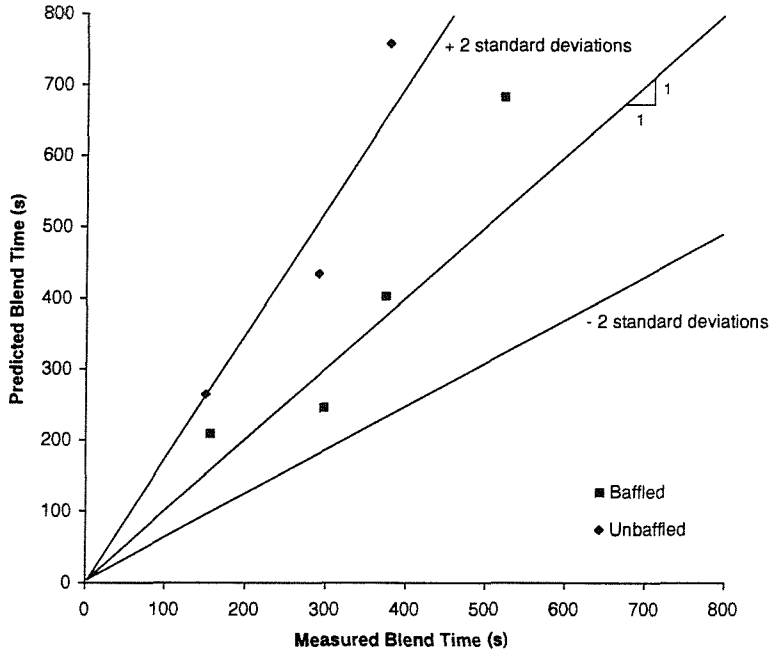

Figure C.1: Predicted blend time verses measured for an impeller mixed vessel in 0.3% CMC

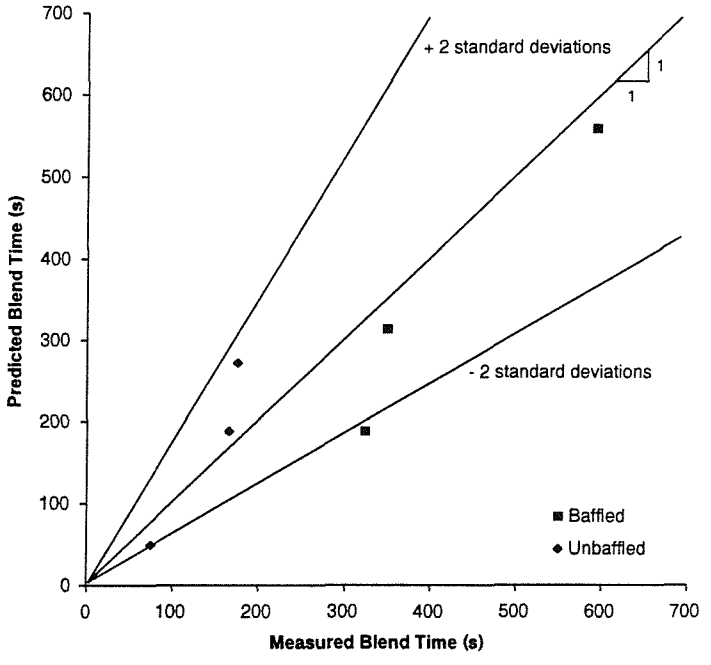

Figure C.2: Predicted blend time verses measured for impeller mixed vessel in 0.6% CMC

plained by a slight difference in tracer addition technique. The volume and concentration of tracer used in this work was representative of that used in the gas mixing tests in that it was scaled down from full scale digesters. 500ml of slightly salted water warmed to 2°C above the bulk temperature was used. It was added via a pump and a fixed inlet pipe located at $T/10$ below the surface and away from the wall. The addition time itself took 40s. The aim of the tracer concentration was that it was neutrally buoyant and the salt concentration had to be low to avoid density effects and also to reduce the deterioration of the CMC rheology.

Grenville (1992) used a pulse addition which lasted only a few seconds and was much smaller in volume. A saturated salt solution was used to ensure a distinct point at which the vessel was mixed. Initial investigations into density effects caused by tracer addition, performed in this work showed that a small increase in the amount of salt concentration resulted in a significant downward flow of the tracer, into the mixing zone. Therefore, adding a small quantity of a saturated salt solution into a turbulent vessel could mean that the tracer arrived at the impeller region much faster than the author's method, resulting in a shorter blend time.

Despite these differences, the accuracy of the transitional correlation is good compared to the experimental data implying that the blend time technique used is representative of that used by Grenville (1992).

Appendix D

Digester Mixing: Theory and Practice

This Appendix contains a copy of the paper written by the author of this thesis that was presented as a result of this work at the 3rd European Biosolids and Organic Residuals Conference organised by Aqua-Enviro in Wakefield, UK on the 16th to the 18th November, 1998.

Digester Mixing: Theory and Practice

by

Jacqueline Barker and Dr Mick Dawson

BHR Group Limited, The Fluid Engineering Centre, Cranfield, Bedfordshire. MK43 0AJ

Abstract

The anaerobic digestion of sewage sludge is an extensively used biological treatment process due to its ability to stabilise many sludge types prior to their application to agricultural land as a fertiliser. Because of greater sludge production and tight restrictions on disposal routes[1], many sludge producers want to increase their digestion capacity.

The throughput of existing digesters can be increased in a number of ways; by reducing retention times (some plants operate at mean retention times longer than the 12 days required by the DoE Code of Practice[2]); by reducing dead zones, thereby increasing the effective digester volume; or by digesting sludges with a higher dry solids content. Successful increase in volume utilisation and digestion of higher solids sludges are dependent on the detailed design of the mixing systems involved.

However, published design values for digester mixing are scarce. The US Environmental Protection Agency (EPA)[3] and Degrémont[4] provide the only two quantified design guidelines in the literature. These design guidelines result in inconsistencies when changing scale, aspect ratio or mixer operation. The values of mixing power input found in actual digesters surveyed were typically lower than the guideline values.

Keywords:

Anaerobic; digestion; mixing; gas; unconfined

Introduction:

Anaerobic digestion is the biological decomposition of sewage sludge in the absence of oxygen to produce biogas (a combination of methane and carbon dioxide) together with an inoffensive, black, tarry substance suitable as an agricultural fertiliser. The process of anaerobic digestion is one that has evolved over the past century where improvements have been made as a result of problems that have arisen during this time. Many of the parameters and variables involved in digestion are still not fully understood. Due to the recent increase in sludge produced and the reduction in available disposal routes, anaerobic digestion is now being looked at from a fresh angle in an attempt to optimise the process.

Effective mixing is critical for efficient digester performance in order to provide contact between feed sludge and biomass, to utilise the whole vessel volume, reduce downtime due to solids accumulation, improve process kinetics and increase gas production. However, poor mixing within digesters is inherent in a wide variety of existing designs and as a result, the effective volume of many digesters can be greatly reduced with many operating at 60 to 70% of their digestion capacities.

A review of the available literature on digester mixing has been carried out and some of the findings are reported here. The mixer design values found in the literature are discussed and compared with those found in practice as well as those reported by other researchers.

Mixer types

A survey of operational digesters in the Yorkshire region has recently been performed[5] and the majority of digesters were found to be mixed using unconfined gas injection. Figure 1 shows such a system. The main benefit of this type of mixing is that there are no internal moving parts and therefore, the possibility of shutting down the digester for internal equipment maintenance is reduced. In addition, unconfined gas systems have been shown to be effective at eliminating dead-zones and dispersing feed[12].

There are 3 other main types of assisted mixing systems[3,6,7,8] as well as natural mixing[9,10] due to convection and natural gas evolution. These will not be discussed here as they are described in detail elsewhere. The other assisted mixing systems are confined gas injection, mechanical stirring and mechanical pumping.

The gas collection and injection operations of unconfined gas mixed digesters are similar from one site to another. The gas produced by the digesting sludge is collected either in the head space or more commonly, in a separate collection tank. It is then scrubbed and re-enters the digester either through roof-mounted lances or more frequently a series of base mounted diffusers.

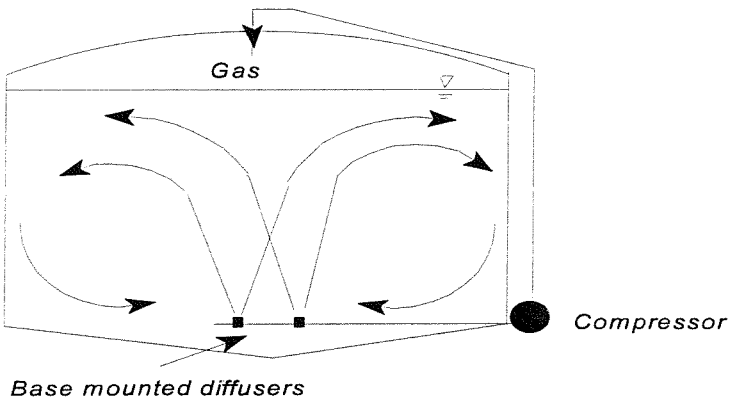

Figure 1 - unconfined gas injection system

Unconfined gas mixer design information from the literature

Actual published design information is scarce with many manufacturers presumably having their own design guidelines which have arisen from years of experience. In 1987, the EPA published a series of papers on the design of digesters[3] and included target values for power input and gas flowrate for a digester. In 1991, Degrémont [4] published target values in their Water Treatment Handbook. Stukenberg[11] has published values of turnover time and draft-tube velocity although these relate to egg-shaped digesters and so are not discussed here. The published values are presented in Table 1 below:

Parameter	Definition	unit	typical value	applies to:
P/V	Power input by mixing equipment divided by digester volume (EPA, 1987)	Wm^{-3}	5-8 2-4	UK/US shapes Egg shapes
Unit gas flow EPA: Degrémont:	Quantity of gas delivered divided by digester volume Quantity of gas delivered divided by digester cross-sectional area	$m^3h^{-1}m^{-3}$ $m^3h^{-1}m^{-2}$	0.27-0.3 0.3-0.42 0.8	Unconfined Confined Not specified

Table 1: Published design values for mixing systems

The figures from the EPA are in terms of gas flowrate per unit volume of the digester whereas the Degrémont values are given as gas flowrate per unit area of the digester (superficial gas velocity). In order to understand these values better, consider the following 3 digesters, X, Y and Z.

Parameter	Digester X	Digester Y	Digester Z
Volume (m^3)	500	1000	1000
Aspect ratio	0.5	1	0.5
Digester height (m)	5.42	10.84	6.83
Digester diameter (m)	10.84	10.84	13.66
Cross-sectional area (m^2)	92.29	92.29	146.56
EPA gas flowrate (m^3h^{-1})	135	270	270
Degrémont gas flowrate (m^3h^{-1})	73.83	73.83	117.25
EPA power input (Wm^{-3})	1.27	1.7	1.38
Degrémont power input (Wm^{-3})	0.69	0.47	0.6

Table 2: Comparison between published gas flowrate values and calculation of Power input for digesters of two different aspect ratios

Table 2 shows the gas flowrates required according to the EPA and Degrémont design guidelines separately and then uses the respective values to calculate power inputs based on isothermal gas expansion.

Consider Digester Y. Using the EPA guideline of 0.27 $m^3h^{-1}m^{-3}$ and multiplying by the vessel volume, the gas flowrate was calculated as 270 m^3h^{-1}. Using the Degrémont guideline of 0.8 $m^3h^{-1}m^2$ and multiplying by the cross-sectional area, the gas flowrate was calculated as 73.83 m^3h^{-1}, almost 4 times less than the EPA value. Application of the two sets of design guidelines result in substantially different gas flowrates at these scales and aspect ratios.

The EPA published guideline values for power input which are between 5 and 8 Wm^{-3} for UK and US style low aspect ratio digesters. In Table 2, the power input has been calculated from isothermal expansion, ignoring any kinetic energy input from the gas:

$$P = nRT\left(\ln\frac{p1}{p2}\right) \qquad \text{(Eqn.1)}$$

where: P = power input (W)
n = molar gas flowrate ($mols^{-1}$)
R = universal gas constant (8.314 $J(mol.K)^{-1}$)
T = temperature (K)
$p1$ = pressure at nozzle (Pa)
$p2$ = pressure at surface (Pa)

Comparing the power inputs for Digesters Y and Z indicates an increase in P/V when increasing aspect ratio using the EPA gas flowrate guidelines and the opposite when using the Degrémont guidelines. Comparing the P/V values for Digesters X and Z shows an increase when increasing scale at constant aspect ratio using the EPA guidelines and a decrease using the Degrémont guidelines. The choice of whether to use gas flowrate per unit area or gas flowrate per unit volume therefore has a substantial effect on the sizing and selection of equipment for unconfined gas mixing.

All of the Table 2 power inputs calculated using isothermal expansion are lower than those recommended by the EPA even though the gas flowrates used to calculate the power inputs used the EPA's gas flowrate recommendation. Power inputs calculated from isothermal expansion and based on EPA gas flowrates increase with increasing digester scale.

A further comparison of the EPA and Degrémont's guidelines shows that the ratio of EPA recommended flowrate (m^3h^{-1}) to Degrémont's recommended flowrate is :

$$\frac{0.27}{0.8} \times \text{vessel height} \qquad \text{(Eqn.2)}$$

For a vessel of aspect ratio 1, (vessel height/vessel diameter = 1):

V (m^3)	$Q_{EPA}/Q_{Degrémont}$ (-)
100	1.7
500	2.9
1000	3.7
5000	6.3

Table 3: Comparison between EPA and Degrémont recommended values

Therefore for vessels of a realistic size, the EPA recommended gas flowrate varies from 1.7 to 6.3 times greater than that recommended by Degrémont.

Actual design values found in practice

During a recent site survey[5], twelve digesters were studied to collect information about the design and operation of their mixing systems. The results were collated from 3 sources: original drawings, operators' knowledge and calculation of missing parameters where relevant information was available to do so. The digesters featured in Table 4 were all built between the mid-eighties and mid-nineties by various manufacturers. Table 4 focuses on the geometry of the digester, its gas injection nozzles and on the unconfined gas power inputs.

The majority of aspect ratios were near to 1.0 with the lowest being 0.5. The number of gas injection nozzles varied from 6 to 24 and they were mostly arranged in two rings located on the digester base. The diameter of the nozzles was not always readily available and one reason might be that they took the form of diffusers rather than nozzles.

The way in which the surveyed mixing systems were operated differed significantly. Only two of the digesters (A and F) operated with a continuous gas supply to all nozzles simultaneously. The remaining digesters featured an intermittant gas supply varying from 10 minutes every four hours to 30 minutes every hour. Of the digesters with an intermittant supply, most used a rotary valve to switch the gas supply from one nozzle to the next in a sequence. Alternatively, intermittant gas supply was provided to all nozzles simultaneously or to each of two rings of nozzles in turn. The relative merits of these different methods of unconfined gas mixer operation have never been reported. One can only assume that the mode of operation will have a significant effect on the mixer performance at a given gas flowrate.

The EPA's recommended power input per unit volume (P/V) was between 5 and 8 Wm^{-3}. If P/V is calculated using the power rating of the compressor and dividing by the volume of sludge in the digester, then the surveyed digesters fall between 3 and 12 Wm^{-3}. These P/V values are likely to be an overestimate because they assume 100% efficiency of the compressor. If the P/V values are calculated on the basis of isothermal expansion of the gas flowrate delivered by the compressor then Table 4 shows that all the digesters except one are within the range 2 to 4 Wm^{-3}. The P/V values from isothermal expansion will be more accurate and suggest that the majority of surveyed digester mixers are underdesigned, according to the EPA guidelines.

Figure 2 shows graphically a plot of actual gas flowrate into the digester against those calculated using the EPA and Degrémont guidelines for each of the digesters in Table 4. In nearly all cases, the Degrémont gas flowrate is closest to the actual gas flowrate when compared with the EPA figure.

Digester	Sludge volume (m^3)	Aspect ratio	N° injection ports	Location	Compressor P/V (Wm^{-3})	Isothermal P/V (Wm^{-3})
A	1755	0.5	16	2/3 depth	10.5	7.3
B	978	0.8	24	base	3.1	1.8
C	450	0.9	12	2 rings on base	6.7	4.0
D	715	1.2	12	2 rings on base	4.2	3.0
E	700	0.8	19	-	7.8	3.9
F	500	0.8	6	1 ring on base	8.0	-
G	2290	0.9	24	2 rings on base	-	1.9
H	530	0.8	12	2 rings on base	5.7	3.3
I	1700	1.1	9	base	12.9	-
J	715	1.1	12	2 rings on base	4.2	3.3
K	537	0.92	12	2 rings on base	5.6	2.8
L	1076	0.90	18	2 rings on base	2.8	1.9

Table 4: Characteristics of surveyed digesters

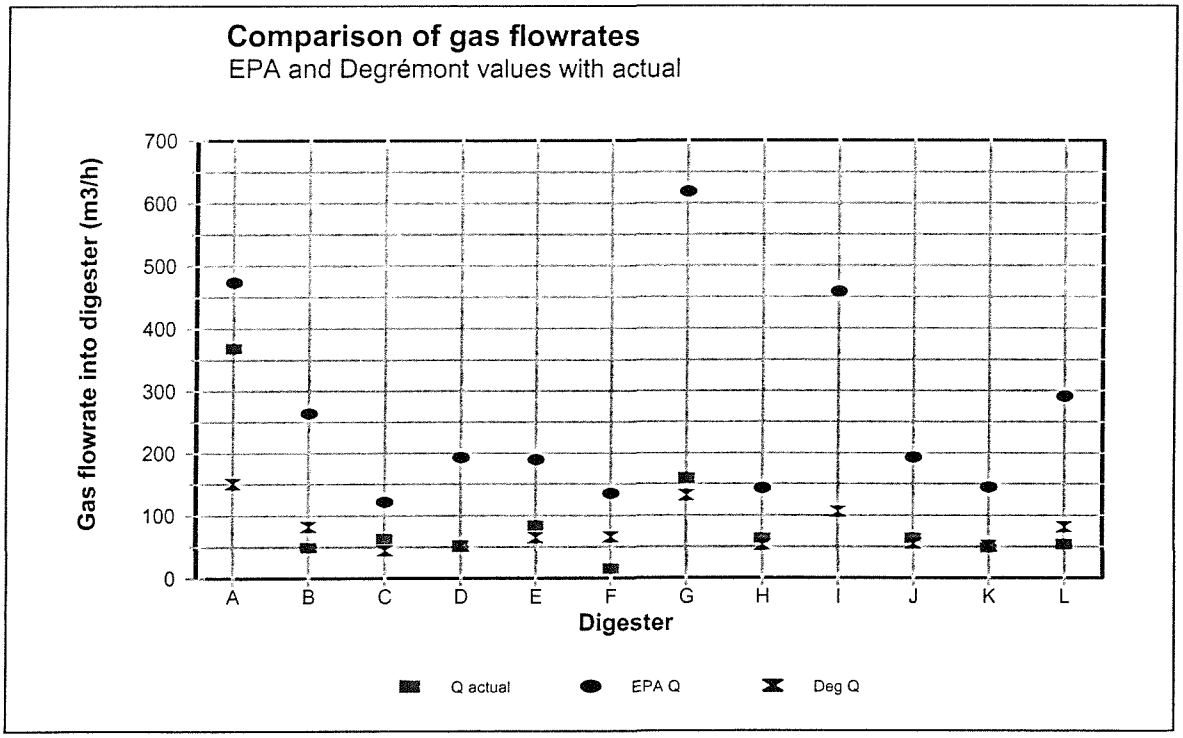

Figure 2: A plot of actual digester flowrates compared to those calculated from EPA and Degrémont design guidelines

Conclusions

The majority of UK anaerobic digesters are mixed using unconfined gas injection. There are only two published sets of design values for sizing unconfined gas mixers. These published design values from the EPA and Degrémont are based on gas flowrate per unit volume and area respectively. The different approaches lead to inconsistencies when changing scale or aspect ratio. Neither set of design values takes into account the effect of different sludge rheological properties on mixing performance.

The unconfined gas mixer design values published in the literature have been compared with those found in practice. Only one of the digesters surveyed met the EPA's power input per unit volume guidelines when calculating power input from isothermal expansion of the gas. None of the digesters met the EPA gas flowrate per unit volume guideline values. The surveyed digesters were found to be much nearer to Degrémont's gas flowrate per unit area recommended value of 0.8 $m^3/h/m^2$.

There is a need for clear design guidelines to be set to improve the design of unconfined gas digester mixers. Some of the questions that need answering are:

- Should designs be based on a gas flowrate per unit volume, gas flowrate per unit area or power input per unit volume?
- What should the power input values be? Literature quotes 5-8 Wm^{-3} whilst most surveyed digesters where found to be 2-4 Wm^{-3}.
- Should gas be supplied continuously or intermittently?
- Should this be supplied to one nozzle at a time or all nozzles together?
- What is the optimum nozzle arrangement?
- What is the effect on mixing requirements for different sludge rheologies?

Once these questions can be answered, the design and operation of unconfined gas mixing systems for anaerobic digesters will be improved.

Acknowledgements

The authors would like to thank Dr Nick Fawcett of Yorkshire Water plc., Pascale Brotier and Sarah Ouziaux for their painstaking data collection and Colin Brade of Monsal Ltd.

References

1. Council of European Communities. Directive concerning urban waste water treatment (91/271/EEC). *Official Journal L135/40*, 21 May, 1991
2. Department of the Environment. Code of Practice for Agricultural Use of Sewage Sludge. Second Edition. HMSO, 1996.
3. U.S. Environmental Protection Agency: Evans, F. III, Gilbert, W.G. and Walsh, T.K. "EPA Design Information Report" *J.Wat.Poll.Control Fed.*, **59**, 3, 162-170, 1987
4. DEGREMONT "Water Treatment Handbook", 6th ed. Paris: Lavoisier Publishing, 1991
5. Yorkshire Water Services plc, internal report,1997.
6. Pagilla K.R., Craney, K.C., Kido, W.H., "Causes and effects of foaming in anaerobic sludge digesters" *Wat.Sci.Tech.* Vol. 36, No. 6-7, pp. 463-470, 1997

7. CIWEM Handbook of UK Wastewater Practice, Sewage Sludge Stabilization and Disinfection,1996
8. Truscott, G.F. "Mixing in Anaerobic Sludge Digesters: A Preliminary Review" *BHRA Fluid Engineering,* 1980
9. Comerford, J.M. and Picken, D.J. " Free-Convective Mixing within an Anaerobic Digester". *Biomass* **6**, 1985, p235-245
10. Verhoff, F.H., Tenney, M.W. and Echelberger, W.F. "Mixing in Anaerobic Digestion" *Biotechnology and Bioengineering*, Vol. XVI, p. 757 - 770, 1974
11. Stukenberg, J.R. "Egg-Shaped Digesters: From Germany to the U.S." *Water Environment & Technology*, p42-51, April 1992
12. Rundle,H and Whyley,J.A., "Comparison of gas recirculation systems for mixing the contents of anaerobic digesters". *Wat.Pollution Control*,1981,**80,** (4), 463 to 490.

Appendix E

A Comparison of Mixing Systems in Model Anaerobic Sewage Sludge Digesters

This Appendix contains a copy of the paper co-written by the author of this thesis that was presented as a result of this work at the 5th European Biosolids and Organic Residuals Conference organised by Aqua-Enviro in Wakefield, UK on the 19th to the 22nd November, 2000.

A Comparison of Mixing Systems in a Model Anaerobic Digester

by

Mick Dawson[a], Jacquie Christodoulides[a], Nick Fawcett[b] and Colin Brade[c]

[a] BHRSolutions, The Fluid Engineering Centre, Cranfield, Bedfordshire, MK43 OAJ. Tel: 01234 750422 Fax: 01234 750074 Email:mdawson@bhrsolutions.com

[b] Yorkshire Water Services [c] Monsal Ltd

ABSTRACT

A wide variety of different equipment types have been used for digester mixing. Digester mixing systems are designed on the basis of work expended in mixing. However design values used are based on rules of thumb. There is a clear need for mixing criteria to be established and for the most effective systems to be identified.

Three different mixing systems were investigated in a cylindrical laboratory scale model digester using non-Newtonian CMC in concentrations of 0.3%, 0.6% and 1% by weight, (equivalent to digested sludges of 2.5%, 5% and 10% dry solids). Actively mixed volumes and blend times were measured over a range of power inputs using unconfined gas mixing, jet mixing and impeller mixing systems.

The performance of two unconfined gas addition methods (sequential and simultaneous), two liquid jet orientations and an impeller system are presented. The blend times and active volumes generated by these different mixing systems were compared at equal net power inputs.

The sequential gas arrangement produced the largest active volume at the lowest power input and one of the shortest blend times. There was a strong effect of viscosity on the active volumes and blend times for all mixers, although the sequential gas arrangement showed the least effect.

KEYWORDS

Digester, mixing, unconfined gas, jet, impeller, sludge rheology

INTRODUCTION

The work described in this paper was undertaken as part of a research project for Yorkshire Water Services and Monsal Limited.

The objectives of digester mixing are to[1,2]:

1 Provide contact between the feed sludge and the active biomass to maximise gas production

2 Provide physical, chemical and biological uniformity within a digester in order to maintain a satisfactory environment for both acid and methane forming bacteria

3 Distribute organics and dilute inhibitory substances

4 Prevent stratification and temperature gradients

5 Use the digester volume effectively to maintain the required biomass residence time, i.e. minimise short-circuiting

6 Minimise the deposition of solids, as this reduces effective digester volume.

7 Minimise the formation of a surface scum layer and foaming

Items 1 to 4 are functions of the rate of liquid blending. Item 5 is determined by the digester flow pattern. Item 6 is related to solid suspension and distribution and item 7 to foam breaking and draw-down from the surface. The research described here has focused on the liquid blending performance and flow pattern generated by digester mixing systems.

There are two main categories of mixing within anaerobic digesters, >natural= mixing and >assisted= mixing. Natural mixing occurs as a consequence of biogas evolution, heating, feeding and drawing off sludge[3].

Originally digesters were neither mixed nor heated and were operated under conditions termed >low rate digestion=. The first trials that involved digesting sludge anaerobically were recorded by W.J.Dibden in 1885, although it was not until 1934 that the first >assisted= mixing device, a screw pump, was installed in the UK[1]. The main purpose of mixing at that time was to break down the deposits of scum that formed on the surface of the digesting sludge.

During the 1920s and 30s, sludge digestion became widespread in the UK with several types of mixing and heating systems employed. However, during the late 1960s and early 1970s, operating difficulties were being reported in the UK and the popularity of anaerobic digestion suffered as a result. This prompted the WPRL survey[4] of 142 sewage treatment works (thought to represent over 90% of digestion works) to categorise operating difficulties. Of the surveyed works, 56 reported problems due to inadequate design or operation, which were or could be mixing related. Heating and mixing improvements to assist higher rate digestion were investigated in the early 1980s[5-9]. Many of the findings from these studies have been implemented.

A wide variety of different equipment types have been used for >assisted= digester mixing. The commonest classes are confined and unconfined gas injection systems, mechanical stirring and mechanical pumping systems. Large digesters sometimes operate multiple mixing systems.

A majority of UK digesters feature unconfined gas mixing systems and external recirculation loops[10]. The sludge gas is collected at the top of the digester, compressed and discharged, intermittently or continuously through multiple nozzles simultaneously or in sequence. The main advantage of unconfined gas mixing is the absence of internal moving parts, this reduces the down-time of the digester for maintenance. Published information concerning mixing quantification within digesters mixed using unconfined gas is relatively scarce[10-13].

Confined gas mixing systems are less common in the UK than unconfined systems. Sludge gas is collected at the top of the digester, compressed and discharged through draft-tubes. The gas rises up the draft-tube either as a stream of small bubbles or as a single slug depending on the flowrate of gas and the diameter of the draft-tube. As gas rises, it causes sludge to rise up the tube and be distributed over the surface. The claimed advantages of confined gas mixing over unconfined gas mixing are that it is more energy efficient and it provides a better movement of bottom deposits[2]. However, as much of the equipment is within the digester, corrosion can be a serious problem.

Mechanical stirring systems feature one or more shaft mounted, rotating impellers. The choice of impeller type, size, speed, etc. is critical in determining mixing effectiveness and, if chosen correctly, the mixing efficiency can be very good. Large diameter impellers were originally avoided because of the requirement to provide a bottom bearing, mounted within the tank. This problem was overcome by the use of a long balanced shaft[9]. Despite the potential benefits, widespread use of impellers in the UK has been limited.This may be partly due to the problems associated with the presence of mechanical equipment inside the digester and partly due to concern about shafts becoming imbalanced as a result of rag accumulation on the impeller. Problems of gas leaks at the shaft seals have also been reported[2].

Mechanical pumping systems can be external or internal. Internal systems typically comprise an impeller in a draft-tube and external systems are typically pumped recirculation loops for heating. Internal systems are claimed[12] to be effective both for grit suspension (downward pumping mode) and for scum control (upward pumping mode) but do have some of the disadvantages of an impeller system. There is often corrosion and wear on the internal equipment; the draft-tube can become blocked by rags during operation and the equipment is sensitive to the liquid level inside the digester[2].

External systems comprise of a pump mounted externally in a recirculation loop which may have a nozzle fitted to promote jet mixing. Multiple external recirculation pumps are sometimes used in large digesters as this eliminates any internal parts, reducing maintenance and down-time. The sludge feed can be introduced into the recirculation line and heated to the digester temperature rather than entering cold.

Currently digester mixing systems are sized on the basis of[2,11]:

Power input per unit volume (Wm^{-3})

Gas flowrate per unit volume of sludge ($m^3h^{-1}m^{-3}$)

Gas flowrate per unit area of digester ($m^3h^{-1}m^{-2}$)

The different approaches result in inconsistencies when changing scale, aspect ratio or mixer type. In addition, published power and gas flowrate design values vary over one order of magnitude[10]. Design values are typically based on past experience of engineers, operators and manufacturers rather than a definitive mixing theory. The values of mixing power input found in actual digesters surveyed are typically

lower than guideline values[10, 13]. Mixing equipment selection appears to have been dictated by market availability and there is little fundamental work establishing criteria for different mixing systems.

To date, a definitive mixing theory has not been developed due to variable sludge composition, limited information on the effects of sludge rheology, wide variety of mixing systems used and lack of data linking process performance to mixing parameters.

Impeller and liquid jet performance has been extensively studied in turbulent and transitional flow regimes in baffled vessels[14]. However, process mixing theory for liquid blending using liquid jets and impellers has not been applied to digesters due to insufficient published research work on typical digester geometries and sludge rheologies.

Residence Time Distribution (RTD) data from Lithium Chloride (LiCl) tracer tests have frequently been fitted using mathematical models to predict the volume of back mixed, plug-flow and dead zones in digesters[15]. This approach is useful in assessing the flowpattern and active volume during commissioning or operation, but is limited and costly for identifying the relative performance of different types of mixing system or system operation.

No thorough examination of the relative efficiencies of different digester mixing systems or operation modes has been reported. The effect of sludge rheology on the performance of different digester mixer types has also not been reported in the literature. The work described in this paper has set out to address some of the gaps in the current knowledge relating to these factors.

OBJECTIVES

To characterise the digester mixer geometries, operating conditions and sludge rheologies from key sites within Yorkshire Water's catchment area.

To find a safe, durable, cost effective and easy to use simulant for three 'typical' digested sludges that would represent the range of rheologies found in practice.

Identify the effects of unconfined gas flowrate, power input, sludge viscosity and mixer geometry on digester blend time and active volume.

Identify the effects of liquid jet flowrate, power input, sludge viscosity and jet geometry on digester blend time and active volume.

Identify the effects of impeller speed, power input, geometry and sludge viscosity on digester blend time and active volume.

Perform comparisons between the mixer types tested.

MATERIALS AND METHODS

Due to limited information on full-scale digester geometry, operation and sludge properties, a survey of 17 digestion sites within the Yorkshire Water area was undertaken. The results from this survey were used to design a laboratory scale model digester and to select a liquid simulant with similar rheological properties to those measured for a range of digested sludges.

Results from this survey are presented in Table 3.1. The dashes in Table 3.1 indicate where no information was available.

Table 3.1: Survey findings from 17 Yorkshire Water digestion sites

Site	Mixing System	Aspect Ratio	Vol. (m^3)	Mixer geometry	Gross P/V (Wm^{-3})	Net P/V (Wm^{-3})	Digested Sludge %DS
A	Unconfined gas	0.94	530	8 diffusers in outer ring 4 diffusers in inner ring	6.7	2.2	3.4
B	Unconfined gas	1.2	728	8 diffusers in outer ring 4 diffusers in inner ring	4.2	1.4	-
C	Unconfined gas	0.53	4900	16 lances	10.5	3.5	3.7
D	Unconfined gas	0.93	4586	24 diffusers in two rings	-	-	-
E	Unconfined gas	0.85	1130	8 diffusers in outer ring 4 diffusers in inner ring	5.7	1.8	-
F	Unconfined gas	1.08	3500	9 diffusers in base	12.9	-	2.5
G	Unconfined gas	1.07	1540	8 diffusers in outer ring 4 diffusers in inner ring	4.2	1.7	-
H	Unconfined gas	0.92	565	8 diffusers in outer ring 4 diffusers in inner ring	5.6	1.5	-
I	Unconfined gas	0.9	2276	18 around the base	2.8	0.9	3.1
J	Unconfined gas	0.53	5670	1 ring of diffusers in base 1 ring of diffusers at mid-height	-	-	3.3
K	Unconfined gas	0.4	105	12 diffusers around the base	-	-	5.0
L	Unconfined gas	0.82	1005	24 diffusers around the base	3.1	0.9	2.4
M	Unconfined gas	0.84	2920	8 diffusers in outer ring 8 diffusers in inner ring 1 central diffuser	7.8	2.1	4.6
N	Unconfined gas	0.81	500	1 ring of diffusers in base	8	-	3.3
O	Confined gas	0.41	10280		2.5	0.5	4.0
P	Confined gas	0.36	3400		8.8	1.0	-
Q	Mechanical mixing & sludge recirculation	0.51	4038		-	-	2.4

The unconfined gas gross power inputs were determined using compressor power ratings and assuming 100% efficiency. The net power inputs were determined using the isothermal expansion of the rising gas plume:

$$P = \dot{n} RT \ln\left(\frac{p_1}{p_2}\right) \qquad \text{(Eqn.3.1)}$$

Where P = Power input (W)

n = molar gas flow-rate (mol/s)

R = Universal gas constant (J/mol/K)

T = Temperature (K)

P = pressure (Pa)

The net P/V values are approximately one third of the gross P/V values suggesting a compressor efficiency of about 30%.

Digester geometry

Most of the digesters surveyed had shallow conical sloping bases with an angle of 7° or so whilst two had a steeper slope of 20°. The majority of digester inlets were located at the top by the wall, two inlets were located in the base by the wall and one was situated centrally at mid-depth. All of the outlets were overflow weirs positioned at the top of the digesters. In some cases, the inlet and outlet were positioned close together which could result in short-circuiting of the feed sludge.

Digester operation

The majority of the digesters surveyed were fed on a semi-continuous basis, with a frequency of several minutes per 20 to 30 minute cycle. The feed sludge usually entered the recirculation loop where it was preheated to the digesting sludge temperature.

The method of gas addition for the unconfined gas injection digesters varied. The gas was either supplied in a pre-arranged sequence to each diffuser for a set period or was supplied simultaneously to all of the diffusers. Gas could also be supplied continuously or intermittently throughout the day, the latter case being the preferred method within the surveyed digesters.

Sludge rheology

Samples of sludge were withdrawn from each of the digesters surveyed and their rheological properties measured. Sludges exhibit non-Newtonian behaviour where the shear rate and shear stress do not vary proportionally as for a Newtonian fluid such as water. Due to the different composition of sludges, their rheological behaviour varies between sludge types and between sites. Samples of 22 digested sludges from different sites were taken to provide a more complete understanding of their rheologies, and ultimately, to help select suitable simulants for use in the laboratory.

Rheology measurements

Brookfield LVDV-II+ and DVIII rheometers were used in the 'open-sea' method where the spacing between the concentric cylinders is wide enough to avoid the effect of solids suspended in the sludge[16]. The rheological properties were determined by performing linear regressions on the shear stress-shear rate data and fitting to the Herschel-Bulkley model:

$$\tau = \tau_y + k\dot{\gamma}^n \qquad \text{(Eqn.3.2)}$$

The effect of digesting high dry solids sludges was investigated in this work. The surveyed digested sludges ranged from 2.5 to 5% DS. To provide thicker sludge samples a 10%DS sludge was formed by evaporation in an oven at 35°C. Three sludges (2.5% DS, 5% DS and 10% DS) were chosen as representative of the surveyed range of sludge rheologies shown in Figure 3.1

Simulant selection

A simulant was required for each of the three representative sludges of 2.5%, 5% and 10%DS. The simulant needed to be durable, easy to make-up and use, transparent for flow visualisation, non-hazardous and cost effective. After trying several types of polymer solutions, Grade 7H4C CMC (Sodium carboxymethylcellulose) was chosen for use in concentrations of 0.3%, 0.6% and 1% by weight. Figure 3.2 shows the viscosity v. shear rate data for these simulant concentrations with the corresponding data from the sludges being simulated.

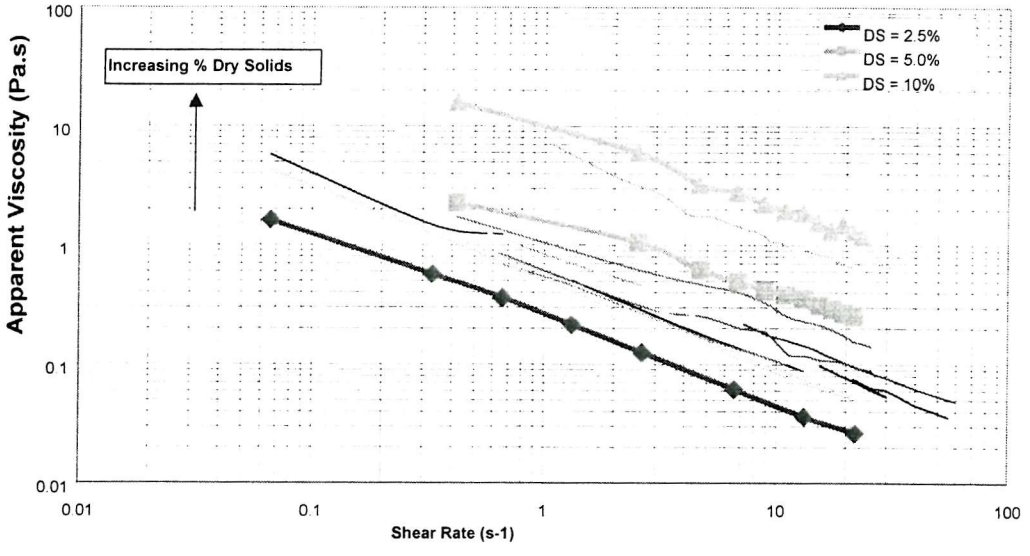

Figure 3.1: Range of apparent sludge viscosities found from site survey

A laboratory scale model digester was designed to reflect the vessel and mixer geometries found during the site survey. The result was a 0.61m diameter cylindrical Perspex vessel, with a flat base. In addition, a pilot scale 2.67m diameter cylindrical vessel was used for a number of tests.

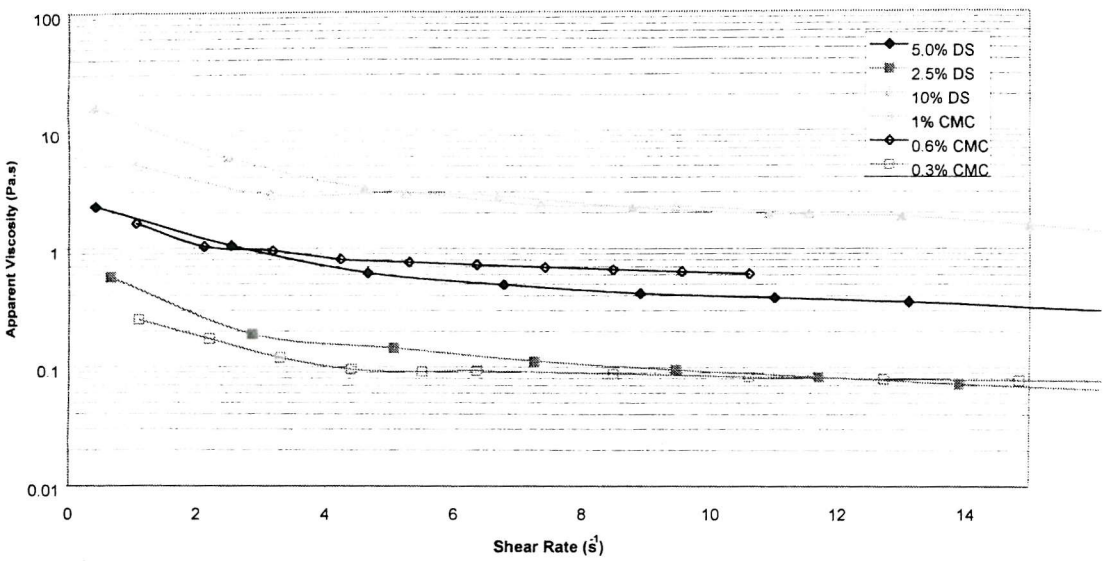

Figure 3.2: Comparison of Sludge and Simulant apparent viscosities.

Model digester unconfined gas blending

Two gas sparger arrangements were investigated and are shown in Figure 3.3. Sparger A consisted of a central ring of 4 diffusers with gas supplied simultaneously to all 4, this represents a system found commonly in practice. Sparger B consisted of a central ring of 4 diffusers and an outer ring of 12 diffusers with air supplied to each diffuser in sequence.

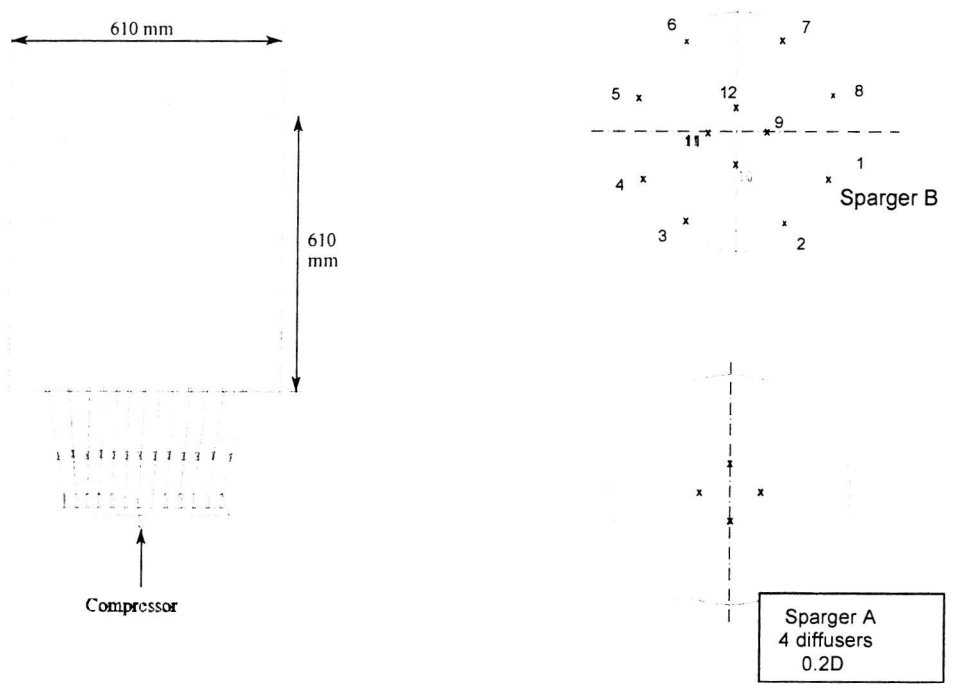

Figure 3.3: Unconfined gas injection with Spargers A and B

Jet blending

Figure 3.4 shows the two liquid jet orientations studied: a vertical downward jet and a tangential jet.

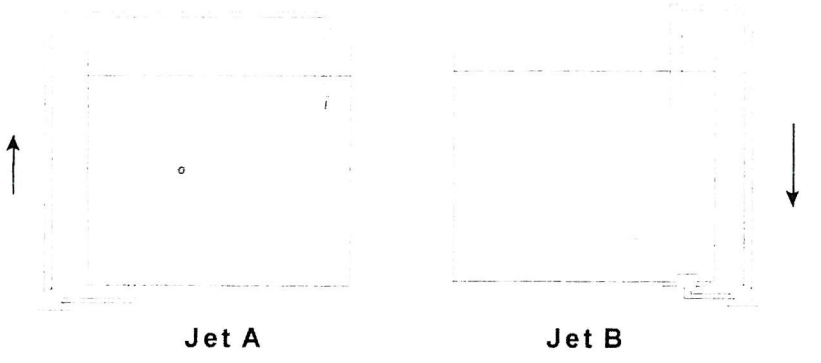

Figure 3.4: Jet orientations A and B

Impeller blending

Figure 3.5 shows a 4-blade, T/3 diameter, downward pumping, 45° pitch-blade turbine impeller, which was studied at a clearance of T/3 from the vessel base both with and without baffles.

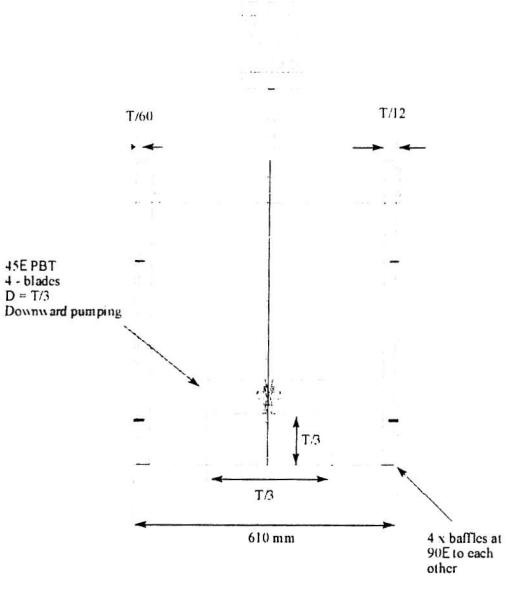

Figure 3.5: Impeller geometry

Experimental Methods

A range of gas flow-rates was used for the two unconfined gas sparger geometries to give net power inputs per unit volume spanning the range of values found on-site. Jet flow-rates were selected to provide a similar range of net power inputs. Jet Reynolds numbers were in the transitional and turbulent flow regimes. Impeller speeds were selected to ensure turbulent flow (impeller Reynolds number). At the laboratory scale the speeds required to achieve turbulent flow in 0.6% and 1% CMC resulted in unrealistically high power inputs. As a result, impeller and unconfined gas results in the more viscous simulants could only be

compared at 2.67m scale.

Blend time determination

The rate of liquid blending can be determined by measuring the time taken for the concentration of a tracer material to become uniform throughout all of the test volume. Here a salt tracer (NaCl solution) was used to follow the rate of blending. The tracer was added to the vessel and its concentration measured using 5 miniature conductivity probes. The blend time experiments were conducted in batch fashion with the tracer addition position and relative volume matched to those found during the site survey. It soon became clear that the responses of the probes in different regions of the model digester could vary significantly. This indicated that fully turbulent flow was not present throughout the model under all test conditions. Visual observation clearly showed the extent of 'active' and 'inactive' zones. Probe responses in the 'active' zones agreed well, leading to the adoption of an 'active' zone blend time. All the blend time results presented in this paper are for the 'active' zone.

Active volume determination

Flow patterns were recorded using a combination of dye and flow followers (neutrally buoyant coloured plastic shapes). Visual observation and video footage were used to determine the approximate size and locations of both 'active' and 'inactive' zones in the model digester. Both active volume and blend time results are presented in the next section.

RESULTS AND DISCUSSION

Figure 4.1 compares actively mixed volumes using continuous (Sparger A) and simultaneous (Sparger B) unconfined gas addition. The sequential addition of gas through nozzles distributed across the digester

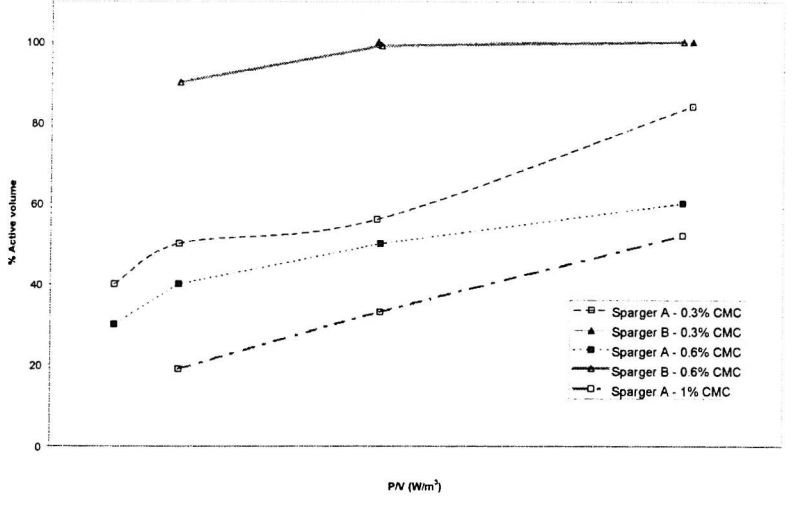

Figure 4.1: % Active volume Vs P/V for unconfined gas spargers A and B

floor resulted in a much larger actively mixed volume than simultaneous gas addition at equal net power

input in simulants equivalent to sludges of 2.5% to 5%DS. As expected, increasing sludge thickness from 2.5%DS to 10%DS significantly reduced the actively mixed volume whereas increasing net power input increased active volume.

Figure 4.2 is a representation of the actively mixed volumes observed using Sparger A. The last regions to become active were around the circumference of the digester base. As viscosity increases or power input falls the actively mixed volume shrinks until it forms a narrow cylinder around the gas plume rising from the four cenrally placed nozzles. Sequential gas addition through a larger number of well-spaced nozzles prevents the formation of persistent stagnant or 'inactive' zones.

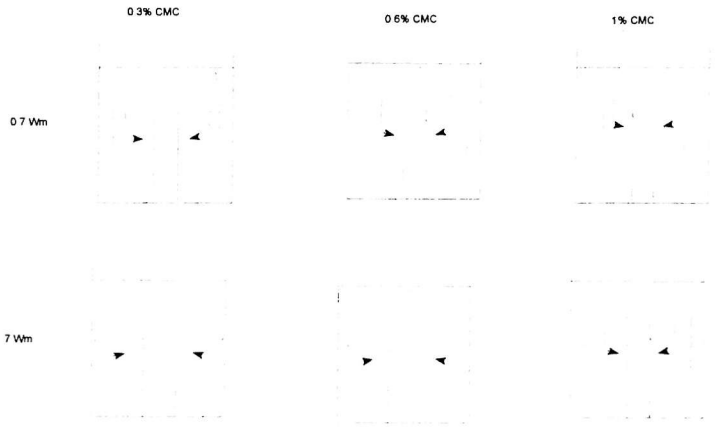

Figure 4.2: Representation of active volumes for sparger A

The blend times measured in the actively mixed volumes using unconfined gas spargers A and B are shown in Figure 4.3. The blend times for the two sparger types were similar in 0.3% CMC (simulating approx. 2.5%DS digested sludge). However, as the simulated sludge thickness increased, the sequential gas addition (Sparger B) provided active volume blend times that were significantly shorter at equal net power input. It was also evident that as sludge thickness increased not only did the active volume shrink but the blend time within it also rose.

The actively mixed volumes achieved using the two orientations of jets tested are shown in Figure 4.4. There was little difference between the orientations in 0.3% CMC where the jets were effective at turning over the fluid in the model digester. However, the actively mixed volumes decreased in 0.6% CMC (equivalent to 5% sludge DS) where the tangential Jet B with a longer path length performed better than the vertical Jet A. As simulated sludge thickness increased further (1% CMC equivalent to 10%DS sludge) the jets became even less effective. Active volumes in 1% CMC were so small at the highest net power inputs that the experiments were terminated.

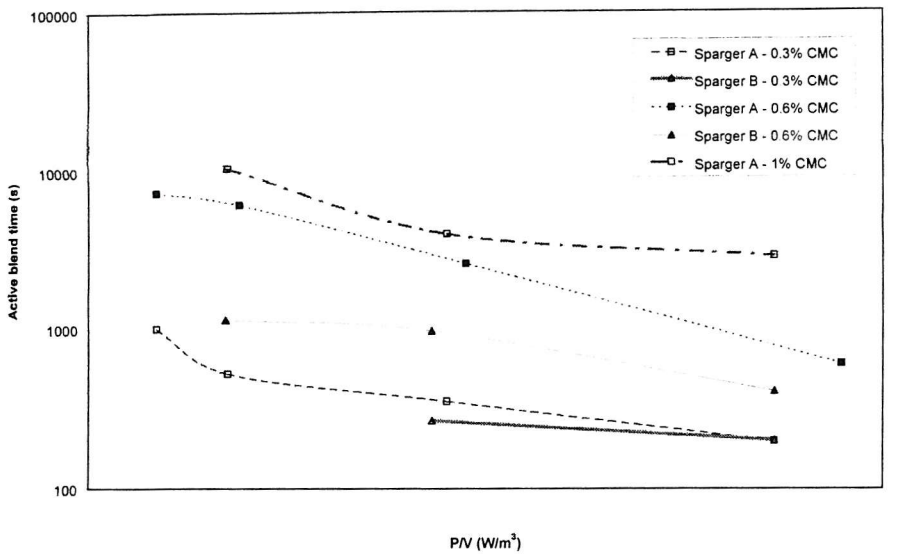

Figure 4.3: Active blend time Vs P/V for unconfined gas spargers A and B

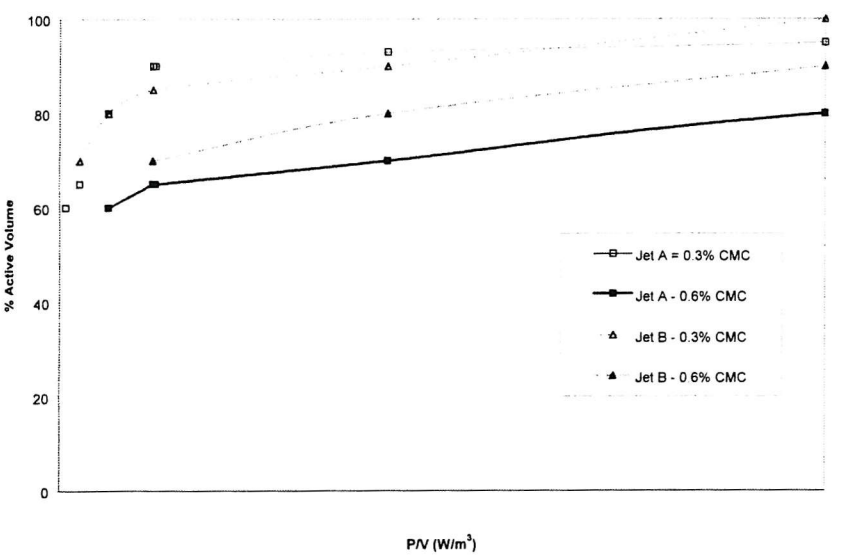

Figure 4.4: % Active volume Vs P/V for liquid jet orientations A and B

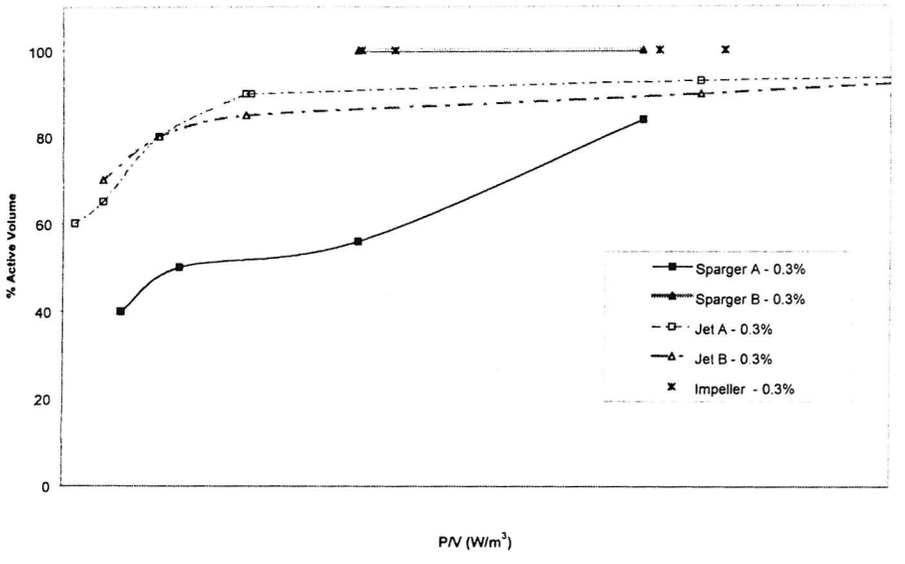

Figure 4.5: % Active volume Vs P/V in 0.3% CMC

An actively mixed volume comparison of all the mixer types tested in 0.3% CMC (2.5%DS sludge equivalent) is shown in Figure 4.5. The most effective mixers were the sequential gas Sparger B and the impeller. The two liquid jet orientations were only marginally worse in this low viscosity simulant, whilst the simultaneous gas addition (Sparger A) gave the lowest active volume. The corresponding active volume blend times are shown in Figure 4.6. The shortest blend times were achieved using the sequential gas Sparger B although tests have yet to be carried out at the lower end of the power-input range. The simultaneous gas Sparger B, impeller and vertical jet A showed similar active volume blend times. Overall in 0.3% CMC, accounting for both the size of the actively mixed volume and the blend time within it, the sequential Sparger B performed best followed by the impeller, liquid jets and finally simultaneous Sparger A.

A comparison of the actively mixed volumes in 0.6% CMC (equivalent to 5%DS sludge) is shown in Figure 4.7. The sequential gas Sparger B provided significantly greater active volumes than the jet orientations. The simultaneous Sparger A performed poorly compared with the other mixers tested. The active volume blend times in 0.6% CMC are presented in Figure 4.8. The sequential gas Sparger B gave much shorter blend times particularly at low net power inputs. Both liquid jet orientations showed longer blend times in smaller active volumes. The simultaneous Sparger A performed better than the liquid jets at high net power inputs. Overall, in simulant equivalent to 5%DS digested sludge, blend times for all mixers except Sparger B increased by roughly an order of magnitude compared with those in simulant equivalent to 2.5%DS sludge. The sequential gas Sparger B blend times increased with increasing viscosity, but at a slower rate than the other mixers.

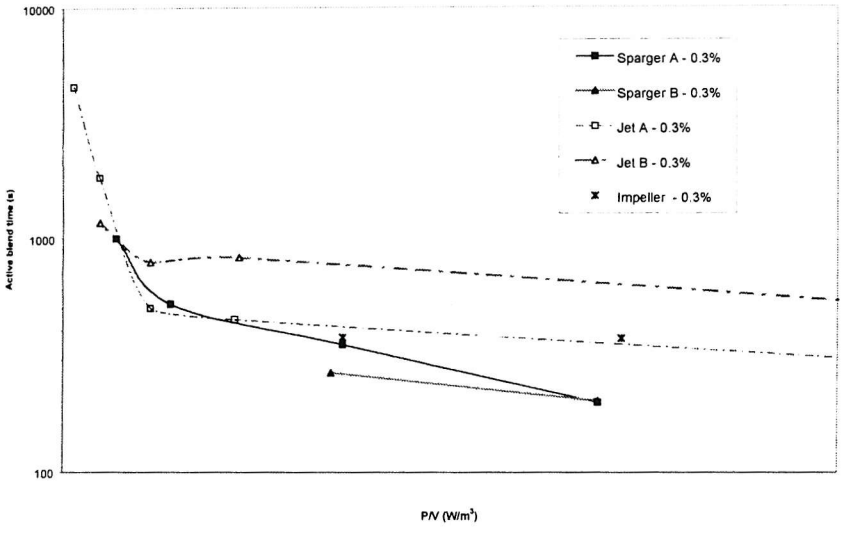

Figure 4.6: Active blend time Vs P/V in 0.3% CMC

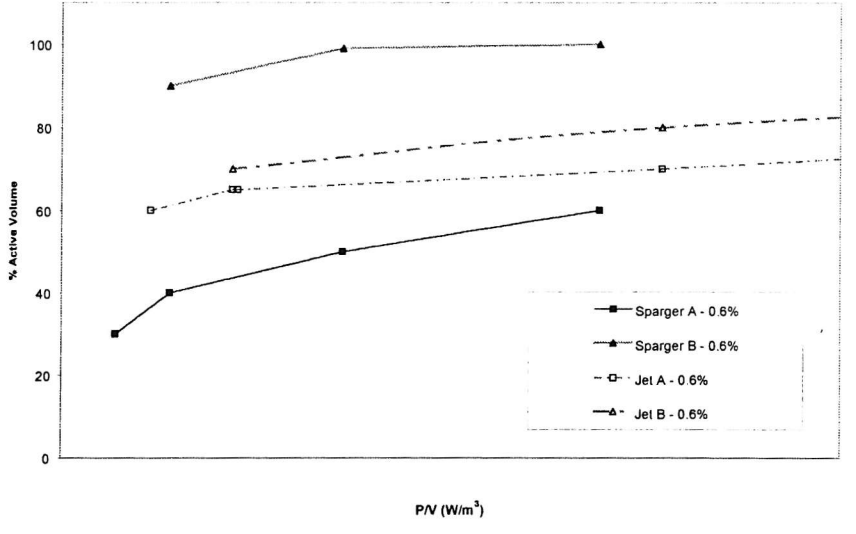

Figure 4.7: % Active volume Vs P/V in 0.6% CMC

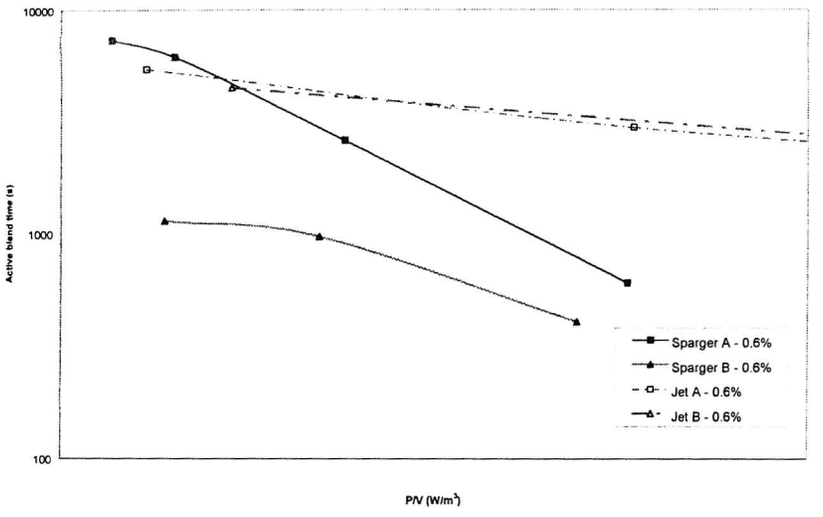

Figure 4.8: Active blend time Vs P/V in 0.6% CMC

The impeller mixing system could not be compared with the jet and unconfined gas systems at the laboratory scale in 0.6% CMC because of the high net power inputs required to achieve turbulent impeller Reynolds numbers. This shortcoming was rectified by comparing experimental blend time results using gas Sparger A in a $15m^3$ volume 2.67m diameter pilot scale vessel with impeller blend time data for the same scale and liquid calculated using blend time correlations[17]. The comparison is shown in Figure 4.9. The predicted impeller blend times were somewhat shorter than those measured for Sparger A at equal net power input. The tenfold increase in blend time with increasing sludge viscosity from 2.5%DS to 5%DS equivalents was similar to that seen at the laboratory scale.

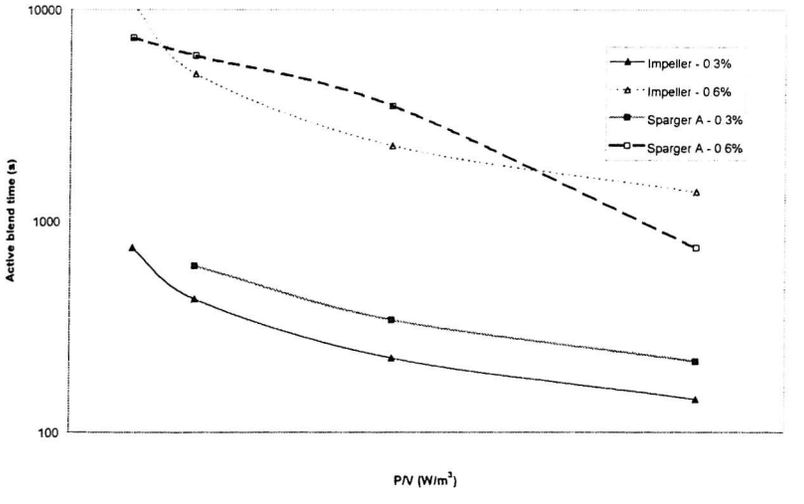

Figure 4.9: Active blend time vs P/V for Impeller and Sparger A in a pilot scale model digester

CONCLUSIONS AND FURTHER WORK

Most digesters in the UK currently use unconfined gas mixing systems with net power inputs of 1.5 to 3.5 W/m^3, a majority of these systems feature simultaneous rather than sequential gas addition. At equal net power inputs with well-spaced diffusers, the manner in which gas flow was introduced into model digesters had a very significant impact on the size of the actively mixed volume and blend time within the actively mixed volume. By switching the total gas flow from one diffuser to the next in sequence considerably greater active volumes and shorter blend times could be achieved when compared with continuously dividing the total gas flow between all the available diffusers. The superiority of the sequential gas arrangement increased as the sludge dry solids content and hence viscosity increased. In addition, the sequential gas addition system provided greater actively mixed volumes which is becoming increasingly important with new controls over pathogen content and the need for guaranteed residence times.

Comparison of impeller, liquid jet and unconfined gas mixing systems was carried out at equal net power inputs. The sequential unconfined gas system was the most efficient overall, followed by the impeller system with marginally longer blend times. The liquid jet systems performed reasonably at low sludge viscosity but deteriorated sharply at high dry solids equivalents. The unconfined gas system where gas was supplied simultaneously to all diffusers was the least efficient mixing system.

Significant power savings can therefore be achieved by replacing simultaneous gas addition systems with sequential systems.

Further work to extend the range of test conditions using the sequential gas mixing system is planned. In addition, more test work at pilot scale (15 m^3)and the use of full-scale data is planned to provide greater precision when scaling –up the laboratory findings.

REFERENCES

1. The Chartered Institution of Water and Environmental Management. Handbooks of UK Wastewater Practice. *ASewage Sludge:, Stabilisation and Disinfection≅ CIWEM,* 1995

2. U.S. Environmental Protection Agency : Evans, F. III, Gilbert, W.G. and Walsh, T.K. AEPA Design Information Report≅ *J. Wat. Pollut. Control Fed.*, **59**, 3, 162-170, 1987.

3. Casey, T.J. ARequirements and Methods for Mixing in Anaerobic Digesters≅ in *Anaerobic Digestion of sewage sludge and organic agricultural wastes; seminar, Athens, Greece, Elsevier Applied Science Publishers Ltd. Essex, England,* May 14-15, 1984.

4. Swanwick, J.D., Shurben, D.G. and Jackson, S. AA Survey of the Performance of Sewge Sludge Digesters in Great Britain≅ *Wat.Pollut. Control* **68**, (6), 639 - 661, 1969

5. Brade, C.E. and Noone, G.P. AAnaerobic Sludge Digestion - Need it be expensive? Making more of existing resources≅ *Wat. Pollut. Control,* 70-94, 1981.

6. Brade, C.E., Noone, G.P., Powell, E., Rundle, H. and Whyley, J. AThe Application of Developments in Anaerobic Digestion within Severn-Trent Water Authority≅ *Wat. Pollut. Control,* **81**, (2), 200 - 219, 1982

7. Brade, C.E., Smith, P.B. and Newton, G. ASteam-Heated Digester Performance≅ *Wat. Pollut. Control,* **85**,

(3). 356 - 365. 1986

8. Noone. G.P. and Brade. C.E. ALow-Cost Provision of Anaerobic Digestion: II. High-Rate and Prefabricated Systems≅ *Wat.Pollut. Control* **81**. (4). 479 - 510. 1982

9. Rundle. H. and Whyley. J. AA Comparison of Gas Recirculation Systems for Mixing of Contents of Anaerobic Digesters≅ *Wat. Pollut. Control*. **80**. (4). 463 - 490. 1981

10. Barker.J. and Dawson.M .'Digester Mixing: Theory and Practice'. 3rd European Biosolids & Organics Residuals Conference. 1998.

11. DEGREMONT AWater Treatment Handbook≅. 6th ed. Paris: Lavoisier Publishing. 1991.

12. Stukenberg. J.R.. Clark. J.H.. Sandino. J. and Naydi. W.R. AEgg-shaped digesters: From Germany to the U.S.≅ *Water Environment & Technology*. 42 - 51. 1992.

13. Williams. P.A. AMixing in anaerobic digesters≅ *Ph.D. Thesis. Cranfield University of Science and Technology*. 1994

14. Tatterson. G.B.. AFluid Mixing and Gas Dispersion in Agitated Tanks≅ *McGraw-Hill Inc.* 1991

15. Williams. S. AMixing in sewage slude digestion≅ paper from Joint meeting of the water and fluid mixing subject groups IChemE one-day seminar. *The Water Industry and Mixing Technology*. 1992

16. Whorlow.R.W.. Rheological Techniques. Ellis Horwood Ltd.. 1980.

17. Ruskowski. S.W.. 'A Rational Method for Measuring Impeller Blending Performance and Comparison of Different Impeller Types'. 8th European Conference on Mixing. University of Cambridge. UK. I.Chem.E Symposium series No136.p283-291.1994

References

Acharya, A., R. Mashelkar, and J. Ulbrecht (1977). *Chemical Engineering Science 24*, 348.

Astarita, G. and G. Apuzzo (1965). Motion of gas bubbles in non-Newtonian fluids. *American Institution of Chemical Engineers Journal 11*, 815.

Balmer, P. (1999, March/April). Experiences with flat-bottomed, high digesters. *Water Quality International* , 41–43.

Barker, J. S. and M. Dawson (1998). Digester mixing: Theory and practice. In *3rd European Biosolids and Organic Residuals Conference, Aqua-Enviro, Wakefield, UK. 16-18 November.*

Barnes, H. A., J. F. Hatton, and K. Walters (1989). *An Introduction to Rheology.* Elsevier, Amsterdam.

Barnett, S., A. E. Humphrey, and M. Litt (1966). *American Institution of Chemical Engineers Journal 12*, 253.

Baumann, P. G. and G. L. Huibregste (1982). Evaluation and comparison of digester gas mixing systems. *Journal of the Water Pollution Control Federation 54*(8), 1194–1206.

Bhaga, D. and M. E. Weber (1980). In-line interaction of a pair of bubbles in a viscous liquid. *Chemical Engineering Science 35*(12), 2467–2474.

Bhavaraju, S., R. Mashelkar, and H. Blanch (1978). Bubble motion and mass transfer in non-Newtonian fluids - single bubble in Power Law and Bingham fluids. *American Institution of Chemical Engineers Journal 24*(6), 1063–1070.

Bode, H. and E. Klauwer (1999, March/April). Advantages and disadvantages of different shapes in digester design. *Water Quality International* , 35–40.

Brade, C. E. (1997). The IMPACT programme anaerobic digester mixing: Notes on current best practice for unconfined gas mixing. (unpublished).

Brade, C. E. and G. P. Noone (1981). Anaerobic sludge digestion - need it be expensive? Making more of existing resources. *Water Pollution Control 80*(1), 70–94.

Brade, C. E., G. P. Noone, E. Powell, H. Rundle, and J. Whyley (1982). The application of developments in anaerobic digestion within Severn-Trent Water Authority. *Water Pollution Control 81*(2), 200–219.

Brookfield (1996). More Solutions to Sticky Problems. Technical Manual from Brookfield Engineering Laboratories Inc., 240, Cushing Street, Stoughton, Massachussetts 02072 USA.

Buzzell, J. C. and C. N. Sawyer (1963). Biochemical vs. physical factors in digester failure. *Journal of the Water Pollution Control Federation 35*, 205.

Calderbank, P. H., D. S. L. Johnson, and J. Loudon (1970). Mechanics and mass transfer of single bubbles in free rise through some Newtonian and non-Newtonian liquids. *Chemical Engineering Science 25*, 235–256.

Carrol, W. D. and R. D. Ross (1983). A full-scale comparison of confined and unconfined gas lift mixing systems in anaerobic digesters. In *Proceedings of the WRc Conference on Stabilisation and Disinfection of Sewage Sludge, Manchester.* Cited in Casey, 1984.

Casey, T. J. (1984). Requirements and methods for mixing in anaerobic digesters. In *Anaerobic Digestion of Sewage Sludge and Organic Agricultural Wastes Seminar, Athens, Greece. May 14-15. ISBN:0 85334 431 0*, pp. 90–103. Elsevier Applied Science Publishers Ltd.

Chen, M. H. and S. S. S. Cardoso (2000). The mixing of liquids by a plume of low-Reynolds number bubbles. *Chemical Engineering Science 55*(14), 2585–2594.

Chhabra, R. P. (1993). *Bubbles, Drops and Particles in Non-Newtonian Fluids.* CRC Press, Florida.

CIWEM (1996). Handbooks of UK wastewater practice. Sewage sludge: Stabilisation and disfinfection. ISBN:1 870875 24 4. Technical report, The Chartered Institution of Water and Environmental Management.

Clift, R., J. R. Grace, and M. E. Weber (1978). *Bubbles, drops, and particles.* Academic Press Inc. ISBN 0-12-176950-X.

Colella, D., D. Vinci, R. Bagatin, M. Masi, and E. ABu Bakr (1999). A study on coalescence and breakage mechanisms in three different bubble columns. *Chemical Engineering Science 54*, 4767–4777.

Costes, J. and C. Alran (1978). Models for the formation of gas bubbles at a single submerged orifice in a non-Newtonian fluid. *International Journal of Multiphase Flow 4*, 535.

Crabtree, J. R. and J. Bridgwater (1969). Chain bubbling in viscous liquids. *Chemical Engineering Science 24*, 1755–1768.

Crabtree, J. R. and J. Bridgwater (1971). *Chemical Engineering Science 26*, 839.

Davidson, J. F. and B. O. G. Schuler (1960a). Bubble formation at an orifice in a viscous fluid. *Transactions of the Institute of Chemical Engineers 38*, 145.

Davidson, J. F. and B. O. G. Schuler (1960b). Bubble formation at an orifice in an inviscid liquid. *Transactions of the Institute of Chemical Engineers 38*, 335.

Deckwer, W. D. and A. Schumpe (1993). Improved tools for bubble column reactor design and scale-up. *Chemical Engineering Science 48*, 889–912.

Degrémont (1991). *Water Treatment Handbook - Vol.II.* Lavoisier Publishing.

Dekée, D., P. J. Carreau, and J. Mordarski (1986). Bubble velocity and coalescence in viscoelastic liquids. *Chemical Engineering Science 41*(9), 2273–2283.

Dekée, D. and R. P. Chhabra (1988). A photographic study of shapes of bubbles and coalescence in non-Newtonian polymer solutions. *Rheol. Acta 27*, 656.

Department of the Environment (1996). Code of practice for agricultural use of sewage sludge. Technical report, HMSO.

Dewsbury, K., D. Karamanev, and A. Margaritis (1999). Hydrodynamic characteristics of free rise of light solid particles and gas bubbles in non-Newtonian liquids. *Chemical Engineering Science 54*, 4825–4830.

DoE (1996). *Department of the Environment, Code of Practice for Agricultural Use of Sewage Sludge* (Second ed.).

Edgington, R. (2000). Digestion: Are we getting what we expect? In *5th European Biosolids and Organic Residuals Conference, Aqua-Enviro, Wakefield, UK. 19-22 November.*

Edwards, M. F. (1997). *Mixing in the Process Industries* (Second Edition ed.)., Chapter 8, pp. 137–158. Butterworth-Heinemann, Oxford.

Elefsiniotis, P. and W. K. Oldham (1994). Effect of HRT on acidogenic digestion of primary sludge. *Journal of Environmental Engineering 120*(3), 645–660.

EPA (1987). EPA design information report. *Journal of the Water Pollution Control Federation 59*(3), 162–170.

ESDU (1982, December). Non-Newtonian fluids: introduction and guide to classification and characteristics. Technical Report Item No. 82036, ESDU International plc, London.

EU (1991, May). 991/271/EEC directive concerning Urban Wastewater Treatment. Technical report, Council of European Communities.

Fawcett, N. F. (1997). Personal communication.

Frost, R. C. (1983). How to design sewage sludge pumping systems. Technical Report TR185, Water Research centre.

Grenville, R. K. (1992). *Blending of Viscous Newtonian and Pseudo-Plastic Fluids.* Ph. D. thesis, Cranfield Institute of Technology.

Grenville, R. K. and J. Tilton (1997). Turbulence or flow as a predictor of blend time in turbulent jet mixed vessels. *Récents Progrès en Génie des Procédés. 11*(51), 67–74. ISBN: 2 910239 25 x.

Gujer, W. and A. J. B. Zehnder (1983). Conversion processes in anaerobic digestion. *Water Science Technology 15*(8), 127–167.

Haque, M. W., K. D. P. Nigam, and J. B. Joshi (1986). Hydrodynamics and mixing in highly viscous pseudo-plastic non-Newtonian solutions in bubble columns. *Chemical Engineering Science 41*(9), 2321–2331.

Haque, M. W., K. D. P. Nigam, V. K. Srivastava, J. B. Joshi, and K. Viswanathan (1987). Studies on mixing time in bubble columns with pseudoplastic (carboxymethyl) cellulose solutions. *Industrial Engineering Chemical Research 26*, 82–86.

Haque, M. W., K. D. P. Nigam, K. Viswanathan, and J. B. Joshi (1988). Studies on bubble rise velocity in bubble columns employing non-Newtonian solutions. *Chemical Engineering Communications 73*, 31–42.

Harnby, N., M. F. Edwards, and A. W. Nienow (Eds.) (1997). *Mixing in the Process Industries* (Second Edition ed.)., Chapter 8, pp. 322–363. Butterworth-Heinemann, Oxford.

Hassager, O., C. Bisgaard, and K. Ostergaard (1980). Measurements of velocity fields around objects moving in non-Newtonian liquids. *Plastics in Medicine and Surgery (International Conference) 2*, 17–21.

Hertle, C. K. and M. L. Lever (1987, March). Mixing in anaerobic sludge digesters. *Water 14*(1), 16–20,37.

Hirose, T. and M. Moo-Young (1969). *Canadian Journal of Chemical Engineering 47*, 265.

Hirose, T. and M. Moo-Young (1972). *Industrial Engineering Chemical Fundamentals 11*, 281.

Imhoff, K. R. (1983). Design and operation of anaerobic sludge digesters in Germany. In *Proceedings of the WRc Conference on Stabilisation and Disinfection of Sewage Sludge, Manchester.* Cited in Casey, 1984.

Jacobs, B. E. A. (1994). *Design of slurry transport systems.* Elsevier Science publishers Ltd ISBN 1-85166-634-6.

Joshi, J. B. and M. M. Sharma (1976). A circulation cell model for bubble columns. *Transactions of the Institution of Chemical Engineers 57*, 244–251.

Kawase, Y. and M. Moo-Young (1986a). Influence of non-Newtonian flow behaviour on mass transfer in bubble columns with and without draft tubes. *Chemical Engineering Communications 40*, 67–83.

Kawase, Y. and M. Moo-Young (1986b). Liquid phase mixing in bubble columns with Newtonian and non-Newtonian fluids. *Chemical Engineering Science 41*(8), 1969–1977.

Khang, S. J. and T. J. Fitzgerald (1975). A new probe and circuit for measuring electrolyte conductivity. *Industrial Engineering Chemistry Fundamentals 14*, 208–213.

Kumar, R. and N. R. Kuloor (1970). The formation of bubbles and drops. *Advances in Chemical Engineering 8*, 255.

Li, H. Z. (1999). Bubbles in non-Newtonian fluids: Formation, interactions and coalescence. *Chemical Engineering Science 54*, 2247–2254.

Lin, K. C. and M. E. J. Pearce (1991). Effects of mixing on anaerobic treatment of potato-processing wastewater. *Canadian Journal of Civil Engineering 18*, 504–514.

Lotito, V., L. Spinosa, G. Mininni, and R. Antonacci (1997). Rheology of sewage sludge at different steps of treatment. *Water Science and Technology 36*(11), 79–85.

McDonough, R. J. (1992). *Mixing for the process industries.* Van Nostrand Reinhold, New York.

Metzner, A. B., R. H. Feehs, H. L. Ramos, R. E. Otto, and J. D. Tuthill (1961). Agitation of viscous Newtonian and non-Newtonian fluids. *American Instiution of Chemical Engineers Journal 7*(3), 3–9.

Metzner, A. B. and R. E. Otto (1957). Agitation of non-Newtonian fluids. *American Institution of Chemical Engineers Journal 3*(3), 3–10.

Monteiro, P. (1997). The influence of the anaerobic digestion process on the sewage sludges rheological behaviour. *Water Science and Technology 36*(11), 61–67.

Nienow, A. W. (1997). *Mixing in the Process Industries* (Second Edition ed.)., Chapter 1, pp. 1–24. Butterworth-Heinemann, Oxford.

Nishikawa, M., H. Kato, and K. Hashimoto (1977). Heat transfer in aerated tower filled with non-Newtonian liquid. *Industrial Engineering Chemical Process Design and Development 16*, 133–137.

Noone, G. P. and C. E. Brade (1982). Low-cost provision of anaerobic digestion: II. High-rate and prefabricated systems. *Water Pollution Control 81*(4), 479–510.

Novaes, R. F. V. (1986). Microbiology of anaerobic digestion. *Water Science Technology 18*(12), 1–14.

Ouziaux, S. (1997). Mixing in digesters - site survey on Yorkshire Water anaerobic digesters. Technical Report 97/19, Yorkshire Water Services Process Development. (unpublished).

Pandit, A. B. and J. B. Joshi (1983). Mixing in mechanically agitated gas-liquid contactors, bubble columns and modified bubble columns. *Chemical Engineering Science 38*(8), 1189–1215.

Revill, B. K. (1997). *Mixing in the Process Industries* (Second Edition ed.)., Chapter 9, pp. 159–183. Butterworth-Heinemann, Oxford.

Rietema, K. and S. P. P. Ottengraph (1970). Laminar liquid circulation and bubble street formation in a gas-liquid system. *Transactions of the Institution of Chemical Engineers 48*, T54–T62.

Rundle, H. and J. Whyley (1981). A comparison of gas recirculation systems for mixing of contents of anaerobic digesters. *Water Pollution Control 80*(4), 463–480.

Ruszkowski, S. (1994). A rational method for measuring blending performance, and comparison of different impeller types. In *Eighth European Conference on Mixing. IChemE Symposium No.136. University of Cambridge, 21-23 September.*

Schmidt, J., R. Nassar, and A. Lubbert (1992). Local dispersion in the liquid phase of gas-liquid reactors. *Chemical Engineering Science 47*(13-14), 3363–3370.

Shah, Y. T., B. G. Kelkare, S. P. Godbole, and W. D. Deckwer (1982). Design parameters estimations for bubble column reactors. *American Institution of Chemical Engineers Journal 28*(3), 353–379.

Shekarriz, A., G. Douillard, and C. D. Richards (1996). Velocity measurements in a turbulent non-Newtonian jet. *Journal of Fluids Engineering 118*, 872–874.

Shiloh, K. S., S. Sideman, and W. Resnick (1973). *Canadian Journal of Chemical Engineering 51*, 542.

Skelland, A. H. P. (1967). *Non-Newtonian Flow and Heat Transfer.* Wiley, New York.

Slatter, P. T. (1997). The rheological characterisation of sludges. *Water Science and Technology 36*(11), 9–18.

Smith, L. C. (1996). Mixing in upflow anaerobic filters and its influence on performance and scale-up. *Water Research 30*(12), 3061–3073.

Sridhar, T. and O. E. Potter (1980). Interfacial areas in gas-liquid stirred vessels. *Chemical Engineering Science 35*, 683–695.

Stafford, D. A. (1982). The effects of mixing and volatile fatty acid concentration on anaerobic digester performance. *Biomass 2*, 43–55.

Stukenberg, J. R., J. H. Clark, J. Sandino, and W. R. Naydi (1992). Egg-shaped digesters: From Germany to the US. *Water Environment Technology 4*(4), 42–51.

Swanwick, J. D., D. G. Shurben, and S. Jackson (1969). A survey of the performance of sewage sludge digesters in Great Britain. *Water Pollution Control 68*(6), 639–661.

Tatterson, G. B. (1991). *Fluid Mixing and Gas Dispersion in Agitated Tanks.* McGraw-Hill Inc., New York. ISBN: 0 07 062933 1.

Tatterson, G. B. (1994). *Scaleup and Design of industrial mixing processes.* McGraw-Hill Inc., New York. ISBN: 0 07 062939 0.

Tchobanoglous, G. and F. L. Burton (1993). *Wastewater Engineering - Treatment, Disposal and Reuse* (third ed.). McGraw-Hill International, Singapore. ISBN: 0 07 100824 1. Metcalf and Eddy Inc.

Truscott, G. F. (1980, March). Mixing in anaerobic digesters: A preliminary review. TN1598. Technical report, BHRA Fluid Engineering.

Ulbrecht, J. J. and L. E. Baykara (1981). Significance of the central plume velocity for the correlation of liquid phase mixing in bubble columns. *Chemical Engineering Communications 10*, 165–185.

Ulbrecht, J. J., Y. Kawase, and K. F. Auyeung (1985). More on mixing of viscous liquids in bubble columns. *Chemical Engineering Communications 35*, 175–191.

Vaahto (1996). Vaahto Sales Info. 27, Berthas Field, Didmarton, Badminton, Avon. GL9 1EB. UK.

Verhoff, F. H., M. W. Tenney, and W. F. Echelberger, Jr. (1974). Mixing in anaerobic digestion. *Biotechnology and Bioengineering XVI*, 757–770.

Wadley, R. J. (1994). *Studies of a Bubble Column Reactor System for Fine Chemical Production.* Ph. D. thesis, U.M.I.S.T.

Walters, K. (1975). *Rheometry.* Chapman and Hall, London.

Wiedemann, F. (1977). Einrichtungen zur umwälzung des schlammes in faulräumen. *GWF-wasser-abwasser 118*, 278.

Williams, P. A. (1994). Mixing in anaerobic digesters. Master's thesis, Cranfield University of Science and Technology.

Zlokarnik, M. (1998). Problems in the application of dimensional analysis and scale-up of mixing operations. *Chemical Engineering Science 53*(17), 3023–3030.

Zoltek, J. and A. L. Gram (1975). High-rate digester mixing study using radioisotrope tracer. *Journal of the Water Pollution Control Federation 47*(1), 79–84.